

**UNIVERSITY OF ROME  
“LA SAPIENZA”**



Faculty of Civil and Industrial Engineering  
Astronautic, Electrical and Energetic Engineering Department  
PhD School on Science and Technology for the Industrial Innovation

PhD in Electrical Engineering  
ING-IND/33 – Electrical Systems for Energy  
25° cycle – 2009/2012

**SELECTED PROBLEMS  
FOR THE PROTECTION OF ELECTRICAL  
AND ELECTRONIC SYSTEMS AGAINST  
LIGHTNING OVERVOLTAGES**

PhD thesis  
Tomasz Dominik Kisielewicz

Tutor  
Prof. Eng. Carlo Mazzetti di Pietralata

To my mother and my father

## **ACKNOWLEDGEMENT**

In this special occasion, finishing my PhD studies in Italy, it gives me a great pleasure to express my gratitude to all people who have supported me and contributed to my scientific work.

I would like to express the deepest appreciation to Prof. Eng. Carlo Mazzetti di Pietralata (Professor of High Voltage Technique at University of Rome La Sapienza), for all effort, cooperation, support and encouragement during the PhD studies, especially for patience and motivation given to finish this thesis.

I am grateful to one of my best work guides, Dr Eng. Giovanni Battista Lo Piparo (President TC 81 CEI, Secretary of TC 81 IEC and CENELEC), for fruitful discussions and inspiration for researches.

I would like to thank Prof. Eng. Zdobyslaw Flisowski (Professor of High Voltage Technique at Warsaw University of Technology), Prof. Eng. Andrzej Jakubiak (Professor of Telecommunication Technique at Warsaw University of Technology) and Dr Eng. Boleslaw Kuca (Researcher and students Mentor at Warsaw University of Technology) from my mother university for significant and valuable contributions to my researches before and during my PhD studies in Italy.

In the last, I would like to thank my family and friends for all support and comprehension during my studies.

# Contents

<b>1. Introduction.....</b>	<b>8</b>
<b>2. Lightning physics .....</b>	<b>12</b>
2.1. Thunderstorm occurrences .....	12
2.2. Types of lightning discharge .....	14
2.2.1. Nature of lightning flashes .....	14
2.2.2. Lightning classification according to protection issues .....	17
2.3. Lightning currents and related parameters .....	21
2.3.1. General survey.....	21
2.3.2. Lightning current shapes .....	22
2.3.3. Lightning current statistics .....	26
2.3.4. Lightning current parameter for LPL according to IEC standards.....	29
2.4. Frequency of lightning discharges to earth.....	33
2.5. Lightning location and warning systems .....	36
2.5.1. Measurements techniques .....	36
2.5.2. EUCLID network .....	41
2.5.3. Thunderstorm warning systems .....	46
2.6. Summary.....	48
<b>3. Classification and characteristics of critical occurrences: damage source determination .....</b>	<b>50</b>
3.1. Critical occurrences determination.....	50
3.2. Flashes to the structure: source of damage S1 .....	58
3.2.1. Prevailing parameters determination and calculation .....	58
3.2.2. Dangerous events frequency .....	66
3.3. Flashes near the structure: source of damage S2.....	68
3.3.1. Prevailing parameters determination and calculation .....	68
3.3.2. Dangerous events frequency .....	70
3.4. Flashes to the services connected to the structure: source of damage S3 .....	72
3.4.1. Prevailing parameters determination and calculation .....	72
3.4.2. Dangerous events frequency .....	75
3.5. Flashes near the services connected to the structure: source of damage S4.....	80
3.5.1. Prevailing parameters determination and calculation .....	80
3.5.2. Dangerous events frequency .....	85
3.6. Summary.....	90
<b>4. Characteristic and technology of selected protection measures: numerical representation for computer simulations .....</b>	<b>92</b>
4.1. Surge protective devices.....	92
4.1.1. Introduction .....	92
4.1.2. SPD switching type.....	96
4.1.3. SPD limiting type.....	100



4.1.4. Computer implementation of surge protective devices.....	104
4.2. Isolation transformer .....	107
4.2.1. Introduction .....	107
4.2.2. Isolation transformer construction features.....	110
4.2.3. Computer implementation of isolation transformer.....	112
4.3. Summary.....	114
<b>5. Criteria for protection measures selection according to the international standards</b> .....	<b>116</b>
5.1. Introduction .....	116
5.1.1. Standardisation bodies.....	116
5.1.2. Lightning protection.....	117
5.2. Establishment of lightning protection zones .....	119
5.3. Protection by surge protective devices.....	120
5.3.1. SPD inside LPZ.....	120
5.3.2. Selection with regard to voltage protection level.....	122
5.3.3. Selection with regard to discharge current.....	124
5.3.4. Coordinated SPD system.....	125
5.4. Protection by isolation transformer.....	128
5.5. Summary .....	129
<b>6. Criteria for protection measures selection: experimental tests and computer</b> <b>simulations for surge protective devices .....</b>	<b>131</b>
6.1. Introduction .....	131
6.2. Laboratory tests of surge protective devices .....	132
6.3. Computer simulation of surge protective devices: models development.....	137
6.3.1. Introduction .....	137
6.3.2. Lightning source current .....	137
6.3.3. Low voltage SPD .....	139
6.3.4. Supply line.....	140
6.3.5. Transformer.....	142
6.3.6. Grounding system .....	142
6.4. Comparison of numerical and experimental results.....	150
6.5. Factors influencing the selection and installation of surge protective devices for low voltage systems: upstream SPD.....	157
6.5.1. Introduction .....	157
6.5.2. Selection with regard to discharge current.....	157
6.5.3. SPD selection with regard to protection level.....	161
6.5.4. Inductive voltage drop $\Delta V$ on the connection leads of SPD.....	164
6.5.5. SPD dimensioning.....	165
6.5.6. Conclusions relevant to the upstream SPD .....	166
6.6. Factors influencing the selection and installation of surge protective devices for low voltage systems: downstream SPD .....	167
6.6.1. Introduction .....	167
6.6.2. Induced voltage .....	168

6.6.3. Induced current.....	169
6.6.4. Voltage drop $\Delta V$ on SPD connecting leads due to induced current .....	174
6.6.5. Feeding effect: transmitted current .....	175
6.6.6. Induction and feeding effects composition: current on SPD and voltage drop $\Delta V$ on its connection lead.....	178
6.6.7. SPD dimensioning.....	181
6.6.8. Conclusions relevant to the downstream SPD .....	185
6.7. Summary .....	186
<b>7. Criteria for protection measures selection: experimental tests and computer simulations for the isolation transformer .....</b>	<b>188</b>
7.1. Introduction .....	188
7.2. Characteristic of surge transfer by an isolation transformer .....	189
7.3. Laboratory tests of isolation transformers effectiveness.....	192
7.3.1. Introduction .....	192
7.3.2. Determination of tests condition .....	193
7.3.3. Computer simulation of isolation transformer: models development.....	195
7.3.4. Tests results .....	195
7.4. Summary .....	203
<b>8. Case study: selected aspects of lightning protection for photovoltaic power generation systems .....</b>	<b>205</b>
8.1. Introduction .....	205
8.2. Risk assessment.....	209
8.2.1. Introduction .....	209
8.2.2. Risk assessment for the roof top PVPG .....	211
8.2.3. Risk assessment for the ground based PVPGS .....	217
8.3. Protection of control and measurement apparatus by means of SPD.....	219
8.3.1. Introduction .....	219
8.3.2. Results of laboratory tests .....	220
8.4. Influence of load conditions on apparatus protection by means of SPD.....	225
8.4.1. Introduction .....	225
8.4.2. Results of computer simulations .....	226
8.5. Influence of parallel consumers on SPD protection features .....	230
8.5.1. Introduction .....	230
8.5.2. Results of computer simulations .....	230
8.6. Grounding conditions influence on apparatus protection by means of SPD.....	234
8.6.1. Resistive coupling for an extended earth arrangement .....	234
8.6.2. Bonding conditions for control and measurement apparatus protection.....	237
8.7. Summary .....	245
<b>9. Summary and conclusions.....</b>	<b>247</b>
<b>REFERENCES.....</b>	<b>249</b>

# **Chapter 1**

# 1. Introduction

Nowadays electrical and electronic apparatus forming complex systems within a structure can provide many benefits, e.g. automation of operation, increment of control precision etc. However the regular operations of these systems can be influenced by different not demand occurrence dependent and not dependent on humans. Certainly the range of influence depends on the damage source type e.g. water, fire, overvoltages, storms or negligence, theft. The percentage representation of different incidence based on the statistics of more than 15200 apparatus failures is shown in Fig. 1.1. [1, 2].

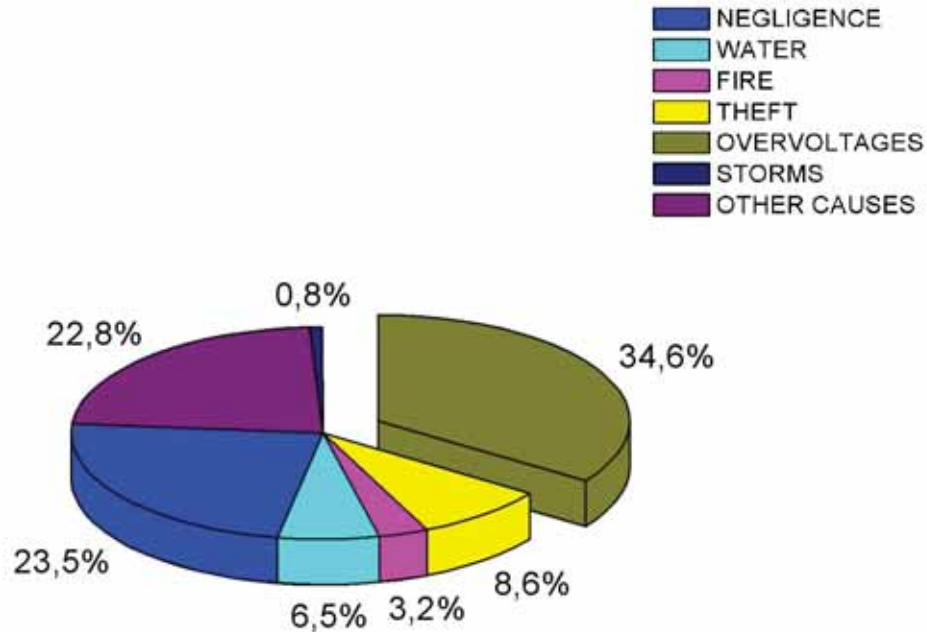


Figure 1.1. Statistics based on >15.200 apparatus failures.

It is to note that the overvoltages consist of the main component of possible damage sources. This fact is influenced by modern apparatus features, namely high operation frequencies as well as low operation voltage.

These overvoltages can be caused by electrical currents of different sources and especially by current of direct and nearby lightning strikes. For this reason to assure electrical and electronic apparatus operations many scientific studies relevant to their protection are developed in the frame of scientific conferences (ICLP, CIGRE, SIPDA, ...) [1-9]. Moreover, it is important to mention that different institutions deal with this problem of protection of electrical and electronic systems against lightning surges: International Electrotechnical Commission (IEC), European Committee for Electrotechnical Standardization (CENELEC), Institute of Electrical and Electronics Engineers (IEEE) and the relevant National Bodies (i.e. CEI in Italy); they give normalized requirements and procedures of lightning protection measures and systems.

Aim of the thesis work is to analyse selected aspects of protection of electrical and electronic systems within a structure against lightning overvoltages. Selection and

coordination problems of the main protection measures recommended by International Standards (IEC), such as surge protective devices (SPD) and isolation transformers, are investigated by means of laboratory tests and computer simulations.

The present work is organised as follows.

After the short introduction in this first chapter, the second chapter reports selected aspects concern lightning phenomena. Survey is started with description of thunderstorm occurrences. Meteorological definition is given, as well as some principal facts regarding these physical aspects. Moreover, lightning discharge are classified. Principal mechanism of lightning occurrences are given taking into account natural issues. The classification is also focused on protection issues taking into account standard requirements. The lightning protection level concept referring to IEC standard is discussed, and respectively parameters for severe cases are presented. Frequency of lightning discharges to ground is mentioned, and examples of lightning flash density maps are given. Special focus is dedicate for lightning location, to present current state of technologies associated with this natural phenomena. The measurements techniques are defined. An example of lightning location network is given.

In the third chapter the source of damage due to lightning are analysed. The survey is started from general recognition of lightning current influence on objects. Possible dangerous occurrences are subdivided into four general categories: flashes to the structure (S1); flashes to ground or to grounded objects near the structure (S2); flashes to the connected lines (S3); flashes nearby the connected lines (S4), taking into account the lightning point termination. The attention is paid on the description of significant parameters belonging to each occurrence. Special focus is dedicated also for the calculation of dangerous events frequency. To sum up, even if the source of damage S1 is not so frequent as the indirect influence of lightning flashes to an object, such source represents the most severe case in respect to the other damage sources taking into account lightning current values.

The forth chapter includes two characteristic parts, according to the analysed protection measures to reduce the effects of different sources of damage.

The first part of this chapter includes general information about surge protection devices and their application field. The basic criteria for SPD selection and fundamental parameters are introduced. The classification presented is based on the international standards and literatures [1, 2, 10-12]. Paragraph on surge protective devices (SPD) limiting type includes information about the internal features of this protection measure based on varistors. The principal of physics as well as typical characteristics of this element are described. Paragraph on SPD switching type includes similar information for protection measures based on spark gaps.

The second part includes information about isolation transformers. The general survey presents that such transformer can do more than transferring electrical energy from one voltage to another and is able to reduce the transfer of common mode lightning overvoltages. Special focus is dedicated to some technological aspects of such device.

In the fifth chapter the standardisation aspects of lightning protection are presented. The survey starts of standardisation bodies overview with reference to the application fields



and territories. In terms of lightning protection, it is possible to distinguish two international bodies IEC and ITU. IEC deals with electrical systems. ITU deals with communication and signalling networks systems. Special focus is dedicated for IEC standard due to SPD and isolation transformer consideration. Moreover the lightning protection zones (LPZ) concept is discussed. Examples of protection measures installation in these zones are shown. The SPD selection according to the voltage and current threat is argued.

The sixth chapter intends to give criteria for protection measures selection, installation and coordination, namely SPD switching and limiting type, against lightning overvoltages. The worst case of damage source S1, where failure of apparatus can be caused due to resistive as well as inductive coupling of lightning current flowing to the earthing system is considered. The analyses are developed by several computer simulations performed by means of commercial transient software EMTP-RV, adopting suitable computer models validated by experimental tests in HV Laboratory of Warsaw University of Technology as well as in the HV Laboratory of University of Rome La Sapienza. The special focus is dedicated for the comparison of the laboratory and computed results to ascertain models accuracy. The results evaluation seems to be satisfactory and further analyses of apparatus protected by means of SPD are developed. The first examination include proper selection of SPD installed at the entry point of power line into the structure, namely upstream SPD. The results of this first part of work demonstrated that the installation of further, downstream SPD is needed. The selection of downstream SPD have to be coordinated with upstream SPD with regard to both the protection level and the discharge current. Finally, some simple rules for the selection of downstream and upstream SPD are proposed. Comments and comparison with the requirements of the international standard IEC/ EN 62305-4 are presented.

In the seventh chapter selected criteria for the electronic and electrical apparatus protection by means of an isolation transformer are discussed. Special focus is dedicated on the mechanism of surge transfer through an isolation transformer especially when a fast front source is applied. Laboratory tests as well as computer simulations are performed with aim to investigate the influence of grounding condition of screen on protection effectiveness. For this reason different types of source are also taken into account. Some practical recommendation for installation issues are formulated.

In the eighth chapter selected aspects of lightning protection for photovoltaic power generation systems (PVGS) are presented. The investigations include: risk assessment, protection of control and measurement apparatus by means of SPD, influence of load conditions on apparatus protection by means of SPD, influence of parallel consumers on SPD protection features, grounding and bonding conditions influence on apparatus protection.

In the ninth chapter briefly summary of present work as well as some general conclusions are reported.

# **Chapter 2**

## 2. Lightning physics

### 2.1. Thunderstorm occurrences

According to meteorologists requirements a storm is classified as a thundercloud or thunderstorm if thunder is heard. Generally this peculiar and intense acoustic disturbance is caused by the presence of lightning, if no other natural source exist. The storms, habitually composed of strongly convective cumulonimbus clouds, are usually accompanied by strong wind gusts and rain. Sometimes rain can be substituted by hail or snow. In natural conditions thunderclouds are results of atmospheric instability and develop as the warm, moist air near the earth rises and replaces the denser air aloft. This overturn often results in the condensation of atmospheric water vapour forming a visible cloud of water droplets. When this occurs, the heat associated with the phase changes of water acts to speed the overturn: release of the heat of vaporization by condensing water vapour enhances the updraughts, while cooling, caused by evaporation of condensed water, can help drive the downdraughts which replace some of the ascending subcloud air. Moreover it is possible to describe that, thunderclouds are large atmospheric heat engines with water vapour as the primary heat-transfer agent. The output of these engines is the mechanical work of the vertical and horizontal winds produced by the storm, electrical work on free charge resulting in lightning discharges and an outflow of condensate in the form of rain and hail from the bottom of the cloud and of small ice crystals from the top of the cloud. In addition, thunderclouds increase the local stability of the atmosphere, transport horizontal momentum vertically, and are believed to maintain the atmosphere's electrical potential relative to the earth. During daylight, the snow crystals that are blown away from the top of the cloud in the form of cirrus by the high level winds, reflect much of the incoming solar radiation back to space thus reducing solar heating of the earth's surface and suppressing the development of other thunderclouds [13]. The processes in a thundercloud during lightning occurrences are varied, complex and still under consideration of scientific research groups [14].

The climatological observations, performed by means of modern measurement systems indicate that, at any time is about 1,000 thunderstorms are continuously in progress over the surface of the earth. Generally the primary activity presents in the lower latitudes. Sometimes, thunderclouds occur in the polar regions. The global distribution of thunderstorms shows their convective origin [15]. The greatest frequency is to be found where and when vertical convective activity is at a maximum and much of this is controlled by radiation processes: solar heating warms the surface of the earth each day with a thermal input of about  $1 \text{ kW m}^{-2}$  of perpendicular surface while the upper troposphere is cooled continually by the outward thermal radiation from water molecules and aerosol particles. As the earth rotates beneath the sun, new thunderstorms form in the subsolar area so that a wave of thunderstorm development moves westward each day.

Thunderstorms occur commonly over warm sea coasts when breezes from the surrounding ocean are induced to flow inland after sunrise as the land surface is warmed by solar radiation. Similarly, because mountains are heated before the valleys, they often aid the onset of convection in unstable air. In many parts of the world, diurnal thunderstorms occur over mountainous terrain.



In addition to air-mass convection (and sometimes superimposed upon it) is the intense convective activity that occurs when cold air meets warmer, moister air, slides under and lifts it: vigorous thunderstorms occur along an active cold front and in squall lines in the warm air ahead. While most thunderstorms develop around midday in the spring and summer months when the potential for convection is usually the greatest and adequate water vapour is available, they have been observed at all times throughout the year in temperate latitudes, as a result of frontal activity. Further, thunderstorms frequently develop over the North Atlantic Ocean during the winter when cold Arctic air flows over the warmer Gulf Stream [13].

Water vapour concentrations in excess of 7 g of water  $\text{kg}^{-1}$  of dry air are required generally for warm-season thunderstorm formation although lightning has been reported in winter clouds over the unfrozen Great Lakes when the water vapour mixing ratio could not have exceeded 4 g  $\text{kg}^{-1}$  of air [13].

The global thunderstorm activity now occurring has presumably been taking place from times early in the development of the earth's atmosphere. The evidence for this inference is obtained from geological information: when lightning strikes dry sand, the resultant high temperature melts and vitrifies the silica, forming tubes known as fulgurites, similar to the contemporary formations which are found in our beaches and deserts. Ancient fulgurites believed to be 250 million years old have been detected in geological deposits. Speculations have been advanced by a number of scientists that lightning has played a significant role in the modification of the early atmosphere to its present state and in the origin of life on the planet [13].

Lightning rarely occurs in cumuli with depths smaller than about 3 km but it has been observed in volcanic eruption clouds with dimensions of less than 500 m. Normal lightning and thunder occur frequently in large clouds. The greatest activity occurs in the largest convective systems which approach 20 km in depth. The temperature of the air and the phase of cloud water at cloud-base and cloud-top levels do not seem to be critical for the development of cloud electrification. The main requirements are that sufficient water vapour be present to power the cloud and that the atmosphere be unstable to vertical motions. Lightning in clouds everywhere warmer than 0 °C has been reported, conversely, electrification has been observed in clouds everywhere colder than 0 °C and in clouds of ice crystals [13].

Active thundercloud systems range in horizontal extent from about 3 km in diameter to dimensions greater than 50 km. Along cold fronts merged thunderclouds may occur in lines extending for hundreds of kilometres.

The life of an "air-mass" thundercloud over the New Mexican mountains is typically about 2 hours. Smaller, electrically active clouds in the subtropics have been observed with durations of less than 30 minutes. On the other hand, large, frontal-cloud disturbances have persisted for more than 48 hours and moved more than 2,000 km [13].

## 2.2. Types of lightning discharge

### 2.2.1. Nature of lightning flashes

A natural lightning flash is a complex phenomenon composed of successive events, also called flash components, with different physical properties in terms of discharge type and propagation, radio frequency radiation type, current properties, duration. General survey of lightning flashes observed by human being is shown in Fig. 2.1.

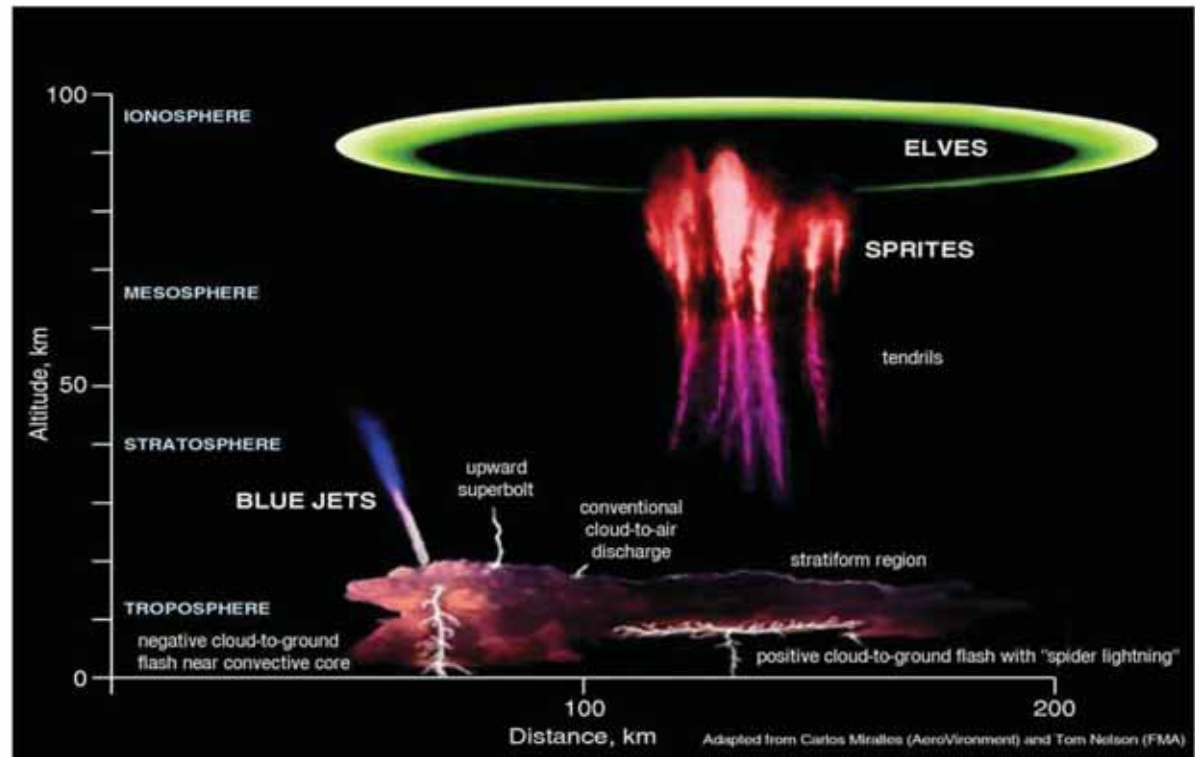


Figure 2.1. Lightning discharges observed by human being [16].

The negative cloud to ground flash, positive cloud to ground flash, conventional cloud to air discharge as well as blue jets, upward superbolt, tendrils, sprites and elves are presented in technical literature [13, 14]. The classical lightning protection concept include only interferences of lightning flashes to the earth and in special cases aspect of lightning flashes between clouds is considered. The disturbance source has an impact for electrical and electronic apparatus protection. Taking into account civil apparatus protection, the lightning flashes to the earth should be considered.

Lightning flash to the earth is result of thundercloud present. The conditions necessary for these occurrence initiation are shortly described in 2.1. In typical cases, the thundercloud characterizes the negative charges in the lower parts and positive charges in the higher region. The prevailed charge defines the lightning current polarity. Prevailing positive charge defines positive cloud and results a flash called positive flash while negative charge defines negative cloud and results a negative flash. In a positive flash a positive current flows from cloud to earth, in a negative flash the current is described as negative. Beside the polarity of lightning current, a direction of lightning discharge development can be selected as

classification of lightning flashes. This criterion consist of downward and upward leader progresses. In a downward leader the direction is from the cloud to earth. An upward leader progress from earth to the cloud. An upward connecting leader is a discharge from earth (or an earthed object) which meets a downward leader and discharges it to earth. The polarity of a leader may be defined either by the polarity of the electric charge involved or by that of the resulting current. Either a downward leader lowers positive charge from the cloud by means of a positive current or it lowers a negative charge by means of a negative current. Such a leader therefore has always the same polarity of charge and current. An upward leader, on the other hand, has opposite polarities of charge and current [14].

The leader stroke is invariably initiated at a point of high electric field strength. This can occur either between positive and negative charge centres in a thundercloud or between a negative (or positive) charge centre in the cloud and its induced countercharge in the ground. The first case starts as an intra-cloud flash between the charges of opposite polarity. Depending on the height of the cloud above ground and the transient field change between cloud and earth, such a discharge can be confined to a pure intra-cloud flash or it can proceed towards ground, thus producing an earth flash. The second case leads to a leader stroke from the cloud charge to its induced charge in the ground. The highest field strength can then arise either at the lower boundary of the cloud or on a very tall earthed object. This, in turn, leads either to a downward flash from cloud to earth or to an upward leader which develops from the earthed object towards the cloud.

An overview of the lightning discharges subdivision is shown in Fig. 2.2. – 2.5. The four leader types are shown. Moreover the return strokes belong to these typical occurrences are added consist of comprehensive review [14].

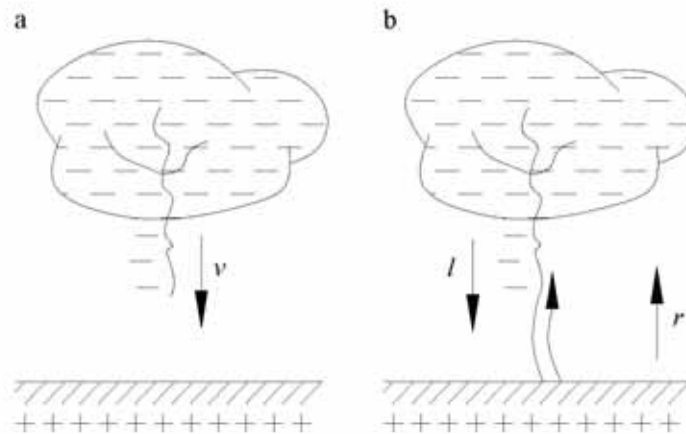


Figure 2.2. Downward negative discharge, where:  $l$  - leader;  $r$  - return stroke;  $v$  - direction of propagation.

The first type of lightning discharge is shown in Fig. 2.2, a and b. Fig. 2.2 a shows that the discharge begins with a downward leader from a negative cloud. This is predominantly the case over open country without very tall objects. The leader is negatively charged and its current is negative. If it does not reach earth (air discharge), no return stroke ensues; it constitutes a cloud discharge. Fig. 2.2 b shows a case when the negative downward leader reaches the earth, the very fast upward moving return stroke develops and this discharges the

leader and part of the cloud charge to earth. This sequence can occur once, producing a single-stroke flash, or it can be repeated, producing a multi-stroke flash. The phenomenon is defined as negative downward flash.

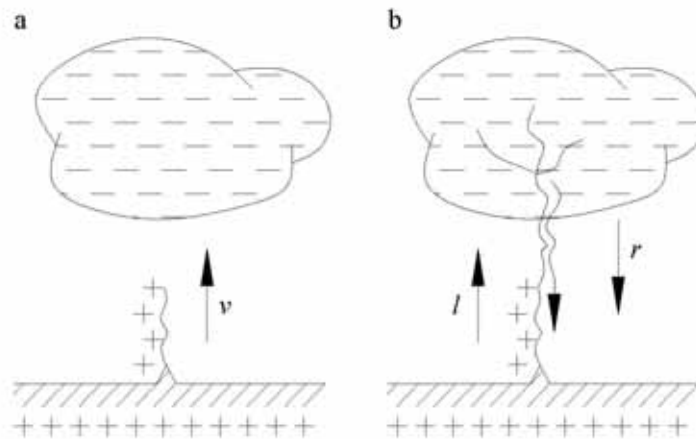


Figure 2.3. Upward positive discharge, where:  $l$  - leader;  $r$  - return stroke;  $v$  - direction of propagation.

The second type of lightning discharge is shown in Fig. 2.3, a and b. Fig. 2.3 a shows that the discharge is initiated by an upward leader from earth. In practical case this situation can occurred when tall earthed objects e.g. tower or mountain top are present, progressing towards a negative cloud. The leader is charged positively. The charge flowing to earth, and thus the currents in the object are negative. This phenomenon is defined as positive upward leader/negative continuous flash. Type Fig. 2.3 b shows initial stage as for type Fig. 2.3 a, followed by subsequent strokes, each having a downward leader and upward return stroke as type shown in Fig. 2.2 b. This phenomenon is defined as positive upward leader/negative multiple flash.

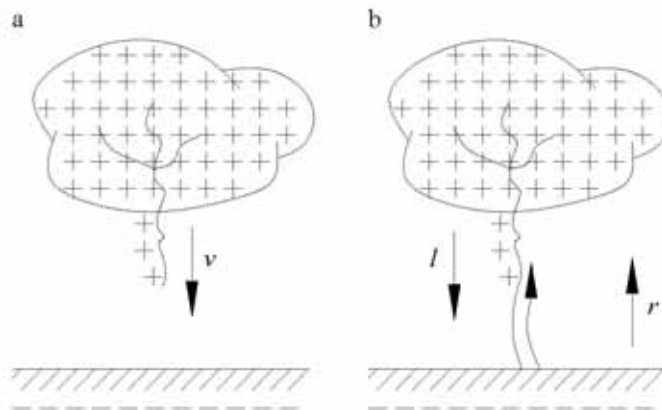


Figure 2.4. Downward positive discharge, where:  $l$  - leader;  $r$  - return stroke;  $v$  - direction of propagation.

The third type of lightning discharge is shown in Fig. 2.4, a and b. Fig. 2.4 a corresponds to type shown in Fig. 2.2 a but under a positive cloud. Both the charge on, and the current in the leader are positive. Since the leader does not reach earth, a displacement current flows in the ground. Fig. 2.4 b shows when the positive downward leader reaches the earth, it gives rise to



a positive upward return stroke by which the leader and part of the cloud are discharged. This phenomenon is defined as positive downward flash.

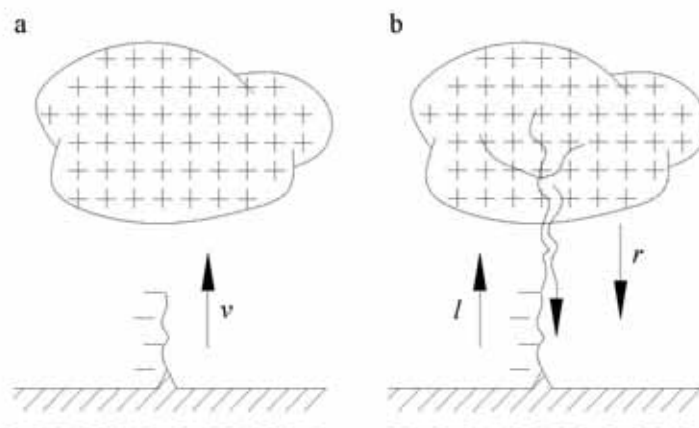


Figure 2.5. Upward negative discharge, where:  $l$  - leader;  $r$  - return stroke;  $v$  - direction of propagation.

The fourth type of lightning discharge is shown in Fig. 2.5, a and b. Fig. 2.5 a shows case when from earth an upward leader is initiated under a positive cloud. The leader is negatively charged (the tip of the structure constitutes the cathode). The charge flowing to earth is positive and so is the current which, being of long duration, is described as a continuous current. In real cases this can occur if tall earthed objects are present. Type Fig. 2.5 b is initiated as type Fig. 2.5 a but the upward leader is followed, after 4 to 25 ms, by an exceptionally severe positive downward discharge which must be regarded as a return stroke. The negative upward leader progresses in the form of a very long "connecting leader" into an existing intra-cloud flash which, first, caused the transient field by which the upward leader was initiated and, later, is discharged to earth through this "connecting leader". These phenomena are defined as negative upward leader/positive impulse-current flash, or in short, positive impulse current flash (mountain type).

Mostly downward flashes occur in flat territory, and to lower structures, whereas for exposed and/or higher structures upward flashes become dominant. With effective height, the probability of a direct strike to the structure increases and the physical conditions change. The additional component in upward flashes is the first long stroke with or without up to some ten superimposed impulses. But all impulse current parameters of upward flashes are less than those of downward flashes. A higher long stroke charge of upward flashes is not yet confirmed. Therefore the lightning current parameters of upward flashes are considered to be covered by the maximum values given for downward flashes. A more precise evaluation of lightning current parameters and their height dependency with regard to downward and upward flashes is under consideration [17].

### 2.2.2. Lightning classification according to protection issues

The protection issues of electrical and electronic apparatus are subject of technical standards. Topical publications include usually source of damage definition and define lightning currents. The IEC 62305 standard suggests the following general subdivision criterion for lightning flashes to earth [18]:

- downward flashes initiated by a downward leader from cloud to earth (Fig. 2.2 and Fig. 2.4);
- upward flashes initiated by an upward leader from an earthed structure to cloud (Fig. 2.3 and Fig. 2.5).

Further subdivision of strokes comes from their polarity (positive or negative) and from their position during the flash (first, subsequent, and superimposed).

The possible components of current for downward flashes are shown in Fig. 2.6.

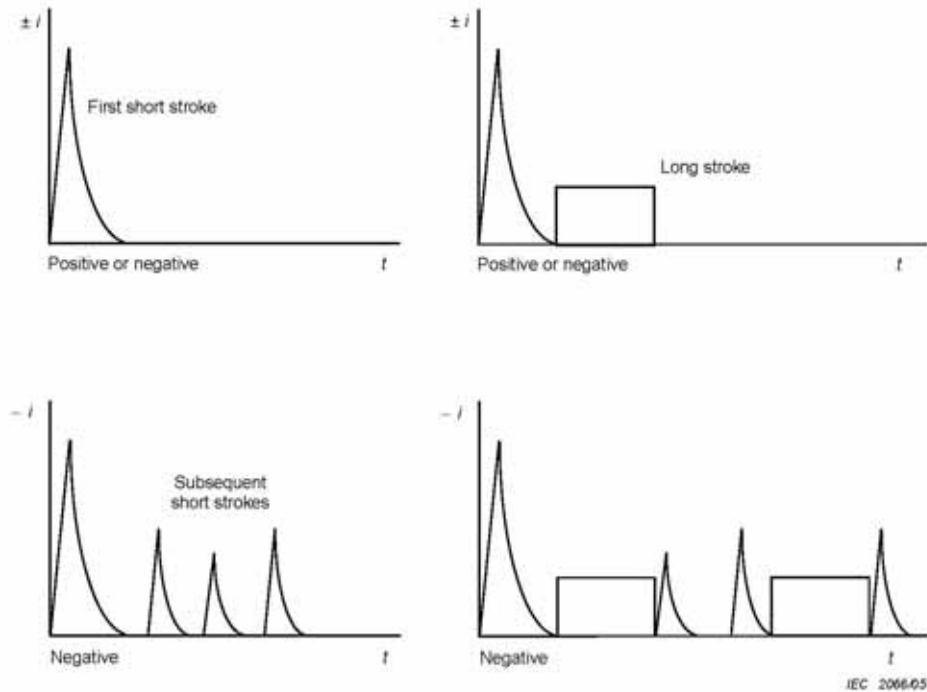


Figure 2.6. Possible components of downward flashes (typical in flat territory and to lower structures) [17].

Schematic illustration of phenomenon shown in Fig. 2.6. is founded on the base of experimental measurements of lightning current performed in the last century. An example of data corresponding to the negative downward lightning is shown in Fig. 2.7.

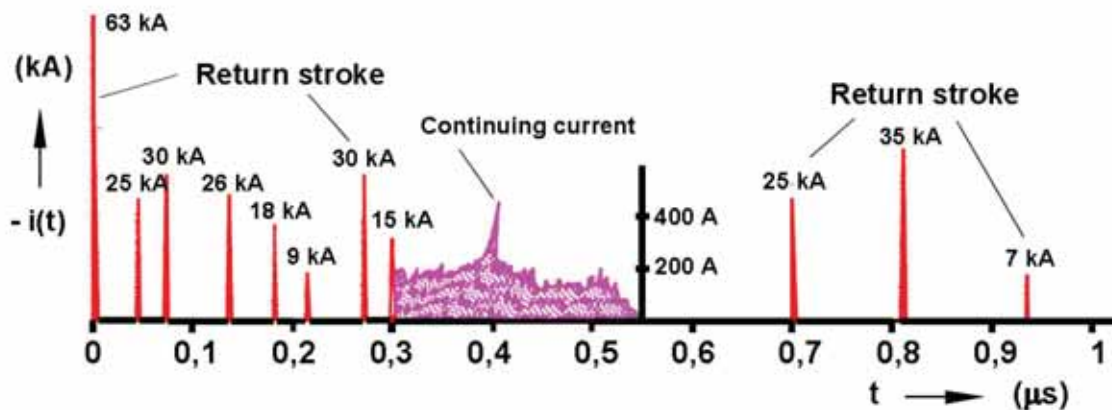
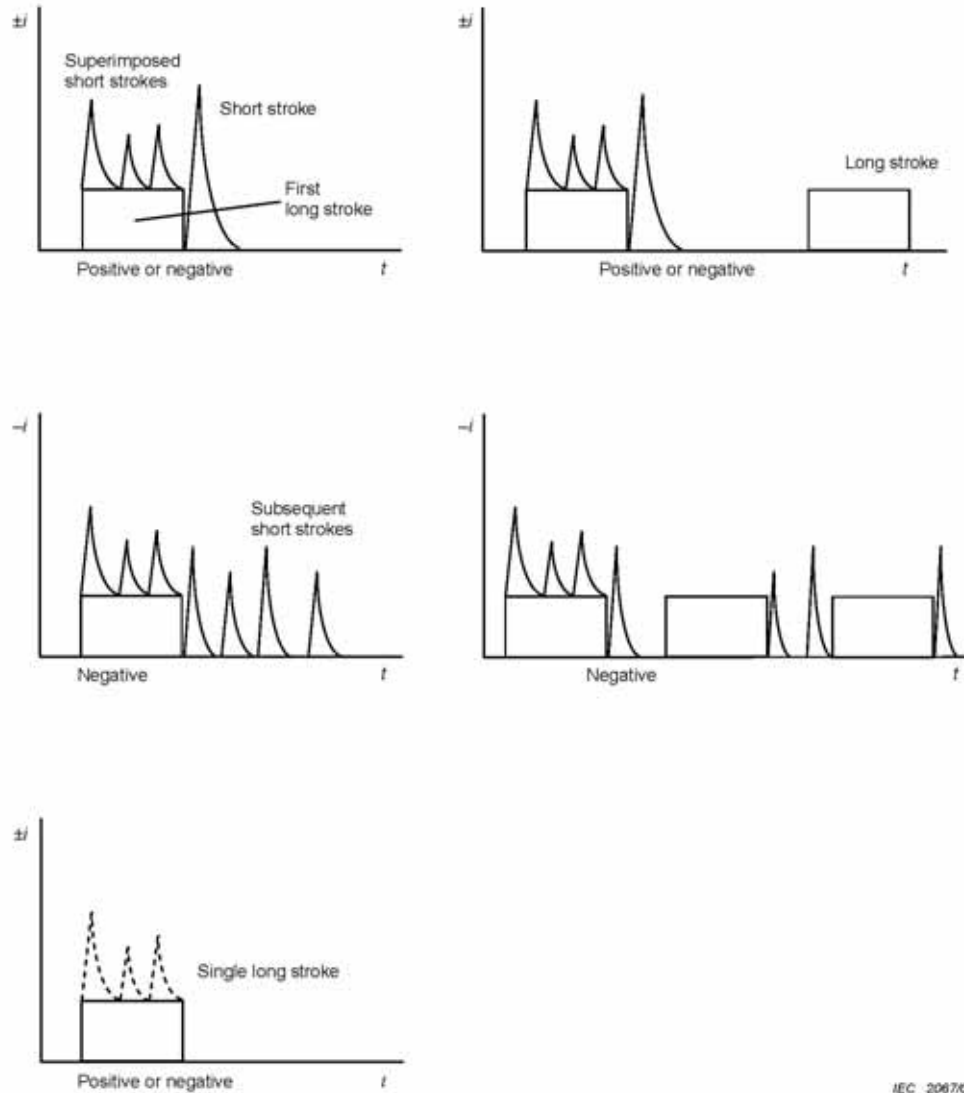


Figure 2.7. Current of a multiple stroke negative downward lightning with 11 return strokes and one continuing current [19].

This occurrence example consisting of 11 return strokes and one continuing current. The continuing currents always follow immediately after a return stroke current, in present case after the 8<sup>th</sup> return stroke. The peak currents of the subsequent return stroke are in the range of 10 kA and thus much smaller than the peak currents of the first strokes. On the other hand, the subsequent return strokes have short rise times and therefore higher  $di/dt$  values compared to the first return strokes. The continuing currents differ from the return stroke currents significantly having much lower current amplitudes in the range of some 100 A, but much longer duration in the range of some 100 ms [19].

The possible components of current for upward flashes are shown in Fig. 2.8.



IEC 200705

Figure 2.8. Possible components of current of upward flashes (typical to exposed and/or higher structures) [17].

An example of data corresponding to the negative upward flash measured at the Peissenberg tower is shown in Fig. 2.9.

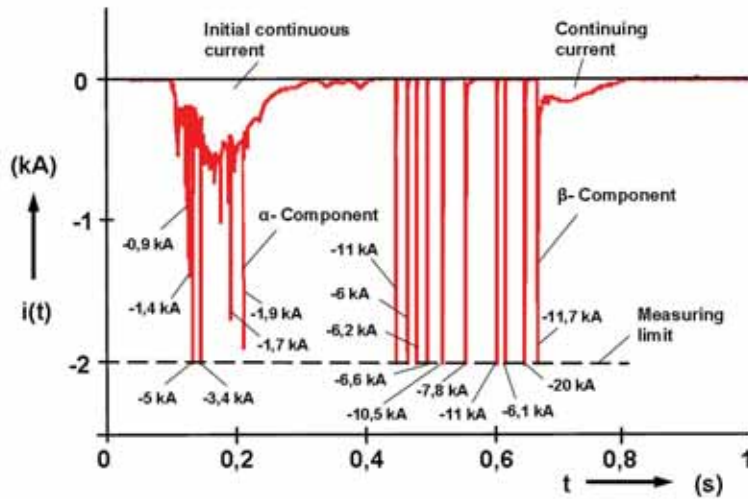


Figure 2.9. Current of a negative upward lightning measured at the Peissenberg tower, Germany [19].

Impulse currents are superimposed to the initial continuous current. These so-called  $\alpha$  components are short duration currents with amplitudes up to several kA. After the cessation of the initial continuous current  $\beta$  components may follow, which are similar to the currents of the subsequent return strokes. Furthermore, a small continuing current may occur immediately after a  $\beta$  component as shown in Fig. 2.9 [19].



## 2.3. Lightning currents and related parameters

### 2.3.1. General survey

The lightning current is the most important single parameter of the lightning discharge. The scientific aspects of lightning protection as principal factors include the wave-shape and amplitude of an occurrence. The knowledge of these two parameters seem to be sufficient to solve electrical problems belong to lightning protection operation. Up to the beginning of the 20<sup>th</sup> century lightning protection measures were mostly based on empirical knowledge. Misconceptions occasionally keep on long after improved information has been available. It may have been the flickering appearance of a multiple lightning discharge which first gave rise to the idea that the lightning current was oscillatory. Arguing from experiments with Leyden jars. Sir Oliver Lodge (1892) convinced himself that lightning was an oscillatory phenomenon with a frequency of about 1 MHz. Later it became fashionable to calculate this frequency by visualizing a capacitor, formed by a charged cloud and the earth, discharging to earth through the channel which was represented by its internal resistance and inductance. As late as 1924 this circuit was regarded as sufficiently valid for Creighton to suggest that the current amplitude could reach 1,450 kA and its rate of rise  $400 \text{ kA } \mu\text{s}^{-1}$ . In a paper which even today would be remarkable for its wide scope Humphreys argued, in 1918, that the lightning current was more likely to be aperiodic than oscillatory and this was explained by the suggestion that the internal resistance of the lightning channel exceeded the critical value for damping. However, with the numerical values adopted by Peek (1924) a cloud was assumed to be discharged in one single stroke and this led to the conclusion that the lightning current would last no more than a few microseconds. On this basis Fortescue (1930) pointed out that, if a charge of 20 C, a figure which had been established by Wilson (1920), was discharged in  $2 \mu\text{s}$ , this would require a current amplitude of 10,000 kA. The argument about the oscillatory or aperiodic nature of the lightning current lasted several decades [13].

In the middle of 20<sup>th</sup> century has been established that the lightning current is almost invariably unidirectional and Ampere's law could be used to measure the current peak value with small magnetic links. The first device for lightning current measurement consist of small bundles of parallel steel wires were located in glass tubes [20]. The magnetic links were installed close to the down conductors. In case of a lightning strike they became magnetized. The residual magnetism retained by the steel wires allow to derive the peak value and polarity of the lightning current. Moreover the magnetic links were relatively cheap, what permitted to widespread this technique, e.g. ten thousands of them were installed at high-voltage power lines in Germany [21, 22]. Similar experiments were carried out at high-voltage power lines and other high objects in Russia [23] and at high chimneys in Poland [24]. In Czechoslovakia more than 1000 lightning currents were measured from 1958 to 1985 at buildings with heights ranging from 25 m up to 140 m [25].

The current waveform of lightning stroke probably was recorded by means of oscilloscopes as the first by McEachron at the Empire State Building in New York, USA during the thirties of the last century [26]. The use of storage oscilloscopes allowed resolving the whole current waveform including the fast rising current front and the slow decay. With this method, Berger measured the lightning currents at two 70 m high towers on the mountain

San Salvatore, Switzerland During a period of about 10 years Garbagnati and Lo Piparo recorded lightning currents at two 40 m high telecommunication towers located at Foligno and Monte Orsa in Italy [27]. In South Africa the lightning currents were measured for more than 15 years at a 60 m high mast [28]. Because the probability of lightning strikes increases with the structure height, in Russia even tethered balloons were used to erect a 1000 m high steel wire [29]. Most of the lightning strikes to tall towers are upward discharges developing from the top of the structure. At very high towers, like the 540 m high Ostankino tower in Moscow, Russia, however, it was found that lightning may also terminate at the lower parts of the tower [30, 31]. More recently upward lightning was measured at the Peissenberg tower in Germany [32], the Gaisberg tower in Austria [33], the CN-tower in Canada [34] and the San Chrischona tower in Switzerland [35]. The upward lightning typically occur in winter when the thundercloud base is lower and closer to the tower top. From the measurements in Japan at several high objects it is known that the lightning during winter thunderstorm may be very severe transferring high charges to ground [36, 37]. Because even at high towers the number of lightning strikes is restricted to a few up to some ten events per year [38], rockets are used to artificially trigger the lightning discharges. The rocket quickly brings up a trailing metal wire in a strong electric field which acts similar to a high tower where upward discharges are initiated. Newman was the first who did such experiments when he started rockets from a boat located at the coast of Florida in 1962 [39]. Meanwhile triggered lightning experiments have been performed by several research group, e.g in Japan [40], China [41], France [42] and the USA [43-45]. The results reveal that the rocket triggered upward lightning has current components similar to the current component of normal upward lightning. The most important data originate from the experiments of Berger who measured the lightning currents from 1943 to 1971 at two telecommunication towers on the mountain San Salvatore, Switzerland. The top of this mountain is 915 m above sea level and 640 m above the Lake of Lugano. Both towers have a height of 70 m including the Franklin rod installed at the top. All in all, the currents of more than one thousand upward and more than 200 downward lightning discharges could be successfully recorded during this extensive measuring period. Up to now, these results are the basis for the lightning protection standard series IEC 62305 edited by the Technical committee TC 81 of IEC[19]. Nowadays lightning parameters are continuously collecting by means of lightning location systems (LLS) to determine a present lightning activity and establish a new distribution of lightning current.

### **2.3.2. Lightning current shapes**

As shown in paragraph 2.2. lightning occurrence may consist of different flashes. For any kind of flash is possible to determinate a specific lightning current, with a wave shape typical for occurrence. The knowledge of lightning current shapes consist of principals for lightning protection. This aspect is important for two reasons, as a first for risk assessment and as a second for adequate protection measure selection. The IEC 62305-1 standard defines that a lightning current consists of one or more different strokes:

- impulses with duration less than 2 ms;
- long strokes with duration longer than 2 ms.

Normalized definition of impulse current with duration less than 2ms is shown in Fig. 2.10. The peak value and front steepness of shape made of prevalent parameters. The time to half value responds to energetic aspects of discharge.

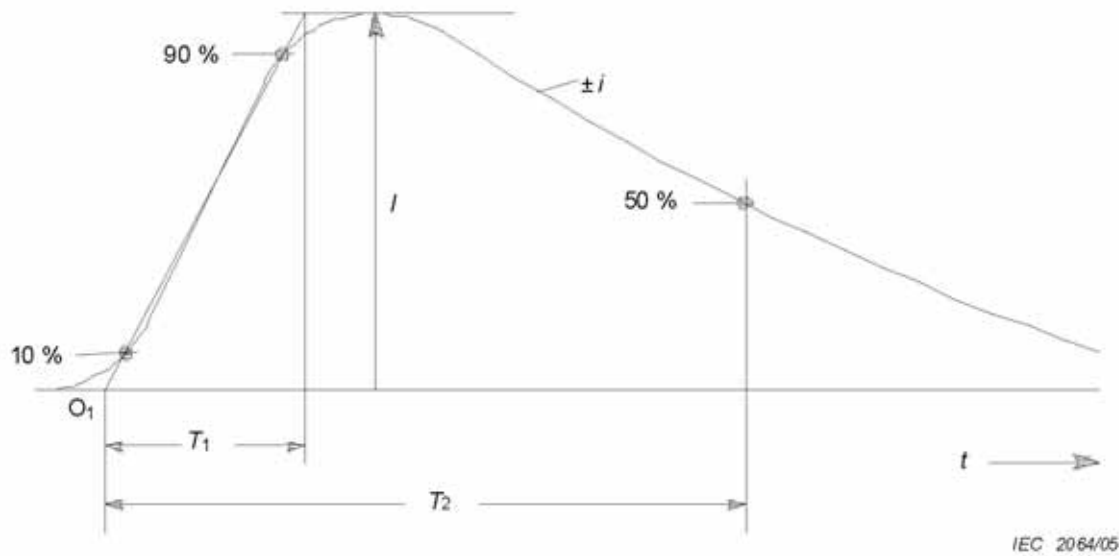


Figure 2.10. Definitions of impulse current parameters (typically  $T_2 < 2$  ms), where:  $O_1$  - virtual origin;  $I$  - peak current;  $T_1$  - front time;  $T_2$  - time to half value [17].

Normalized definition of impulse current with duration longer than 2ms is shown in Fig. 2.11. The time duration and total charge made of prevalent parameters. The front time as well as time to half value can be neglected.

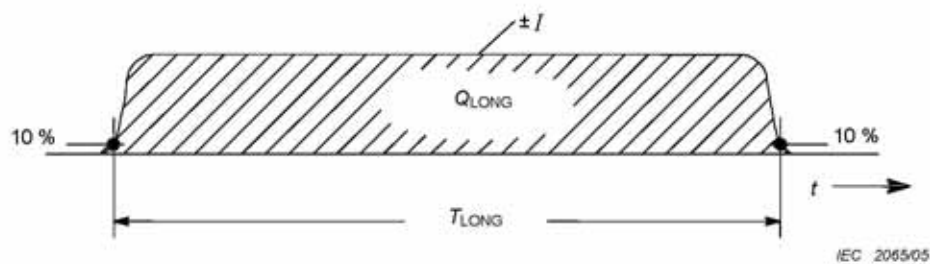


Figure 2.11. Definitions of long duration stroke parameters (typically  $2 \text{ ms} < T_{LONG} < 1 \text{ s}$ ), where:  $T_{LONG}$  - duration time;  $Q_{LONG}$  - long stroke charge [17].

For analysis purposes commonly as impulses with duration less than 2 ms three types of current wave form are used. Namely, first positive impulse with a wave form 10/350  $\mu\text{s}$ , first negative impulse with a wave form 1/200  $\mu\text{s}$  and subsequent negative impulse with a wave form 0,25/100  $\mu\text{s}$ . These forms is possible to determine by means following equation, suggested by [18]:

$$I = \frac{I_p}{k} \cdot \frac{(t/\tau_1)^{10}}{1 + (t/\tau_1)^{10}} \cdot \exp(-t/\tau_2) \quad (2.1)$$

where:

$k$  – correction factor for the peak current;

$t$  – time;

$I_p$  – peak value of the lightning current;

$\tau_1$  – front time constant;

$\tau_2$  – tail time constant.

The current shapes parameters of the first positive impulse, the first negative impulse and the subsequent negative impulses are given in Tab. 2.1.

Table 2.1. Parameters for Equation 2.1

Parameters	First positive impulse	First negative impulse	Subsequent negative impulse
$k$	0,93	0,986	0,993
$\tau_1$ ( $\mu\text{s}$ )	19	1,82	0,454
$\tau_2$ ( $\mu\text{s}$ )	485	285	143

Examples of impulses with duration less than 2 ms of lightning current shape represent Fig. 2.12 and Fig. 2.13, Fig. 2.14 and Fig. 2.15, Fig 2.16 and Fig 2.17 for first positive, first negative and subsequent negative impulse respectively.

The long stroke for analyses purposes can be described by a rectangular wave shape with an average current  $I$  and a duration  $T_{LONG}$  according to [18].

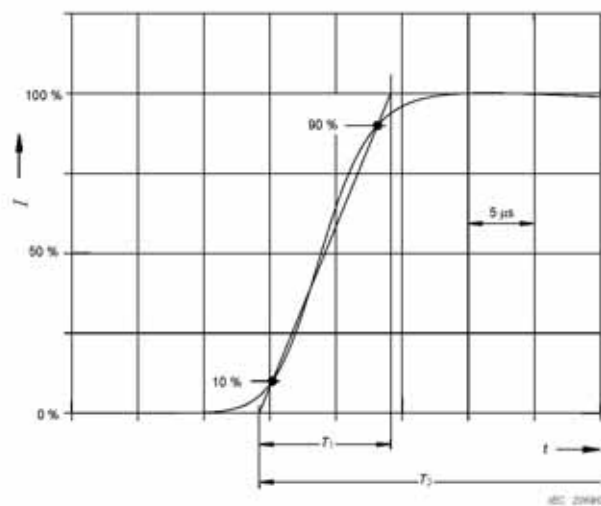


Figure 2.12. Shape of the current rise of the first positive impulse [17].

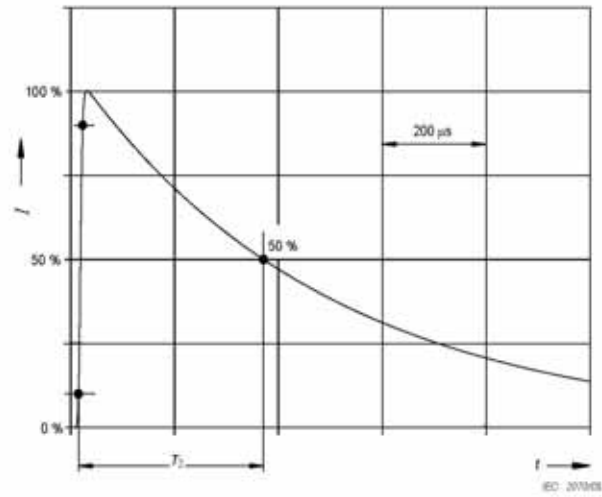


Figure 2.13. Shape of the current tail of the first positive impulse [17].

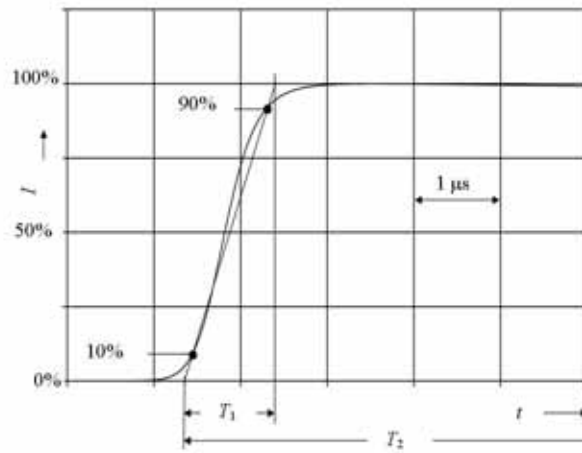


Figure 2.14. Shape of the current rise of the first negative impulse [17].

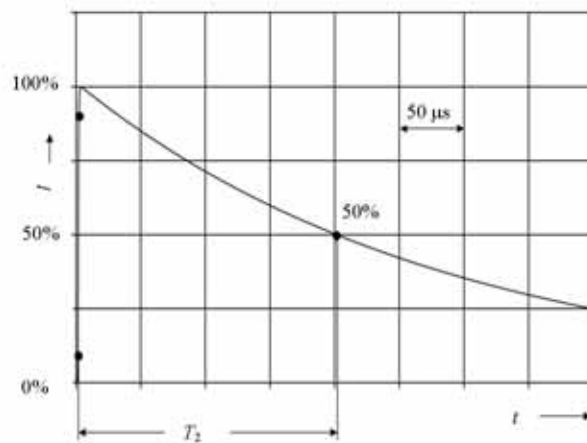


Figure 2.15. Shape of the current tail of the first negative impulse [17].

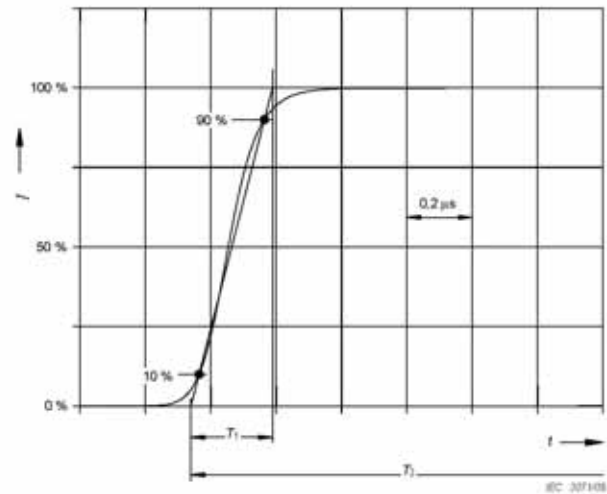


Figure 2.16. Shape of the current rise of the subsequent negative impulses [17].

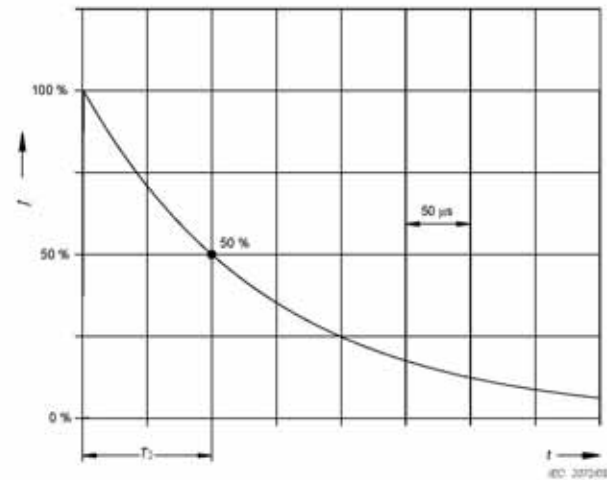


Figure 2.17. Shape of the current tail of the subsequent negative impulses [17].

### 2.3.3. Lightning current statistics

Lightning parameters were investigated from the middle of the last century and a reliable synthesis of the collected data were published within CIGRE activities [46-48]. These parameters are usually obtained from measurement taken on high objects. These data are used for the aim of lightning protection each structure according to standards IEC 62305 [17]. The tabulated values of lightning current parameters are given in Tab. 2.2. Their statistical distribution can be assumed to have a logarithmic normal distribution. The corresponding mean value  $\mu$  and the dispersion  $\sigma_{\log}$  are given in Tab 2.3.

Table 2.2. Tabulated values of lightning current parameters taken from CIGRE [47].

Parameter	Fixed values for LPL I	Values			Type of stroke	Line in Fig. 2.18
		95 %	50 %	5 %		
$I$ (kA)		4 <sup>b</sup>	20 <sup>b</sup>	90	*First negative short	1A+1B
	50	4,9	11,8	28,6	*Subsequent negative short	2
	200	4,6	35	250	First positive short (single)	3
$Q_{FLASH}$ (C)		1,3	7,5	40	Negative flash	4
	300	20	80	350	Positive flash	5
$Q_{SHORT}$ (C)		1,1	4,5	20	First negative short	6
		0,22	0,95	4	Subsequent negative short	7
	100	2	16	150	First positive short (single)	8
$W/R$ (kJ/ $\Omega$ )		6	55	550	First negative short	9
		0,55	6	52	Subsequent negative short	10
	10 000	25	650	15 000	First positive short	11
$di/dt_{max}$ (kA/ $\mu$ s)		9,1	24,3	65	*First negative short	12
		9,9	39,9	161,5	*Subsequent negative short	13
	20	0,2	2,4	32	First positive short	14
$di/dt_{30\%/90\%}$ (kA/ $\mu$ s)	200	4,1	20,1	98,5	*Subsequent negative short	15
$Q_{LONG}$ (C)	200				Long	
$T_{LONG}$ (s)	0,5				Long	
Front duration ( $\mu$ s)		1,8	5,5	18	First negative short	
		0,22	1,1	4,5	Subsequent negative short	
		3,5	22	200	First positive short (single)	
Stroke duration ( $\mu$ s)		30	75	200	First negative short	
		6,5	32	140	Subsequent negative short	
		25	230	2 000	First positive short (single)	
Time interval (ms)		7	33	150	Multiple negative strokes	
Total flash duration (ms)		0,15	13	1 100	Negative flash (all)	
		31	180	900	Negative flash (without single)	
		14	85	500	Positive flash	

a) Parameters and relevant values reported on [47]  
b) The values of  $I = 4$  kA and  $I = 20$  kA correspond to a probability of 98 % and 80 %, respectively.

Table 2.3. Logarithmic normal distribution of lightning current parameters – Mean  $\mu$  and dispersion  $\sigma_{\log}$  calculated from 95 % and 5 % values from CIGRE [18, 46-48].

Parameter	Mean $\mu$	Dispersion <sup>b</sup> $\sigma_{\log}$	Stroke type	Line in Fig. 2.18
$I$ (kA)	(61,1)	0,576	<sup>a</sup> First negative short (80 %)	1A
	33,3	0,263	<sup>a</sup> First negative short (80 %)	1B
	11,8	0,233	<sup>a</sup> Subsequent negative short	2
	33,9	0,527	First positive short (single)	3
$Q_{\text{FLASH}}$ (C)	7,21	0,452	Negative flash	4
	83,7	0,378	Positive flash	5
$Q_{\text{SHORT}}$ (C)	4,69	0,383	First negative short	6
	0,938	0,383	Subsequent negative short	7
	17,3	0,570	First positive short (single)	8
$W/R$ (kJ/ $\Omega$ )	57,4	0,596	First negative short	9
	5,35	0,600	Subsequent negative short	10
	612	0,844	First positive short	11
$di/dt_{\text{max}}$ (kA/ $\mu$ s)	24,3	0,260	<sup>a</sup> First negative short	12
	40,0	0,369	<sup>a</sup> Subsequent negative short	13
	2,53	0,670	First positive short	14
$di/dt_{30\%/90\%}$ (kA/ $\mu$ s)	20,1	0,420	<sup>a</sup> Subsequent negative short	15
$Q_{\text{LONG}}$ (C)	200		Long	
$T_{\text{LONG}}$ (s)	0,5		Long	
Front duration ( $\mu$ s)	5,69	0,304	First negative short	
	0,995	0,398	Subsequent negative short	
	26,5	0,534	First positive short (single)	
Stroke duration ( $\mu$ s)	77,5	0,250	First negative short	
	30,2	0,405	Subsequent negative short	
	224	0,578	First positive short (single)	
Time interval (ms)	32,4	0,405	Multiple negative strokes	
Total flash duration (ms)	12,8	1,175	Negative flash (all)	
	167	0,445	Negative flash (without single)	
	83,7	0,472	Positive flash	
a) Parameters and relevant values reported on [47]				
b) $\sigma_{\log} = \log(X_{1\%}) - \log(X_{50\%})$ where X is the value of parameter.				



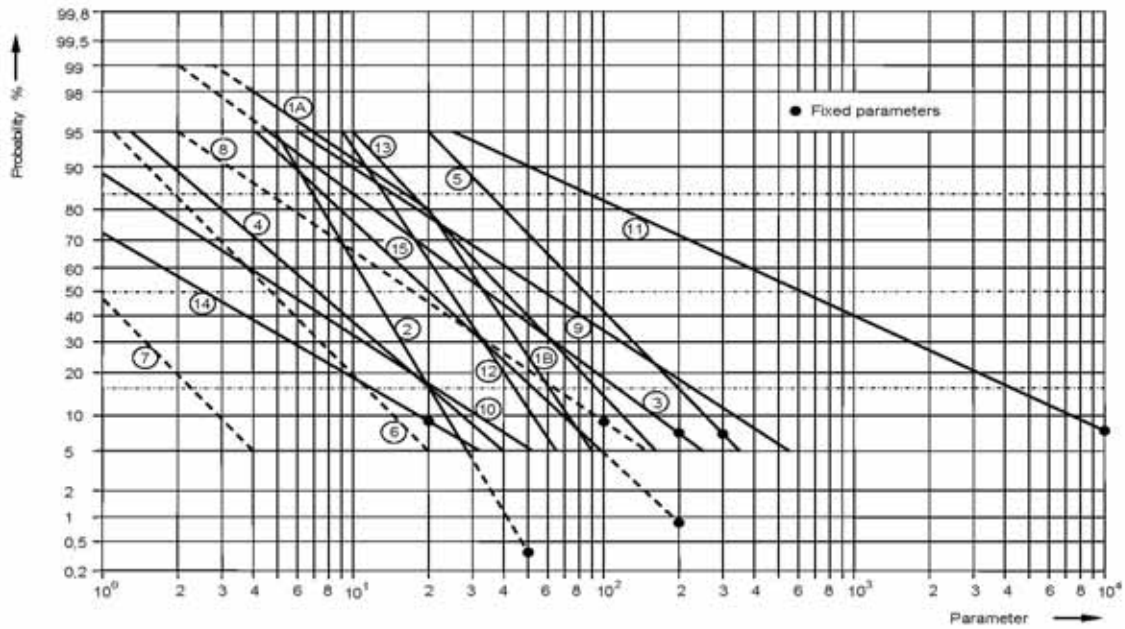


Figure 2.18. Cumulative frequency distribution of lightning current parameters (lines through 95 % and 5 % value) [18].

The value of the probability of occurrence of lightning current peak values exceeding the previously considered is shown in Fig. 2.19.

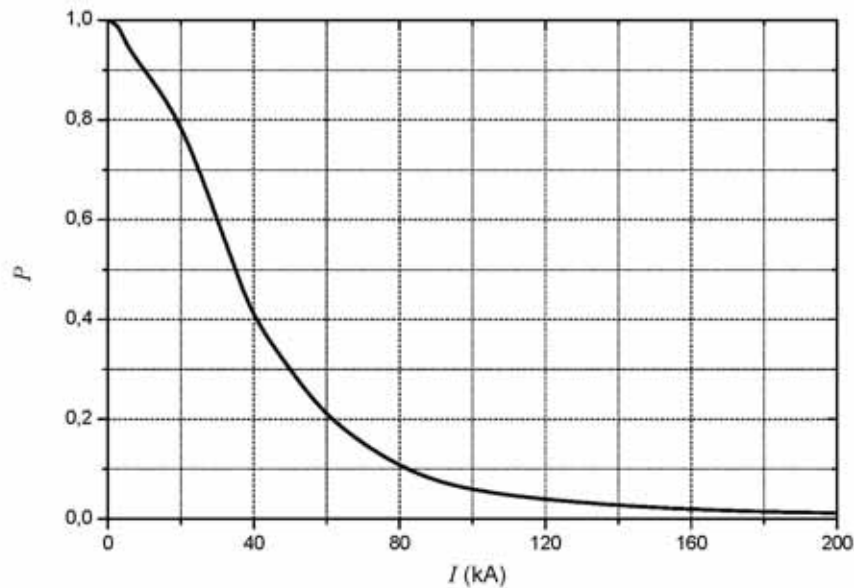


Figure 2.19. Values of the lightning current amplitude  $I$  and the relevant probability  $P$  of occurrences.

### 2.3.4. Lightning current parameter for LPL according to IEC standards

The IEC standard 62305 series propose four lightning protection levels (LPL), called LPL I, LPL II, LPL III and LPL IV. The subdivision of LPL is based on the lightning current values. This fact is strongly related with protection of structures based on the risk assessment threat [17]. The minimal and maximal values of lightning current for each level are given in Tab 2.4.

Table 2.4. Parameters of lightning current according to LPL defined by IEC standards [17].

Type of discharge	LPL							
	I		II		III		IV	
	$I_{\min}$ (kA)	$I_{\max}$ (kA)	$I_{\min}$ (kA)	$I_{\max}$ (kA)	$I_{\min}$ (kA)	$I_{\max}$ (kA)	$I_{\min}$ (kA)	$I_{\max}$ (kA)
First positive impulse	3	200	5	150	10	100	16	100
First negative impulse	3	100	5	75	10	50	16	50
Subsequent negative impulse	3	50	5	37,5	10	25	16	25

Taking into account lightning current statistics (2.3.3.) and the criterion of LPL, the following comments can be formulated respect to lightning protection issues:

- peak value of the first stroke - the lowest values of the statistical distribution of current amplitude of downward flashes are important for the choice of the number and position of the air termination system to prevent direct lightning flashes to the structure to be protected; the highest values of the statistical distribution of current amplitude are important for sizing of protection measures (electrodynamic effects, etc.);
- maximum rate of rise - the highest values of the statistical distribution are important for the dimensioning the protection measures in order to avoid inductive effects of lightning current (induced overvoltages) and dangerous sparking;
- flash duration and total charge in the flash - the highest values of the statistical distribution are important for the sizing of the air terminations system aimed at limiting the thermal effects at the impact point of the lightning flash;
- specific energy in a flash - the highest values of the statistical distribution are important for the selection of the conductor of the protective system, aimed at preventing damage due to thermal effects and for setting up a suitable earthing system in order to prevent life hazard.

In terms of lightning protection fixing the minimum lightning current parameters is also important. This parameter has an influence for the interception efficiency of an air-termination system. The geometrical boundary of areas which are protected against direct lightning flashes can be determined using the rolling sphere method. The minimum value of lightning current influences for the dimension of rolling sphere radius. Moreover following the electro-geometric model, the rolling sphere radius  $r$  (final jump distance) is correlated with the peak value of the first impulse current. The electro geometrical model [49] can be describe by means of following equation accepted by the international standard [18]:

$$r = 10 \cdot I_p^{0.65} \quad (2.2)$$

where

$r$  – rolling sphere radius (m);

$I_p$  – peak current (kA).

For a given rolling sphere radius  $r$  it can be assumed that all flashes with peak values higher than the corresponding minimum peak value  $I_p$  will be intercepted by natural or dedicated air terminations.

The lightning current parameters of LPL I for lightning protection purposes consist of severe case. The mechanical effects of lightning are related to the peak value of the current ( $I$ ), and to the specific energy ( $W/R$ ). The thermal effects are related to the specific energy ( $W/R$ ) when resistive coupling is involved and to the charge ( $Q$ ) when arcs develop to the installation. Overvoltages and dangerous sparking caused by inductive coupling are related to the average steepness ( $di/dt$ ) of the lightning current front. Each of the single parameters ( $I$ ,  $Q$ ,  $W/R$ ,  $di/dt$ ) tend to dominate each failure mechanism.

For positive impulse and long stroke the values of  $I$ ,  $Q$  and  $W/R$  related to mechanical and thermal effects are determined from positive flashes (because their 10 % values are much higher than the corresponding 1 % values of the negative flashes). From Fig. 2.18. (lines 3, 5, 8, 11 and 14) the following values with probabilities below 10 % can be taken:

$$I = 200 \text{ kA}$$

$$Q_{\text{FLASH}} = 300 \text{ C}$$

$$Q_{\text{SHORT}} = 100 \text{ C}$$

$$W/R = 10 \text{ MJ}/\Omega$$

$$di/dt = 20 \text{ kA}/\mu\text{s}$$

For a first positive impulse, these values give a first approximation for the front time:

$$T_1 = I / (di/dt) = 10 \mu\text{s} (T_1 \text{ is of minor interest})$$

For an exponentially decaying stroke, the following formulae for approximate charge and energy values apply ( $T_1 \ll T_2$ ):

$$Q_{\text{SHORT}} = (1/0,7) \times I \times T_2$$

$$W/R = (1/2) \times (1/0,7) \times I_2 \times T_2$$

These formulas, together with the values given above, lead to a first approximation for the time to half value:

$$T_2 = 350 \mu\text{s}$$

For the long stroke, its charge can be approximately calculated from:

$$Q_{\text{LONG}} = Q_{\text{FLASH}} - Q_{\text{SHORT}} = 200 \text{ C}$$

Its duration time may be estimated as:

$$T_{\text{LONG}} = 0,5 \text{ s}$$

The first negative impulse for some inductive coupling effects, leads to the highest induced voltages, e.g. for cables within cable ducts made of reinforced concrete. From Fig. 2.18. (lines 1 and 12) the following values with probabilities below 1 % can be taken:

$$I = 100 \text{ kA}$$

$$di/dt = 100 \text{ kA}/\mu\text{s}$$

For a first negative impulse these values give a first approximation for its front time of:

$$T_1 = I / (di/dt) = 1,0 \mu\text{s}$$

Its time to half value may be estimated from the stroke duration of first negative impulses:  
 $T_2 = 200 \mu\text{s}$  ( $T_2$  is of minor interest).

For subsequent impulse, the maximum value of average steepness  $di/dt$  related to the dangerous sparking caused by inductive coupling is determined from subsequent impulses of negative flashes (because their 1 % values are somewhat higher than the 1 % values from first negative strokes or the corresponding 10 % values of the positive flashes). From Fig. 2.18. (lines 2 and 15) the following values with probabilities below 1 % can be taken:

$$I = 50 \text{ kA}$$

$$di/dt = 200 \text{ kA}/\mu\text{s}$$

For a subsequent impulse these values give a first approximation for its front time of:

$$T_1 = I / (di/dt) = 0,25 \mu\text{s}$$

Its time to half value may be estimated from the stroke duration of negative subsequent impulses:

$$T_2 = 100 \mu\text{s}$$
 ( $T_2$  is of minor interest).

In Fig. 2.20 the amplitude density of the lightning current according to LPL I is shown. It is to note that the lightning current frequency can achieved range of MHz.

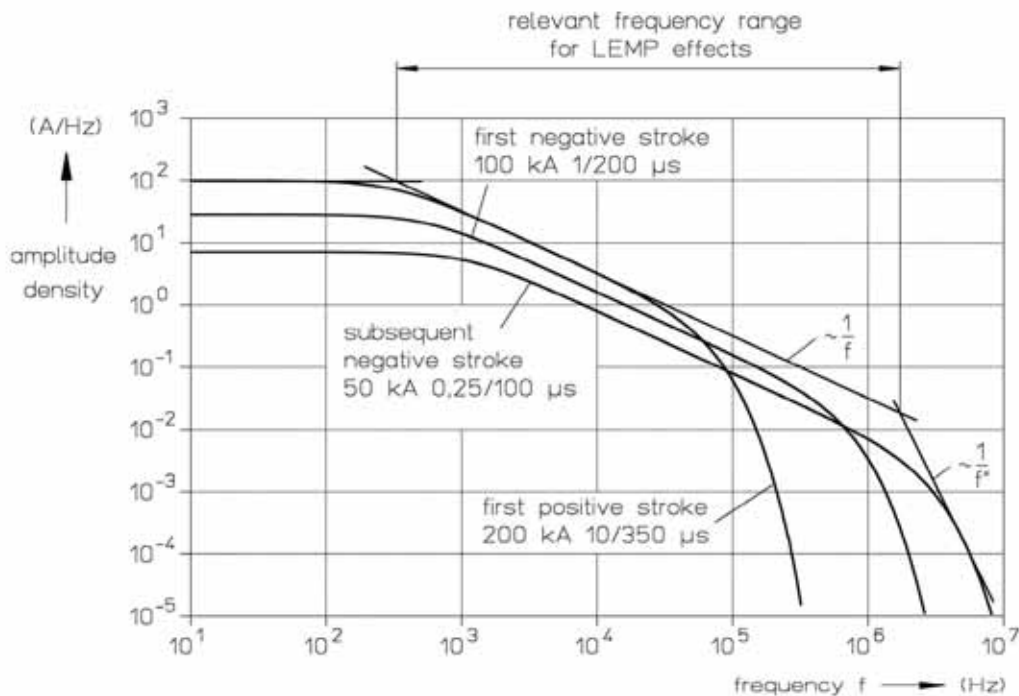


Figure 2.20. Amplitude density of the lightning current according to LPL I [17].

#### 2.4. Frequency of lightning discharges to earth

Frequency of lightning discharges can be a topic of interest diversified professional groups. Recent interest in how global lightning activity might change in the future as a result of global warming, and how the distribution and frequency of lightning activity changes from year to year as a result of the phenomena, has led to renewed interest in determining the global flash rate. Lightning frequency is used in the parameterization and validation of global chemical transport models used to understand the impacts of trace gases and the variations in the Earth's ozone are requiring increased spatial and temporal details of global lightning, an important natural source of NO<sub>x</sub> [15]. The global flash rate has an impact for Schuman resonance (SR) observations and finally frequency of lightning discharges has a place in field of protection against lightning. Unanimously lightning frequency is key aspects of the climatology. Its value include regional differences, land/ocean variability, and zonal and meridional decomposition. The time of observation has also an influence for its value. In global scale the thunder day statistics determined by human observers and compiled by the World Meteorological Organization (WMO) is one of the best sources of proxy information concerning lightning activity worldwide [15]. Nowadays in regional European scale the thunder day statistics obtain by means of EUCLID network is also reliably information, confirmed by several studies [50].

To utilize information on the occurrence of lightning flashes, a value which describes the number of events per unit area and time. i.e. the density, is needed. Ideally, to obtain this for each type of flash, an arbitrary area should be agreed on and a record of the occurrence in the area of each type kept for a statistically useful period. Convenient units are  $\text{km}^{-2} \text{s}^{-1}$  or  $\text{km}^{-2} \text{yr}^{-1}$ . For regional studies, the area is assumed to be of the order of  $1,000 \text{ km}^2$ .

Reports of extreme values of observed flashing rates during severe thunderstorms are difficult to assess as the circumstances are seldom stated, e.g. Israel (1973) gives 1,000 flashes in 15 minutes and Lane (1966) states that in Pretoria 360 flashes occurred in 3 minutes, and for about an hour 100 flashes per minute were recorded. Shackford (1960) reported a maximum of 1,800 flashes per hour for storms in New England (U.S.A.) within 1 mile of the observer. Presumably a number of cells were active simultaneously and all types of flash were counted. Thomas (1955) reported from the Persian Gulf that on one evening the lightning was so frequent and intense as to appear as one continuous, vivid light. There appears to be little information on the possible relationship between the types of thunderstorm and the incidence of the different types of flash. From temperate climate studies, Holzer (1953) states that the proportion of ground flashes is higher for frontal than for air mass thunderstorms. He also noted that intra-cloud flashes became relatively more frequent than ground flashes in the latter stages of the life of the cell. Blcivins and Marwitz (1968) found that the proportion of ground flashes to total flashes decreased as the total flashing rate increased. Thus the proportion varied from 90% at 0 to 10 flashes per minute to 9% at over 70 per minute. A five-year study in a subtropical climate (Prentice, 1960), in which lightning-caused faults to an electricity distribution system (1,000 km route length) were recorded, showed that frontal and trough thunderstorms together caused about three times the number of faults attributed to air mass thunderstorms [13].



Global estimates of lightning incidence are few but the following are some examples. Brooks (1925) has given 200 flashes per hour as the most probable mean value for a severe thunderstorm in the temperate zone or for an intermediate thunderstorm in the tropical zone. Later work, reported by Israel (1973), gives an estimate of approximately 60 ground flashes per hour. Brooks (1925) also estimated that about 100 flashes per second occur over the earth's surface. Kolokolov (1971) gave a similar value, 117, noting that 69% were cloud flashes and 31% ground flashes. Loch (1972), from narrow-sector of direction-tinder studies states that, for the centre of European U.S.S.R., the mean flashing rate (all types) may be taken as  $0.25 \text{ km}^{-2} \text{ h}^{-1}$  [13].

The internationally accepted parameter of lightning incidence is the thunder-day (i.e. a calendar day on which thunder is heard at a station), denoted by  $T_d$ . The established method of summarizing thunderday data is the isokeraunic map, and from such a map the areas of differing levels of thunderstorm incidence are obvious. The map may be global or regional. Generally speaking, the highest incidence is near the equator and the lowest near the poles. Maps based on thunderdays per month also show the change in seasonal incidence, typically a maximum in the local summer and a minimum in the winter. In the equatorial zone, the variation in incidence is less than elsewhere and there may be two peaks in the annual variation.

An example of annualized distribution of total lightning activity is shown in Fig. 2.21 [15].

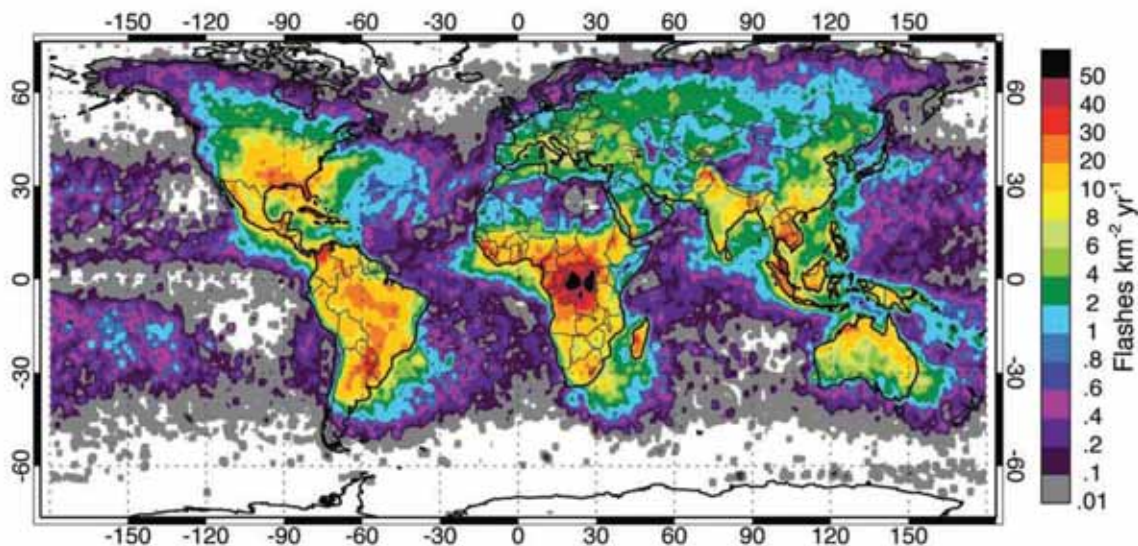


Figure 2.21. The annualized distribution of total lightning activity (in units of flashes  $\text{km}^{-2} \text{ yr}^{-1}$ ) [15].

The time of observation influences significant for registered values, what is shown in Fig. 2.22 [15].

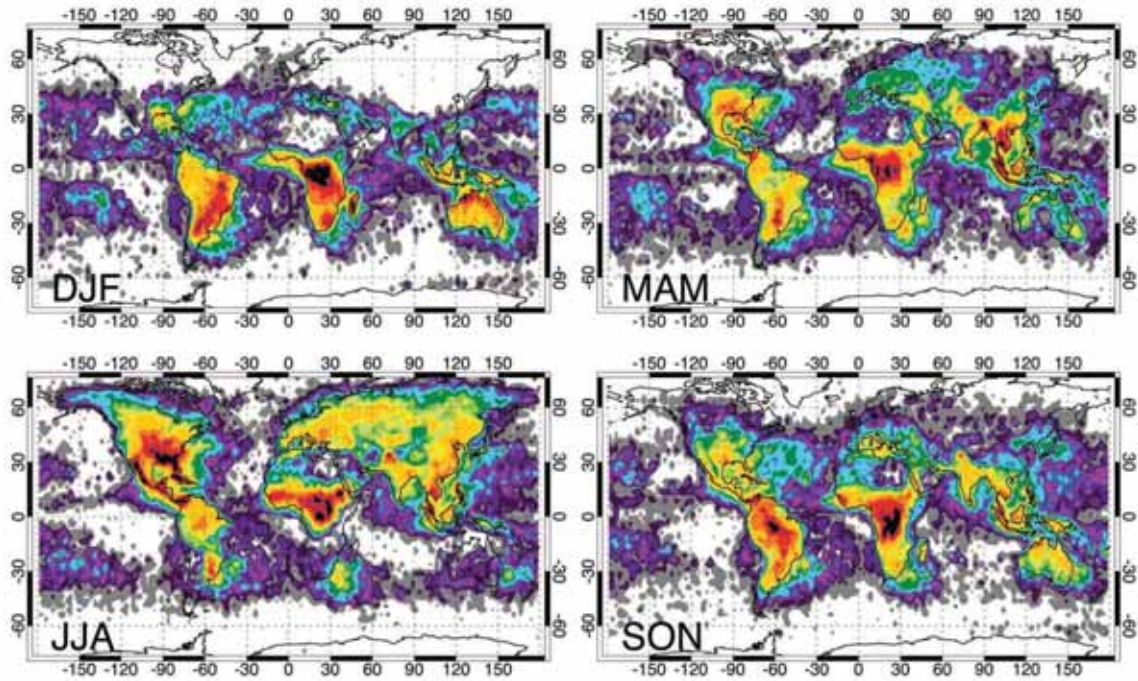


Figure 2.22. The seasonal distribution of lightning activity (annualized in units of flashes  $\text{km}^{-2} \text{yr}^{-1}$ ). The contour levels are identical to those of Fig. 2.21. (a) December, January, and February. (b) March, April, and May. (c) June, July, and August. (d) September, October, and November [15].

The lightning ground flash density  $N_g$  is the number of lightning flashes per  $\text{km}^2$  per year. This value is available from ground flash location networks in many areas of the world, but no common rule exists giving requirements neither for their performances nor for the elaboration of the measured data. In order to make reliable and homogeneous the values obtained from lightning location systems in various countries using such systems, an international standard is needed.

According to the IEC standard [17] if a map of  $N_g$  is not available, in temperate regions it may be estimated by:

$$N_g \approx 0,1 \cdot T_d \quad (2.3)$$



## 2.5. Lightning location and warning systems

### 2.5.1. Measurements techniques

The development of lightning location systems (LLS) has been driven by both basic scientific interest and by a variety of applications and practical needs. The requirements for applications come in many forms, including new value-producing capabilities, improvements in quality/reliability of the information, and loss reduction. Locating lightning is a complex task and involves numerous distinct areas as lightning physics, propagation of transient electromagnetic fields over finitely conducting ground, applied sensor technology, local site conditions of each sensor, applied location method, parameterization of location algorithm and finally the reliability of communication between sensor and central analyser [14]. An example of block representation of simplified LLS is shown in Fig. 2.23.

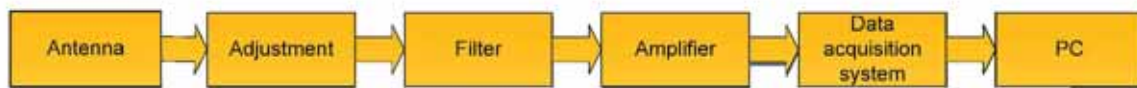


Figure 2.23. Block representation of the measurement system.

Presently lightning occurrences are mapped by means of different LLS ground systems [14, 45, 51, 52]. The accuracy of measurement is verified by means of fast cameras [53] or from space [54]. Generally all LLS sensors are exposed to electric and magnetic field signals from various discharge types during thunderstorm activity. Although the fields produced by return strokes in flashes are by far the largest VLF/LF lightning signal, other components of in-cloud and intra-cloud flashes are also detected in this frequency range, especially from sensors nearby the storm. It is a complex task to correctly identify and classify each lightning emitted electromagnetic pulse. Sensors are frequently reporting different waveform parameters as a result of signal attenuation when propagating over ground of finite conductivity (Fig. 2.24.).

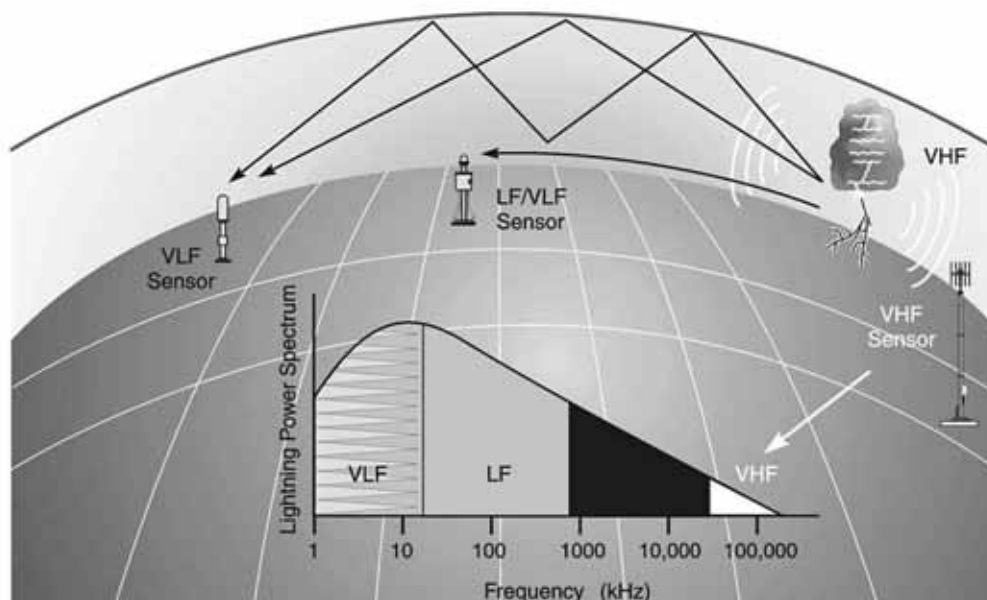


Figure 2.24. Illustration of lightning locating techniques and operating frequencies [54].



Most LLS utilize the VLF/LF band from  $\sim 1$  kHz to several 100 KHz, whereby dominant emission comes from  $\sim 10$  KHz (wave length  $\sim 30$  km). As long as ranges shorter than  $\sim 600$  km are relevant, the detected signals represent ground waves that propagate with distance,  $D$ , according to  $\sim 1/D$ . They are quite indifferent to obstacles, and follow the curvature of the Earth. Receivers use simple rods or loops as antenna for the electric or magnetic field of the lightning pulse. The electric field delivers the stroke amplitude and its polarity; detection of only the magnetic flux yields the polarity only after the stroke location has been determined in the network. Depending on the noise level and system thresholds relatively small signals can be detected, but stroke locating succeeds only when the signal arrives at a sufficient number of sensors. Thus, the network efficiency depends also on the baseline of the receivers. Stroke locating can be achieved with direction finding (DF), time of arrival (TOA), or a combination of both technique.

DF operates at VLF/LF and first time used in 1920. For lightning discharges the initial field peak of the radiated magnetic (and electric) field occurs at a time, when the upward propagating return stroke has reached a height of a few hundred meters. DF systems determine the direction just at the time of initial peak field incidence from signals measured by crossed loop antennas. Hence the resulting direction vector points as closely as possible to the location where the lightning stroke attached to ground. Sampling of the electric field is also required at this time to determine the stroke polarity.

In a typical network three or more sensors report a discharge and an optimization which minimizes the angle disagreement between the reporting sensors can be employed as shown in Fig. 2.25.

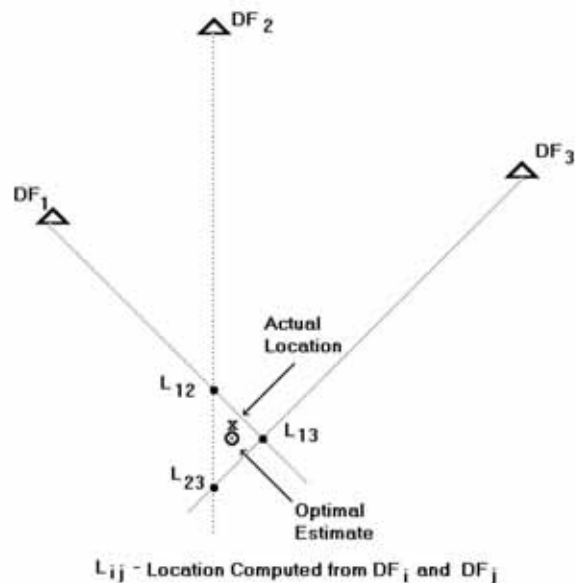


Figure 2.25. Optimal location algorithm for direction finding [55].

Proper location of lightning with DF sensors requires implementation of the so called site error correction in the location algorithm. Local sensor site conditions (nearby objects, metal fences, buried cables or other conducting installations) are causing a more or less significant change in the direction of field incidence, which can be up to  $10^\circ$  or even more for a poor sensor site. It is possible to determine these systematic site errors for each DF sensor site from

historical data in form of a correction function  $\Delta\phi = f(\phi)$  and consider these correction in the location algorithm. An example of such a typically two-sinusoidal site error function is shown in Fig. 2.26.

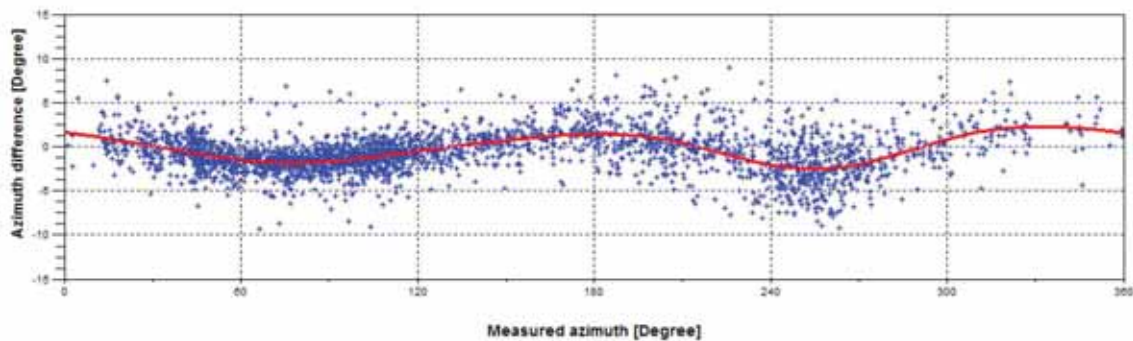


Figure 2.26. Typical site error function of a DF sensor. (+) Error values determined from historical data, solid line represents n-harmonic fit to the point data and is used as error correction function in the location algorithm [55].

TOA operates at VHF and first time used in 1970. This techniques measure the arrival time of a lightning electromagnetic pulse at the detector as accurate as possible. Since the travel times from the lightning source to the employed detectors depend on the respective distance, the measured arrival times will differ characteristically. Least-squares procedures, standard in high-precision data analysis, allow determining the lightning source point such that the differences between measured and recalculated travel times are minimized. A constant difference in the arrival time at two stations defines a hyperbola, and multiple stations provide multiple hyperbolas whose intersections define the source location (Fig. 2.27).

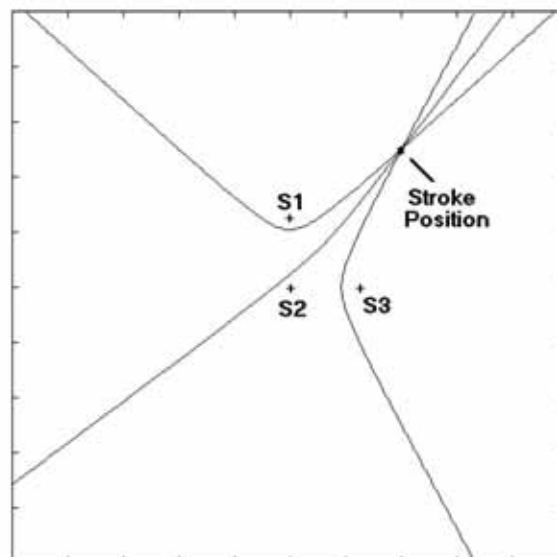


Figure 2.27. Hyperbolic intersection method for locating lightning using three sensors [55].

Locating lightning by TOA method requires precise synchronization of the sensors, which is available from GPS satellite signals today, and a minimum of three sensors reporting a

stroke. Under some geometrical conditions, curves produced from only three sensors will result in two intersections, leading to an ambiguous location as shown in Fig. 2.28.

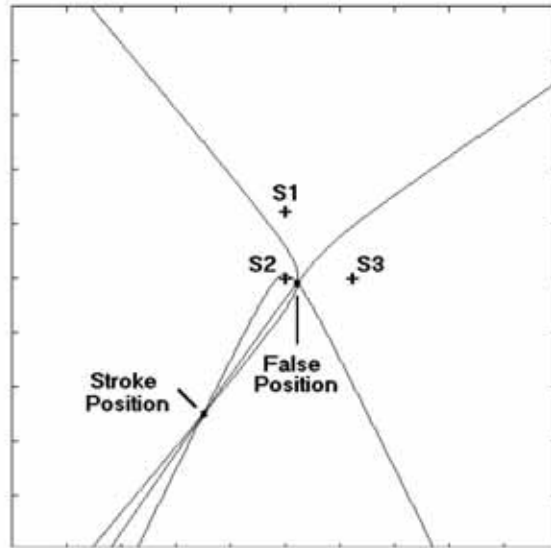


Figure 2.28. Example of an ambiguous location for a three sensor hyperbolic intersection [55].

Each of sensors measures time of detection. Difference between stroke time and the moment, when sensor detects LEMP of discharge is equal to time, that is needed for wave to travel from stroke location  $P_0(x_0, y_0)$  to the sensor (Fig 2.29).

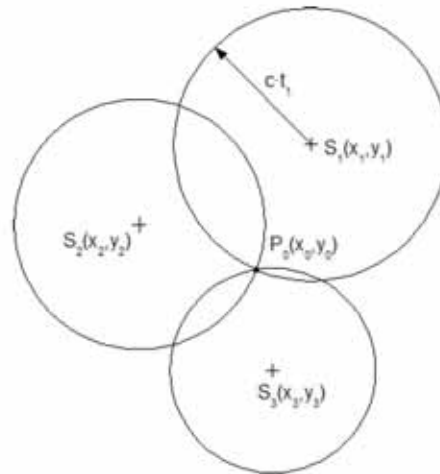


Figure 2.29. Theoretical aspect of lightning occurrence localization with the help of three TOA sensors [56].

Considering three-sensor network, the following three equations for determining stroke time  $t_0$  in point  $P_0(x_0, y_0)$  can be presented:

$$t_0 = t_1 - \frac{\sqrt{(x_1 - x_0)^2 + (y_1 - y_0)^2}}{c} \quad (2.4)$$

$$t_0 = t_2 - \frac{\sqrt{(x_2 - x_0)^2 + (y_2 - y_0)^2}}{c} \quad (2.5)$$

$$t_0 = t_3 - \frac{\sqrt{(x_3 - x_0)^2 + (y_3 - y_0)^2}}{c} \quad (2.6)$$

Solution of this equation system is quadratic equation, what results two solutions shown in Fig. 2.30.

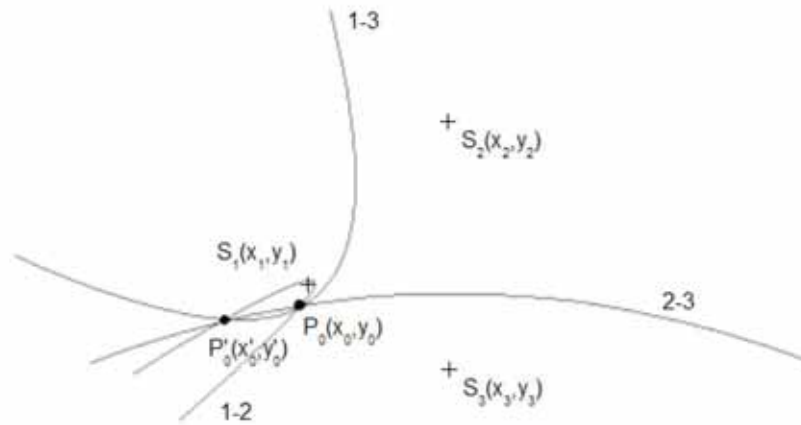


Figure 2.30, Ambiguous solution of three-hyperbola system [56].

Presented problem of location is generally avoided if four sensors are required to locate a discharge. For this reason, advanced LLS employ both a sufficient number of sensors and sophisticated analysis software. In principle, four non-redundant reports suffice for a 2D-location. Determination of 3D-locations and redundancy of solutions suggest the use of more than four sensors.

Combined Direction Finding and Time-of-Arrival (DF + TOA) method combining both techniques and referred to as IMPACT (IMProved Accuracy using Combined Technology) method was introduced by Global Atmospheric in the early 1990's. In this approach, direction finding provides azimuth information and absolute arrival time provides range information. The combined DF + TOA method has redundant information which allows an optimized estimate of the three unknown parameters - latitude, longitude, and discharge time, even when only two sensors provide both timing and angle information. Both techniques have some advantages and disadvantages over each other. These (dis-)advantages regard base line, level of detail and cover of lightning type and one or both techniques can be chosen depending on the application it will serve. Combining both techniques is a powerful way to gain performance in detecting lightning-discharges.

Independently of technique used, LLS characteristic determines:

- detection efficiency;
- location accuracy;
- detection capacity;
- detection range;
- susceptibility to disturbances.

Detection efficiency is fundamental parameter to describe LLS and determine its usefulness. Since a flash can consist of several strokes, detection of a flash is already achieved with the detection of at least one of the strokes or of other discharge components. Generally,



strong strokes are detected with high efficiency close to 100%, whereas the detection efficiency decreases to zero when the strokes become weaker. The lower limit varies greatly in different LLS; mostly, range-normalized stroke currents are efficiently detected above some 10 kA, although it turned out that the most frequent stroke currents are usually found below 10 kA.

### **2.5.2. EUCLID network**

Meteorological services utilize lightning data for many different purposes, dominantly in the context of national duties, public services, and international commitments.

Real-time lightning data is observed by forecasters and may be overlaid with radar and satellite images (cloud images, brightness temperature) in order to produce nowcasting information and to check the necessity for issuing warning in specific areas for the public, protection services, and many industrial branches. A first lightning signal is considered as a serious indication for a situation having the potential for an upcoming storm. As regards early recognition of severe weather conditions it is generally accepted that, among others, the event rate of efficiently measured cloud lightning represents a useful indicator. Automated warning tools in pre-defined regions benefit from LLS that provide accurate stroke positions and reliable border areas of storm cells, with a minimum of false reports.

In aviation it is a vital objective to provide reliable storm information for extended, mostly supra-regional areas to airlines and pilots so that carriers can adjust flight paths in time to avoid dangerous thunderstorm clouds with lightning, hail and strong wind gusts. At present, lightning data is provided mostly for self-briefing by the specific user groups. Onboard lightning detection is widely used, but neither compulsory nor sufficiently accurate; for this reason, a number of projects are under way with the aim of transferring advanced meteorological data with the inclusion of lightning parameters into the cockpits, and to arrive at equal information levels on the ground and in the air.

Basic numerical weather prediction with the aim of storm warning, nowcasting and forecasting use lightning data and combinations with other meteorological data sources. Numerous advanced tools are under development, often with co-operations of scientific institutions and involvement of educational programs. Analysis of lightning occurrence as a function of time, and for different areas is part of studies in climatology.

Among the practical applications of lightning data are expert's reports on the probability that lightning was the cause for some ground damage, mostly in connection with insurance cases.

For these reasons, European Cooperation for Lightning Detection (EUCLID) is established. EUCLID is a collaboration among national lightning detecting networks with the aim to identify and detect lightning all over the European area. The countries involved are Germany, Austria, Hungary, Czech Republic, Slovenia, Holland, Belgium, Luxembourg, Italy, Poland, Slovakia, Norway, Finland, Denmark, Sweden, France, Croatia and Serbia (see Fig. 2.31).

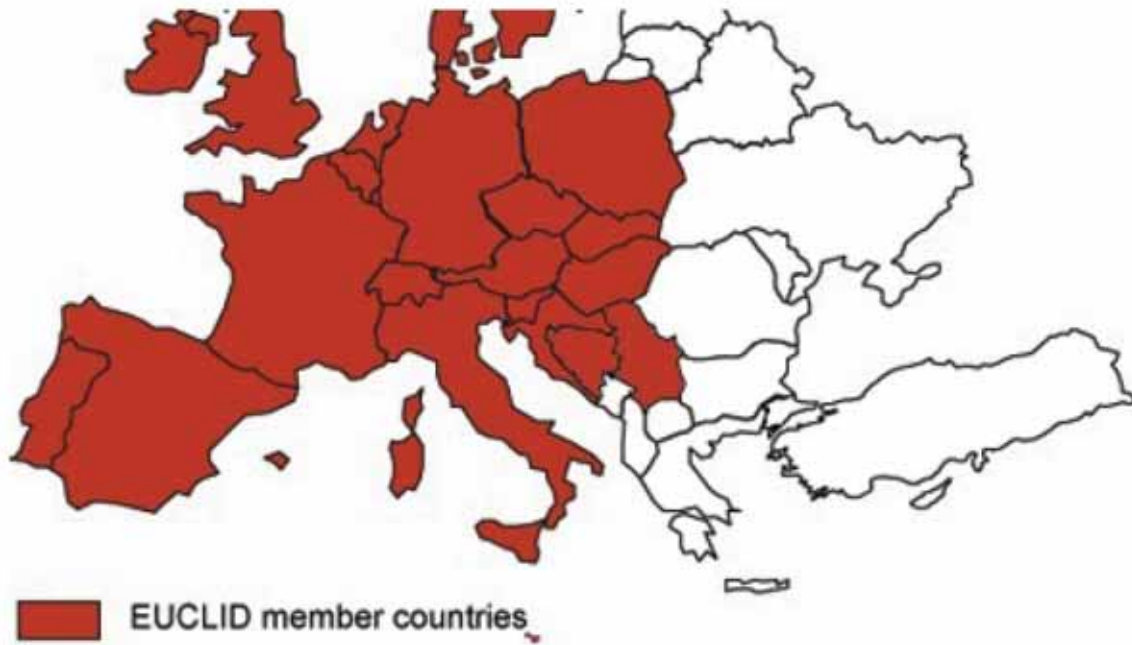


Figure 2.31. Members of the EUCLID Network [56].

At the moment the complete network consists of about 140 sensors, in these 19 countries, contributing to the detection of lightning. The position of sensors is shown in Fig. 2.32.

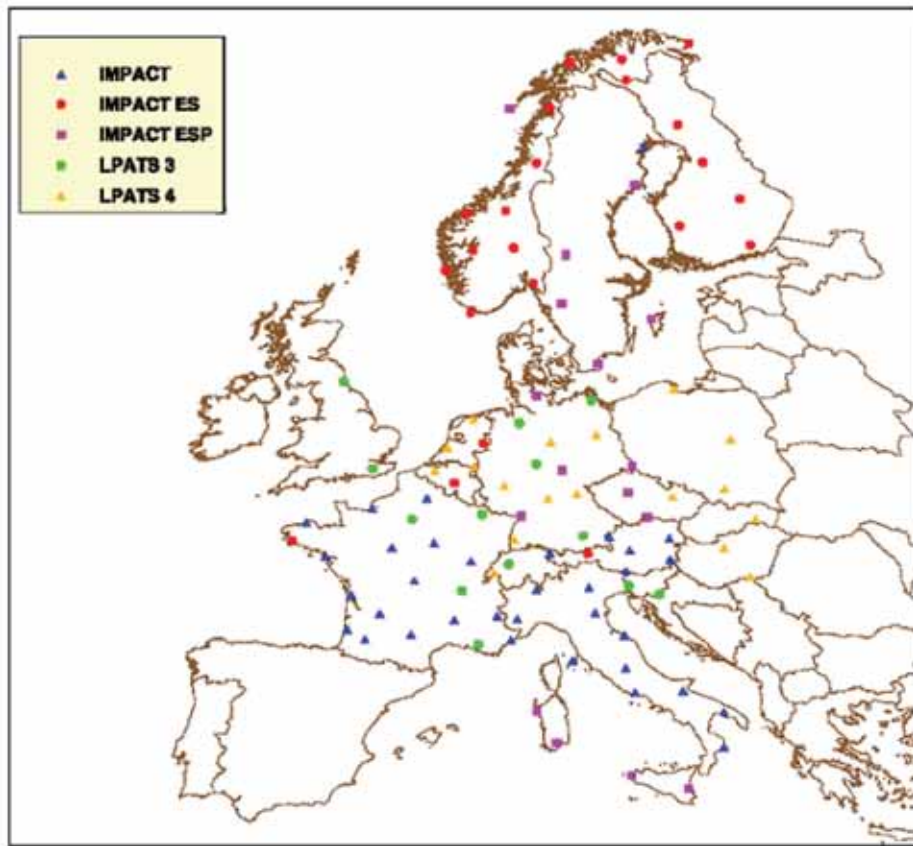


Figure 2.32. Sensors position of the EUCLID Network [56].



All the lightning data is detected by means of electromagnetic sensors, which send raw data to a central analyser. The technology involved is provided by Vaisala [57]. Each sensor detects the electromagnetic signal emitted by the lightning return stroke. This technology uses GPS Satellite signals for time information. For each lightning stroke the main parameters are recorded, namely the time of event, the impact point (Latitude and longitude), the current intensity and polarity, and the number of subsequent strokes. The data of all the sensors throughout the network are concentrated in real-time in two Euclid central operational centres. They are computed there immediately to calculate the lightning locations and optimise the data quality. The resulting data are sent in the course of processing to the Euclid service operational centre. This leads to a complete picture of lightning activity in real time. An example of real time data is shown in Fig. 2.33. All lightning data collected is archived as well for post-storm analysis. The Euclid network provides lightning data for Europe with homogenous quality in terms of detection efficiency and location accuracy. Individual participating networks receive real-time access to the complete Euclid data and use this data to serve clients for national lightning data. Each network retains its national independence and provides lightning data for individual user applications in their own country as well. The core operational applications for EUCLID include meteorology, hydrology, electric power utilities, communications, insurance, forestry, defence and aviation. It is the objective of Euclid to benefit the members by interconnecting national lightning detection networks, existing in various countries in Europe, to establish a united network covering the greater part of the European continent on a cooperation basis.

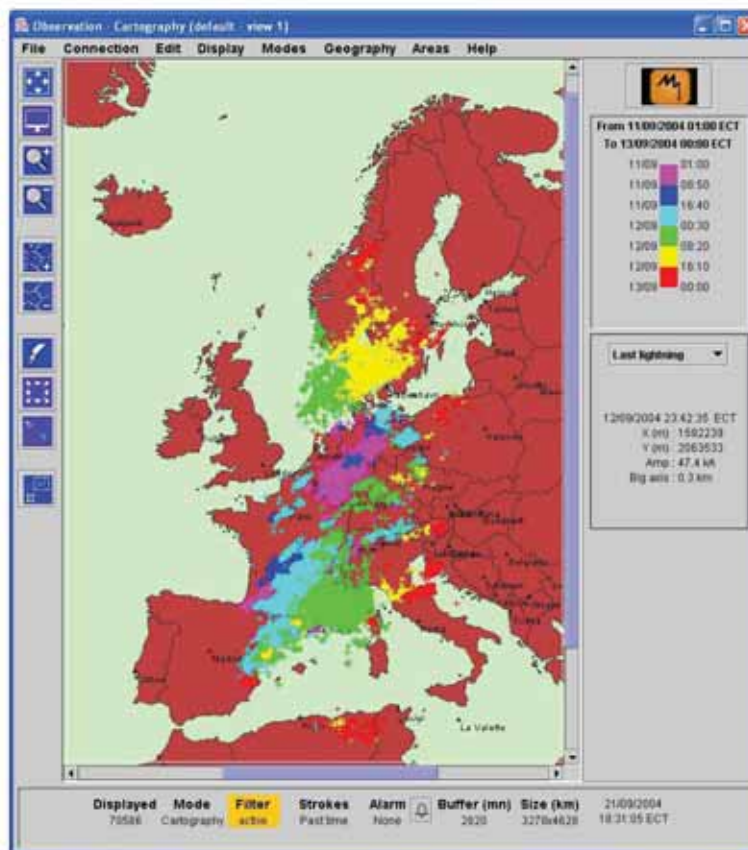


Figure 2.33. Example of lightning thunderstorm over Europe in real time [56].

EUCLID as lightning location network archives all the lightning information into a database and can suit any customers need with off line data and can as well provide any kind of post process information, like evaluate the mean number of flashes to ground or to tell how many lightning strokes hit in a particular area at a particular time. Statistical maps and tailored-studies can be provided, based on the European wide lightning database.

According to the annualized distribution of total lightning activity shown in Fig. 2.21, high values of lightning flash density include the Mediterranean region. This region is covered by EUCLID network by means of Sistema Italiano Rilevamento Fulmini (SIRF) belongs to Centro Elettrotecnico Sperimentale Italiano (CESI).

The Italian lightning detection network is formed by 16 sensors positioned on the Italian territory [58]. Some sensors located nearby the Italian border, in Austria, France and Switzerland, are as well used to enhance the network sensitivity. The sensors localisation is shown in Fig. 2.34. All the sensors are of IMPACT (Global Atmospheric Inc.) technology, that is broadband electromagnetic antennas, with GPS synchronization, TOA and DF calculation methods. They detect the electromagnetic field emitted by any cloud-ground lightning, providing raw data (EM field vector, time, etc.). Each sensor is able to discriminate a lightning signal from the background noise.



Figure 2.34. SIRF Network [59].

The sensors, located in Italy and abroad, send the raw data to the SIRF Operating Center, through dedicated telecommunication lines. Each sensor is linked to the operating center, located in Milan at the CESI headquarter, through a dedicated ISDN line. Any of these lines transmit the raw data to the SIRF central Router and send commands from the operating center to the sensor, in case of remote controls or operations. The Router as well sends the raw data both to the central analyser and to the backup analyser. Once calculated, the



lightning data are sent to the SIRF Central Database via the SIRF internal network. Data coming from each sensor are received and elaborated by the central analyser, which calculate, in a few seconds, the impact geographic coordinates, the time of impact and the electric parameters of each lightning event (current amplitude, polarity, number of strokes).

Calculated data are thus ready to be sent to customers or to be saved into the central database. From this database all the information can be extracted at any time and in any format (statistics, maps, tables, ASCII file, and so on). Examples of lightning activity detection over Italy are shown in Fig. 2.35 and Fig. 2.36.



Figure 2.35. Example of lightning thunderstorm over Italy in real time [59].

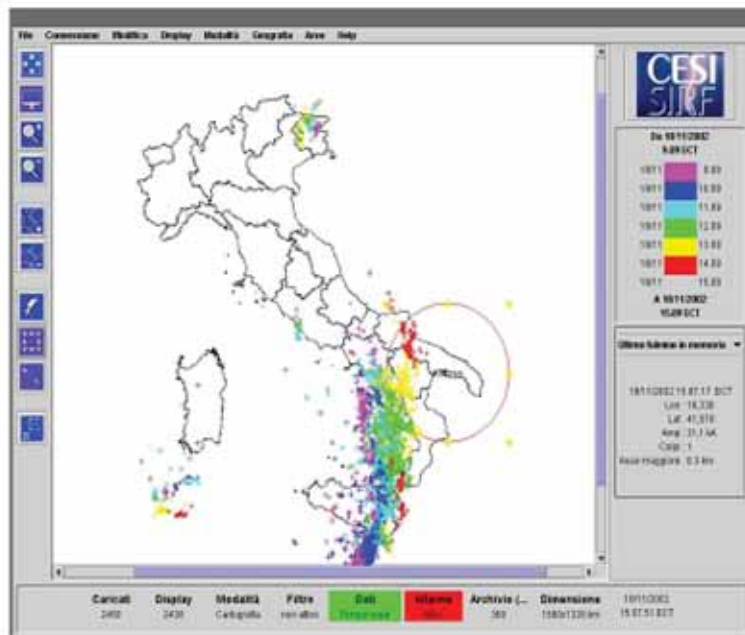


Figure 2.36. Example of lightning activity over Italy [59].

### 2.5.3. Thunderstorm warning systems

Thunderstorm Warning Systems (TWS) provides information in real-time on atmospheric electrical activity in order to monitor for preventive means [60].

This information can be particularly helpful in following field of application:

- people in open areas: maintenance people, labour, sports or other open-air activities, competitions, crowded events, agricultural activities, farms and fisheries;
- wind farms, larger solar power systems, power lines, etc.;
- occupational health and safety prevention;
- safeguarding sensitive equipment: computer systems, electric or electronic systems, emergency systems, alarms and safety;
- prevention of losses in operations and industrial processes;
- prevention of serious accidents involving dangerous (e.g. flammable, radioactive, toxic, and explosive) substances;
- prevention in specified environments or activities with special danger of electrostatic discharges (e.g. space and flight vehicle operations);
- operations in which the continuity of the basic services needs to be guaranteed (e.g. telecommunications, the generation, transport and distribution of energy, sanitary services and emergency services);
- infrastructures: ports, airports, railroads, motorways and cableways;
- civil defence of the environment: forest fires, landslide and floods;
- managing traffic (e.g. airplanes.) or wide networks (e.g. power lines, telecommunication lines) may also benefit from having early detection of thunderstorms.

The European Standard EN 50536 provides information on the characteristics of thunderstorm warning systems and information for the evaluation of the usefulness of lightning real time data and/or storm electrification data in order to implement lightning hazard preventive measures. This standard defines the basic parameters related to thunderstorms and to TWS as well as how to use these parameters for preventive actions [60].

In general terms, TWS are useful to control, prevent or reduce loss of life, damages to goods, services or properties (with the associated economic losses) and environmental hazard.

Risk management for the application of TWS has to consider a wide range of situations. In general terms, a TWS attempts to reduce risks due to dangerous events by means of anticipating temporary preventive measures allowing reducing the exposure time to the threat and/or cutting off lines conducting surges into the structure. More specifically a TWS is not able to substitute or replace a lightning protection system and protection against lightning associated surges addressed in IEC 62305.

TWS provide real-time information on atmospheric electrical activity, thus the statistical data referred to thunderstorms might have no direct relation with the evaluation of the prevention advisability. So, the advisability of implementing lightning safeguard procedures in a certain area depends on the characteristics of the activity performed, the public zones exposed to thunderstorms, its human presence and the possibility of taking effective preventive actions as a consequence of the information provided by the TWS.

In particular, risks calculated according to IEC 62305-2 can be reduced by the use of TWS as follows [60]:

Risk  $R_1$  can be reduced by either stopping a process or transferring people to a safe shelter or avoiding dangerous activity. It is also possible to disconnect external services and use only local generators for example. This may apply to a complete structure, to a zone or to a particular service.

Risk  $R_2$  can be reduced by use of a TWS if the production of the service to the public can still be offered while a specific procedure is followed. But, by nature, all the external services need to be operational for providing the service. As such, power, telecom and gas services cannot use TWS to reduce the risk. Only services provided at distance (for example TV and radio) can have their risk reduced by storm detectors. The TWS can be used to move from external power supply to a power generator inside the structure but all other lines, generally cannot be disconnected. As the storm detector has a Failure To Warn Ratio, the lines need to be considered but risk related to some of them (mainly power lines) can be reduced.

Risk  $R_3$  can be reduced by disconnecting external services and using only local generators even if TWS cannot avoid lightning striking an historical or national heritage building. This is similar to above.

Risk  $R_4$  can in general benefit from using a TWS.

The risk components affected by the use of TWS and the amount of their reduction should be evaluated by the lightning protection designer according to the fixed plan of action of the protection measures to be undertaken in coordination with TWS.



## 2.6. Summary

In the present chapter selected aspects concerning lightning phenomena are reported. Survey is started with description of thunderstorm occurrences. Meteorological point of view is given, as well as some principal physical aspects are described. A natural lightning flash is a complex phenomenon composed of successive events, also called flash components, with different physical features, namely discharge type and propagation, radio frequency radiation type, current values, and time duration.

Lightning discharge are classified. A special focus is dedicated to lightning discharges to earth. Principal mechanism of lightning occurrences are specified taking into account four fundamental cases, namely: downward negative discharge, upward positive discharge, downward positive discharge, upward negative discharge.

The classification given is focused on protection issues defined by means of international standards of lightning protection. The possible components of lightning current for downward and upward flashes are reported. Moreover some examples of lightning current are presented, namely current of a multiple stroke negative downward lightning, and current of negative upward lightning.

The lightning currents and related parameter issues are examined. The overview cross the historical aspects of knowledge of some fundamental lightning parameters e.g. peak value. The present state of art is also presented. Lightning current subdivision is described and respectively wave shape forms are shown. Furthermore actual data of lightning current probabilistic distribution are reported.

The lightning protection level (LPL) concept referring to IEC standard is discussed. The subdivision of LPL is based on the lightning current values. This fact is strongly related with structures protection based on the risk assessment threat. The maximal values of lightning current for four lightning protection level are given. The influence of lightning current features on structure protection issues is discussed.

Selected aspects of frequency of lightning discharges to earth are reported. The definition of lightning ground flash density is given. Examples of lightning flash density maps are also given.

Special focus is dedicate to lightning location systems (LLS) with aim to present current state of technologies relevant to the lightning phenomena. The measurements technique concept is presented. Available, common used techniques, namely DF, TOA and DF+TOA are reported. The features determining LLS are presented. An example of lightning location network based on the European Cooperation for Lightning Detection (EUCLID) is given. Some details on Sistema Italiano Rilevamento Fulmini (SIRF), managed by Centro Elettrotecnico Sperimentale Italiano (CESI), covering Mediterranean region are shown. Moreover some aspects of thunderstorm warning systems are given.

# **Chapter 3**

### 3. Classification and characteristics of critical occurrences: damage source determination

#### 3.1. Critical occurrences determination

Current of a lightning discharges related to a structure can result in damage to the structure itself and to its occupants and contents, including failure of apparatus and especially of electrical and electronic systems. The damages and failures may also extend to the surroundings of the structure and may even involve the local environment e.g. fire spread. The scale of danger extension depends on the characteristics of structure and on the characteristics of lightning flash which is corresponding to location of structure. Effects of lightning on a structure include, construction, function, occupants and contents, entering installations, measures to limit consequential effects of damages, scale of the extension of danger. The correctly determination of damage source is crucial to a civil structure safety, as well as critical structure e.g. Nuclear Power Plant [17, 61-64].

Unambiguous the source of damage is the lightning current. The causes of damage depend from the position of the stricken point in relation to the structure. The following situations can be distinguished [17]:

- flashes to the structure, this occurrence in the international standards is called: source of damage S1;
- flashes near the structure, this occurrence in the international standards is called: source of damage S2;
- flashes to the services connected to the structure, this occurrence in the international standards is called: source of damage S3;
- flashes near the services connected to the structure, this occurrence in the international standards is called: source of damage S4.

The dangerous occurrences related to the structure are presented in Fig. 3.1.

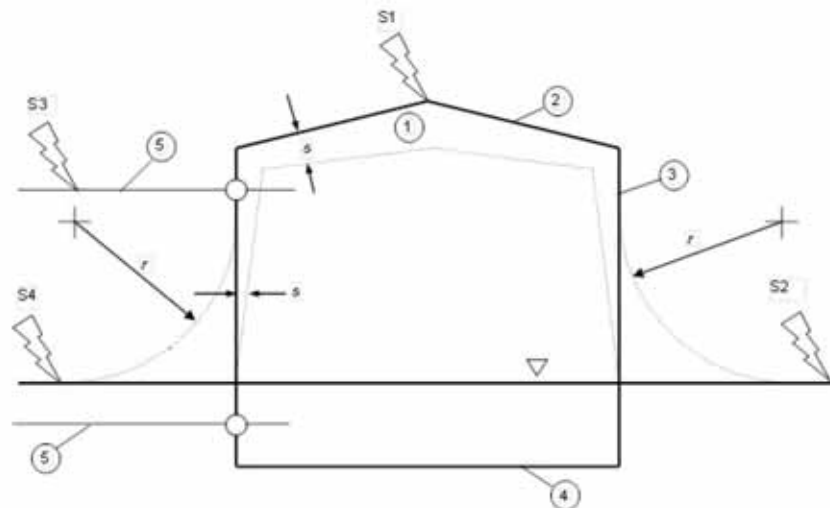


Figure 3.1. Dangerous occurrences related to the structure: 1 - structure; 2 - air termination system; 3 - down conductor system; 4 - earth termination system; 5 - incoming lines; S1 - flash to the structure; S2 - flash near to the structure; S3 - flash to a service connected to the structure; S4 - flash near a service connected to the structure;  $r$  - rolling sphere radius;  $s$  - separation distance against dangerous sparking or too high magnetic field;  $\nabla$  - ground level. [18]

Effects of lightning on various types of structures are reported in Tab. 3.1.

Table 3.1. Effects of lightning on typical structures [17].

Type of structure according to function and/or contents	Effects of lightning
Dwelling-house	Puncture of electrical installations, fire and material damage Damage normally limited to objects exposed to the point of strike or to the lightning current path Failure of electrical and electronic equipment and systems installed (e.g. TV sets, computers, modems, telephones, etc.)
Farm building	Primary risk of fire and hazardous step voltages as well as material damage Secondary risk due to loss of electric power, and life hazard to livestock due to failure of electronic control of ventilation and food supply systems, etc
Theatre, Hotel, School Department store Sports area	Damage to the electrical installations (e.g. electric lighting) likely to cause panic Failure of fire alarms resulting in delayed fire fighting measures
Bank Insurance company Commercial company, etc.	As above, plus problems resulting from loss of communication, failure of computers and loss of data
Hospital Nursing home Prison	As above, plus problems of people in intensive care, and the difficulties of rescuing immobile people
Industry	Additional effects depending on the contents of factories, ranging from minor to unacceptable damage and loss of production
Museums and archeological sites Church	Loss of irreplaceable cultural heritage
Telecommunications Power plants	Unacceptable loss of services to the public
Firework factory Munition works	Consequences of fire and explosion to the plant and its surroundings
Chemical plant Refinery Nuclear plant Biochemical laboratories and plants	Fire and malfunction of the plant with detrimental consequences to the local and global environment

The source of damage S1 can cause: immediate mechanical damage, fire and/or explosion due to the lightning channel itself, or its current (over-heated conductors) and its charge (melted metal); fire and/or explosion initiated by sparks caused by overvoltages resulting from resistive and inductive coupling; injuries to people by step and touch voltages resulting

from resistive and inductive coupling; failure or malfunction of electrical and electronic systems due to the flowing of part of the lightning currents and to overvoltages resulting from resistive and inductive coupling (LEMP).

The source of damage S2 can cause failures or malfunction of electrical and electronic systems due to overvoltages resulting from LEMP.

The source of damage S3 (mains, telecommunication and data lines) or other services can cause: fire and/or explosion triggered by sparks due to overvoltages appearing on external power lines entering the structure; injuries to people due to overcurrents and to overvoltages appearing on external lines connected to the structure; failures or malfunction of electrical and electronic systems due to overvoltages appearing on external lines connected to the structure.

The source of damage S4 can cause: failures or malfunction of electrical and electronic systems due to LEMP in external lines connected to the structure.

The services from the lightning protection point of view are special treated. Lightning affecting a service can cause damage to the physical means itself (line or pipe) used to provide the service, as well as to connected electrical and electronic equipment. The scale of this extension depends on the characteristics of the service, on the type and extension of the electrical and electronic systems and on the characteristics of the lightning flash. Effects of lightning on a service include, construction (line: overhead, underground, screened, unscreened, fibre optic; pipe: above ground, buried, metallic, plastic), function (telecommunication line, power line, pipeline), structure supplied (construction, contents, dimensions, location), existing or provided protection measures (e.g. shielding wire, SPD, route redundancy, fluid storage systems, generating sets, uninterruptible power systems).

The following situations shall be taken into account, depending on the position of the point of strike relative to the service considered:

- flashes to the supplied structure (S1);
- flashes to the service connected to the structure (S3);
- flashes near the service connected to the structure (S4).

In Tab. 3.2. effects of lightning flashes on typical services are reported.

Table 3.2. Effects of lightning on typical services [17].

Type of service	Effects of lightning
Telecommunication line	Mechanical damage to line, melting of screens and conductors, breakdown of insulation of cable and equipment leading to a primary failure with immediate loss of service Secondary failures on the optical fibre cables with damage of the cable but without loss of service
Power lines	Damages to insulators of low voltage overhead line, puncturing of insulation of cable line, breakdown of insulation of line equipment and of transformers, with consequential loss of service
Water pipes	Damages to electrical and electronic control equipment likely to cause loss of service
Gas pipes Fuel pipes	Puncturing of non-metallic flange gaskets likely to cause fire and/or explosion Damage to electrical and electronic control equipment likely to cause loss of service



Flashes to the supplied structure can cause: melting of metallic wires and of cable screens due to parts of the lightning current flowing into the services (resulting from resistive heating); breakdown of insulation of lines and of the connected equipment (due to the resistive coupling); puncturing of non-metallic gaskets in flanges of pipes, as well as gaskets in insulating joints.

Flashes to a service connected to the structure can cause: immediate mechanical damage of metallic wires or piping due to electrodynamic stress or heating effects caused by lightning current (breaking and/or melting of metallic wires, screens or piping), and due to the heat of the lightning plasma arc itself (puncturing of plastic protective cover); immediate electrical damage of lines (breakdown of insulation) and of connected equipment; puncturing of thin overhead metallic pipes and of non-metallic gaskets in flanges, where consequences may extend to fire and explosion depending on the nature of conveyed fluids.

Flashes near a service connected to the structure can cause: breakdown of insulation of lines and of the connected equipment due to inductive coupling (induced overvoltages).

To add up, the lightning current appearance can result in different dangerous effects. Their character depends strictly on the strike position as well as on the structure features.

Thermal effects linked with lightning current are relevant to the resistive heating caused by the circulation of an electric current flowing through the resistance of a conductor or into an lightning protection system (LPS). Thermal effects are also relevant to the heat generated in the root of the arcs at the attachment point and in all the isolated parts of an LPS involved in arc development (e.g. spark gaps). Resistive heating takes place in any component of an LPS carrying a significant part of the lightning current. The instantaneous power dissipated as heat in a conductor due to an electrical current is expressed as:

$$P(t) = i^2 \cdot R \quad (3.1)$$

The thermal energy generated by the complete lightning pulse is therefore the ohmic resistance of the lightning path through the LPS component considered, multiplied by the specific energy of the pulse. This thermal energy is expressed in units of Joules (J) or Watt-seconds (W·s).

$$W = R \cdot \int i^2 \cdot dt \quad (3.2)$$

In a lightning discharge, the high specific energy phases of the lightning flash are too short in duration for any heat generated in the structure to be dispersed significantly. The phenomenon is therefore to be considered adiabatic. The temperature of the conductors of the LPS can be evaluated as follows:

$$\theta - \theta_0 = \frac{1}{\alpha} \left( \exp \left( \frac{\frac{W}{R} \cdot \alpha \cdot \rho_0}{q^2 \cdot \gamma \cdot c_w} \right) - 1 \right) \quad (3.3)$$

where:

$\theta - \theta_0$  - temperature rise of the conductors (K);

$\alpha$  - temperature coefficient of the resistance (1/K);

$W/R$  - specific energy of the current impulse (J/ $\Omega$ );

$\rho_0$  - specific ohmic resistance of the conductor at ambient temperature ( $\Omega\text{m}$ );

$q$  - cross-sectional area of the conductor ( $\text{m}^2$ );

$\gamma$  - material density ( $\text{kg}/\text{m}^3$ );

$c_w$  - thermal capacity (J/kgK).

Mechanical effects caused by the lightning current depend on the amplitude and the duration of the current as well as on the elastic characteristics of the affected mechanical structure. Mechanical effects also depend on the friction forces acting between parts of the LPS in contact with one another, where relevant. Magnetic forces occur between two current-carrying conductors or, if only one current-carrying conductor exists, where it forms a corner or a loop. When a current flows through a circuit, the amplitude of the electrodynamic forces developed at the various positions of the circuit depend on both the amplitude of the lightning current and the geometrical configuration of the circuit. The mechanical effect of these forces, however, depends not only on their amplitude but also on the general form of the current, its duration, as well as on the geometrical configuration of the installation. Electrodynamic forces developed by a current,  $i$ , flowing in a conductor having long parallel sections of length  $l$  and distance  $d$  (long and small loop), as shown in Fig. 3.2, can be approximately calculated using the following equation:

$$F(t) = \frac{\mu_0}{2\pi} i^2(t) \frac{l}{d} \quad (3.4)$$

where:

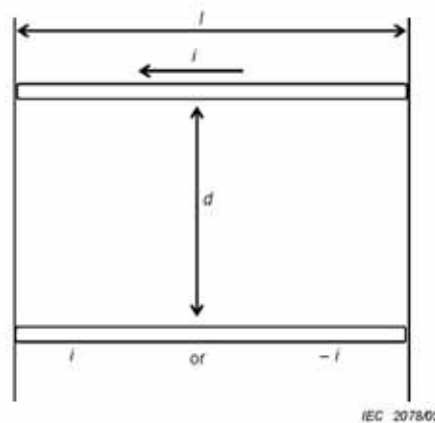
$F(t)$  - electrodynamic force (N);

$i$  - current (A);

$\mu_0$  - magnetic permeability of free space (vacuum) ( $4\pi \times 10^{-7}$  H/m);

$l$  - length of conductors (m);

$d$  - distance between the straight parallel sections of the conductor (m).



IEC 207805

Figure 3.2. General arrangement of two conductors for the calculation of electrodynamic force [17].

In practice, both thermal and mechanical effects occur simultaneously. If the heating of the material of the components (rods, clamps, etc.) is sufficient to soften the materials, much greater damage can occur than otherwise. In extreme cases, the conductor could explosively fuse and cause considerable damage to the surrounding structure. If the cross-section of the metal is sufficient to safely handle the overall action, only mechanical integrity need be checked.

Sparking is generally important only in flammable environments or in the presence of combustible materials. Two different types of sparking can occur, i.e. thermal sparking and voltage sparking. Thermal sparking occurs when a very high current is forced to cross a joint between two conducting materials. Most thermal sparking occur near the edges inside a joint if the interface pressure is too low; this is due primarily to high current density and inadequate interface pressure. The intensity of the thermal sparking is linked to the specific energy and therefore, the most critical phase of the lightning is the first return stroke. Voltage sparking occurs where the current is forced to take convoluted paths, e.g. inside a joint, if the voltage induced in such a loop exceeds the breakdown voltage between the metal parts. The induced voltage is proportional to the self-inductance multiplied by the steepness of the lightning current. The most critical lightning component for voltage sparking is therefore the subsequent negative stroke.

Finally the lightning current causes of transient overvoltages. This value strictly determine the apparatus operation safety which are connected to the endanger structure. Overvoltages due to direct lightning strikes can take two forms. As the first, when lightning strikes a lightning conductor or the roof of a building which is earthed, the lightning current is dissipated into the ground. The impedance of the ground and the current flowing through it create large difference of potential what results overvoltages. These overvoltages then propagate throughout the services in a structure e.g. supply lines, what can result apparatus failures. As the second form when lightning strikes an overhead low voltage line, the latter conducts high currents which penetrate into the structure creating large overvoltages. The damage caused by this type of overvoltage is usually spectacular (e.g. fire in the electrical switchboard causing the destruction of buildings and apparatus) and results even in explosions. The overvoltages previously mentioned are also found when lightning strikes in the near a structure, due to the increase in potential of the ground at the point of impact. The electromagnetic fields created by the lightning current generate inductive and capacitive coupling, leading to other overvoltages. Within a radius up to several kilometres, the electromagnetic field caused by lightning in clouds can also create sudden increases in voltage. Although less spectacular than in the previous case, irreparable damage is also caused to so called sensitive equipment such as fax machines, computer power supplies and safety and communication systems.

Overvoltages can be describe be means of wave threat. The strong relation between electrical and electromagnetic filed exist. The electrical field change results in appearance of electromagnetic field which results electrical field appearance. The energy exchanges between these two fields proceed with a high value of frequency, often this value is higher respect to the nominal system frequency.

The basic relation of electromagnetic field, spot well strictly relation between electrical and magnetic component in a macroscopic point of view can be represent by means of following Maxwell equations:

$$\text{rot } \vec{H} - \gamma \vec{E} + \varepsilon \frac{\partial \vec{E}}{\partial t} = \vec{J} + \frac{\partial \vec{D}}{\partial t} \quad (3.5)$$

$$\text{rot } \vec{E} = -\mu \frac{\partial \vec{H}}{\partial t} = -\frac{\partial \vec{B}}{\partial t} \quad (3.6)$$

where:

$\vec{H}$  – vector of magnetic field intensity;

$\vec{E}$  – vector of electrical field intensity;

$\vec{D}$  – vector of electrical induction;

$\vec{J}$  – vector of current density;

$\vec{B}$  – vector of magnetic induction;

$\varepsilon$  – absolut value of electrical permeability;

$\mu$  – absolut value of magnetic permeability;

$\gamma$  – environment conductivity.

In Fig. 3.3. character of lightning overvoltages with respect to the all types of possible electrical disturbance is shown.

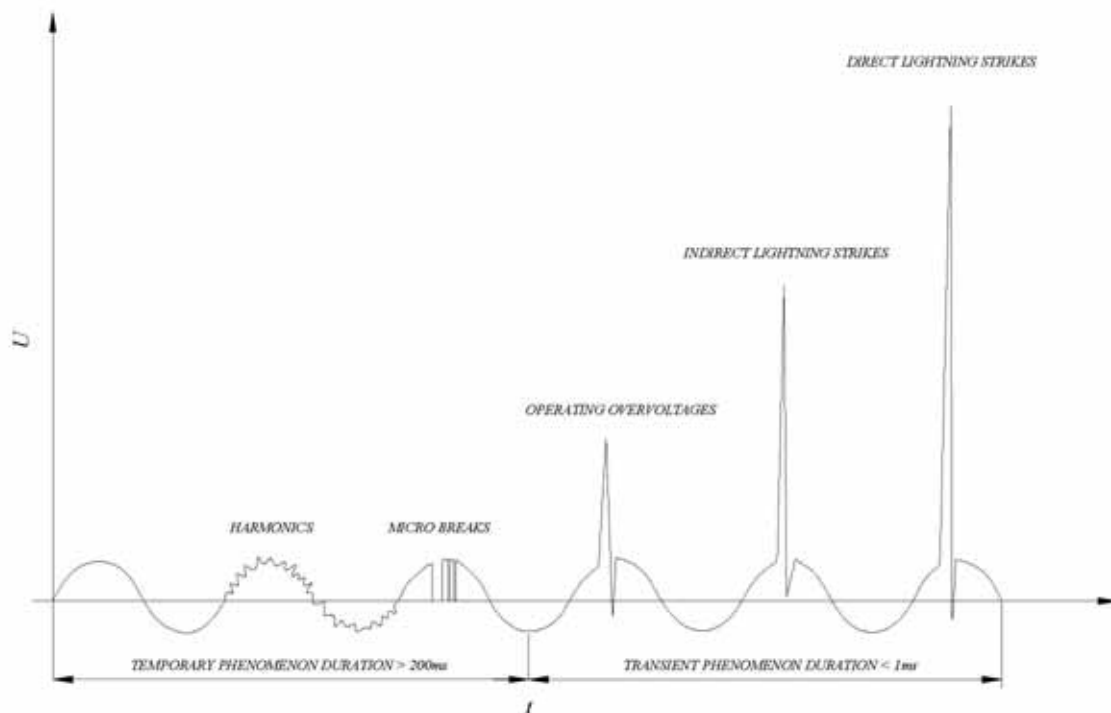





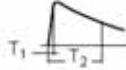
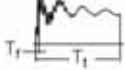
Figure 3.3. Representation of the various disturbances on electrical networks.

Overvoltages may occur:

- between different phases or circuits, they are said to be differential mode;
- between live conductors and the frame or earth, they are said to be common mode.

Tab. 3.3. represents classification of lightning overvoltages according to the IEC 71 standard [65].

Table 3.3. Representative overvoltage shapes and tests considered by IEC 71.

Overvoltage class	Low frequency		Transient		
	Permanent	Temporary	Slow front	Fast front	Very fast front
Shape					
Shape range	$f = 50 \text{ or } 60 \text{ Hz}$ $T_1 \geq 3,600 \text{ s}$	$10 < f < 500 \text{ Hz}$ $3,600 \geq T_1 \geq 0,03 \text{ s}$	$5,000 > T_p > 20 \mu\text{s}$ $20 \text{ ms} \geq T_2$	$20 > T_1 > 0,1 \mu\text{s}$ $300 \mu\text{s} \geq T_2$	$100 > T_f > 3 \text{ ns}$ $0,3 < f_1 < 100 \text{ MHz}$ $30 < f_2 < 300 \text{ kHz}$ $3 \text{ ms} \geq T_i$
Standardised shape	$f = 50 \text{ or } 60 \text{ Hz}$ $T_1 (*)$	$48 \leq f \leq 62 \text{ Hz}$ $T_1 = 60 \text{ s}$	$T_p = 250 \mu\text{s}$ $T_2 = 2,500 \mu\text{s}$	$T_1 = 1,2 \mu\text{s}$ $T_2 = 50 \mu\text{s}$	(*)
Standardised withstand test	(*)	Short duration power frequency test	Switching impulse test	Lightning impulse test	(*)
Note: (*) – to be specified by the relevant product committee					



## 3.2. Flashes to the structure: source of damage S1

### 3.2.1. Prevailing parameters determination and calculation

The lightning current in case of a direct stroke to a structure results overvoltages due to resistive and inductive coupling [18, 66, 67]. These two types overvoltages can be danger for electrical and electronic apparatus installed within the structure.

Fig. 3.4. represents a case, where the lightning strikes the external air termination system consist of one mast. Moreover it is assumed, that the whole lightning current is flowing to the earthing system, without any losses.

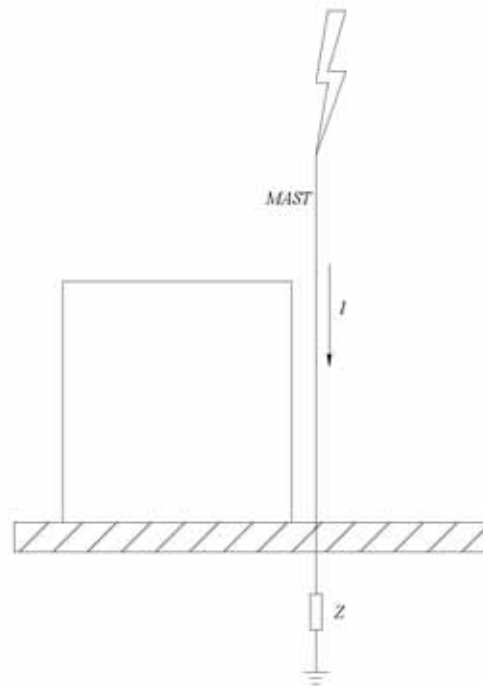


Figure 3.4. Schematic representation of damage source S1.

In this basic example overvoltages due to resistive coupling can be calculated as follows:

$$U_R = Z \cdot I \quad (3.7)$$

where:

$Z$  – conventional earthing impedance of the earth-termination system;

$I$  – lightning current.

The maximal value of overvoltage depends on the peak value of lightning current as well as on the impedance value.

In practice, the situations are much more complex due to develop a number of air termination system, external systems, and so on. In these cases the current division threat should be applied. An example of current distribution is shown in Fig. 3.5.

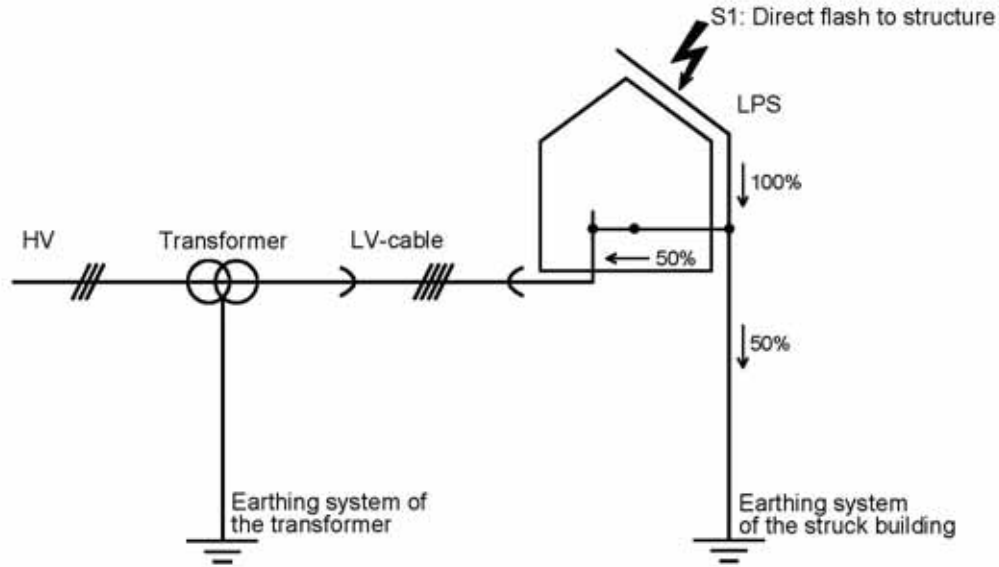


Figure 3.5. Basic example of balanced current distribution.

In present situation when impedance of earthing system of the transformer is equal of impedance of earthing system of the struck building, the IEC standards [17, 18] suggest the lightning current division consist of 50% and 50% when the LPS of structure is connected to the earthing system and external services.

The lightning current ( $I_g$ ) flowing to the earthing system, in case of different values of impedance or different number of conductors can be calculated by means of following general formula:

$$I_g = \frac{Z_e}{n_1 Z + Z_e} I \quad (3.8)$$

$Z_e$  – conventional earthing impedance of the external parts or lines;  
 $n_1$  – number of services.

The lightning current ( $I_s$ ) flowing to the service, in case of different values of impedance or different number of conductors can be calculated as follows:

$$I_s = \frac{Z}{n_1 Z + Z_e} I \quad (3.9)$$

The IEC standards [17, 18] for simplification introduce the current sharing factor  $k_e$  and then equations (3.4) and (3.5) can be derive as follows:

$$I_g = k_e \cdot I \quad (3.10)$$

$$I_s = k_e \cdot I \quad (3.11)$$

The value of  $k_c$  factor similarly takes into account:

- the number of parallel paths;
- their conventional earthing impedance for underground parts, or their earth resistance, where overhead parts connect to underground, for overhead parts;
- the conventional earthing impedance of the earth-termination system.

The values of conventional earthing impedance of a buried conductor under impulse condition 10/350  $\mu$ s are reported in Tab. 3.4.

Table 3.4. Conventional earthing impedance values  $Z$  and  $Z_1$  according to the resistivity of the soil [17].

$\rho$ $\Omega\text{m}$	$Z_1^a$ $\Omega$	Conventional earthing impedance related to the type of LPS <sup>b</sup>		
		$Z \Omega$		
		I	II	III – IV
$\leq 100$	8	4	4	4
200	11	6	6	6
500	16	10	10	10
1 000	22	10	15	20
2 000	28	10	15	40
3 000	35	10	15	60

<sup>a</sup> Values referred to external parts length over 100 m. For length of external parts lower than 100 m in high resistivity soil ( $> 500 \Omega\text{m}$ ) values of  $Z_1$  could be doubled.

<sup>b</sup> Earthing system complying with 5.4 of IEC 62305-3:2010.

In practice the amplitude and shape of lightning current flowing in power line ( $I_s$ ) depend on:

- cable length, this effect can influence current sharing and shape characteristics;
- different impedances of neutral and phase conductors, this effect can influence current sharing among line conductors;
- different transformer impedances, this effect can influence current sharing (negligible, if the transformer is protected by SPDs bypassing its impedance);
- the relation between the conventional earthing impedance of the transformer and the items on the load side, this effect can influence current sharing (the lower the transformer impedance, the higher is the surge current flowing into the low voltage system);
- parallel consumers cause a reduction of the effective impedance of the low voltage system which may increase the partial lightning current flowing into this system.

In case of direct stroke to a structure of lightning current with a wave shape 10/350  $\mu$ s with telecommunication or signalling lines as first approximation, it can be assumed that one half of the lightning current ( $I$ ), flows in the earth termination system and the remaining 50 % of the current is shared between the  $n$  services entering the structure [68].

The aspect of lightning current division and influence of system installation conditions for different stressing wave shapes, normalized by the standards, is examined in chapter 6.

If the entering telecommunication or signalling line is unscreened or not routed in metal conduit, each of the  $m$  conductors of the line carries an equal peak part,  $I_f$ , of the lightning current which may be evaluated as follows [68]:

$$I_f = \frac{0,5 \cdot I_p}{n \cdot m} \quad (3.12)$$

For shielded (or routed in metal conduit) entering lines bonded at the entrance of the structure, the peak values  $I_f$ , of current entering each of the  $m$  conductors, is given by:

$$I_f = \frac{0,5 \cdot I_p \cdot R_s}{n \cdot (m \cdot R_s + R_c)} \quad (3.13)$$

where:

$R_s$  - ohmic resistance for unit length of the shield or the metal conduit;

$R_c$  - ohmic resistance for unit length of the conductor.

The lightning current injected into a structure apart of overvoltages due to resistive coupling, causes overvoltages due to inductive coupling. This special kind of interferences of lightning current is also recognize as LEMP interferences [69-72]. The quantity of influences primary depends on the lightning current steepness:

$$U = -L \frac{di}{dt} \quad (3.14)$$

A simple example of possible loops formed into endangered structure is shown in Fig. 3.6.

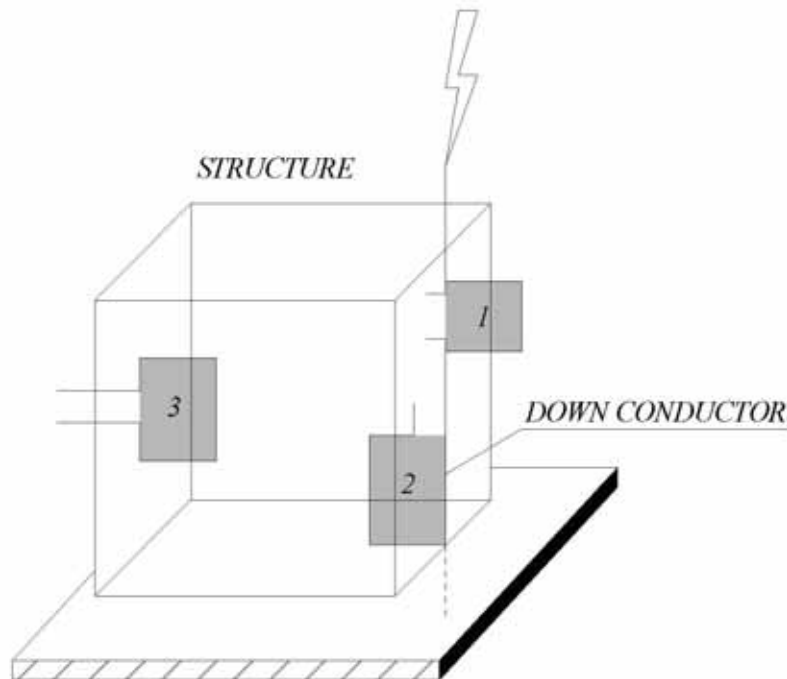


Figure 3.6. Schematic representation of loops formed into structure: 1 – natural loop with down conductor, 2 – loop formed by down conductor, 3 – installation loop.

The loop principal features include, self-inductance  $L_s$  and mutual-inductance  $L_m$ . The  $L_s$  determine an essential parameter for the loop 1 and 2. The  $L_m$  determine an essential parameter for the loop 3, where the loop is disconnected from any part of LPS.

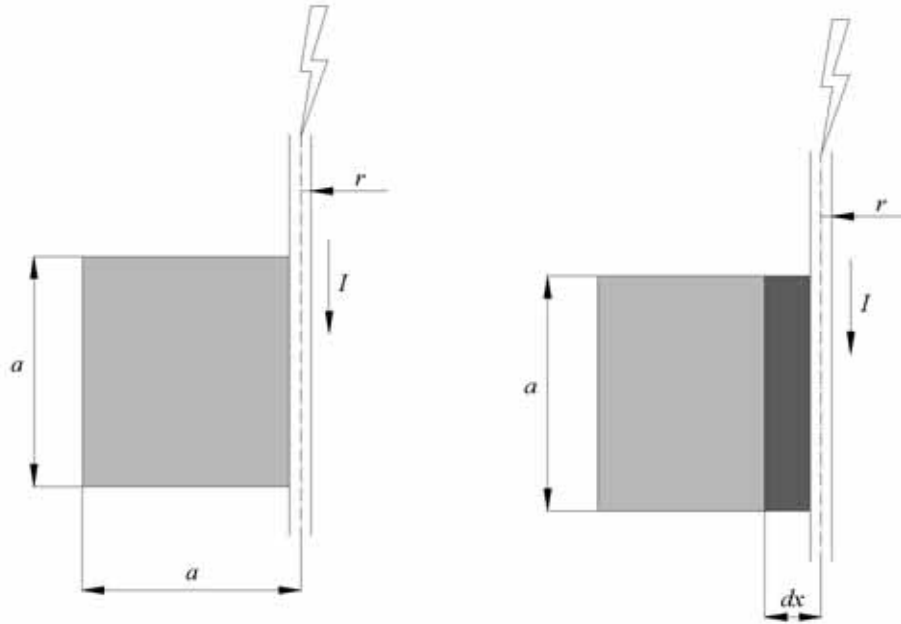


Figure 3.7. Examples of loop with  $L_s$  prevailing parameter.

For the cases shown in Fig 3.7. following equations can be formulated:

$$B = \mu_0 \frac{i(t)}{2\pi \cdot x} \quad (3.15)$$

$$d\Phi = B \cdot dS = B \cdot a \cdot dx \quad (3.16)$$

$$U = \left( \frac{\mu_0 \cdot a}{2\pi} \cdot \int_r^l \frac{dx}{x} \right) \cdot \frac{di}{dt} \quad (3.17)$$

$$L_s = \frac{4\pi \cdot 10^{-7}}{2\pi} \cdot a \cdot \int_r^l \frac{dx}{x} = 0,2 \cdot \ln\left(\frac{l}{r}\right) \quad (3.18)$$

In Fig 3.8. influence of arrangement dimensions as well as influence of cross section of conductor through lightning current passing, on self-inductance values is shown.



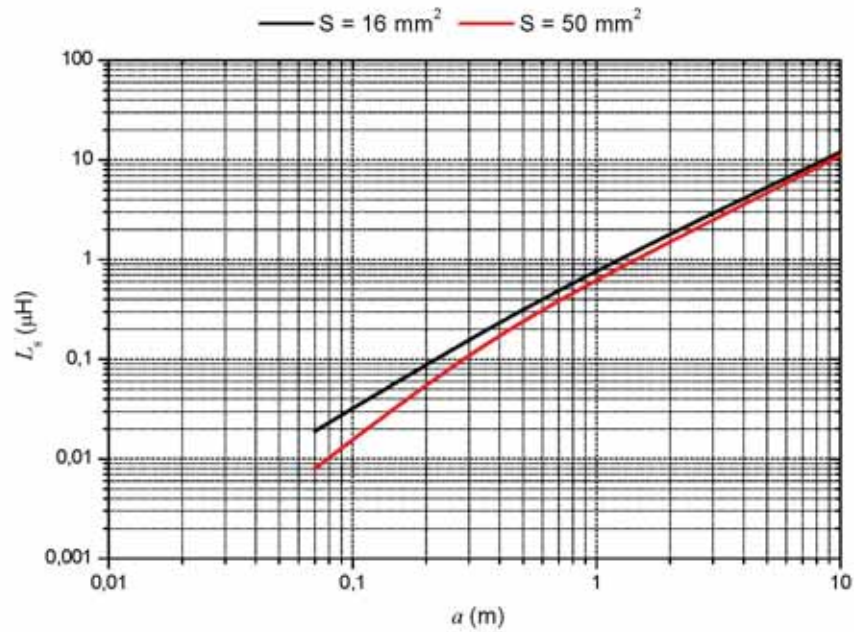


Figure 3.8.  $L_s$  parameter as a function of dimension of loop formed by square arrangement for two cross section of conductor, namely  $16 \text{ mm}^2$  and  $50 \text{ mm}^2$ .

Fig. 3.9. shows a case where a loop is disconnected from the path of lightning current. In this case the  $L_m$  is prevailing.

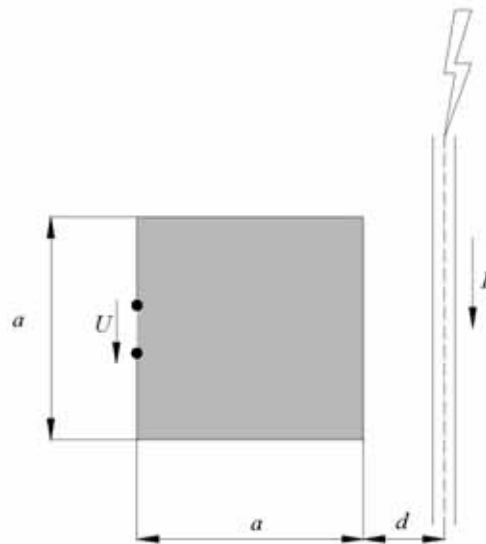


Figure 3.9. Example of loop with  $L_m$  prevailing parameter.

Its value in simplification can be calculated as follows:

$$L_m = 0,2 \cdot a \cdot \ln\left(\frac{d+a}{d}\right) \quad (3.19)$$

Fig 3.10. shows influence of distance between formed loop and lightning current path as well as influence of arrangement dimensions, on mutual-inductance values.

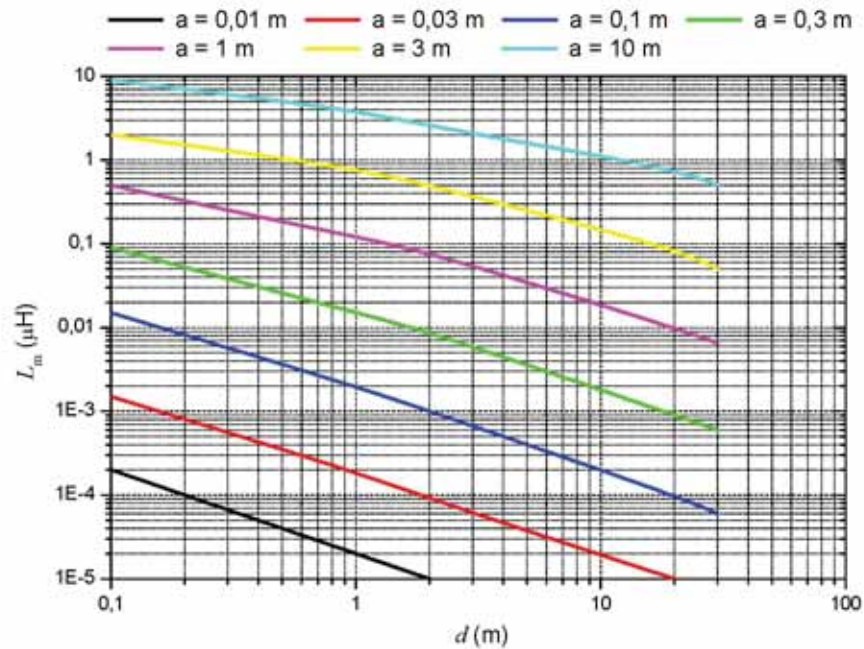


Figure 3.10.  $L_m$  parameter as a function of distance between formed loop and current path for different dimension arrangements.

In general cases the value of self-inductance and mutual-inductance can be calculated by means of following formulas:

$$\begin{aligned}
 L_s = & 0,8 \cdot \sqrt{l^2 + w^2} - 0,8 \cdot (l + w) + 0,4 \cdot l \cdot \ln\left(\frac{2w}{r \cdot \left(1 + \sqrt{1 + \left(\frac{w}{l}\right)^2}\right)}\right) \\
 & + 0,4d \cdot \ln\left(\frac{2l}{r \cdot \left(1 + \sqrt{1 + \left(\frac{l}{w}\right)^2}\right)}\right)
 \end{aligned} \tag{3.20}$$

$$L_m = 0,2 \cdot l \cdot \ln\left(\frac{d+l}{d}\right) \tag{3.21}$$

where:

$l$  - loop length (m);

$w$  - loop width (m);

$d$  - distance between lightning current flowing in the electrical conductor and the induced circuit loop (m);

$r$  - wire radius (m).

Moreover in some cases, even  $L_m$  is prevailing parameter, especially: circuits with shielding elements or equipotential conductors, the calculation of induced current  $I_i$  is needed.

The current flowing in the short circuit loops, created during endangered occurrence can destroyed elements of circuit due to exceeding isolation level. In mentioned case, the induced current in the loop  $I_i$  can be calculated by means of following equation [73]:

$$L_s \frac{dI_i}{dt} + R_s I_i = L_m \frac{dI}{dt} \quad (3.22)$$

where:

$R_s$  – ohmic resistance of conductors formed loop.

In simplification, where the resistance of loop can be neglected, its value can be determinate as follows:

$$I_i \approx \frac{L_m}{L_s} I \quad (3.23)$$

In this case the induced current  $I_i$  maintain the same shape of the inducing current  $I$ .

If the loop resistance is not negligible, the shape of induced current is shorter as shown in Fig. 3.11.

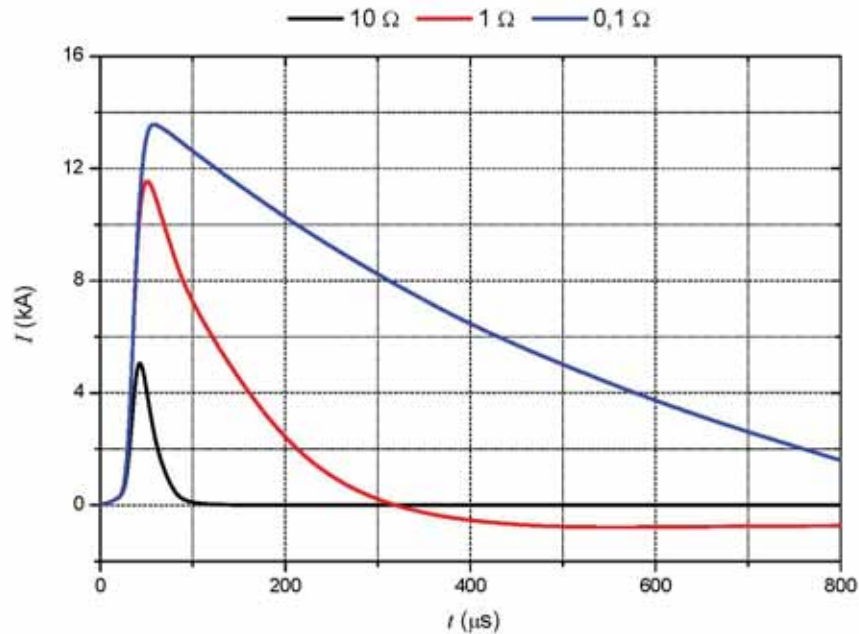


Figure 3.11. Induced current in a loop of 50 m<sup>2</sup> area for different values of its resistance; inducing current of a first stroke flowing in a vertical down conductor at 1 m distance from the loop.

In case where the lightning current is flowing directly through circuit elements, the lightning current division threat should be applied. Moreover the energetic coordination is needed if two phenomenon can occur.

### 3.2.2. Dangerous events frequency

The dangerous events frequency in case of damage source S1 according to the [17, 18] can be expressed by estimated annual number of dangerous events for the structure  $N_D$ .

$N_D$  may be evaluated as the product:

$$N_D = N_g \cdot A_D \cdot C_D \cdot 10^{-6} \quad (3.24)$$

where:

$N_g$  - lightning ground flash density ( $1/\text{km}^2 \times \text{year}$ );

$A_D$  - collection area of the structure ( $\text{m}^2$ );

$C_D$  - location factor of the structure.

The lightning ground flash density  $N_g$  can be taken from isokeuranic maps or estimated taking into account the number of thunder storm days (see chapter 2).

In simplification for isolated structures on flat ground, the collection area  $A_D$  is the area defined by the intersection between the ground surface and a straight line with 1/3 slope which passes from the upper parts of the structure (touching it there) and rotating around it.

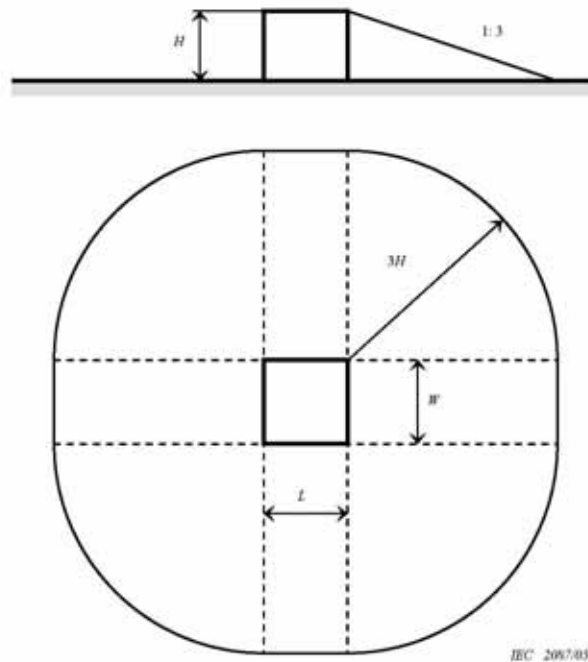


Figure 3.12. Example of collection area  $A_D$  of an isolated structure [18].

For an isolated rectangular structure on flat ground as shown in Fig. 3.12, the collection area can be calculated as follows:

$$A_D = L \cdot W + 2 \cdot (3 \cdot H) \cdot (L + W) + \pi \cdot (3 \cdot H)^2 \quad (3.25)$$

where:

$L$  – length (m);

$W$  – width (m);

$H$  – height (m).

If the structure has a complex shape such as elevated roof protrusions (Fig. 3.13), a graphical method should be used to evaluate  $A_D$ .

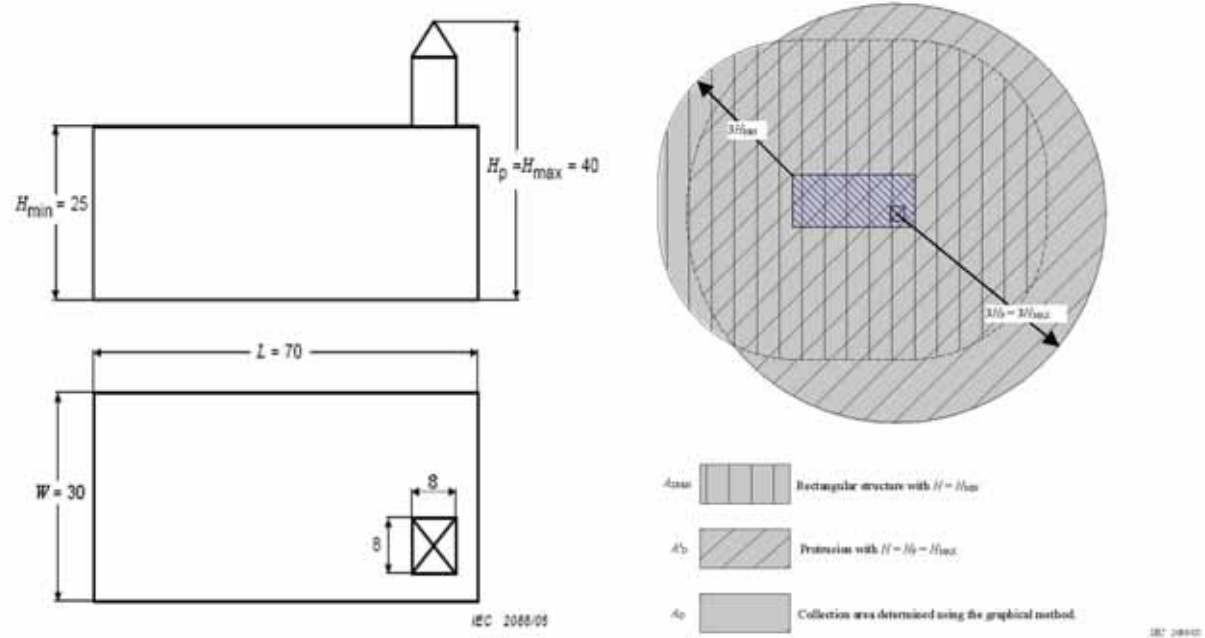


Figure 3.13. Example of collection area  $A_D$  of complex shaped structure [18].

The relative location of the structure takes into account local effects of localization. Tab 3.5. reports values of  $C_D$  factor proposed by [18].

Table 3.5. Structure location factor  $C_D$ [17].

Relative location	$C_D$
Structure surrounded by higher objects	0,25
Structure surrounded by objects of the same height or smaller	0,5
Isolated structure: no other objects in the vicinity	1
Isolated structure on a hilltop or a knoll	2



### 3.3. Flashes near the structure: source of damage S2

#### 3.3.1. Prevailing parameters determination and calculation

The source of damage S2 occur due to lighting flash near the structure. The distance should be at least  $3h$  as shown in Fig. 3.14 (other case S1 occurs) and not exceed 500m [17].

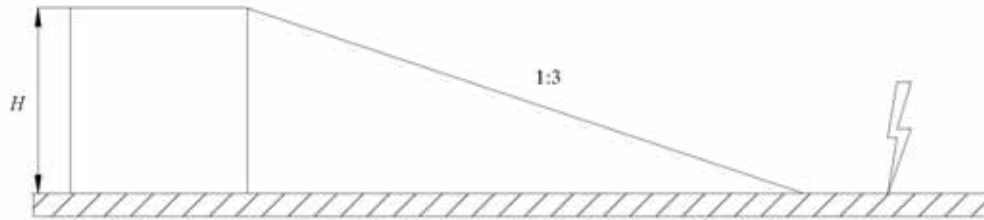


Figure 3.14. Schematic representation of damage source S2.

In this case the source of damage is caused by LEMP. The overvoltages inside the structure can be created in common mode as well as differential mode due to inductive coupling of lightning current. This type of damage can be particular dangerous for low voltage apparatus and controlling system due to possible overvoltages characterized by high peak value over of the rated impulse withstand voltage ( $U_w$ ) of apparatus installed.

The value of magnetic field ( $H_p$ ) due to lightning stroke influences on a loop can be calculated as follows:

$$H_p = \frac{I_p}{2 \cdot \pi \cdot d} \quad (3.26)$$

where:

$I_p$  – maximal peak value of lightning current;

$d$  – distance between lightning stroke and loop.

The overvoltage value in this simple case can be calculated as follows:

$$U = \frac{d\Phi}{dt} = \frac{\mu S}{2\pi d} \cdot \frac{dI}{dt} \approx \frac{\mu S}{2\pi d} \frac{I_{max}}{T_1} \quad (3.27)$$

where:

$\frac{I_{max}}{T_1}$  – current steepness  $\left(\frac{kA}{\mu s}\right)$ ;

$S$  – loop area ( $m^2$ ).

In real cases the situation is much more complex. An example of arrangement is shown in Fig. 3.15.

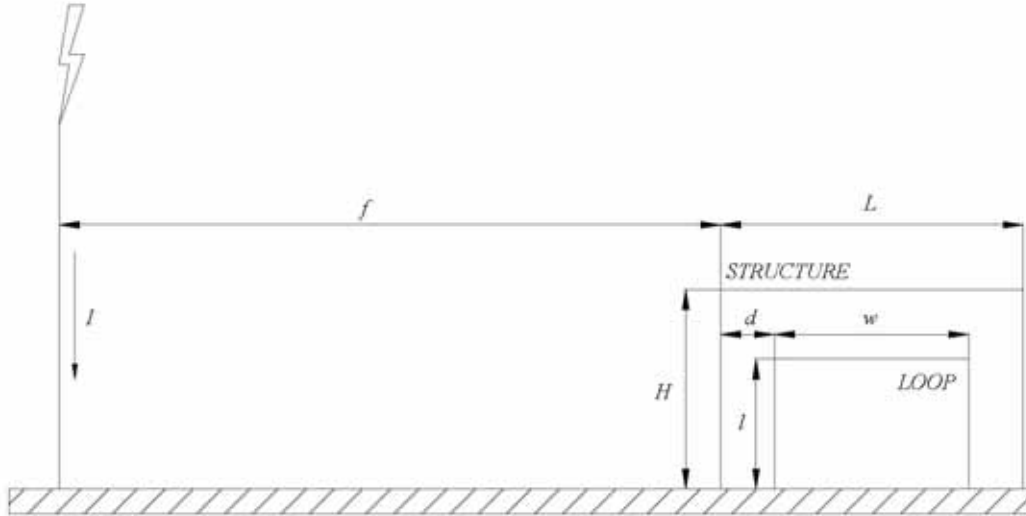


Figure 3.15. Schematic representation of damage source S2.

The peak value of open circuit voltage  $U_{io}$  induced in the loop inside the structure by a lightning near the structure can be calculated as follows:

$$U_{io} = L_m \cdot \frac{di}{dt} = L_m \cdot \frac{I_p}{T_1} \quad (3.28)$$

where:

$I_p$  – peak value of lightning current;

$T_1$  – front time of the lightning current.

Approximated value of  $L_m$  ( $\mu\text{H}$ ) can be calculated as follows:

$$L_m = 0,2 \cdot \eta \cdot K_s \cdot l \cdot \ln\left(\frac{f+d+w}{f+d}\right) \quad (3.29)$$

where:

$l$  – loop length (m);

$w$  – loop width (m);

$f$  – distance from the lightning channel to the wall of the structure (m);

$d$  – distance of the loop from the wall of the structure (m);

$\eta = 0,12 \cdot w$  – shielding factor of the structure shield (shield of LPZ 1), being  $w \leq 5$  m the mesh width of the grid-like spatial shield;

$K_s$  – shielding factor taking into account the shielding effect of the cable shield.

The peak value of the short circuit current  $I_{sc}$ , if the ohmic resistance of the loop wires is neglected can be calculated as follows:

$$I_{sc} = \frac{U_{io} \cdot T_1}{L_s} = \frac{L_m}{L_s} \cdot I_p \quad (3.30)$$

According to [68] in this more extended case (as shown in Fig. 3.15) the self-inductance ( $L_s$ ) can be calculated as follows:

$$L_s = 0,8 \cdot \sqrt{l^2 + w^2} - 0,8 \cdot (l + w) + 0,4 \cdot w \cdot \ln\left(\frac{2 \cdot l}{r \cdot \left(w + \sqrt{w + \left(\frac{l}{w}\right)^2}\right)}\right) + 0,4 \cdot l \cdot \ln\left(\frac{2 \cdot w}{r \cdot \left(w + \sqrt{w + \left(\frac{w}{h}\right)^2}\right)}\right) \quad (3.31)$$

### 3.3.2. Dangerous events frequency

According to [17] the dangerous events frequency is estimated by average annual number of dangerous events  $N_m$ . An overview of analysed situation is shown in Fig. 3.16. The lighting occurrences belong to S2 type of damage include surface determine by  $x - R$ .

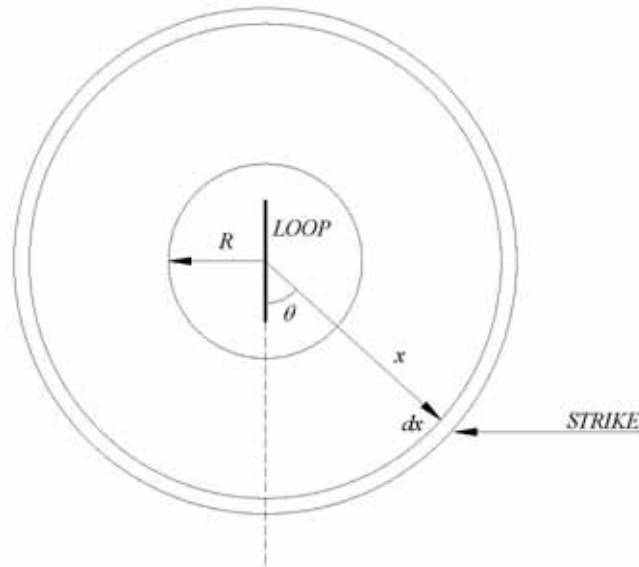


Figure 3.16. Reference configuration for evaluation of the surge induced into a loop by a lightning near a structure.

The total number of strikes  $N_m$  can be calculated as follows:

$$N_m = 4 \cdot N_g \int_R^{\infty} \int_0^{\pi/2} \int_0^{\pi/2} p(i) \cdot di \cdot \cos\theta \cdot d\theta \cdot x \cdot dx \quad (3.32)$$

where:

$R$  - minimum distance from the loop for which the lightning will not strike directly the structure ( $R = 3H + L/2$ );

$p(i)$  - probability function of the strike current;

$\theta$  - angle between the loop and a straight line linking the strike and the loop;

$x$  - distance between the strike and the centre of the loop;  
 $I_p$  - peak strike current that will induce the voltage  $U$  at the loop.

According to [17]  $N_M$  may be evaluated as the product:

$$N_m = N_g \cdot A_M \cdot 10^{-6} \quad (3.33)$$

where:

$A_M$  - collection area of flashes striking near the structure ( $m^2$ ).

$$A_M = 2 \cdot 500 \cdot (L + W) + \pi \cdot 500^2 \quad (3.34)$$

### 3.4. Flashes to the services connected to the structure: source of damage S3

#### 3.4.1. Prevailing parameters determination and calculation

Fig. 3.17 represents typical case where a lightning flash terminates on overhead lines. This occurrence according to [17] consist of source of damage S3. In this event overvoltages have a conventional wave shape 1,2/50  $\mu$ s [18]. Its value can be calculated as follows:

in common mode:

$$U_G = \frac{1}{2} \cdot Z_c \cdot i(t) \quad (3.35)$$

in differential mode:

$$U_D = \frac{1}{2} \cdot Z_c \cdot \left(1 - \frac{Z_{2c}}{Z_c}\right) \cdot i(t) \quad (3.36)$$

where:

$Z_c$  – self-impedance of conductor;

$Z_{2c}$  – mutual-impedance of two conductors;

$i(t)$  – lightning current.

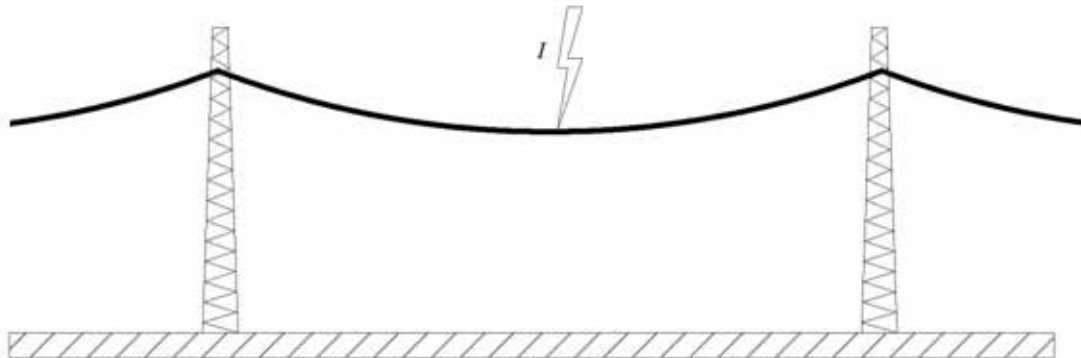


Figure 3.17. Schematic representation of damage source S3.

In case of lightning flash to the line pole, the overvoltages in simplification can be calculated as follows:

$$U_{S3P} = Zi(t) + L \frac{di(t)}{dt} \quad (3.37)$$

where:

$Z$  – conventional earthing impedance;

$L$  – pole equivalent inductance.

In the case of direct lightning flashes to connected lines to a structure, partitioning of the lightning current in both directions of the line and the breakdown of insulation should be taken into account.



Fig. 3.18. represents a situation where due to lightning stroke, overvoltage  $U_L$  occurs. In this simple example the whole lightning current form overvoltage directed to an apparatus  $U_w$  through the line distance  $d$ .

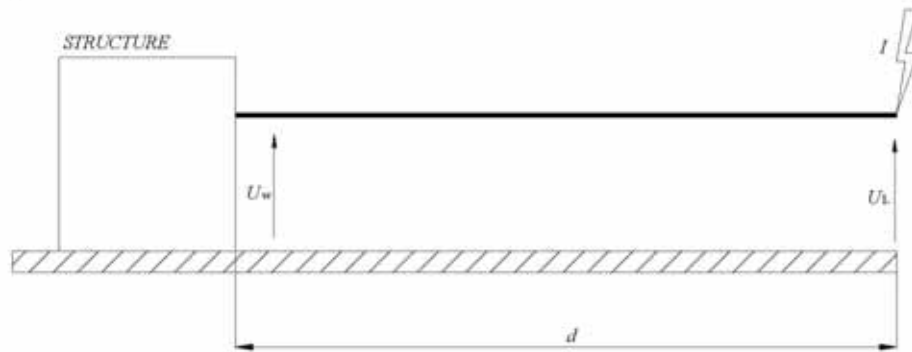


Figure 3.18. Schematic representation of propagation of overvoltages toward apparatus.

In this case the value of overvoltages can be calculated as follows:

$$U_w = e^{-\alpha_L d} U_L \quad (3.38)$$

$$d = \frac{-1}{\alpha_L} \ln \left( \frac{U_w}{U_L} \right) \quad (3.39)$$

where:

$U_w$  – withstand voltage of apparatus to be protected;

$U_L$  – voltage value in point of stroke;

$\alpha_L$  – line attenuation coefficient;

$d$  – line length.

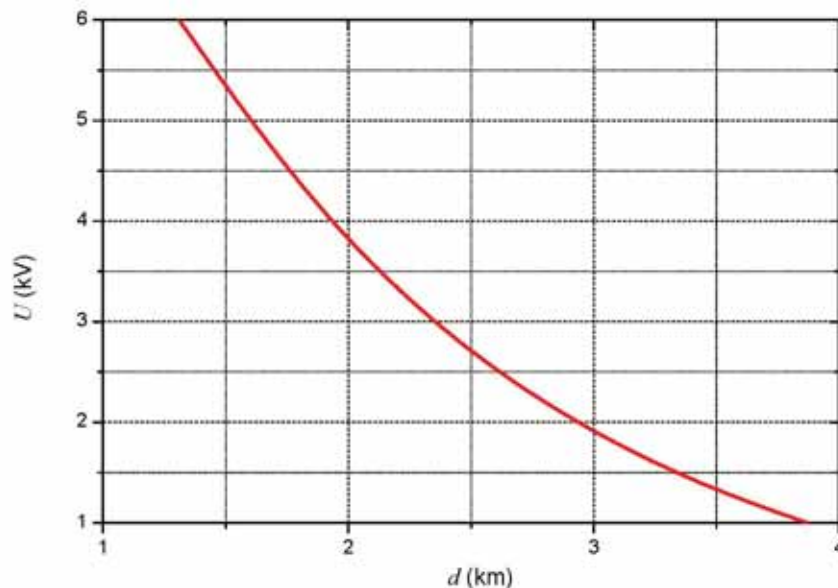


Figure 3.19. Expected voltage value ( $U_w$ ) on apparatus terminals as a function of lightning termination distance ( $d$ ).

In case of low voltage systems, where isolating level of overhead line is 15 kV,  $\alpha_L = 0,7 /\text{km}$  [1, 17], results showing influence of distance  $d$  on the incoming overvoltage value  $U_w$  are shown in Fig. 3.19.

In case e.g. of medium voltage line the presence of transformer should be considered. Schematic representation of simplified arrangement is shown in Fig. 3.20.

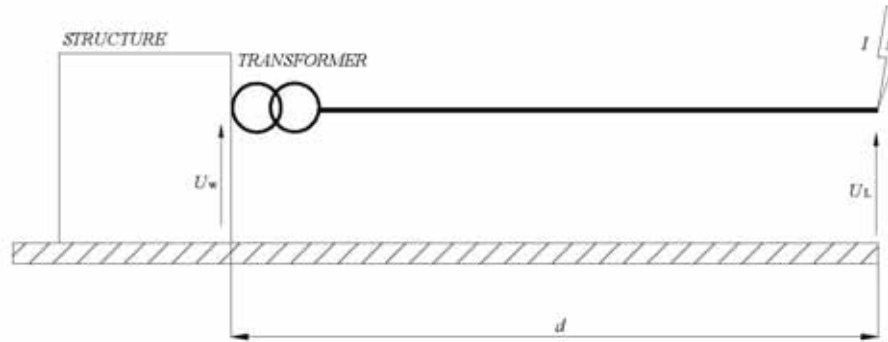


Figure 3.20. Schematic representation of propagation of overvoltages through line connected to transformer.

In this case overvoltages incoming to the apparatus can be calculated as follows:

$$U_w = e^{-\alpha_L d} (\alpha_t \cdot U_L) \quad (3.40)$$

$$d = \frac{-1}{\alpha_L} \ln \left( \frac{U_w}{\alpha_t \cdot U_L} \right) \quad (3.41)$$

where:

$\alpha_t$ – transformer attenuation coefficient.

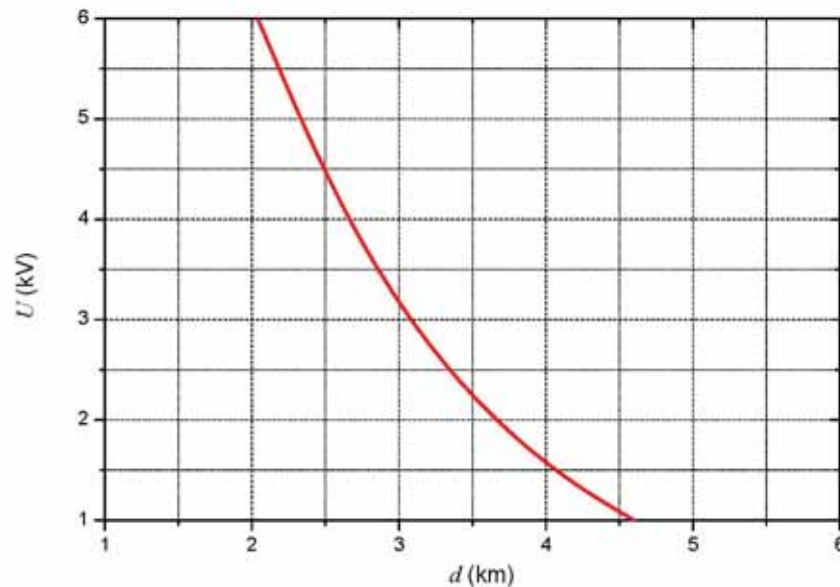


Figure 3.21. Expected voltage value ( $U_w$ ) on apparatus terminals as a function of lightning termination distance ( $d$ ).

In case of medium voltage systems, where isolating level of overhead line is 125 kV,  $\alpha_L = 0,7$  /km, and  $\alpha_t = 0,2$  [1, 17], results showing influence of distance  $d$  on the incoming overvoltage value  $U_w$  are shown in Fig. 3.21.

According to [68] for telecommunication or signalling line are two possible situations classified as S3 damage source, namely the striking point is far away from the structure, the striking point is close to the structure. In both situation, the lightning current entering the telecommunication or signalling line is described by 10/350  $\mu$ s waveshape and by the peak value  $I_t$ . Neglecting the propagation effects, the same 10/350  $\mu$ s waveshape is assumed for the current expected in different sites of the network (exchange or customer's building or remote sites).

If the telecommunication or signalling line is unscreened or not routed in metal conduit, each of the  $m$  conductors of the line carries an equal peak part,  $I_t$ , of the lightning current which may be evaluated for an shielded line by:

$$I_t = \frac{0,25 \cdot I_p}{n \cdot m} \quad (3.42)$$

with  $n = 1$  or  $2$ ; the latter case applies for example when telecommunication and power lines are close to each other, e.g. they share the same poles.

The value given by equation (3.39) shall be equal to or lower than the following value:

$$I_t \leq 8 \cdot A \quad (3.43)$$

where:

$A$  - cross sectional area of the telecommunication or signalling conductor ( $\text{mm}^2$ ).

For shielded (or routed in metal conduit) entering lines bonded at the entrance of the structure, the peak values  $I_t$ , of current entering each  $m$  conductors, is given by:

$$I_t = \frac{0,25 \cdot I_p \cdot R_s}{n \cdot (m \cdot R_s + R_c)} \quad (3.44)$$

where:

$R_s$  - ohmic resistance for unit length of the shield or the metal conduit;

$R_c$  - ohmic resistance for unit length of the conductor.

The open circuit voltage between conductor and shield is approximately proportional to the product of the shield resistance and the portion of the lightning current that flows through the shield, limited by the breakdown voltage of the core conductors to the shield. Where the shield is periodically earthed, the shield current attenuates as it propagates away from the strike point. Propagation of the surge along the cable leads to dispersion and increase of the decay time.

### 3.4.2. Dangerous events frequency

Dangerous events frequency due to damage source S3 express average annual number of dangerous events  $N_L$  due to flashes to a line. Moreover [17] estimated this value only with overvoltages over 1kV and can be calculated by:

$$N_L = N_g \cdot A_L \cdot C_I \cdot C_E \cdot C_T \cdot 10^{-6} \quad (3.45)$$

where:

$C_I$  - installation factor of the line;

$C_T$  - line type factor;

$C_E$  - environmental factor.

Tab. 3.6., Tab. 3.7. and Tab. 3.8. reports values of factors  $C_I$ ,  $C_T$  and  $C_E$  respectively.

Table 3.6. Line installation factor  $C_I$ .

Routing	$C_I$
Aerial	1
Buried	0,5
Buried cables running entirely within a meshed earth termination	0

Table 3.7. Line type factor  $C_T$ .

Installation	$C_T$
LV power, telecommunication or data line	1
HV power (with HV/LV transformer)	0,2

Table 3.8. Line environmental factor  $C_E$ .

Environment	$C_E$
Rural	1
Suburban	0,5
Urban	0,1
Urban with tall buildings (higher than 20 m)	0,01

The collection area (in  $m^2$ ) for flashes to a line according to [17] can be calculated as follows:

$$A_L = 40 \cdot L_L \quad (3.46)$$

where:

$L_L$  - length of the line section (m).

In case where the length of a line section is unknown,  $L_L = 1\ 000$  m is to be assumed.

The collection area for flashes to a line can be also estimated by means of electro-geometrical model proposed by Eriksson [49]. The equivalent area of line section for direct flashes shows Fig. 3.22.

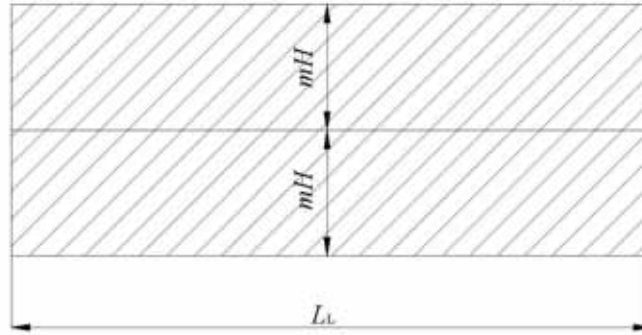


Figure 3.22. Equivalent area of line section for direct flashes.

Its value depends on the line length and pole high multiply by coefficient  $m$  related to the peak value of lightning flash and can be calculated as follows:

$$A_L = 2 \cdot m \cdot H \cdot L_L \quad (3.47)$$

where:

$m$  – coefficient of Eriksson electro-geometrical model;

$H$  – pole high (m).

The coefficient value can be estimated by means of following general equation corresponding to direct stroke[49]:

$$r = m \cdot H \quad (3.48)$$

where:

$r$  – radius of direct stroke.

The radius of direct stroke is different for masts and lines. Its value can be calculated as follows for masts:

$$r = 0,84 \cdot H^{0,6} \cdot I^{0,74} \quad (3.49)$$

As follows for lines:

$$r = 0,67 \cdot H^{0,6} \cdot I^{0,74} \quad (3.50)$$

Finally the value of coefficient  $m$  for lines can be calculated as follows:

$$m = \frac{0,67 \cdot H^{0,6} \cdot I^{0,74}}{H} \quad (3.51)$$

e.g. for a lightning current  $I = 35$  kA:

$$m = 14 \cdot H^{-0,4} \quad (3.52)$$

Fig. 3.23. shows the values of coefficient  $m$  taking into account the influence of the pole height.



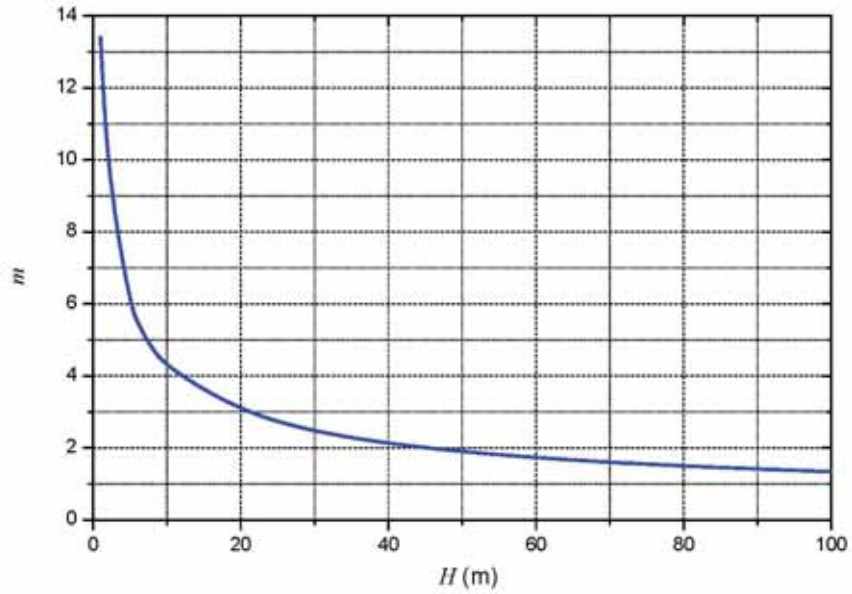


Figure 3.23. Value of coefficient  $m$  as a function of pole height for a lightning stroke  $I = 35\text{kA}$ .

In case of low-voltage overhead line, with poles show in Fig. 3.24, the collection area for lightning flashes with 35kA current peak value can be calculated as follows:

$$A_L = 28 \cdot H^{0.6} \cdot L_L \quad (3.53)$$

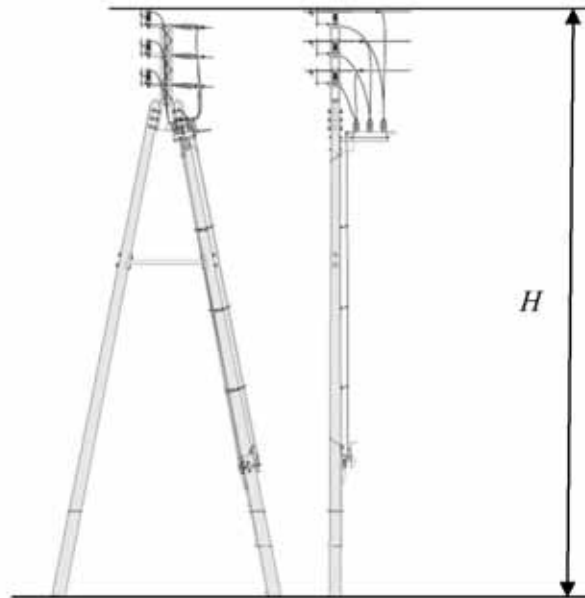


Figure 3.24. Example of low-voltage pole.

Results for different pole height in comparison to [17] are shown in Fig. 3.25.

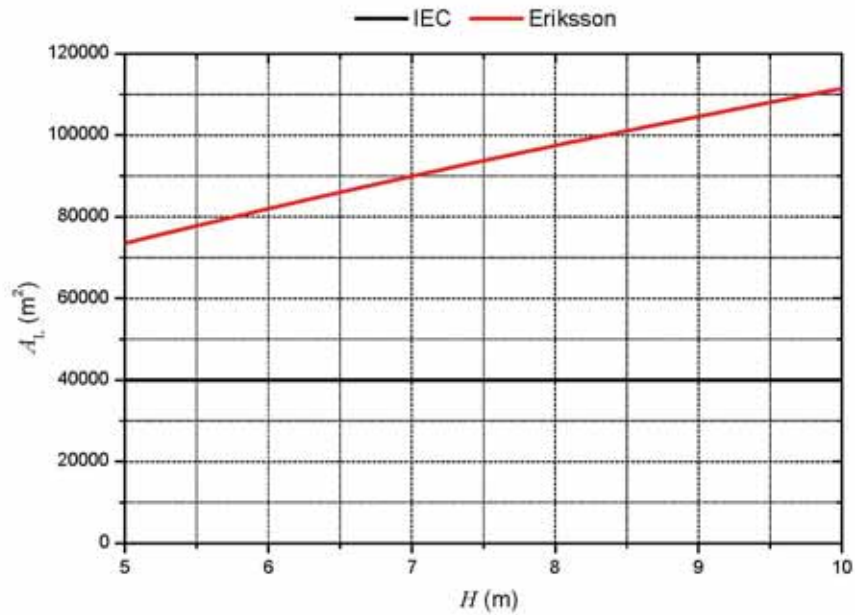


Figure 3.25. Value of equivalent collection area of flashes to a line as a function of pole height for 1 km line section.

In case of high-voltage overhead lines poles with two shielding wires at distance ( $a$ ) the collection area for lightning flashes with 35kA current peak value can be calculated taking into account pole span ( $a$ ) as follows:

$$A_L = (28 \cdot H^{0.6} + a) \cdot L_L \quad (3.54)$$

### 3.5. Flashes near the services connected to the structure: source of damage S4

#### 3.5.1. Prevailing parameters determination and calculation

Lightning flashes that terminate on the earth or on any adjacent object, including clouds itself, near the distribution or transmission line, consist of damage source S4. In this situation lightning current induce voltages on the phase conductors, on the ground wires and across the insulation. Schematic representation of S4 occurrence is shown in Fig. 3.26.

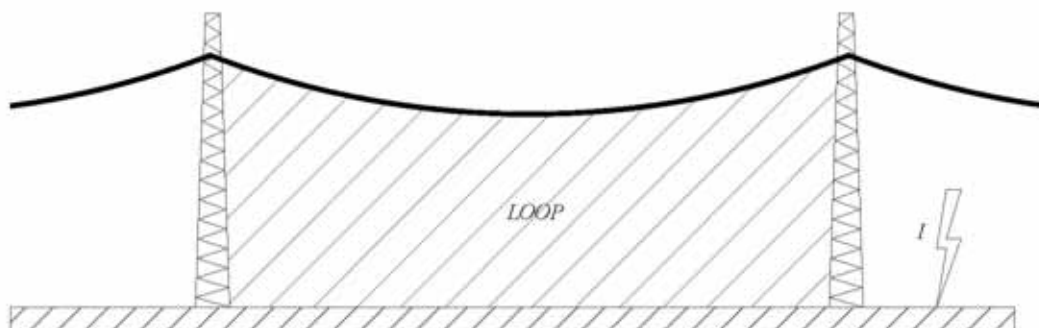


Figure 3.26. Schematic representation of damage source S4.

This type of damage is particular danger due to elevate number of occurrences and high peak value of overvoltages appearance, even in case where the lightning flash terminate far from considerate line [1, 74, 75]. Until about 1930 this source of damage was only considerate as damage source for overhead lines [76]. The accurate calculation of lightning-induced overvoltages on distribution networks is essential for the optimal choice of the characteristics, number and installation location of protective/mitigation devices (surge arresters, shielding wire and relevant groundings). Additionally, it is only by means of accurate calculations that it becomes possible to correlate nearby lightning events—detected by lightning location systems—with voltage dips and/or interruptions, an issue that is receiving growing attention due to the economic impact of power quality problems.

Several theories have been developed to calculate lightning induced voltages on lines and equipment [77, 78]. One of those that has survived all kinds of tests is the one proposed in 1957 by S. Rusck [79]. In his thesis, Rusck developed, from Maxwell's equations, an analytical expression for the lightning induced voltage on ideal infinite lines. Rusck's theory calculates the voltages, along the line, induced by a lightning discharge, at any time. This can be viewed as generalized voltage/current sources distributed on the line. At each of these sources, traveling waves are generated. The propagation of the waves must be calculated to properly simulate the whole interaction between the lightning discharge and the line.

The electric field created by the lightning discharge is calculated by Rusck using the following classical expression:

$$E = -\nabla V_i - \frac{\partial A_i}{\partial t} \quad (3.55)$$

where:

$V_i$ - scalar potential;

$A_i$ - Vector magnetic potential.

In his theory, Rusck proposed that the induced voltage in a homogeneous infinite transmission line is calculated by:

$$V(x,t) = U(x,t) + h \frac{\partial A_1(x,t)}{\partial t} \quad (3.56)$$

$$U(x,t) = \left( \frac{1}{2v_0} \right) \cdot \int_{-\infty}^{+\infty} \frac{\partial V_i \left( u, t - \frac{|x-u|}{v_0} \right)}{\partial t} du \quad (3.57)$$

where:

$x$  – point in the line;

$t$  – time;

$v_0$  – velocity of the return stroke;

$u$  – integrational variable;

$h$  – height of the line.

Rusck showed in his thesis that (3.55) can be solved by the application of current sources along the transmission line. Rusck's theory readily yields the injected current sources from the scalar potential  $V_i$ .

The current source to be injected in the line to represent the scalar potential can be calculated as follows:

$$I_{ci}(x,t) = \frac{1}{v_0 \cdot Z} \cdot \frac{\partial V_i(x,t)}{\partial t} \cdot \Delta x \quad (3.58)$$

where:

$Z$  – surge impedance of the line.

Current source from the vector magnetic potential can be calculated as follows:

$$I_{vi}(x,t) = -h \frac{\partial A_1(x,t)}{\partial t} \quad (3.59)$$

According to [68] calculations of surge induced by a lightning near the line can be calculated also in simplification. Fig. 3.27. shows a line section  $L_L$  and lightning termination in the middle point of the line. In a central point between  $U_0$  and  $U_2$  in a distance above  $d$  (direct flash to a line) the lightning current forms overvoltage  $U_1$ . It is the worst case where the whole electromagnetic field consist of overvoltages creation.

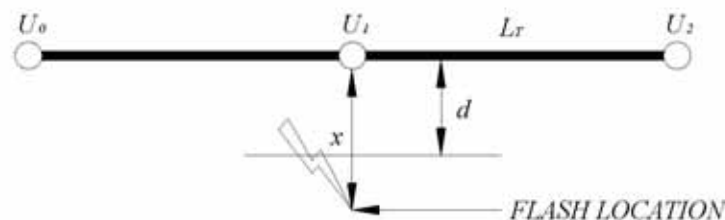


Figure 3.27. Schematic representation of arrangement configuration for surge evaluation induced by a lightning near the line.

In case of perfectly conducting soil, the peak value of the voltage  $U_1$  can be calculated as follows:

$$U_1 = \frac{30 \cdot I_p \cdot h}{d} \left( 1 + \frac{v}{\sqrt{2-v^2}} \right) \quad (3.60)$$

The peak value of the voltages  $U_0$  and  $U_2$  at the line terminations can be estimated by the following equation:

$$U_0 = U_2 = \frac{30 \cdot I_p \cdot h}{d} \quad (3.61)$$

where:

$I_p$  – peak value of lightning current;

$v$  – ratio between the return-stroke velocity ( $v = 1,3 \cdot 10^8$  m/s is assumed) and the velocity of the light ( $c = 3 \cdot 10^8$  m/s).

$$v = 0,43 \text{ and } \left( 1 + \frac{v}{\sqrt{2-v^2}} \right) = 1,3.$$

The peak value of the short circuit current  $I_{sc}$  can be estimated as follows:

$$I_{sc} = \frac{U_1}{Z} \quad (3.62)$$

where:

$Z$  – characteristic line impedance, an overhead transmission line  $400 \Omega$ .

Nowadays calculations of induced overvoltages can be performed by means well developed software. The evaluation and the analysis of the lightning electromagnetic pulse response of distribution networks require the availability of accurate models of LEMP-illuminated lines and their implementation into software tools able to calculate lightning-induced electromagnetic transients in distribution systems. The complexity of these models calls for an implementation into computer codes since, in general, they require a numerical integration of the relevant equations. Accurate evaluation of lightning-induced overvoltages on a multiconductor line above a lossy ground can be obtained by using the LIOV computer code [80-83], developed in the framework of an international collaboration involving the University of Bologna (Department of Electrical Engineering), the Swiss Federal Institute of Technology (Power Systems Laboratory), and the University of Rome 'La Sapienza' (Department of Electrical Engineering).

The LIOV code allows for the calculation of lightning-induced voltages along a multiconductor overhead line as a function of lightning current waveshape (amplitude, front steepness, and duration), return-stroke velocity, line geometry (height, length, number and position of conductors), values of resistive terminations, ground resistivity and relative permittivity. It allows also taking into account induction phenomena due to the leader field



[84], nonlinear phenomena such as corona [85] and the presence of surge arresters [83]. Schematic representation of geometry calculation is shown in Fig. 3.28.

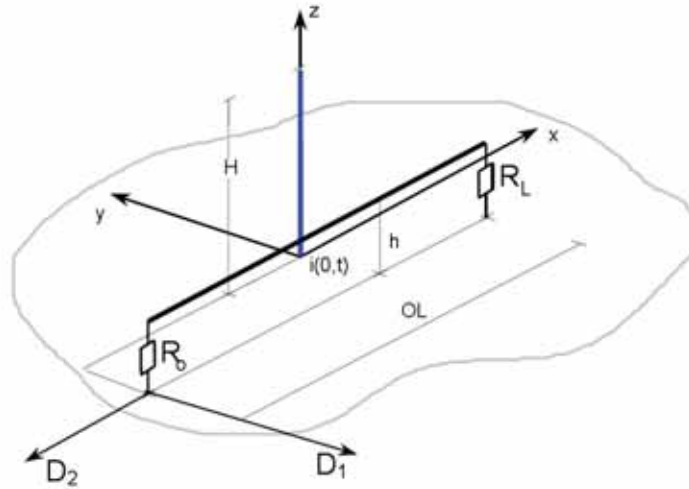


Figure 3.28. Schematic representation of cases can be calculated by LIOV code [80].

The lightning current is defined as sum of three lightning current function:

$$i(0,t) = i_{H1}(0,t) + i_{H2}(0,t) + i_{DE}(0,t) \quad (3.63)$$

where the individual component of lightning current are defined as follows:

$$i_{H1}(0,t) = \frac{I_{01}}{\eta_1} \frac{\left(\frac{t}{\tau_{11}}\right)^{\eta_1}}{1 + \left(\frac{t}{\tau_{11}}\right)^{\eta_1}} e^{-\frac{t}{\tau_{12}}} \quad (3.64)$$

$$i_{H2}(0,t) = \frac{I_{02}}{\eta_2} \frac{\left(\frac{t}{\tau_{21}}\right)^{\eta_2}}{1 + \left(\frac{t}{\tau_{21}}\right)^{\eta_2}} e^{-\frac{t}{\tau_{22}}} \quad (3.65)$$

$$i_{DE}(0,t) = I_D \left( (1 - e^{-\alpha t}) - (1 - e^{-\beta t}) \right) \quad (3.66)$$

$$\eta_1 = e^{-\left(\frac{\tau_{11}}{\tau_{12}}\right)^{\eta_1} \left(\frac{\tau_{12}}{\tau_{11}}\right)^{\frac{1}{\eta_1}}} \quad (3.67)$$

$$\eta_2 = e^{-\left(\frac{\tau_{21}}{\tau_{22}}\right)^{\eta_2} \left(\frac{\tau_{22}}{\tau_{21}}\right)^{\frac{1}{\eta_2}}} \quad (3.68)$$

where:

$\alpha$  – front time coefficient;

$\beta$  – tail time coefficient.

An example of results obtained by means of LIOV code for an overhead line section 100m consisting a part of infinity system and the pole high 6 meters, with assumption that lightning strokes terminated symmetrically over 26,4 m from the line results only source of damage S4, are shown in Fig. 3.29 and Fig. 3.30 for the  $O$  and  $L$  observation point.

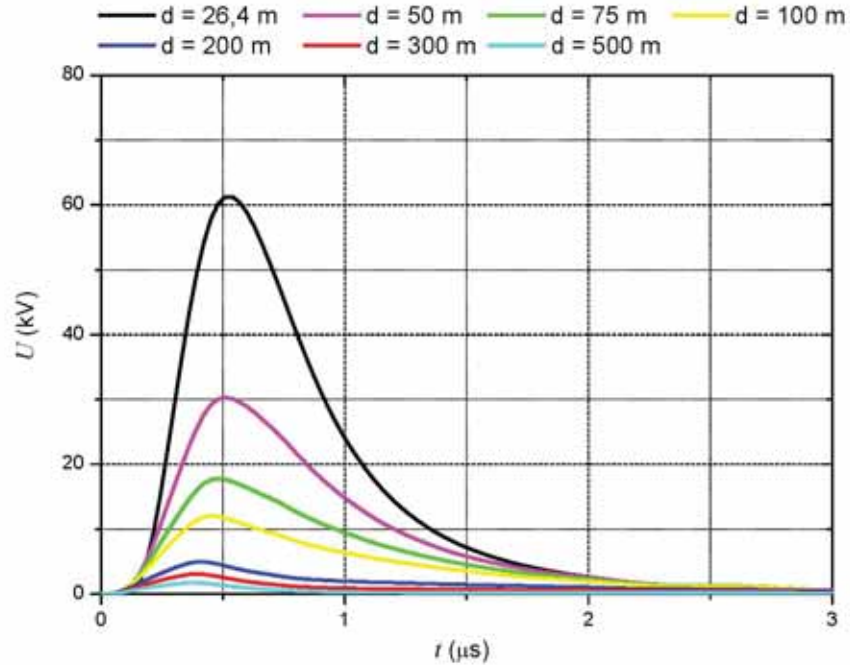


Figure 3.29. Simulated values of overvoltages observed in the  $O$  and  $L$  points, as a function of time for different distance to the line of lightning striking point.

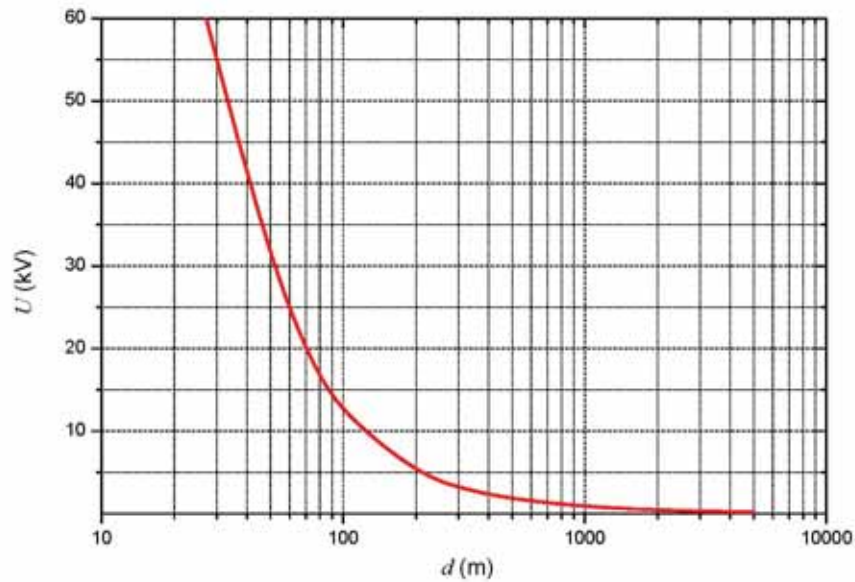


Figure 3.30. Peak value of overvoltages in the  $O$  and  $L$  points as a function of distance to the line of lightning striking point.

On the base of performed simulation is demonstrated that the induced overvoltages consist of damage source. Probability of damage due to S4 depends on the point of lightning current termination. Maximal overvoltage values are obtained for cases where the lightning stroke terminated in a limit of direct stroke termination into overhead lines. Overvoltages values decrease with point of termination, and change their wave shape [86, 87]. The peak value of overvoltage appearances strongly depends on the peak value of lightning current and on its wave shape, namely front steepness. The symmetrical analyses of lightning termination shown that the value of overvoltages obtained at extreme points are each other equal.

### 3.5.2. Dangerous events frequency

The dangerous events frequency of flashes near a line is defined in [17] as the average annual number  $N_I$  of overvoltages over 1kV. A transmission line may consist of several sections. For each section of line, the value of dangerous events frequency may be calculated as follows:

$$N_I = N_g \cdot A_l \cdot C_I \cdot C_E \cdot C_T \cdot 10^{-6} \quad (3.69)$$

where:

$C_I$  – installation factor;

$C_T$  – line type factor;

$C_E$  – environmental factor.

The collection area for flashes near a line according to [17] can be calculated as follows:

$$A_L = 4000 \cdot L_L \quad (3.70)$$

where the length of a line section is unknown,  $L_L = 1\ 000$  m is to be assumed.

The dangerous events frequency can calculate also by means of different models. In case of overhead lines the theoretical model of Rusck, improved by Borghetti et al. [74, 75], experimental data collected by Popolansky [88] or CIGRE recommendation [89] can be applied.

The theoretical model of Rusck is based on the theoretical aspects of electromagnetic field and can be applied for calculation of total number of overvoltages appearances on the overhead line. In this investigation all significant factors are taken into account. An example of parameters which have to be defined are given below:

Definition of lightning current includes:

- medium value of lightning current;
- minimum value of lightning current;
- maximal value of lightning current;
- range of overvoltages induced;
- dispersion of the lightning current distribution.

Definition of area includes:

- lightning flash activity.

Definition of line includes:

- pole high;
- section length.

Originally the theoretical approach proposed by Rusck [79], is dedicate for 100km of line section and the number of induced occurrence could be calculated as follows:

$$N_1 = 200 \cdot N_g \int_0^{\infty} [f(U, I_m - y_{\min})] \cdot \frac{\partial g(I_m)}{\partial I_m} dI_m \quad (3.71)$$

where:

$$d_g = \frac{\partial g(I_m)}{\partial I_m} dI_m \quad (3.72)$$

$$d_g = \frac{1}{\sqrt{2\pi} \cdot I \cdot \delta_1} \cdot \exp\left[-\frac{1}{2} \cdot \frac{\ln^2 \frac{I}{I_m}}{\delta_1^2}\right] dI_m \quad (3.73)$$

Finally equation (3.70) for 1 km of line section obtains following form:

$$N_1 = 2000 \cdot N_g \cdot 10^{-6} \int_{I_{\min}}^{I_{\max}} \left[ \left( \frac{Z_o \cdot I \cdot h}{U} \right) - y_{\min} \right] \cdot \frac{1}{\sqrt{2\pi} \cdot I \cdot \delta_1} \cdot \exp\left[-\frac{1}{2} \cdot \frac{\ln^2 \frac{I}{I_m}}{\delta_1^2}\right] dI_m \quad (3.74)$$

The minimal distance ( $y_{\min}$ ) below which the lighting strike directly to the line can be calculated in two modes, approximately and precisely. In simplification its value can be calculated as follows:

$$y_{\min} = r_s \quad (3.75)$$

$$r_s = 0,67 \cdot h^{0,6} \cdot I^{0,74} \quad (3.76)$$

$$y_{\min} = 0,67 \cdot h^{0,6} \cdot I^{0,74} \quad (3.77)$$

In complex form, as follows:

$$y_{\min} = d_1 \quad (3.78)$$

$$d_1 = \sqrt{r_s^2 - (r_g - h)^2} \quad (3.79)$$

$$r_g = 0,9 \cdot r_s \quad (3.80)$$

$$d_1 = \sqrt{0,67 \cdot h^{0,6} \cdot I^{0,74^2} - \left(0,9 \cdot \left(0,67 \cdot h^{0,6} \cdot I^{0,74}\right) - h\right)^2} \quad (3.81)$$

$$y_{\min} = \sqrt{0,67 \cdot h^{0,6} \cdot I^{0,74^2} - \left(0,9 \cdot \left(0,67 \cdot h^{0,6} \cdot I^{0,74}\right) - h\right)^2} \quad (3.82)$$

Example of calculations is performed for a case where:

- medium value of lightning current: 33,5(kA);
- minimum value of lightning current: 2 (kA);
- maximal value of lightning current: 200 (kA);
- range of induced overvoltages: 1-30 (kV);
- dispersion of the lightning current distribution: [17];
- lightning current activity: 1 (flash/km<sup>2</sup>/anno);
- pole high: 6 (m);
- section length: 1000 (m).

The annual number of overvoltages calculated according to theoretical approach proposed by Rusck is shown in Fig. 3.31.

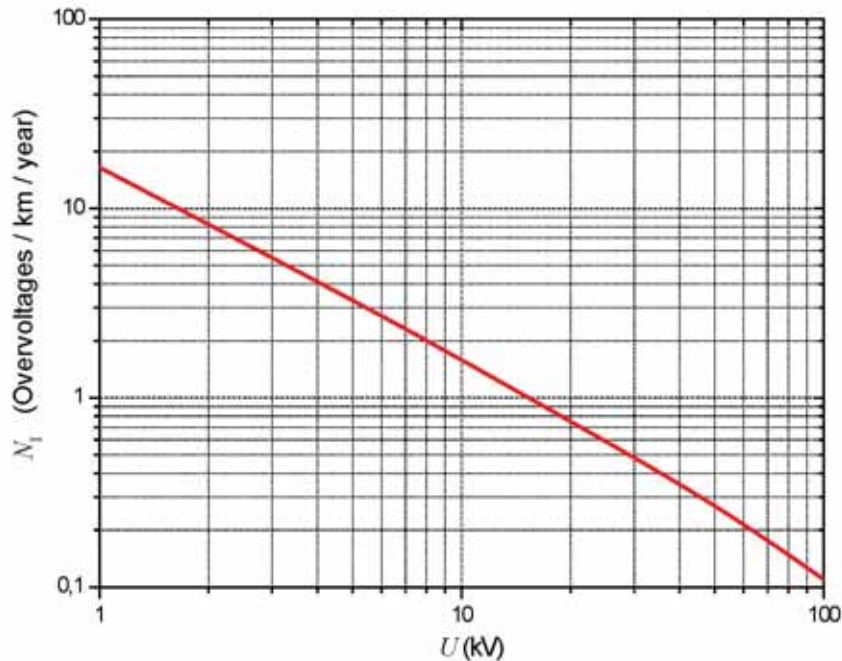


Figure 3.31. Annual number of overvolatlegs due to lightning stroke termination near the line as a function of induced peak value for Rusck model.

It should be stressed that the obtained results are similar for both ways of  $y_{\min}$  parameter determination, expressed by equations (3.77) and (3.82). Moreover, it is to note that the results obtained by (3.74) are identical if only the medium value of lightning current  $I_m$  is considered, so that the following simplified equation (3.83) may be derived:

$$N_1 = 2000 \cdot N_g \cdot 10^{-6} \left[ \left( \frac{Z_o \cdot I_m \cdot h}{U} \right) - (0,67 \cdot h^{0,6} \cdot I_m^{0,74}) \right] \quad (3.83)$$

According to empirical formula proposed by Popolansky [88], the annual number of overvoltages can be estimated as follows:

$$N_1 = N_g \cdot a \cdot U^{-b} \quad (3.84)$$

where:

$a$  – empirical constant ( $a = 18$ );

$b$  – empirical constant ( $b = 1,3$ ).

The calculations are performed similar to the previous case. The annual number of overvoltages is shown in Fig. 3.32.

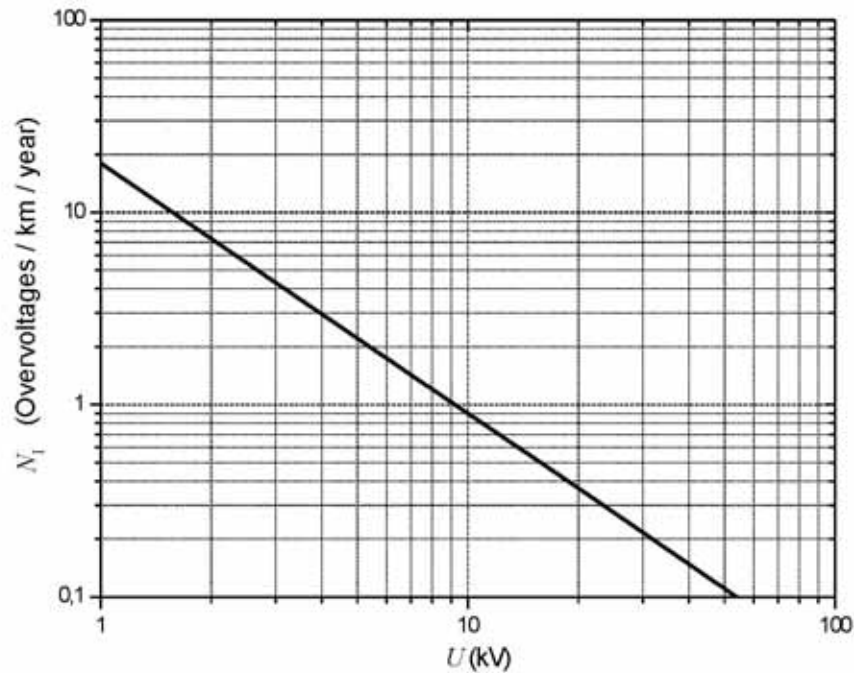


Figure 3.32. Annual number of overvoltages due to lightning stroke termination near the line as a function of induced peak value from Popolansky formula (3.84).

In technical report [89] the estimation of annual number of overvoltages due to lightning near the line is defined as follows:

$$N_1 = 1,9 \cdot 10^{-6} \cdot N_g \cdot H \cdot L \cdot \left[ 3,5 + 2,5 \cdot \log \frac{30 \cdot (1-c)}{U} \right]^{3,75} \quad (3.85)$$

where:

$c$  – conductor coefficient ( $c = 0$  for absence of grounded neutral or grounded earth conductor;

$c = 0,7 \div 0,9$  for multiple-grounded neutral conductor in a preassembled bundle).



The calculations are performed similar to the previous case. Annual number of overvoltages is shown in Fig. 3.33.

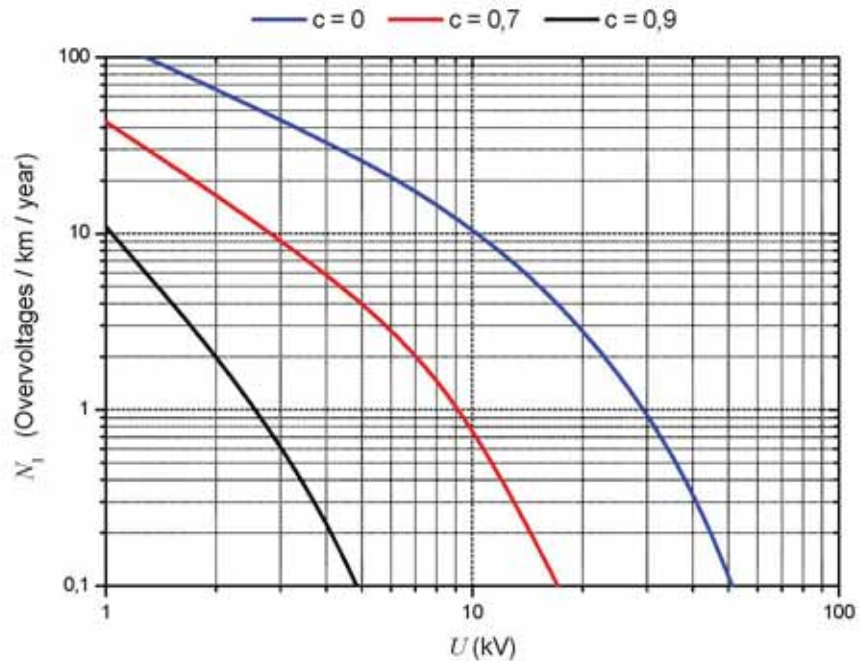


Figure 3.33. Annual number of overvoltages due to lightning stroke termination near the line as a function of induced peak value for three values of coefficient  $c$ .

Results comparison of annual number of overvoltages due to lightning near the line is shown in Fig. 3.34.

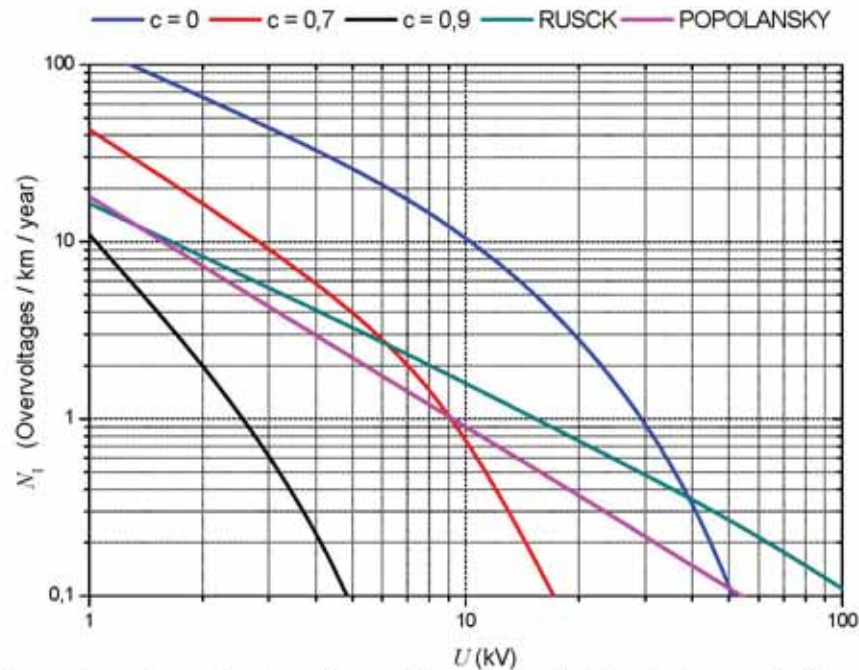


Figure 3.34. Comparison of annual number of overvoltages due to lightning stroke near the line as a function of induced peak value from CIGRE, Rusck and Popolansky.

### 3.6. Summary

In the present chapter the sources of damage due to lightning are analysed. The survey started from general recognition of lightning occurrences and related results to the dangerous events.

Possible dangerous occurrences due to lightning are analysed according to standard recommendation taking into account the lightning point termination.

In terms of lightning protection, the following situations can be distinguished:

- flashes to the structure (S1);
- flashes near the structure (S2);
- flashes to the services connected to the structure (S3);
- flashes near the services connected to the structure (S4).

In case of direct flashes to a structure (S1), the failure of electrical and electronic systems can be due to resistive and inductive coupling of lightning current.

In case of flashes near the structure (S2) the source of damage is caused by LEMP. The overvoltages inside the structure can be created in common mode as well as differential mode due to inductive coupling of lightning current. This type of damage can be particular dangerous for low voltage apparatus and controlling system.

In case of flashes to a line (S3) the source of damage is intended as an overvoltage with a conventional wave shape  $1,2/50 \mu\text{s}$  [18] which can damage apparatus connected.

In case of flashes near the services connected to the structure (S4) lightning current induces voltages on the phase conductors and on the ground wires (if installed), which result in severe stress on the line insulation and apparatus connected.

In paragraphs of this chapter the evidenced sources of damage are described. The prevailing parameters determination and calculation for each type of source is shown and discussed. Moreover special focus is dedicated to the calculation of dangerous event frequency.

On the base of performed analyses, it can be concluded that even if the source of damage S1 is not so frequently as the indirect occurrences, such source is by all means more critical respect to the other damage sources taking into account lightning current values and effects.

The formula suggested by the IEC standards for the estimation of frequency of dangerous events for direct and indirect flashes to a structure seems to give results not on the safety side.

# Chapter 4

## 4. Characteristic and technology of selected protection measures: numerical representation for computer simulations

### 4.1. Surge protective devices

#### 4.1.1. Introduction

This paragraph provides information on the characteristic and technology of surge protective devices (SPD) usually installed for the protection of low voltage systems.

SPD belong to group of measures intended to limit transient overvoltages and divert surge currents by means at least one non-linear component.

Lightning surges frequently cause failure of electrical and electronic systems within a structure due to insulation breakdown or when overvoltages exceed the equipment's common mode insulation level. As discussed in the previous chapter, the dangerous occurrence for instance can be result by lightning flashes to a structure (source of damage S1), near the structure (S2), to a service connected to the structure (S3) and near a service connected to the structure (S4).

Example of switch board failure due to mentioned events is presented in Fig. 4.1., of course magnitude of possible failures depends on lightning current value and are not limited only to the switch board but can also include failures of apparatuses installed in circuits internal to the structure.



Figure 4.1. Low-voltage switch board without SPD singed due to lightning overvoltage [90].

To reduce the risk of these events and assure apparatus operation, SPD can be applied as a protection measure. This protection measure can be located between the phase to be protected and ground (commune mode of installation) in order to discharge to ground incoming surges, in other words the dangerous overvoltages are reduced to the protection level of SPD.



The basic criterion for SPD protection level selection is represented by the following general formula:

$$U_p \leq U_w \quad (4.1)$$

where:

$U_p$  – SPD protection level;

$U_w$  – rated impulse withstand voltage of apparatus to be protected.

In other case if  $U_w$  has a lower value than  $U_p$ , namely the incoming overvoltage exceeds the withstand capability of the electrical apparatus, the insulation of the equipment is destroyed and whole surge current flows through the apparatus to be protected.

The equation (4.1) only introduces to the SPD selection, because the real criteria are much more complex. The detailed aspect of selection and proper installation of SPDs is described in next chapter 6. Fig. 4.2. shows an example of SPD installed in low-voltage switch board.



Figure 4.2. SPD installed in low-voltage switch board [90].

The types and models of SPD can be diversified, however it is possible to distinguish three operation regions for each of theirs:

- first operation region – before overvoltage: SPD has an high value of impedance so the regular function of apparatus installed in the circuit with SPD is assured;
- second operation region – during overvoltages: appearing overvoltage is reducing the impedance of SPD what is a reason of flowing current through SPD and reduce the overvoltage to the protection level of SPD;
- third operation region – after overvoltage: impedance of SPD is increasing, so the conditions to the regular function of apparatus protected by means of SPD are provided.

Principal electrical characteristics of SPD include following parameters:

$U_c$  – maximum continuous operating a.c. or d.c. voltage;

$U_p$  – voltage protection level;

$U_{res}$  – residual voltage;

- $I_c$  – leakage current;
- $I_n$  – nominal current of wave shape 8/20 $\mu$ s;
- $I_{max}$  – maximal current;
- $I_{imp}$  – maximal current of wave shape 10/350 $\mu$ s;
- $I_s$  – current flowing through SPD after overvoltage.

It should be stressed, that from the standard point of view the SPD issues partial or entirely are under consideration of IEC technical committees TC37, TC37A, TC64 and TC81. The committees TC37 and TC37A mostly take a stand on construction features of SPD's. The SPD selection and installation purposes are problem considered by TC64 and TC81 committee.

In accordance with the standard IEC 61643-1 Second Edition 2005-03 the manufacture shall classify the SPDs taking into account specific construction parameters, some of them are described in this section.

Taking into account the internal features of SPD and material used for the construction, it is possible to distinguish three groups of these devices.

One group represents SPD called voltage switching type, where the reduction of incoming overvoltages is assured by means of spark-gaps, gas tubes, thyristors (silicon-controlled rectifiers) or triacs installed inside a box of SPD. This group of SPD is possible called also "crowbar type".

The next group can represents SPD called limiting type, where the reduction of incoming overvoltages is assured by means of non-linear elements like varistor or suppressor diodes. These SPDs are sometimes called "clamping type".

The last group can be composed from SPD where both mentioned elements are applied in the same box of SPD to reduce incoming overvoltages.

Fig. 4.3 represents graphical symbols of SPDs.

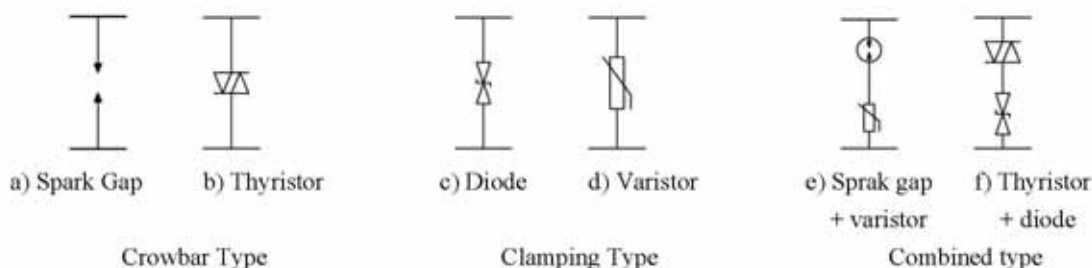


Figure 4.3. SPD symbols.

Another construction classification can be based on accessibility to live parts of SPD. This criterion is composed of two types of SPD with accessible and inaccessible live parts. To the group accessible can belongs SPD which have a free access to live parts of device. To the group inaccessible (out-of-reach) belongs SPD which have no access to live parts without the



use of tools or other equipment. This classification is very useful from the laboratory test point of view.

In accordance with introduced standard some parameters of protective measures have preferred values, for example:

- voltage protection level  $U_p$ : 0,08; 0,09; 0,10; 0,12; 0,15; 0,22; 0,33; 0,4; 0,5; 0,6; 0,7; 0,8; 0,9; 1,0; 1,2; 1,5; 1,8; 2,0; 2,5; 3,0; 4,0; 5,0; 6,0; 8,0 and 10 kV
- r.m.s. or d.c. maximum continuous operating voltage  $U_c$ : 52; 63; 75; 95; 110; 130; 150; 175; 220; 230; 240; 250; 260; 275; 280; 320; 420; 440; 460; 510; 530; 600; 630; 690; 800; 900; 1000 and 1500 V

Moreover the system type can have also an impact for the classification of SPDs. In common use are SPDs dedicated for the alternative current (a.c.) and direct current (d.c.).

The installation aspects of SPD can refer e.g. to the number of ports or location of these measures. The SPD with one port is SPD connected in shunt with the circuit to be protected. A one port device may have separate input and output terminals without a specific series impedance between these terminals. However SPD with two ports is an SPD with two sets of terminals, input and output. A specific series impedance is inserted between these terminals.

Installation location of protection measures can be based on the environment requires causing two general groups like indoor and outdoor SPD. The indoor SPDs are adapted to "friendly" conditions [91]. However the outdoor SPDs shall be contained in a weather shield of glass, glazed ceramic or other acceptable material that is resistant to UV radiation, corrosion, erosion, and tracking to assure correct operation during weather difficulties. The mounting method can also consist a classification of SPD.

Moreover the IEC standards [91] introduce SPD from durability point of view. For this reason the IEC technical committees developed class tests. The conditions of tests are clearly specified in typical standards. The tests are defined as follows:

- class I tests carried out with the nominal discharge current waveshape of 8/20  $\mu$ s, the 1,2/50  $\mu$ s voltage impulse with a virtual front time of 1,2  $\mu$ s and a time to half-value of 50  $\mu$ s, and the maximum impulse current  $I_{imp}$  for class I test defined by three parameters, a current peak value  $I_{peak}$ , a charge  $Q$  and a specific energy  $W/R$ . The parameter values are suggested by IEC 61643-1 standard, namely:  $I_{peak}$  1,0; 2; 5; 10; and 20 kA and  $Q$  charge 0,5; 1; 2,5; 5; and 10 As;
- class II tests carried out with the nominal discharge current, crest value of the current through the SPD having a current waveshape of 8/20  $\mu$ s, the 1,2/50  $\mu$ s voltage impulse with a virtual front time of 1,2  $\mu$ s and a time to half-value of 50  $\mu$ s, and the maximum discharge current  $I_{max}$  has 8/20 $\mu$ s waveshape and magnitude according to the test sequence of the class II operating duty test.  $I_{max}$  is greater than  $I_n$ . The parameter values are suggested by IEC 61643-1 standard and nominal discharge current for class II tests should have the following peak value: 0,05; 0,1; 0,25; 0,5; 1,0; 1,5; 2,0; 2,5; 3,0; 5,0; 10; 15 and 20 kA;
- class III tests carried out with the combination wave (1,2/50  $\mu$ s, 8/20  $\mu$ s). the combination wave is delivered by a generator that applies a 1,2/50  $\mu$ s voltage impulse across an open circuit and an 8/20  $\mu$ s current impulse into a short circuit. The voltage, current amplitude and

waveforms that are delivered to the SPD are determined by the generator and the impedance of the SPD to which the surge is applied. The ratio of peak open-circuit voltage to peak short-circuit current is 2; this is defined as the fictive impedance  $Z_f$ . The parameter value of open-circuit voltage for class III tests is suggested by IEC 61643-1 standard and consist the following row: 0,1; 0,2; 0,5; 1; 2; 3; 4; 5; 6; 10 and 20 kV.

The class tests classification is very useful for the selection appropriate type of SPD according to the lightning protection zones defined in topical standards on lightning protection [11].

#### 4.1.2. SPD switching type

The SPD switching type is used to prevent high current surges. A spark gap has two electrodes separated by an insulation, e.g. air or gas. One of the electrodes is electrically connected to the protected conductor, and the other pin is connected to the earthing system. In case of lightning surge higher than  $U_p$  of SPD considered an electric arc is formed between the electrodes. The area when an electrical arc is formed during ignition of SPD is called striking area. This occurrence provide the lightning current to ground and finally apparatus is exposed to reduced overvoltages. The residual voltage of SPD ( $U_{res}$ ) depends on the construction features like spark gap configuration, namely distance between electrodes, shape of electrodes and so on as well as on the ambience conditions like pressure, humidity or contamination of air or gas.

The Fig. 4.4. shown the operation regions in time of typical SPD switching type. The characteristic parameters  $U_{res}$ ,  $U_{in}$  and the adequate operation regions are specified.

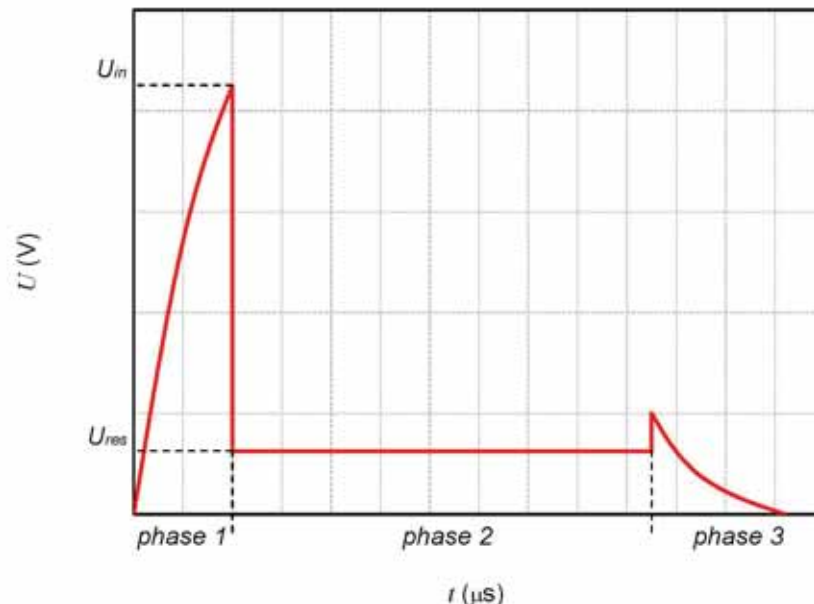


Figure 4.4. Function characteristic of SPD switching type.

The first part of characteristic called phase 1, belong to the ignition of SPD. The wave shape is equal to the stressing overvoltages. The possible delay between these two shape is  $50 \div 100$ ns. The maximal voltage value ( $U_{in}$ ) is determinate by the spark gap condition; its value is assumed to be protection level of SPD ( $U_p$ ). The second phase of characteristic

represents the reduced overvoltage due to electrical arc between electrodes of SPD. The voltage value ( $U_{res}$ ) as well as the time of duration occurrence depends on the overvoltage feature. The  $U_{res}$  is caused due to arc resistance created during ignition of SPD. Generally the maximal value of this voltage is much more lower than operation voltage of circuit to assure apparatus protection. The period of second phase depends only on the overvoltage duration. The interruption of occurrence represents the third phase of characteristic. At the beginning is usually notated a small overshoot of voltage due to the arc magnetic and thermic influences.

Fig. 4.5. represents the trigger voltage of SPD switching type. The characteristic shows that the trigger voltage depends on the overvoltage shape. The higher values of steepness (curve 1) create a situation when the  $U_{in}$  can achieve an higher value and ignition dispersion has a lower value. The long shape of overvoltages (curve 2) cause a situation when the  $U_{in}$  can achieve a lower value and ignition dispersion has a high value.

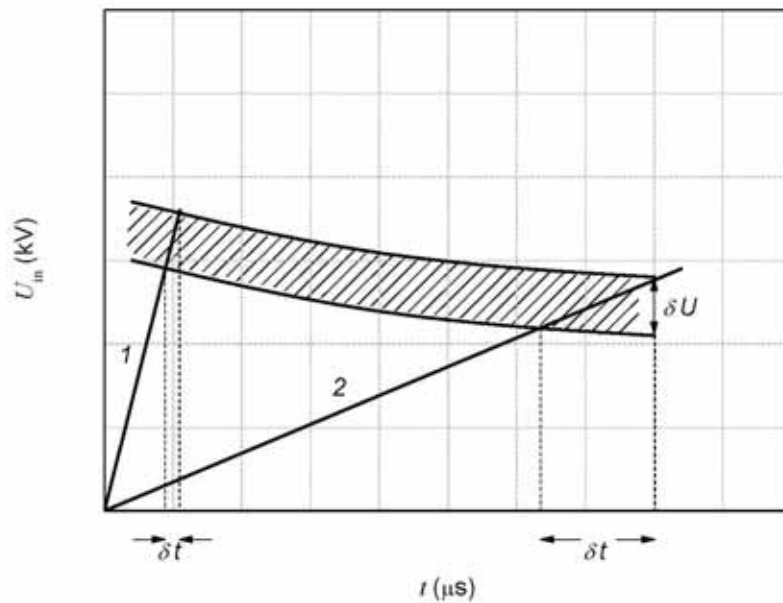


Figure 4.5. The trigger voltage of SPD switching type:  $\delta u$  - trigger voltage dispersion;  $\delta t$  - trigger time dispersion; 1 – overvoltage with a front steepness 10 kV/ $\mu s$ ; 2 – overvoltage with a front steepness 1 kV/ $\mu s$ .

An example of SPD vertical section switching type is shown in Fig. 4.6.

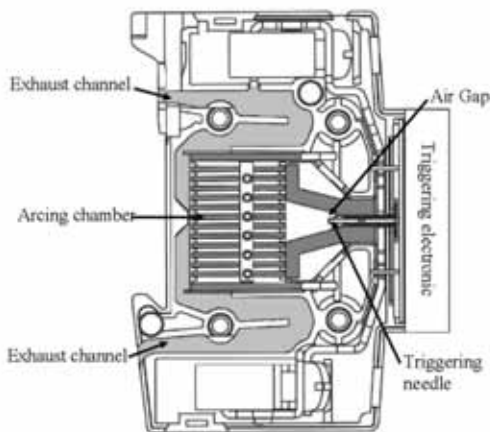


Figure 4.6. Example of SPD switching type - spark gap technology [92].

The technology used for the construction aim can be diversified, however the basic element include always a spark gap with two electrodes.

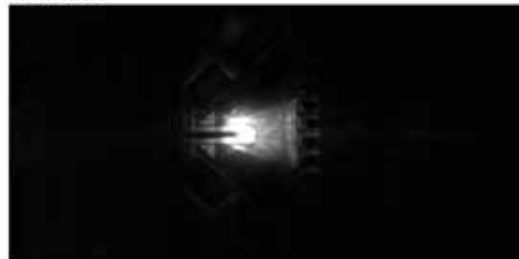
In the example shown in Fig. 4.6 the triggering electronic will detect a surge arrives, and amplify it. The potential between the triggering needle and the electrodes reaches the air breakdown voltage after a few  $\mu\text{s}$  and a little spark is generated at the needle head. The little spark commutes the air gap, thus creating a highly conductive connection between the two electrodes through which the surge energy is driven to ground. The lightning current then flows from the phase to ground and the electrical installation downstream of the SPD is protected. The electric arc is not extinguished spontaneously after the surge pulse and a short-circuit current called the “follow current” therefore continuous to flow. To prevent the installation from being powered down, this follow current should be interrupted without causing the general interrupter devices of the installation, such as circuit-breakers, to open. For this reason, the protection device includes an adapted current interrupter device able to interrupt a high current. This interrupter device generally comprises an arcing chamber (splitter device) taking the form of spaced parallel metal plates used to divide the electric arc into a plurality of small individual arcs in order to build up a high voltage limiting and finally interrupting the follow current. The V shaped electrodes are fixed and enlarge the length of the arc and guide the arc towards the arcing chamber. Hot gas exits passing through the exhaust channels where it is cooled to avoid any fire risk. In the end, this protective device will release neither incandescent material nor burning gas into its immediate environment. It may therefore be installed in the majority of applications [92].

The behaviour of the arc and its moves inside the SPD is shown in Fig. 4.7. The photographs were taken with a highspeed camera (framing rate 10000 frames/s) [92]. The frames show the different phases of the arc from its birth between the needle and the electrode until it extinguishes.

Frame 1



Frame 2



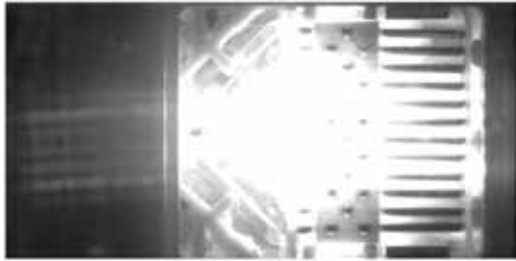
Frame 3



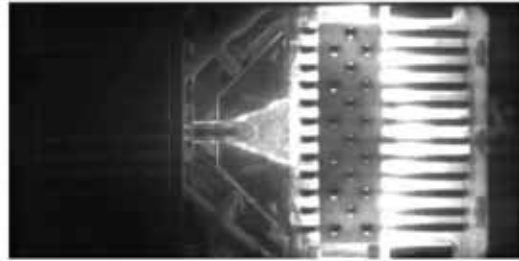
Frame 4



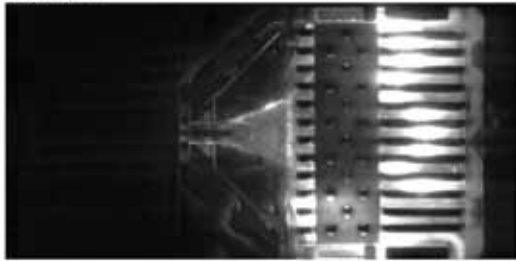
Frame 5



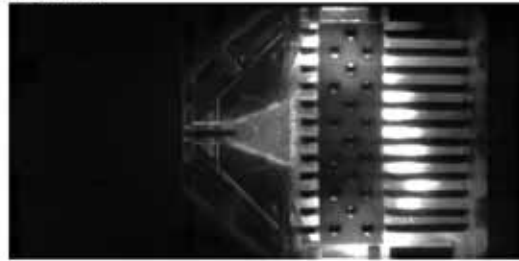
Frame 6



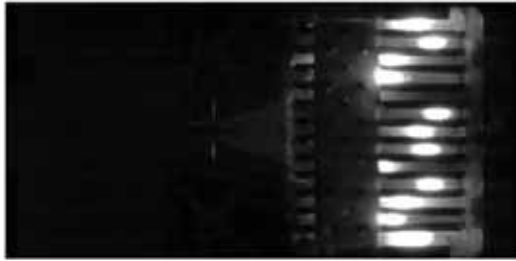
Frame 7



Frame 8



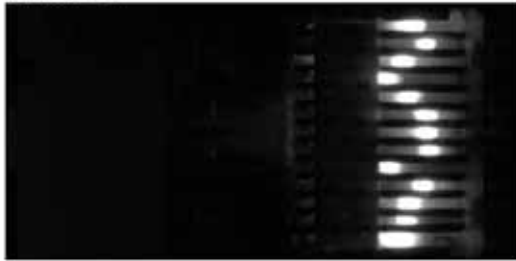
Frame 9



Frame 10



Frame 11



Frame 12



Figure 4.7. Arc initiation, displacement and extinction high speed movie for a 10/350  $\mu$ s pulse with 10 kA peak current. (Framing rate 10000frames/s) [92].

The SPD switching type is able to discharge very heavy lightning currents, of the order of several tens of kilo Ampere. This consist a main feature of these protection measures, moreover to the group of benefits is possible to add also, simple construction, efficient life duration, lossless current protection (leakage current doesn't exist). However, this device has also drawbacks. The first resides in the fact that the electrical arc causes significant release of



hot gases, or even flames, which may damage the immediate environment of the device. The protection based on the arc phenomena create also a difficulties in case of application for low voltage systems. The fact that the electrical arc causes a short circuit between the phase and ground, and it is not quenched spontaneously after the lightning current has passed. The follow current continues to flow to ground and may cause the installation to become inoperative. Moreover the ambient influence has also an impact for protection features, mainly for  $U_{in}$ .

#### 4.1.3. SPD limiting type

The SPD limiting type is based on non-linear elements like varistor or suppressor diodes. Those non-nonlinear elements provide limit incoming overvoltage in range of time about few nanosecond after exceed protection level. In applications of lightning protection varistor SPDs are widespread. Suppressor diodes are in common used in electronic applications. However for both elements  $U / I$  curve consist essential feature. An example of  $U / I$  curve for metal oxide varistor is presented in Fig. 4.8.

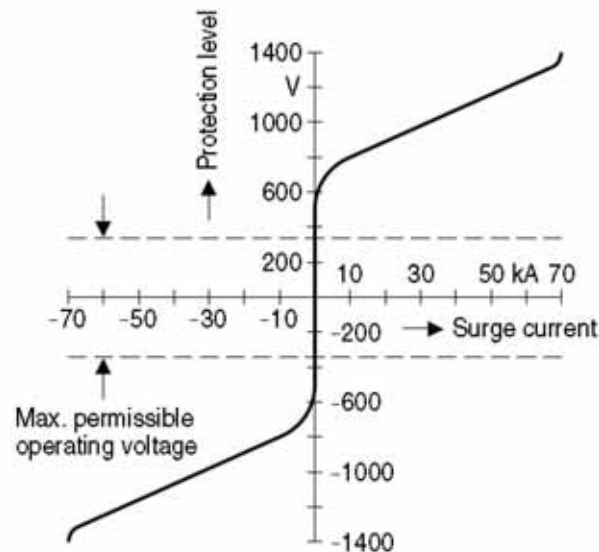


Figure 4.8. Typical  $U / I$  characteristic curve of a metal oxide varistor on a linear scale [93].

The shape of characteristic is obtained by means of the microstructure and conduction mechanism of varistor. Fig. 4.9. in simplified form, presents conducting phenomena. The zinc oxide grains themselves are highly conductive, while the intergranular boundary formed of other oxides is highly resistive. The electrical behavior of the metal oxide varistor, results from the number of microvaristors connected in series or in parallel.

This implies that the electrical properties are controlled by the physical dimensions of the varistor [93]:

- twice the ceramic thickness produces twice the protection level because then twice the number of microvaristors are arranged in series;
- twice the area produces twice the current handling capability because then twice the number of current paths are arranged in parallel;



– twice the volume produces almost twice the energy absorption capability because then there are twice as many absorbers in the form of zinc oxide grains.

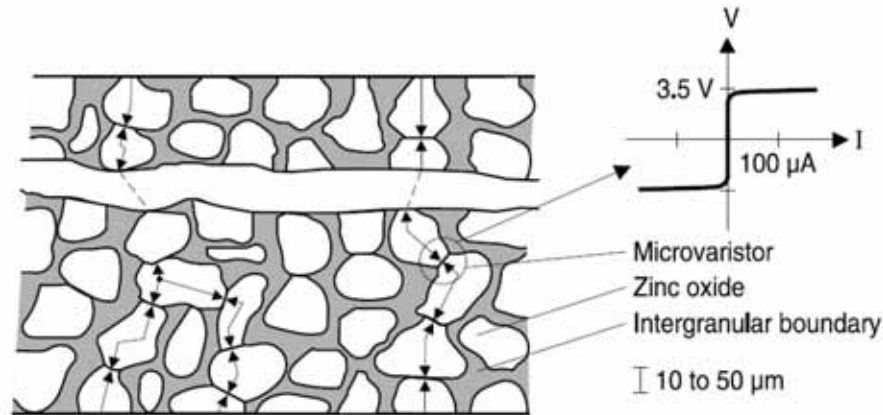


Figure 4.9. Conduction mechanism in a varistor element [94].

The symmetrical non-linear shape is result of resistance decreases with increasing voltage. The voltage dependence of varistor may be approximately characterized by the formula:

$$I = K \cdot U^\alpha \quad (4.2)$$

where:

$I$  – current flowing through varistor;

$K$  - ceramic constant (depending on varistor type);

$U$  - voltage across varistor;

$\alpha$  – nonlinearity exponent (measure of nonlinearity of curve), can be interpreted as a measure of the “steepness” of the  $U/I$  characteristic.

Another possible interpretation of the physical principle underlying the  $U/I$  characteristic curve of a metal oxide varistor is that of a voltage dependent resistance value, and particularly its rapid change at a predetermined voltage.

$$R = \frac{U}{I} = \frac{U}{K \cdot U^\alpha} = \frac{1}{K} \cdot U^{1-\alpha} \quad (4.3)$$

Equations (4.2) and (4.3) can be transformed to the following form:

$$\log I = \log K + \alpha \log U \quad (4.4)$$

and

$$\log R = \log \frac{1}{K} + (1 - \alpha) \log U \quad (4.5)$$

Those equations cannot cover the downturn and upturn regions of characteristics. However simple form express clearly  $U/I$  characteristic issue.

The  $U/I$  characteristic can be also describe as follows:

$$\log U = b_1 + b_2 \cdot \log(I) + b_3 \cdot e^{-\log(I)} + b_4 \cdot e^{\log(I)} \quad (4.6)$$

where:

$b_1$ - $b_4$  – individual parameters of SPD.

However reduced access to the appropriate  $b_1$ - $b_4$  values create some difficulties for practical application [95]. Going back to the principal equations (4.2-5), it is important to mention that  $\alpha$  parameter (as shown in Fig. 4.10.) has different values. This parameter can be calculated as follows:

$$\alpha = \frac{\log I_2 - \log I_1}{\log U_2 - \log U_1} \quad (4.7)$$

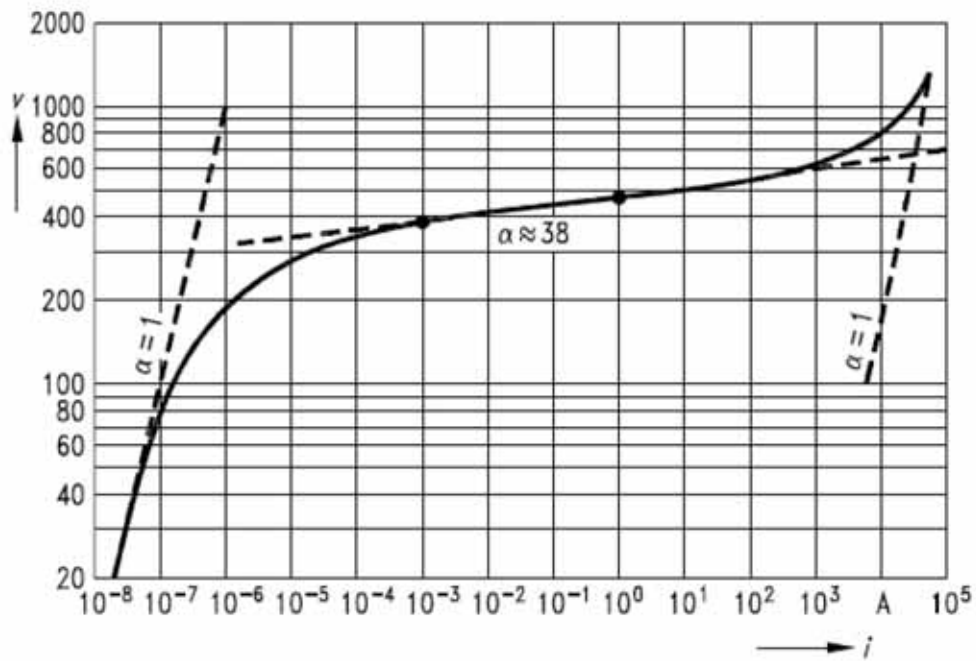


Figure 4.10.  $U / I$  characteristic of a metal oxide varistor with  $\alpha$  parameters regions [94].

First part of characteristic covers leakage current region ( $< 10^{-4}$  A) where  $\alpha = 1$ . In the leakage current region the resistance of an ideal varistor goes towards  $\infty$ .

Second part of characteristic covers normal operating region ( $10^{-5}$  to  $10^3$  A) where  $\alpha > 30$ . Generally this part of characteristic has a more or less a straight line on a log-log scale.

Third part of characteristic covers high-current region ( $> 10^3$  A) where  $\alpha = 1$ . Here the resistance of the ideal varistor approaches zero.

The typical  $R/U$  characteristic of a metal oxide varistor is shown in Fig. 4.11.

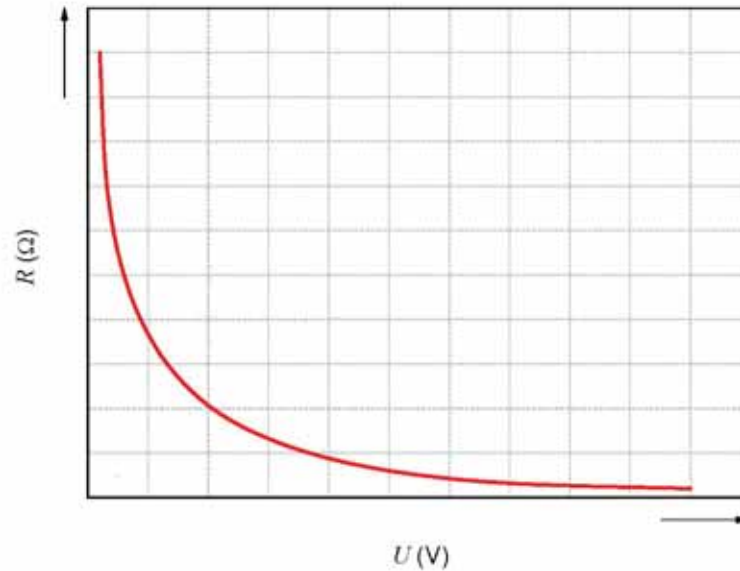


Figure 4.11. Typical  $R/U$  characteristic curve of a metal-oxide varistor.

Fig. 4.12 represents in time domain the typical operation steps of SPD limiting type. This characteristic can be useful to determination energy absorption aspects. In case of SPD limiting type  $U_{res}$  value is assumed to be protection level ( $U_p$ ).

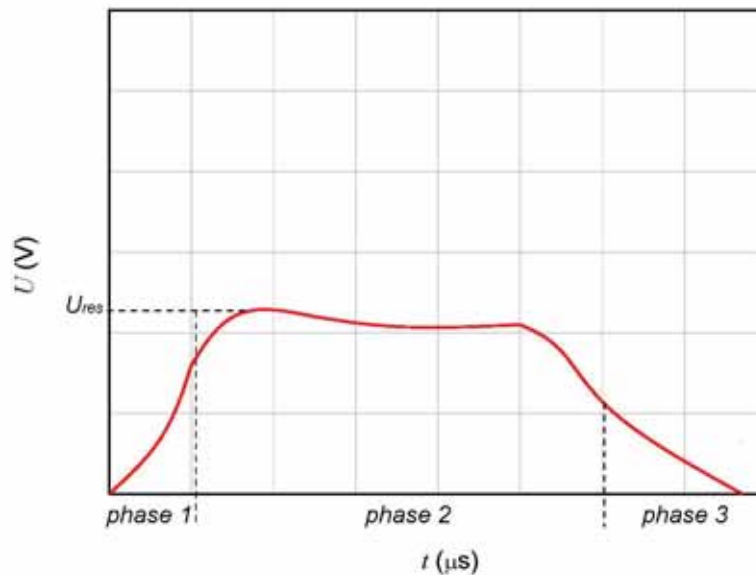


Figure 4.12. Function characteristic of SPD limiting type.

The energy absorption of a varistor is correlated with the surge current.

$$W = \int_{t_0}^{t_k} u(t)i(t)dt \quad (4.8)$$

where:

$u(t)$  - voltage drop across the varistor during current flow;

$i(t)$  - current flow through the varistor.

The varistor SPDs used for the aim of lightning protection have different benefits. Those benefits are composed of very low protection level, perfectly application for low-voltage apparatus, possible high value of residual voltage, precision, short time of delay after exceed protection level. However those elements have also disadvantageous features like reduction possibility to absorb high value of currents, determinate lifetime, leakage current.

#### 4.1.4. Computer implementation of surge protective devices

The proper representation of surge protective devices refers to the state of art of scientific knowledge. For this aim many studies are provided [96-106]. This problem is also considered by members of topical IEEE working group [97].

The knowledge of phenomena occurrences during normal operations of protection measures allows to implement a model of devices. Nowadays is a lot of different engineering's software which permit to simulate electrical circuits. Taking into account the transient character of dangerous events in common use are: Matlab, Orcad, ATP-EMTP and EMTP-RV. These programs have specific own advantages as well disadvantages. This paragraph intends to give an overview on surge protective device representation.

To determinate a characteristic of SPD switching type as well as of SPD limiting type is possible to use different models [96-106]. The SPD representation can have an impact on obtained results, even the same characteristic is implemented [107-109].

In basic models for simulations SPD switching type an ideal switch can be used. The protection level of SPD ( $U_p$ ) can be estimated considering the stressing source characteristic. For this aim the steepness of incoming source and the time duration of flat part of characteristic before the impulsive part, if exist, is needed to determinate the intervention time of switch [96, 98-102]. In more complex models the arc resistance is considered.

In the EMTP-RV program a model of SPD switching type is possible to determinate by means of different methods in order to obtain a desirable  $U/t$  characteristic [110, 111]. In any case some preliminary investigation with aim to determine model correctness is always recommended.

Equivalent circuit of surge protective device limiting type is shown in Fig. 4.13 [12].

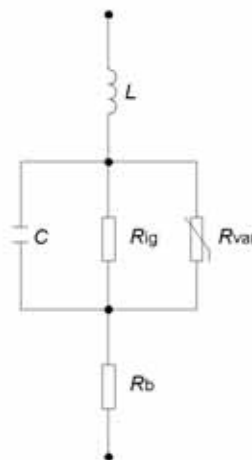


Figure 4.13. Equivalent electrical circuit of SPD limiting type.

where:

$L$  – inductance ( $\approx 1$  nH/mm);

$C$  – capacitance;

$R_{ig}$  – resistance of intergranular boundary ( $\rho \approx 10^{12} \div 10^{13}$   $\Omega$ /cm);

$R_{var}$  – ideal varistor ( $0 \div \infty$   $\Omega$ );

$R_b$  – bulk resistance of ZnO ( $\rho \approx 1 \div 10$   $\Omega$ /cm).

The simplified equivalent circuit (shown in Fig. 4.13) refer to a metal oxide varistor. From this circuit the behavior of the varistor can be interpreted for different current ranges, namely: leakage current region, normal operating region and high current region.

The circuitual representation of leakage current region ( $< 10^{-4}$  A) is shown in Fig. 4.14. In this case the resistance of an ideal varistor goes towards  $\infty$ , so it can be ignored as the resistance of the intergranular boundary will predominate. Therefore  $R_b \ll R_{ig}$ .

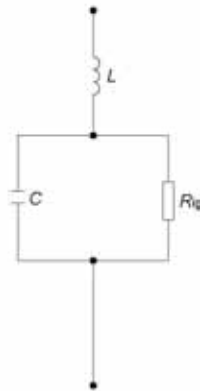


Figure 4.14. Electrical circuit of leakage current region of SPD limiting type.

The ohmic resistance  $R_{ig}$  determines behavior at low currents, the  $U / I$  curve goes from exponential to linear (downturn region).  $R_{ig}$  shows a distinct temperature dependence, so a marked increase in leakage current must be expected as temperature increases.

The circuitual representation of normal operating region ( $10^{-5}$  to  $10^3$  A) is shown in Fig. 4.15. With  $R_v \ll R_{ig}$  and  $R_b \ll R_v$ ,  $R_v$  determines the electrical behavior. The  $U / I$  curve (Fig. 4.10) may be correctly approximated with the simple mathematical description by an exponential function with  $\alpha > 30$ .

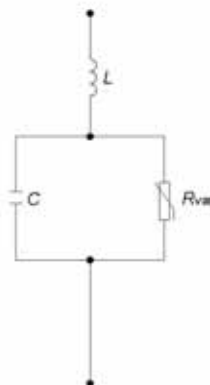


Figure 4.15. Electrical circuit of operating region of SPD limiting type.

The circuital representation of high-current region ( $> 10^3$  A) is shown in Fig 4.16. Here the resistance of the ideal varistor approaches zero. This means that  $R_v \ll R_{ig}$  and  $R_v < R_b$ . The ohmic bulk resistance of ZnO causes the  $U/I$  curve to resume a linear characteristic (upturn region).



Figure 4.16. Electrical circuit of high-current region of SPD limiting type.

In the EMTP-RV program, as for SPD switching type, a model of SPD limiting type is also possible to be implemented by means of different methods in order to obtain a desirable  $U/I$  characteristic [95, 112]. In any case some investigations to model verification are recommended.



## 4.2. Isolation transformer

### 4.2.1. Introduction

Usually electrical transformers are used to transform voltage from a higher level to a lower voltage. These devices attenuate the passage of noise or transients from the primary to the secondary. Transformers can also be used to change the impedance of the electrical circuit to reduce the short-circuit current or to provide a galvanic isolation between two systems. The definition of isolation transformer applies to any transformer where there is no direct connection between the primary and the secondary windings, because the windings are connected only by the magnetic flux in the core [113].

Separation transformers provide a basic separation between the primary and secondary windings. This feature provides a degree of protection against electric shock that is equivalent to a basic insulation. A separation transformer can limit the risks of danger in the event of accidental simultaneous contact with the exposed conductive part and the live parts or metals parts that can become live in the event of an insulation fault. The symbols representation of separation transformer are shown in Fig. 4.17.

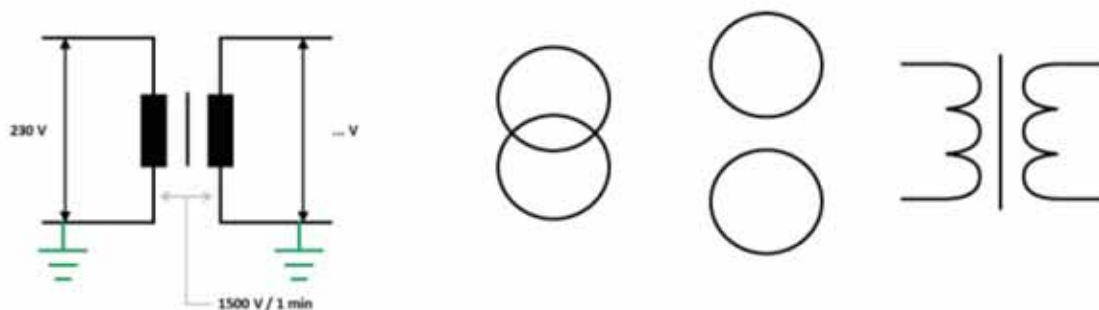


Figure 4.17. Separation transformer symbols representation [113].

Safety transformers provide a limitation of secondary voltage to  $U_L$ , where  $U_L$  is the Safety Extra Low Voltage (SELV) Limit. The symbols representation of safety transformer are shown in Fig. 4.18.

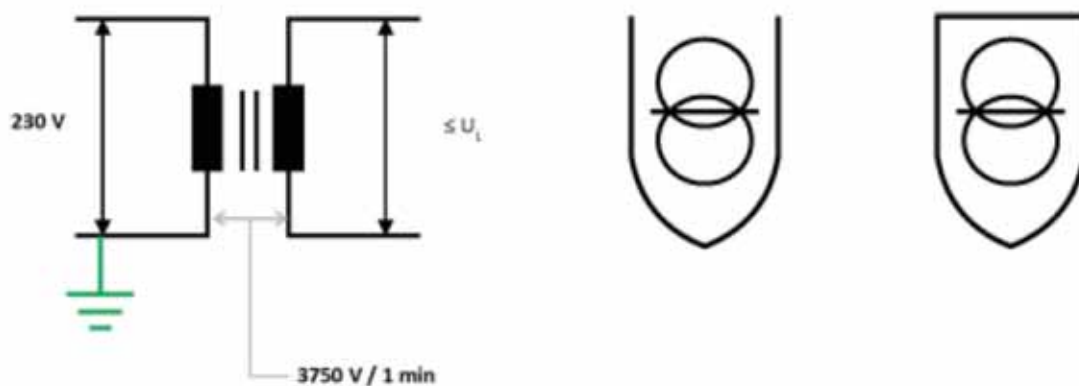


Figure 4.18. Safety transformer symbols representation [113].

Isolation transformers provide insulation between the primary and the secondary windings. An isolation transformer is a transformer used to transfer electrical power from a source of alternating current (AC) power to some apparatus while isolating the powered device from the power source, usually for safety (1:1 under load). Isolation transformers provide galvanic isolation and are used to protect against electric shock, to suppress electrical noise in sensitive apparatus, or to transfer power between two circuits which have to be separated for protection reasons. Suitably designed isolation transformers block interference caused by ground loops. Isolation transformers are commonly designed with careful attention to capacitive coupling between the two windings [114-116]. The symbols representation of isolation transformer are shown in Fig. 4.19.

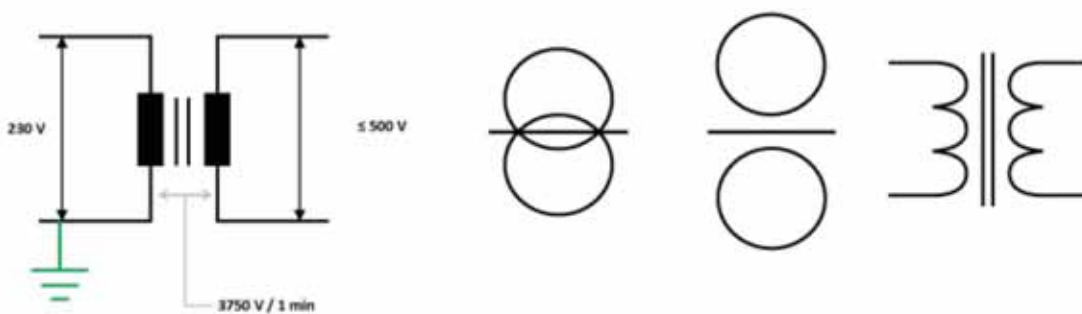


Figure 4.19. Isolation transformer with shield between two windings symbols representation [113].

Standard IEC [117] suggests construction specification of isolation transformer. The rated output voltage shall exceed 50 V a.c. or 120 V ripple-free d.c. but not exceed:

- 250 V a.c. for single-phase portable transformers;
- 400 V a.c. for polyphase portable transformers;
- 500 V a.c. or 708 V ripple-free d.c. for other transformers. In this case, the rated output voltage may be up to 1 000 V a.c. or 1 415 V ripple-free d.c. to be in accordance with the national wiring rules or for a special purpose. This output voltage limitation apply even when output windings, not intended for interconnection, are connected in series.

Moreover the rated output shall not exceed:

- 25 kVA for single-phase transformers;
- 40 kVA for polyphase transformers.

Isolation transformers can be used to protect people from electric shock and as a power supply for sensitive apparatus (computers, medical equipment, laboratory equipment, etc.) or isolate the apparatus from the rest of the electrical installation.

Typical fields of application an isolation transformers include:

- recording studios;
- commercial / residential movie theatres;
- server rooms;
- variable speed drives;
- inverters;

- UPS;
- frequency converters;
- arc welders;
- induction heaters;
- printing presses;
- non-linear loads;
- hid lighting;
- fluorescent lighting;
- power supply of devices not at ground potential.

The isolation between systems avoid loss of power in the case of a first insulation fault. Since there is no return path to the source (the secondary winding of the transformer), in the event of a fault, there will be no fault current flowing and no overcurrent protective device will cut off the supply. Apart from being harmless to persons touching the conductive parts, a first fault will not cause any danger but will also not cut off the supply. Another application of the isolation transformer is to create a star point in grids that do not have such a point. Quite a few applications need the neutral point for controlling purposes. When installing such a machine in a grid without star point, the obvious remedy is to install an isolating transformer. The normal use for isolation transformers is to produce a zone of supply that has no reference to earth [118]. The majority of electric shocks are those involving contact with a live conductor while standing on, or touching an earthed surface. Electrical isolation is considered to be particularly important on medical equipment, and special standards apply [119]. Often the system must additionally be designed so that fault conditions do not interrupt power, but generate a warning. For the safety of the patient in hospitals, all diagnostic or therapeutic medical equipment (medical electrical devices and non-medical electrical devices in the patient environments and/or areas for medical use) should be completely isolated from the supply line (double and strengthened isolation). Complete patient/operator safety is assured by medical isolation transformers with very low leakage current. An example of medical isolation transformer is shown in Fig. 4.20. and its electrical particular symbol in Fig. 4.21.



Figure 4.20. Example of medical isolation transformer [120].



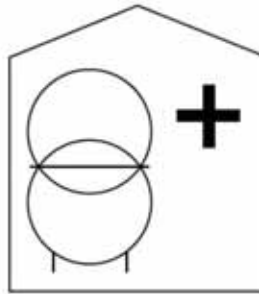


Figure 4.21. Electrical symbol of medical isolation transformer [120].

According to [119, 121] medical transformers are designed:

- to isolate the patient from an electric shock;
- to isolate the operator from an electric shock;
- to protect the equipment from power surges or faulty components.

The [121] suggests that medical transformers:

- should be cooling by air;
- short circuit voltage should fulfilled  $U_{cc} \leq 3\% U_n$ ;
- leakage current of the enclosure to earth  $I_o \leq 3\% I_n$ .

In medical field isolating transformers are used to provide a safer patient environment by minimizing the potential hazards caused by touch voltages and by ensuring that under single fault conditions there is still continuity of supply. The output of the isolating transformer is not connected to earth and so provides better protection from potentially lethal shock hazards by removing the low impedance earth return path. It should be noted that isolating transformers alone are not intended to protect against micro-shock and must be used in conjunction with circuit integrity monitoring devices and equipotential earth bonding. Toroidal transformers are ideal for the use in a medical environment because they are compact, can be completely encapsulated, have low stray-fields and are therefore less likely to cause radiated electromagnetic disturbances. Moreover in this particular field of application, a monitoring device shall be provided to indicate the occurrence of a first fault from a live part to exposed-conductive-parts or to earth. This device shall initiate an audible and/or visual signal that shall continue as long as the fault persists. If there are both audible and visible signals, it is permissible for the audible signal to be cancelled. Nevertheless, the visual alarm shall continue as long as the fault persists. It is recommended that a first fault be eliminated with the shortest practicable delay.

#### 4.2.2. Isolation transformer construction features

Isolation transformers are generally composed of two separate windings with a magnetic shield between these windings to offer noise control as shown in Fig 4.22. and Fig. 4.23. The conducting plate is bonded to the core to form an electromagnetic barrier at frequencies where the skin depth is small relative to the plate thickness, typically above 10÷20 kHz. To reduce eddy current losses, it is necessary to place a small slit in the conducting plate. A double Faraday cage topology, must be used to maintain a high degree of isolation with the slit present [122].

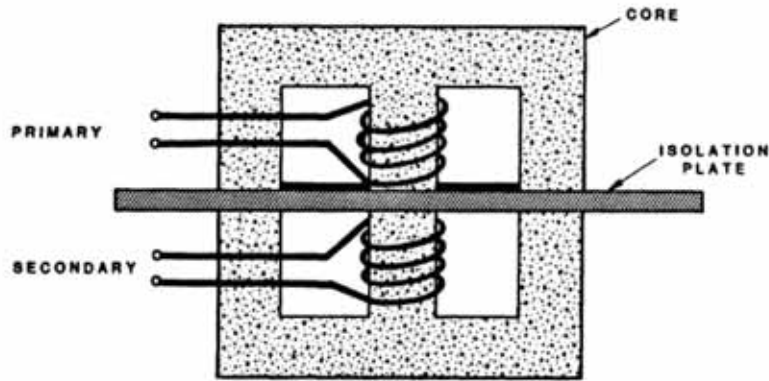


Figure 4.22. Isolation Transformer concept [122].

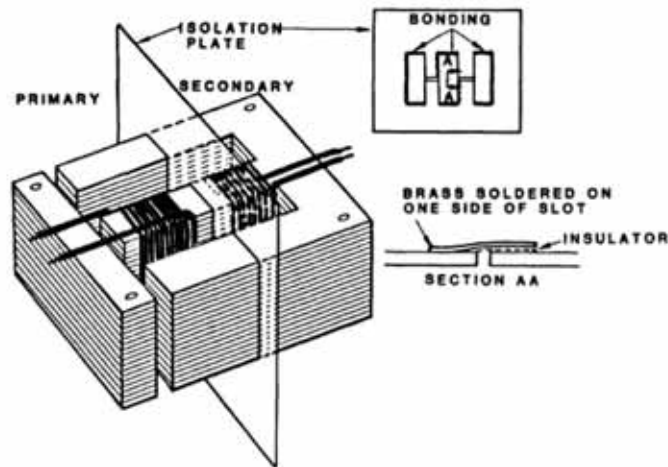


Figure 4.23. Details of conducting isolation plate [122].

The transformer carries the full load current, and thus must be suitably sized. The attenuation of isolation transformers is normally quoted in dB (decibels) for small signal noise conditions (not large transient conditions to which the transformer may offer considerably less attenuation). The main benefit offered by isolation transformers is the input-to-output isolation, where the output circuit can be re-grounded and isolated from input or other ground noise sources. This isolation can also be useful where Ground Potential Rise protection can not be afforded by normal bonding procedures.

Isolation transformer is one of the most effective devices available for rejecting common mode noise. Isolation transformers have very little effect on attenuating differential mode noise, particularly at lower frequencies as they are designed as a “pass” device at power frequencies. When coupled with a suitably grounded or shield, isolation transformers can present an effective barrier to high frequency common mode noise and prevent propagation of this noise to the down-stream equipment via the power supply or ground system as shown in Fig. 4.24. A shielded isolation transformer provides a path for high frequency common mode noise to flow via capacitive coupling to the grounded screen and thus back along the ground.

For this screening to be effective, the screen, transformer core and grounded conductors should be bonded together at a single point.

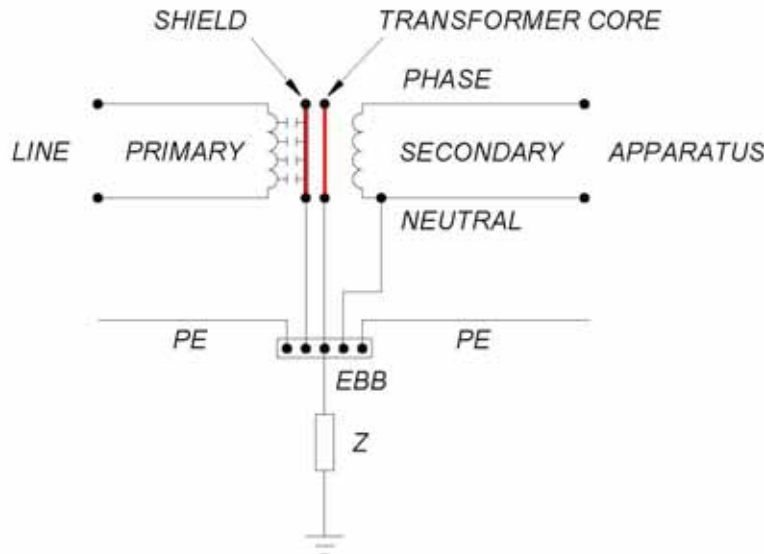


Figure 4.24. Shielded isolation transformer with shield between two windings.

#### 4.2.3. Computer implementation of isolation transformer

During lightning occurrences (high frequencies) the transformer behaves like a filter, suppressing some frequencies and passing others. In this case the inductive elements can be neglected which are important at low frequencies, but capacitive ones are predominant [123-125].

In the present paragraph two examples of transformer representation for lightning studies according to [124, 125] are presented. Moreover, an isolation transformer model and respectively parameters used for analyses in present work is reported in chapter 7.

First model example refers to the power transformer 5 kVA, 13,8/0,23 kV that takes into account the flux leakage, the winding resistance, the non-linear inductance of the core, the capacitance of the high- and low- voltage bushing as well as the capacitance between them is shown in Fig. 4.25.

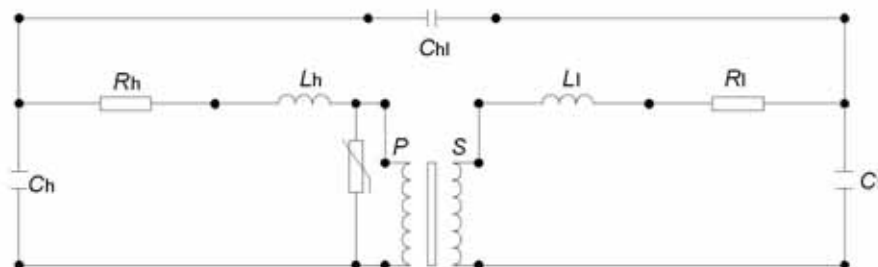


Figure 4.25. Example of transformer model.

The parameters proposed by [125] are given in Tab. 4.1.



Table 4.1. Transformer's model data [125].

Rated power: 5 kVA		
High Voltage (kV)	Low Voltage (kV)	$C_h$ (pF)
13,8	0,23	60
$C_{hl}$ (pF)	$C_l$ (pF)	$R_h$ ( $\Omega$ )
67,97	3200	335,17
$L_h$ (mH)	$R_l$ ( $\Omega$ )	$L_l$ (mH)
702,15	0,093	0,195

The second model reported as an example for computer representation of a transformer of 20 kVA rated power, 13,8/0,22 kV is the circuit model presented by Piantini et al [124]. For this case the transformer is represented by a combination of *RLC* components, the circuitual scheme is shown in Fig 4.26.

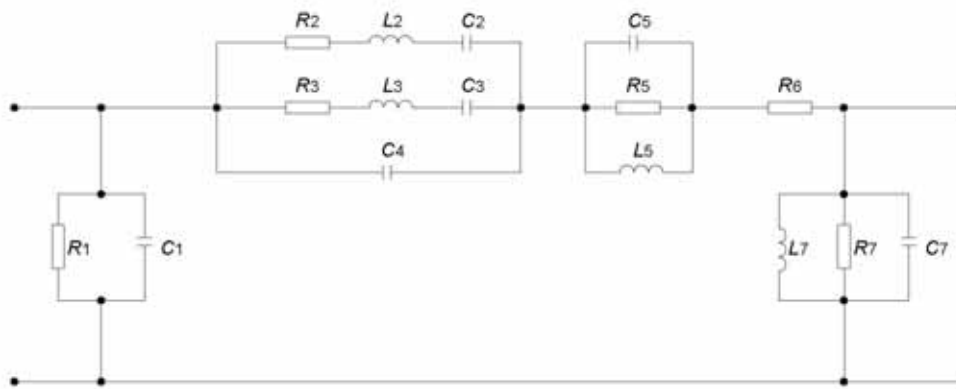


Figure 4.26. Example of transformer model: Piantini et al.

The possible values of the components for model presented in Fig. 4.26 are reported in Tab. 4.2. [124].

Table 4.2. Transformer's model data.

Element	Rate Power: 20 kVA	High Voltage: 13,8 kV	Low Voltage: 0,22 kV
	Resistance (k $\Omega$ )	Inductance (mH)	Capacitance (pF)
1	-	-	493
2	14	16	94,8
3	0,8	1,84	21,51
4	-	-	50
5	-	-	-
6	1,1	-	-
7	1,615	0,05	759,5

### 4.3. Summary

In the present chapter characteristics and technology of selected protection measures, namely, surge protective devices (SPD) as well as isolation transformers are described.

In the first part of work, the basic criteria for SPD selection and fundamental parameters are introduced. These protection measures are classified taking into account international standards recommendations. The typical characteristics defined by these bodies are given.

Paragraph on SPD switching type includes information about spark gaps. Construction features of these devices are described. Typical operational characteristics are shown.

Paragraph on SPD limiting type includes information about varistors. The principal of physics and typical response of this elements are presented. The operational regions are described and some typical characteristics are given.

Models of both types of SPD for computer simulations are presented and discussed in the last section of the first part.

The second part of present chapter includes information about isolation transformers. This protection measure is classified and typical application fields are presented. Special focus is dedicated on computer models development for transient studies.

The summary of considered protection measures taking into account protection issues is reported in Tab. 4.3. [117, 119, 126].

Table 4.3. Protection measures comparison.

<b>Problems</b>	<b>Solution</b>	
	<b>Isolation transformer</b>	<b>SPD</b>
Ground potential rise	Best	No protection
Noise	Better	Good
Common mode transient	Better	Best
Differential mode transient	No protection	Best

# **Chapter 5**

## 5. Criteria for protection measures selection according to the international standards

### 5.1. Introduction

#### 5.1.1. Standardisation bodies

In each technical field, and in particular in the electrical sector, a condition sufficient (even if not necessary) for the realization of plants according to the “status of the art” and a requirement essential to properly meet the demands of customers and of the community, is the respect of all the relevant laws and technical standards. Therefore, a precise knowledge of the standards is the fundamental premise for a correct approach to the problems of the electrical plants which shall be designed in order to guarantee that “acceptable safety level” which is never absolute [127].

#### Juridical Standards

These are all the standards from which derive rules of behaviour for the juridical persons who are under the sovereignty of that State.

#### Technical Standards

These standards are the whole of the prescriptions on the basis of which machines, apparatus, materials and the installations should be designed, manufactured and tested so that efficiency and function safety are ensured. The technical standards, published by national and international bodies, are circumstantially drawn up and can have legal force when this is attributed by a legislative measure [127].

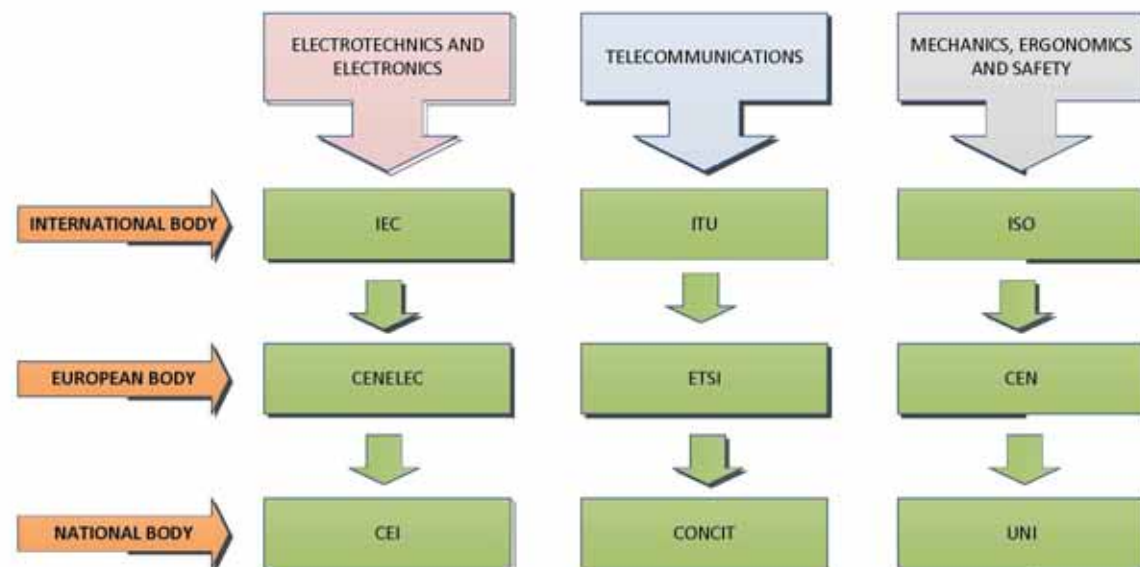


Figure 5.1. Overview of normalization bodies according to application fields.

As shown in Fig. 5.1. it is possible to distinguish three standardization bodies for electrotechnics and electronics fields, namely International Electrotechnical Commission (IEC), European Committee for Electrotechnical Standardization (CENELEC) and national bodies, in Italy CEI.

The International Electrotechnical Commission (IEC) was officially founded in 1906, with the aim of securing the international co-operation as regards standardization and certification in electrical and electronic technologies. This association is formed by the International Committees of over 40 countries all over the world. The IEC publishes international standards, technical guides and reports which are the bases or, in any case, a reference of utmost importance for any national and European standardization activity. IEC Standards are generally issued in two languages: English and French. In 1991 the IEC has ratified co-operation agreements with CENELEC (European standardization body), for a common planning of new standardization activities and for parallel voting on standard drafts [127].

The European Committee for Electrotechnical Standardization (CENELEC) was set up in 1973. Presently it comprises 31 countries (Austria, Belgium, Bulgaria, Cyprus, Croatia, Czech Republic, Denmark, Estonia, Finland, France, Germany, Greece, Hungary, Iceland, Ireland, Italy, Latvia, Lithuania, Luxembourg, Malta, Netherlands, Norway, Portugal, Poland, Romania, Slovakia, Slovenia, Spain, Sweden, Switzerland, United Kingdom) and cooperates with 12 affiliates (Albania, Belarus, Georgia, Bosnia and Herzegovina, Tunisia, Former Yugoslav Republic of Macedonia, Serbia, Libia, Montenegro, Turkey, Ukraine and Israel) which have first maintained the national documents side by side with the CENELEC ones and then replaced them with the Harmonized Documents (HD). There is a difference between EN Standards and Harmonization Documents (HD): while the first ones have to be accepted at any level and without additions or modifications in the different countries, the second ones can be amended to meet particular national requirements. EN Standards are generally issued in three languages: English, French and German. From 1991 CENELEC cooperates with the IEC to accelerate the standards preparation process of International Standards. CENELEC deals with specific subjects, for which standardization is urgently required. When the study of a specific subject has already been started by the IEC, the European standardization body (CENELEC) can decide to accept or, whenever necessary, to amend the works already approved by the International standardization body [127].

### **5.1.2. Lightning protection**

The IEC 62305 series provide guides or, where possible, international standards, for lightning protection [11, 17, 18, 128]. These documents takes into account issues of design, installation, inspection, maintenance and testing of protection measures to reduce the risk due to lightning for persons, structures and electrical and electronic system within structures. However, for their proper application, knowledge of references is needed [91, 129-135]. Basically this standard provides guidelines for cooperation between the designer of the electrical and electronic system, and the designer of the protection measures, in an attempt to achieve optimum protection effectiveness. Practical application comments are given e.g. in [13, 61, 63, 66, 76, 127, 136, 137]. This standard does not deal with detailed design of the electrical and electronic systems themselves. Schematic representation and connections between various parts of IEC 62305 is shown in Fig. 5.2.

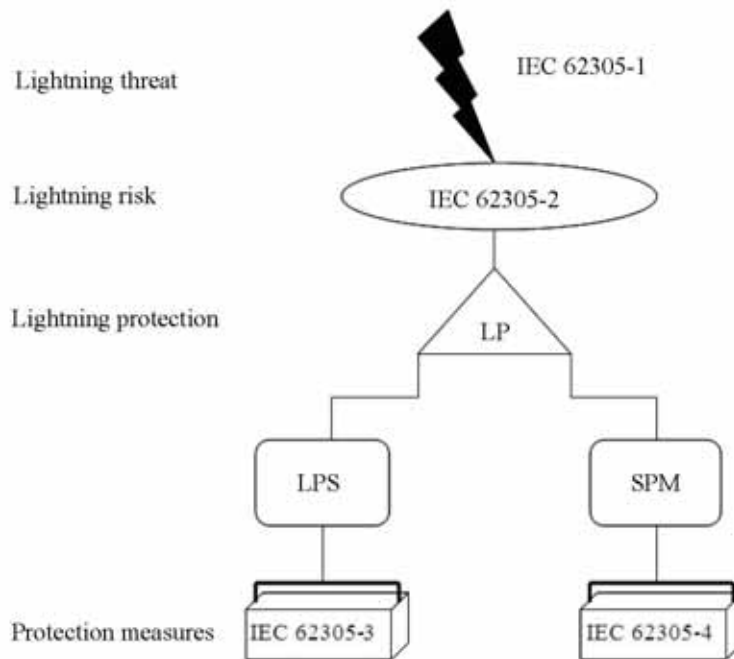


Figure 5.2. Connection between the various parts of IEC 62305 [11].

The protection measures selection according to IEC 62305 recommendations depends on the proper application field and type of damage. Protection measures to reduce injury of living beings by electric shock include: adequate insulation of exposed conductive parts, equipotentialization by means of a meshed earthing system, physical restrictions and warning notices, lightning equipotential bonding (EB). Protection measures to reduce physical damage is achieved by the lightning protection system (LPS) which includes the following features: air-termination system, down-conductor system, earth-termination system, EB, electrical insulation (and hence separation distance) against the external LPS. Protection measures to reduce failure of electrical and electronic systems (SPM) include: earthing and bonding measures, magnetic shielding, line routing, isolating interfaces, coordinated SPD system. In all cases these measures may be used alone or in combination. Their combination form the overall lightning protection. Selection of the most suitable protection measures shall be made by the designer of the protection measures and the owner of the structure to be protected according to the type and the amount of each kind of damage, to the technical and economic aspects of the different protection measures and to the results of risk assessment [17]. Protection measures are effective provided that they comply with the requirements of relevant standards and are able to withstand the stress expected in the place of their installation.

An ideal protection for structures would be to enclose the structure to be protected within an earthed and perfectly conducting continuous shield of adequate thickness, and to provide adequate bonding, at the entrance point into the shield, of the lines connected to the structure. This would prevent the penetration of lightning current and related electromagnetic field into the structure to be protected and prevent dangerous thermal and electrodynamic effects of current, as well as dangerous sparkings and overvoltages for internal systems. In practice, it is often neither possible nor cost effective to go to such measures to provide such full protection.



## 5.2. Establishment of lightning protection zones

The basic criterion of lightning protection zones (LPZ) consist of lightning current influence on apparatus to be protected. Selection and installation protection measures such as LPS, shielding wires, magnetic shields and SPD is based on the LPZ concept. An example of structure division according to this concept is shown in Fig. 5.3.

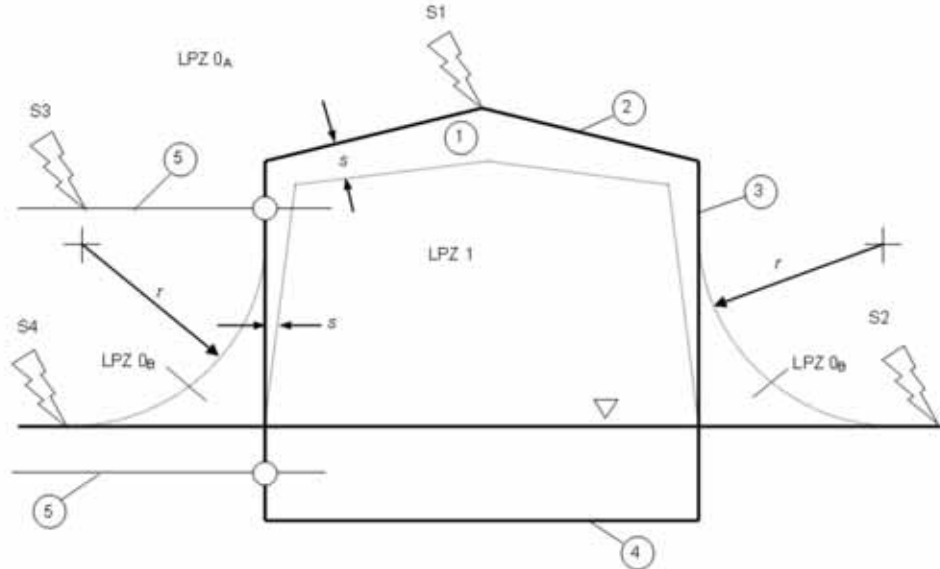


Figure 5.3. Lightning protection zones concept, where: 1 - structure; 2 - air termination system; 3 - down conductor system; 4 - earth termination system; 5 - incoming lines; S1 - flash to the structure; S2 - flash near to the structure; S3 - flash to a service connected to the structure; S4 - flash near a service connected to the structure;  $r$  - rolling sphere radius;  $s$  - separation distance against dangerous sparking; LPZ 0<sub>A</sub> - direct flash, full lightning current; LPZ 0<sub>B</sub> - no direct flash, partial lightning or induced current; LPZ 1 - no direct flash, limited lightning or induced current protected volume inside LPZ 1[11].

With respect to the threat of lightning, the following LPZs are defined:

### Outer zones:

- LPZ 0<sub>A</sub>: zone where the threat is due to the direct lightning flash and the full lightning electromagnetic field. The internal systems may be subjected to full or partial lightning surge current;
- LPZ 0<sub>B</sub>: zone protected against direct lightning flashes but where the threat is the full lightning electromagnetic field. The internal systems may be subjected to partial lightning surge currents;

### Inner zones:

- LPZ 1: zone where the surge current is limited by current sharing and by isolating interfaces and/or SPDs at the boundary. Spatial shielding may attenuate the lightning electromagnetic field;
- LPZ 2, ..., n: zone where the surge current may be further limited by current sharing and by isolating interfaces and/or additional SPDs at the boundary. Additional spatial shielding may be used to further attenuate the lightning electromagnetic field.

In general, the LPZ downstream of the protection measure are characterized by significant reduction of LEMP than that upstream of the LPZ.

### 5.3. Protection by surge protective devices

#### 5.3.1. SPD inside LPZ

To limit conducted surges due to lightning on electrical lines, SPDs should be installed at the entry to any inner LPZ. In buildings with uncoordinated SPDs, damage to the internal system may result if a downstream SPD, or an SPD within the equipment, prevents the proper operation of the SPD at the service entrance. In order to maintain the effectiveness of the protection measures adopted, it is necessary to document the location of all installed SPDs. An example of LPZ with SPD installed at the entrance any inner zone is shown in Fig. 5.4.

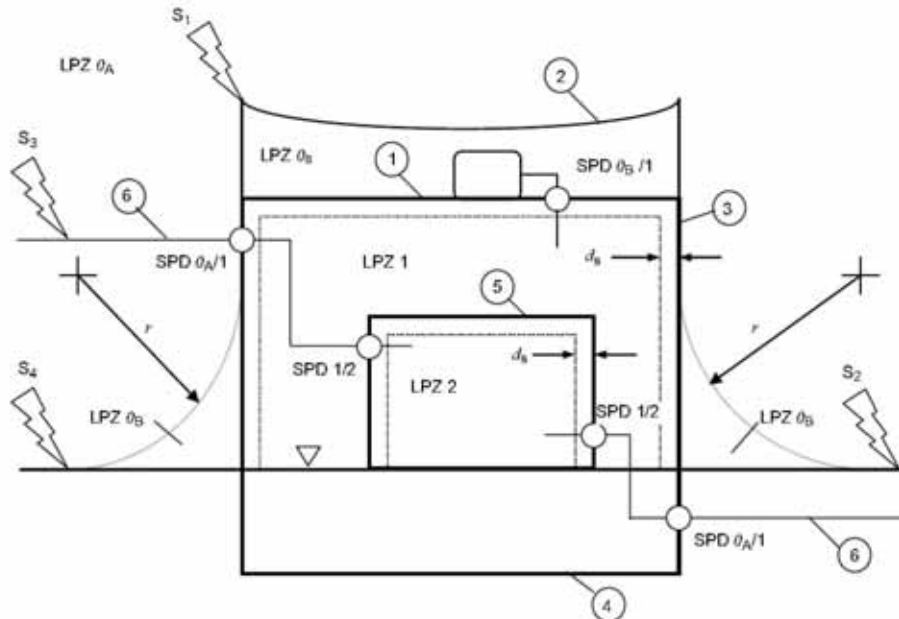


Figure 5.4. LPZ with SPD, where: 1 - structure (shield of LPZ 1); 2 - air termination system; 3 - down conductor system; 4 - earth termination system; 5 - room (shield of LPZ 2); 6 - services connected to the structure; S1 - flash to the structure; S2 - flash near to the structure; S3 - flash to a service connected to the structure; S4 - flash near a service connected to the structure;  $r$  - rolling sphere radius;  $d_s$  - safety distance against too high magnetic field [11].

Depending on the number, type and sensitivity of the electrical and electronic systems, suitable inner LPZs are defined from small local zones (the enclosure of a single electronic equipment) up to large integral zones (the whole building volume). Figs. 5.5 - 5.7 show typical LPZ layouts for the protection of internal systems providing different solutions suitable for existing structures in particular:

Fig. 5.5 shows the installation of a single LPZ 1, creating a protected volume inside the whole structure, e.g. for enhanced withstand voltage levels of the internal systems:

- this LPZ 1 could be created using an LPS, in accordance with [128], that consists of an external LPS (air-termination, down-conductor and earth-termination system) and an internal LPS (lightning equipotential bonding and compliance with the separation distances);
- the external LPS protects LPZ 1 against lightning flashes to the structure, but the magnetic field inside LPZ 1 remains nearly unattenuated. This is because air-terminations and down-conductors have mesh widths and typical distances greater than 5 m, therefore the spatial shielding effect is negligible as explained above;

– the internal LPS requires bonding of all services entering the structure at the boundary of LPZ 1, including the installation of SPDs for all electrical and signal lines. This ensures that the conducted surges on the incoming services are limited at the entrance by SPDs.

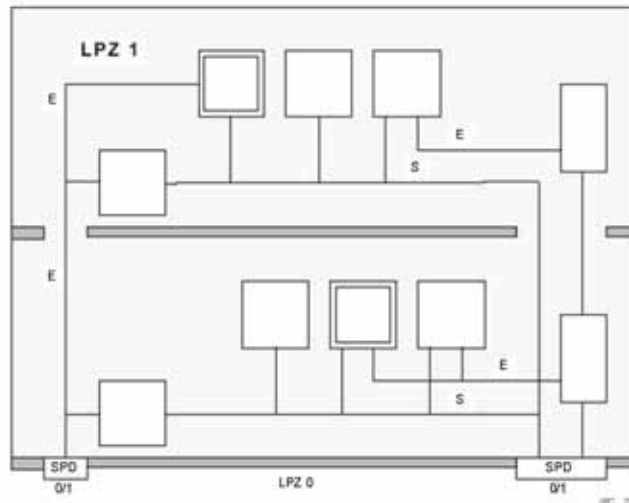


Figure 5.5. Possibilities to establish LPZs in existing structures: Unshielded LPZ 1 using LPS and SPDs at the entrance of the lines into the structure; where: *E* – power lines, *S* – signal lines [11].

Fig. 5.6 shows that in an unshielded LPZ 1, new equipment also needs to be protected against conducted surges. As an example, the signal lines can be protected using shielded cables and the power lines using a coordinated SPD system. This may require additional SPDs tested with  $I_n$  and SPDs tested with a combination wave, installed close to the equipment, and coordinated with the SPDs at the service entrance. It may also require additional Class II “double insulation” of the equipment.

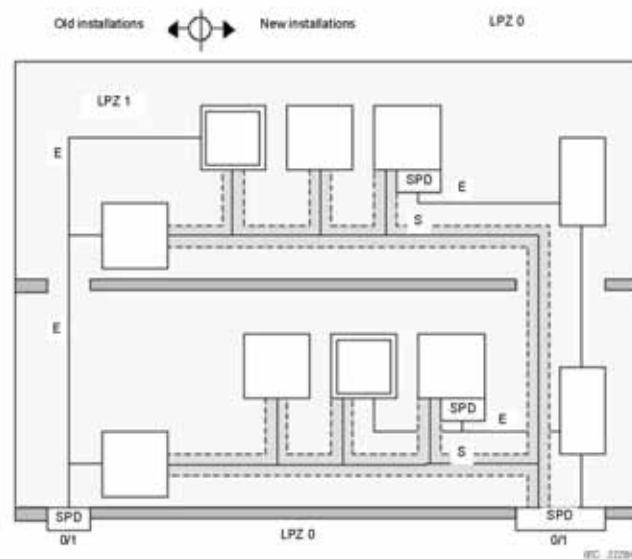


Figure 5.6. Possibilities to establish LPZs in existing structures: Unshielded LPZ 1 with protection for new internal systems using shielded signal lines and coordinated SPDs in power lines; where: *E* – power lines, *S* – signal lines [11].

Fig. 5.7 shows the creation of two smaller LPZs (LPZs 2) inside LPZ 1. Additional SPDs for power as well as for signal lines at the boundary of each LPZ 2 should be installed. These SPDs should be coordinated with the SPDs at the boundary of LPZ 1 in accordance with [133].

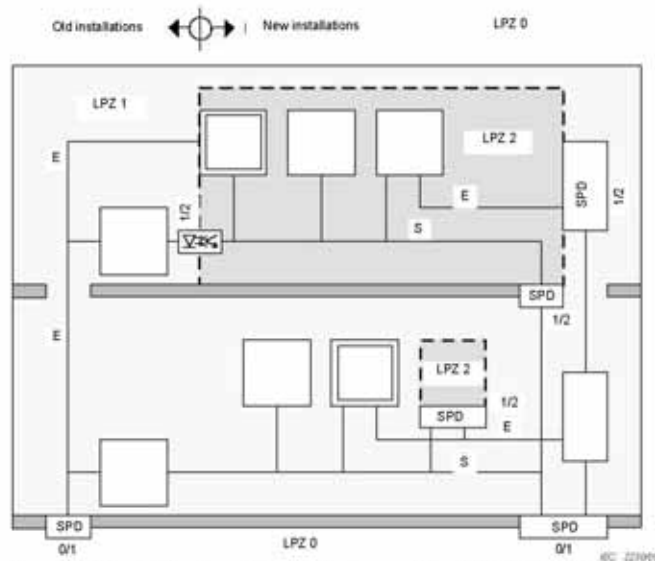


Figure 5.7. Possibilities to establish LPZs in existing structures: Unshielded LPZ 1 and two local LPZs 2 for new internal systems; where: *E* – power lines, *S* – signal lines [11].

### 5.3.2. Selection with regard to voltage protection level

According to [11], selection of the proper voltage protection level of the SPD depends on: the impulse withstand voltage  $U_w$  of the equipment to be protected, length of the connecting conductors to the SPD, length and the routing of the circuit between the SPD and the equipment.

The impulse withstand voltage  $U_w$  of the equipment to be protected should be defined for

- equipment connected to power lines in accordance with [133, 138];
- equipment connected to telecom lines in accordance with [135, [139-141];
- other lines and equipment terminals in accordance with information obtained from the manufacturer.

The protective level  $U_p$  of an SPD is related to the residual voltage at a defined nominal current  $I_n$ . For higher or lower currents passing through the SPD, the value of voltage at the SPD's terminals will change accordingly. The voltage protective level  $U_p$  should be compared with the impulse withstand voltage  $U_w$  of the equipment, tested under the same conditions as the SPD (over voltage and over current waveform and energy, energized equipment, etc). This matter is under consideration. Equipment may contain internal SPD components. The characteristics of these internal SPDs may affect the coordination.

When an SPD is connected to equipment to be protected, the inductive voltage drop  $\Delta U$  of the connecting conductors will add to the protection level  $U_p$  of the SPD. The resulting effective protection level  $U_{p\text{eff}}$ , defined as the voltage at the output of the SPD resulting from the protection level and the wiring voltage drop in the leads/connections (see Fig. 5.8), can be assumed as being:

- for voltage limiting type SPD(s):

$$U_{p/f} = U_p + \Delta U \quad (5.1)$$

- for voltage switching type SPD(s):

$$U_{p/f} = \max(U_p, \Delta U) \quad (5.2)$$

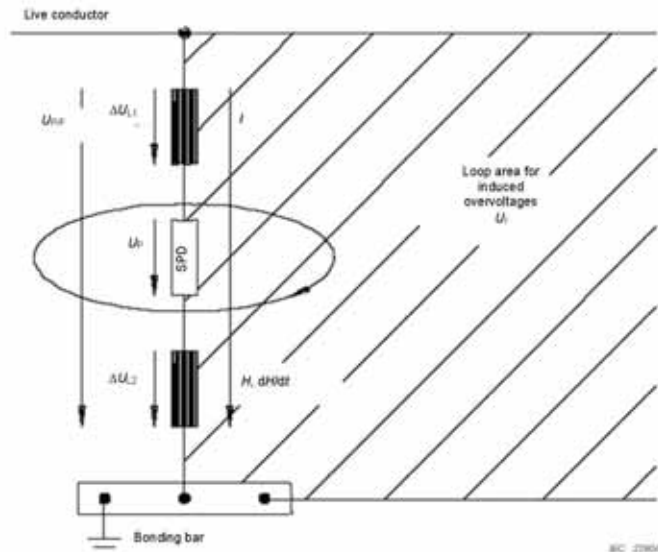


Figure 5.8. Surge voltage between live conductor and bonding bar; where:  $I$  - partial lightning current;  $U_1$  - induced overvoltage;  $U_{p/f} = U_p + \Delta U$  - surge voltage between live conductor and bonding bar;  $U_p$  - limiting voltage of SPD;  $\Delta U = \Delta U_{1,1} + \Delta U_{1,2}$  - inductive voltage drop on the bonding conductors;  $H, dH/dt$  - magnetic field and its time derivative [11].

The surge voltage  $U_{p/f}$  between the live conductor and the bonding bar is higher than the protection level  $U_p$  of the SPD, because of the inductive voltage drop  $\Delta U$  at the bonding conductors (even if the maximum values of  $U_p$  and  $\Delta U$  do not necessarily appear simultaneously). That is, the partial lightning current flowing through the SPD induces additional voltage into the loop on the protected side of the circuit following the SPD. Therefore the maximum voltage endangering the connected equipment can be considerably higher than the protection level  $U_p$  of the SPD.

For some switching type SPDs it may be required to add the arc voltage to  $\Delta U$ . This arc voltage may be as high as some hundreds of volts. For combination type SPDs more complex formulae may be needed.

When the SPD is installed at the line entrance into the structure,  $\Delta U = 1$  kV per m length, should be assumed. When the length of the connection conductors is  $\leq 0,5$  m,  $U_{p/f} = 1,2 \times U_p$  can be assumed. When the SPD is carrying induced surges only,  $\Delta U$  can be neglected.

During the operating state of an SPD, the voltage between the SPD terminals is limited to  $U_{p/f}$  at the location of the SPD. If the length of the circuit between the SPD and the equipment is too long, propagation of surges can lead to an oscillation phenomenon. In the case of an

open-circuit at the equipment's terminals, this can increase the overvoltage up to  $2 \times U_{pT}$  and failure of equipment may result even if  $U_{pT} \leq U_w$ .

Information on the connecting conductors, connecting configurations and fuse withstand levels for SPDs can be found in [129, 133].

Moreover lightning flashes to the structure or to ground nearby the structure, can induce an overvoltage  $U_i$  in the circuit loop between the SPD and the equipment, that adds to  $U_{pT}$  and thereby reduces the protection efficiency of the SPD. Induced overvoltages increase with the dimensions of the loop (line routing: length of circuit, distance between PE and active conductors, loop area between power and signal lines) and decrease with attenuation of the magnetic field strength (spatial shielding and/or line shielding).

In accordance with [11] internal systems are protected if:

- they are energy coordinated with the upstream SPD, and
- one of the following three conditions is fulfilled:
  - 1)  $U_{pT} \leq U_w$ : when the circuit length between the SPD and the equipment is negligible (typical case of an SPD installed at equipment terminals);
  - 2)  $U_{pT} \leq 0,8 U_w$ : when the circuit length is not greater than ten meters (typical case of SPD installed at a secondary distribution board or at a socket outlet); Where failure on internal systems may cause loss of human life or loss of service to the public doubling of voltage due to oscillations should be considered and the criteria  $U_{pT} \leq U_w / 2$  is required;
  - 3)  $U_{pT} \leq (U_w - U_i) / 2$ : when the circuit length is more than ten meters (typical case of SPD installed at the line entrance into the structure or in some cases at the secondary distribution board).

If spatial shielding of the structure (or of the rooms) and/or line shielding (use of shielded cables or metallic cable ducts) are provided, induced overvoltages  $U_i$  are usually negligible and can be disregarded in most cases.

### 5.3.3. Selection with regard to discharge current

SPDs should withstand the discharge current expected at their installation point in accordance with [11]. The use of SPDs depends on their withstand capability, classified in [91] for power, and in [138] for telecommunication systems. The selection of an SPD's discharge current rating is influenced by the type of connection configuration and the type of power distribution network [129, 133].  $I_{imp}$ ,  $I_{max}$  and  $I_n$ , are test parameters used in the operating duty test for Class I and Class II tests. They are related to the maximum values of discharge currents, which are expected to occur at the LPL probability level at the location of installation of the SPD in the system.  $I_{max}$  is associated with Class II tests and  $I_{imp}$  is associated with Class I tests.

SPDs should be selected in accordance with their intended installation location. At the line entrance into the structure (at the boundary of LPZ 1, e.g. at the main distribution board MB):

- SPD tested with  $I_{imp}$  (Class I test): the required impulse current  $I_{imp}$  of the SPD should provide for the (partial) lightning current to be expected at this installation point based on the chosen LPL in accordance with [18];



– SPD tested with  $I_n$  (Class II test): this type of SPD can be used when the lines entering are entirely within LPZ 0<sub>B</sub> or when the probability of failures of the SPD due to sources of damage S1 and S3 can be disregarded. The required nominal discharge current  $I_n$  of the SPD should provide for the surge level to be expected at the installation point based on the chosen LPL and related overcurrents, in accordance with [18]. The risk of failures of the SPDs due to sources of damage S1 and S3 can be disregarded if the total number of direct flashes to structure ( $N_D$ ) and to line ( $N_L$ ) complies with the condition:

$$N_D + N_L \leq 0,01 \quad (5.3)$$

Close to the equipment to be protected (at the boundary of LPZ 2 and higher, e.g. at a secondary distribution board, or at a socket outlet):

– SPD tested with  $I_n$  (Class II test): the required nominal discharge current  $I_n$  of the SPD should provide for the surge current to be expected at this point of the installation, based the chosen LPL and related overcurrents in accordance with [18]. An SPD having the characteristics of Class I and Class II tests may be used in this location;

– SPD tested with a combination wave  $U_{oc}$  (Class III test): this type of SPD can be used when the lines entering are entirely within LPZ 0<sub>B</sub> or when the risk of failures of the SPD due to sources of damage S1 and S3 can be disregarded. The required open circuit voltage rating  $U_{oc}$  of the SPD (from which the short-circuit current  $I_{sc}$  can be determined, since test Class III is carried out using a combination wave generator with a 2  $\Omega$  impedance) should provide for the surge level to be expected at the installation point, based on the chosen LPL and related overcurrents, in accordance with [18].

#### 5.3.4. Coordinated SPD system

The protection of internal systems against surges requires a systematic approach consisting of coordinated SPDs for both power and signal lines. The rules for the selection and installation of a coordinated SPD system are similar in both cases [11]. In SPM using the lightning protection zones concept with more than one inner LPZ (LPZ 1, LPZ 2 and higher), SPD(s) shall be located at the line entrance into each LPZ. In SPM using LPZ 1 only, an SPD shall be located at the line entrance into LPZ 1 at least. In both cases, additional SPDs may be required if the distance between the location of the SPD and the equipment being protected is long [18].

Procedure for installation of a coordinated SPD system. A coordinated SPD system should be installed as follows:

- at the line entrance into the structure (at the boundary of LPZ 1, e.g. at installation point MB) install SPD1 fulfilling the requirements of location and discharge current;
- determine the impulse withstand voltage  $U_w$  of internal systems to be protected;
- select the voltage protection level  $U_{p1}$  of SPD 1;
- check the requirements of voltage protection level are met;

If this requirement is met, the equipment is adequately protected by SPD 1. Otherwise, an additional SPD 2(s) is/are needed.

- if so required, closer to the equipment (at the boundary of LPZ 2, e.g. at the installation point  $S_b$  or  $S_a$ ), install SPD 2 fulfilling the requirements of location and discharge current, and energy coordinated with the upstream SPD 1;

- select the protection level  $U_{p2}$  of SPD 2;

- check the requirements of voltage protection are met;

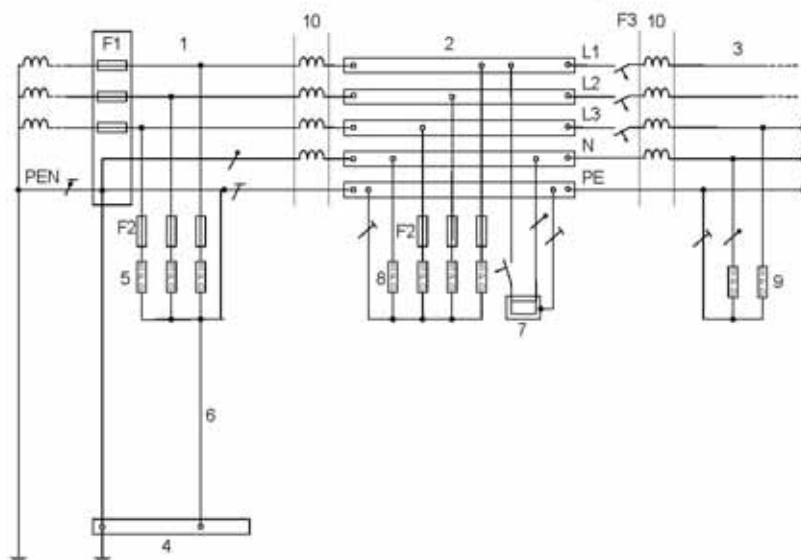
If this requirement is met, the equipment is adequately protected by SPD 1 and SPD 2.

- otherwise, close to the equipment (e.g. at installation point  $S_a$  socket), additional SPD 3(s) is/are needed fulfilling the requirements of location and discharge current, and energy coordinated with the upstream SPD 1 and SPD 2;

- check the condition  $U_{p/F3} \leq U_W$  is fulfilled.

The stress, which an SPD will experience under surge conditions, is a function of many complex and interrelated parameters, like:

- location of the SPD(s) within the structure, as shown in Fig. 5.9;



IEC 64802

Figure 5.9. Installation example of test Class I, Class II and Class III SPDs; where: 1 - origin of the installation; 2 - distribution board; 3 - distribution outlet; 4 - main earthing terminal or bar; 5 - surge protective device, Class I or II tested; 6 - earthing connection (earthing conductor) of the surge protective device; 7 - fixed equipment to be protected; 8 - surge protective device, Class II tested; 9 - surge protective device, Class II or Class III tested; 10 - decoupling element or line length; F1, F2, F3 - overcurrent protective disconnectors [11].

- method of coupling of the lightning strike to the facility – for example, is this via a direct strike to the structure's LPS (S1), or via induction onto building wiring due to a nearby strike (S2), or services feeding the structure (S3 and S4);

- distribution of lightning currents within the structure – for example, what portion of the lightning current enters the earthing system, and what remaining portion seeks a path to remote earths via services which enter the structure such as the power distribution system, metallic pipes, telecom services etc. and the equipotential bonding SPDs used on these;

- the resistance and inductance of services entering the structure, as these components effect the current peak value  $I$  and charge  $Q$  distribution ratios;

- additional conductive services connected to the facility – these will carry a portion of the direct lightning current and therefore reduce the portion which flows through the power

distribution system via the lightning equipotential bonding SPD(s). Attention should be paid to the permanence of such services due to possible replacement by non-conductive parts;

- type of waveshape being considered – it is not possible to consider simply the peak current which the SPD will have to conduct under surge conditions, one also has to consider the waveshape of this surge (for example, 10/350  $\mu$ s covering direct and partial lightning current, 8/20  $\mu$ s covering induced lightning current) and the bulk charge  $Q$ ;
- any additional structures which are interconnected to the primary structure via the power service, as these will also effect the current sharing distribution.

The efficiency of a coordinated SPD system depends not only on the proper selection of the SPDs, but also on their correct installation. Aspects to be considered include: location of the SPD and connecting conductors. The location of the SPDs should comply with [18] and is primarily affected by:

- the specific source of damage e.g. lightning flashes to a structure (S1), to a line (S3), to ground near a structure (S2) or to ground near a line (S4);
- the nearest opportunity to divert the surge current to ground (as close to the entrance point of a line into the structure as possible).

The first criterion to be considered is: the closer the SPD is to the entrance point of the incoming line, the greater the amount of equipment within the structure that will be protected by this SPD (economic advantage). Then the second criterion should be checked: the closer an SPD is to the equipment being protected, the more effective its protection will be (technical advantage). The SPD's connecting conductors should have a minimum cross-sectional area as given in [128].

Moreover, in a coordinated SPD system, cascaded SPDs need to be energy coordinated in accordance with [133, 135]. For this purpose, the SPD manufacturer should provide sufficient information as to how to achieve energy coordination between his different SPDs.

#### 5.4. Protection by isolation transformer

Power-frequency interference currents through the equipment and its connected signal lines can be caused by large loops or the lack of a sufficiently low impedance bonding network. To prevent such interference (mainly in TN-C installations), a suitable separation between existing and new installations can be achieved using isolating interfaces, such as: class II insulated equipment (i.e. double insulation without a PE-conductor); metal-free fibre optic cables; optical couplers and isolation transformers.

The basic criterion of selection an isolation transformer include, nominal operational voltage and maximum output power. However, the lightning protection issues are not specified by topical standards.

In Fig. 5.10 the installation of a large integral LPZ 2 inside of LPZ 1, to accommodate the new internal systems is shown. The grid-like spatial shield of LPZ 2 provides a significant attenuation of the lightning magnetic field. On the left hand side, the SPDs installed at the boundary of LPZ 1 (transition of LPZs 0/1) and subsequently at the boundary of LPZ 2 (transition of LPZs 1/2), should be coordinated in accordance with [133]. On the right hand side, the SPDs installed at the boundary of LPZ 1 should be selected for a direct transition of LPZs 0/2.

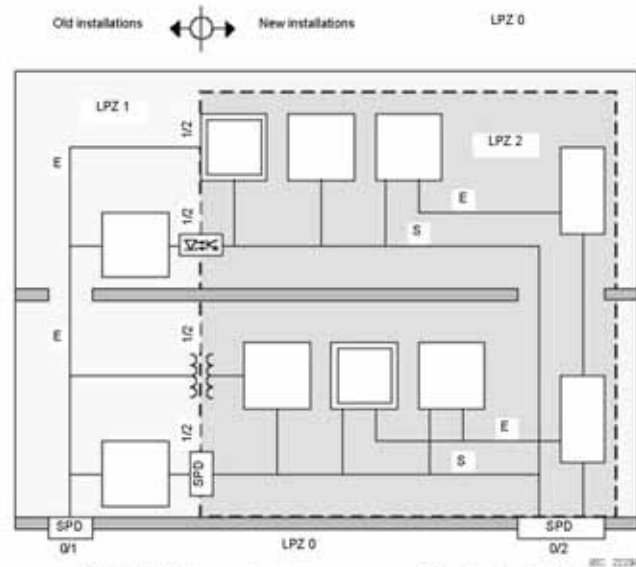


Figure 5.10. Possibilities to establish LPZs in existing structures: Unshielded LPZ 1 and large shielded LPZ 2 for new internal systems; where: *E* – power lines, *S* – signal lines [11].

## **5.5. Summary**

In the present chapter some aspects of standardisation for lightning protection issues are presented. The survey starts with standardisation bodies overview with reference to the application fields and territories. The three standardization bodies for electrotechnics and electronics fields, namely International Electrotechnical Commission (IEC), European Committee for Electrotechnical Standardization (CENELEC) and national bodies (in Italy CEI) are evidenced.

In terms of lightning protection, it is possible to distinguish two international standardisation bodies, namely IEC and ITU. The IEC standards deals with electrical systems. The ITU standards deals with communication and signalling networks systems.

In present work special focus is dedicated to IEC standard on SPD and isolation transformer as selected protection measures against failure of electrical and electronic systems within a structures.

The lightning protection zones concept is examined and discussed. Examples of protection measures installation in these zones are shown.

The SPD selection according to the voltage and current threat is presented. A real case, where more than one SPD exist, is presented and basic rules of coordination systems of SPD are reported.

The selection an isolation transformer is not extensively considered over the topical standards of lightning protection. These publications introduce well isolating interferences concept, where an isolation transformer is one of possible protection measures.

# Chapter 6



## 6. Criteria for protection measures selection: experimental tests and computer simulations for surge protective devices

### 6.1. Introduction

Electrical and electronic apparatus of modern structures are more and more sensitive to electromagnetic fields produced by electrical currents of different sources and especially by current of direct and nearby lightning strikes. Lightning overvoltages stressing electrical and electronic systems within a structure are essentially due to [18, 142]: flashes to the structure (S1); flashes to ground or to grounded objects near the structure (S2); flashes to the connected lines (S3); flashes nearby the connected lines (S4). The influence of lightning currents results in overvoltages, which may be particularly dangerous for the equipment and the application of protection measures is unavoidable. The classification and characteristics of critical occurrences are described in chapter 3.

In order to limit the probability of damage (and then the risk) caused by lightning overvoltages, different protection measures are suggested by the IEC Standards [11, 17], namely:

- a system of surge protective devices properly selected, coordinated and installed from the point of view of the energy and of the protection levels in relation to the impulse withstand voltage ( $U_w$ ) value of the equipment to be protected;
- appropriate earthing and bonding as well as shielding of structure and/or cables;
- routing precautions in the wiring installation.

Surge protective devices (SPD) belong to such measures and they allow to reduce significantly the probability of electrical equipment damage, but their effectiveness depends - within a certain limits - on their proper selection and installation. Every disregard of these two factors may result in an inadmissible voltage increase on terminals of a distant equipment to be protected. It appears mainly due to oscillating phenomena, which in every case should be involved into consideration and calculation of the SPD protection efficiency [143-149].

The present chapter intends to give a contribution to the investigation, by both computer simulations and laboratory tests, on the criteria for the selection of the SPD protection level ( $U_p$ ) in order to limit the voltage at the apparatus terminals to a value less than or equal to its withstand voltage ( $U_w$ ). Such criteria are strongly influenced by installation conditions of SPD. Experimental tests are performed in the HV Laboratory of Warsaw University of Technology as well as in the HV Laboratory of University of Rome La Sapienza. Examples of performed tests are given in paragraph 6.2. The experimental results consist of a first essential step to circuit analyses and further to satisfactory models development. The methods of circuit components representation for computer simulation issues are given in paragraph 6.3. The laboratory and simulation results are compared in paragraph 6.4, where special focus is dedicated for circuits protected by means of SPD limiting type. The analyses of typical low-voltage systems, where SPDs are used as protective devices are reported in paragraph 6.5 and 6.6, where upstream SPD and downstream SPD selection issues are deeply developed. The considered circuit arrangements are simulated by the computer using a commercial transient software EMTP-RV.

## 6.2. Laboratory tests of surge protective devices

The current test consist a fundamental experimental field to estimate SPD essential features, namely the  $U/I$  characteristic for SPD limiting type and clamping voltage for SPD switching type. Moreover this type of test can estimate the durability of SPD. The current tests are possible to carry out with different shapes and peak values, according to specification given in chapter 4. However the laboratory tests are much more complex and go beyond this specification of generator. The type of grounding system, connecting leads, probes, oscilloscopes and son on, have also a major impact for obtained results. In present chapter the current tests are performed with impulse current generator with a standard wave shape (8/20  $\mu$ s). The equivalent electric circuit of the analysed arrangement is shown in Fig. 6.1.

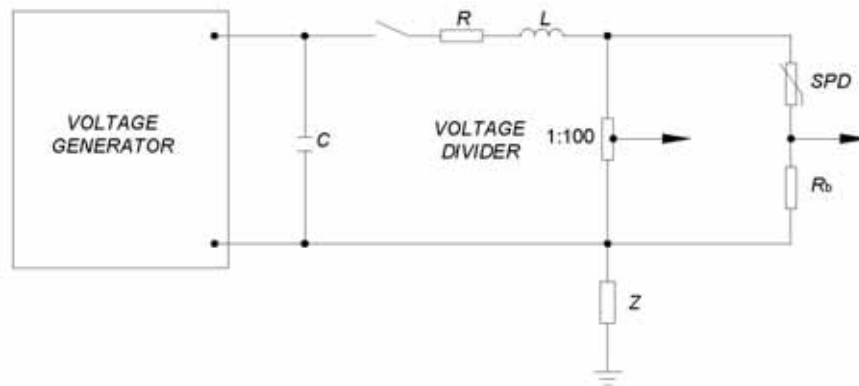


Figure 6.1. Equivalent electric circuit of basic analysed arrangement, where:  $C = 16 \mu\text{F}$ ;  $R = 0,42 \Omega$ ;  $R_b = 10,6 \text{ m}\Omega$ ;  $L = 4\mu\text{H}$ .

The impulse current generator consist on a capacitance which is charged by voltage generator (up to 3kV). The current peak value is regulated by means of voltage generator charging the capacitance  $C$ . The wave form 8/20  $\mu$ s is fixed by the relation of suitable values of  $R$ ,  $L$ ,  $C$  circuit parameters. The arrangement is connected to the local ground system of laboratory where the earth impedance value is 0,1  $\Omega$ . The voltage values are measured by means of voltage divider 1:100, and the current values by means of characteristic resistance  $R_b = 10,6 \text{ m}\Omega$ . Both signals are displayed on the digital oscilloscope Tektronix mod. TDS2002B with maximal samples rate 1 GS/s and bandwidth 60MHz. The oscilloscope is connected to the PC in order to registered test results in digital form. Photos of laboratory configuration are reported in Fig. 6.2.



Figure 6.2. Photos of laboratory during the SPD test.

An example of obtained oscillograms is represented in Fig. 6.3. On the picture is shown the program window of software enclose to the digital oscilloscope with registered waves shapes of voltage and current. The signal of first channel (1) represent the current wave shape flowing through the SPD. The registered voltage on the SPD terminals is shown by the signal of second channel (2).

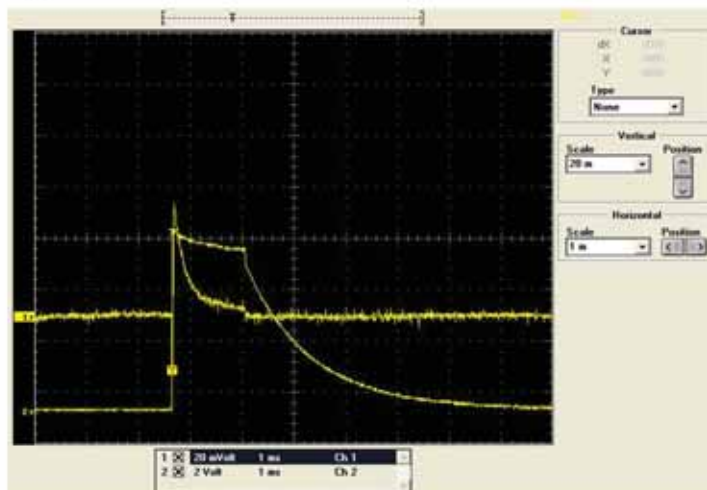


Figure 6.3. Example of obtained oscillograms; CH1 – current, CH2 – voltage.

Preliminary, the  $U / I$  characteristic of SPD limiting type is experimentally determined. The numerical results of performed test are reported in Tab. 6.1. The column CH 1 is related with registered values of voltage drop on the resistance used for the current measure. CH 2 is related with registered values of voltage drop on the voltage divider. On the base of first two columns the values of  $I$  (A) and  $U$  (V) are obtained.

Table 6.1. Registered values of voltage as well as the final values of current and voltage.

CH1	CH2	$I$ (A)	$U$ (V)
0,00333	5,98	0,32	598
0,00393	6,54	0,37	654
0,067	7,07	6,33	707
0,328	7,53	31	753
1,12	8	105,86	800
2,1	8,33	198,49	833
4,93	9,1	465,97	910
7,27	9,47	687,15	947
9,33	9,73	881,85	973
13,7	10,4	1294,89	1040
Note: $I = CH1 / 0,1058$ $U = CH2 \cdot 100$			



On the base of Tab. 6.1 is possible to construct the operational part of  $U/I$  characteristic of the SPD under test. The laboratory results are compared in Fig. 6.4 with a manufacturer characteristic MOD 320 given in [93] and they show a good agreement.

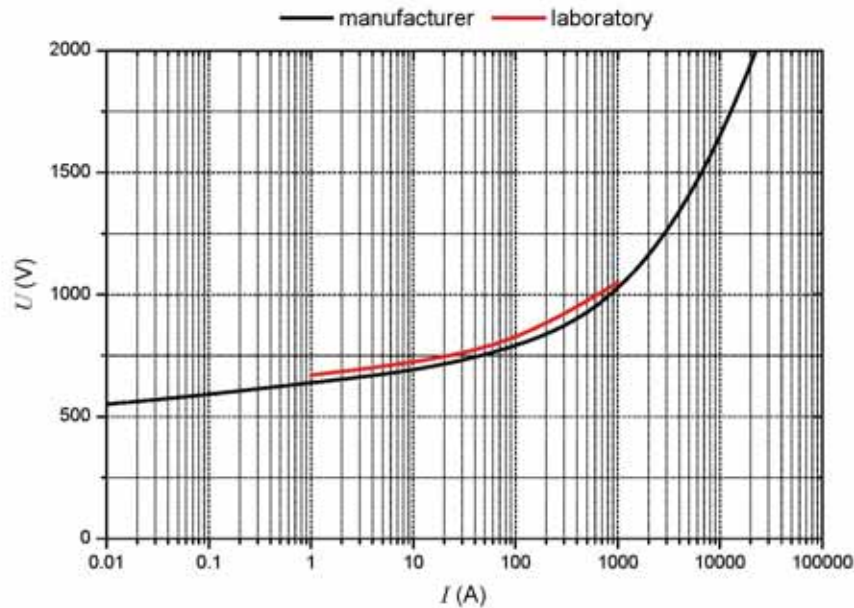


Figure 6.4.  $U/I$  characteristic of used SPD.

The second group of laboratory tests consist of voltage investigation. This character has much more applicative aspect in the case of coordinated system of lightning protection measures as well as of induced voltages. In both cases the current have a small value and the voltage wave shape has a significant influence on apparatus protection, especially in terms of protected distances and withstand voltage ( $U_w$ ) of apparatus to be protected.

The basic circuit for laboratory tests is shown in Fig. 6.5. In such arrangement the impulse voltage generator ( $G$ ) with peak value of 2,5 kV and wave shape 1,2/50  $\mu$ s, the typical low-voltage limiting SPDs, the low-voltage wires with 1,5 mm<sup>2</sup> cross-section for connections have been used.

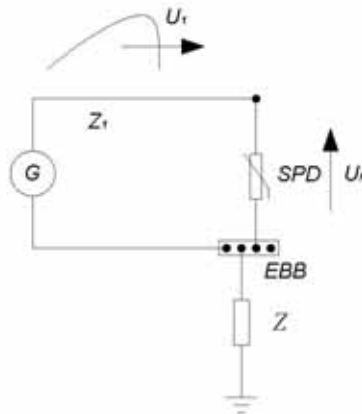


Figure 6.5. Basic analysed arrangement, where:  $G$  - impulse voltage generator;  $U_1$  - surge voltage;  $Z_1$  - surge impedance left by the surge;  $EBB$  - equipotential bonding bar;  $Z$  - conventional earthing impedance;  $U_p$  - voltage on the SPD terminals.

The equivalent schema of the impulse voltage generator used is shown in Fig. 6.6. The impulse generator consists of the voltage generator with maximal continuous voltage up to 3 kV and different parameters of  $R_1$ ,  $C_1$ ,  $R_2$ ,  $C_2$ . To determine the wave shape 1,2/50  $\mu$ s the following parameters  $R_1 = 13 \Omega$ ,  $C_1 = 4 \mu\text{F}$ ,  $R_2 = 17,6 \Omega$ ,  $C_2 = 0,05 \mu\text{F}$  are selected. Photo of described arrangement is shown in Fig. 6.7.

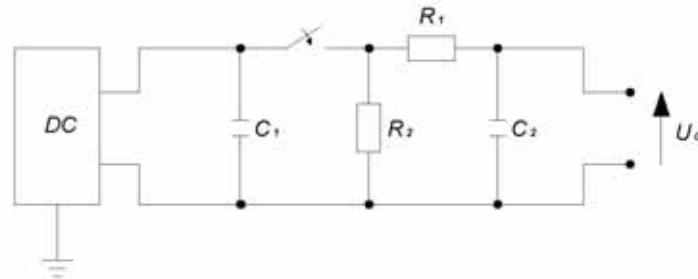


Figure 6.6. Equivalent electric circuit of impulse voltage generator, where:  $R_1 = 13 \Omega$ ,  $C_1 = 4 \mu\text{F}$ ,  $R_2 = 17,6 \Omega$ ,  $C_2 = 0,05 \mu\text{F}$ .



Figure 6.7. Photo of impulse voltage generator.

The SPDs limiting and switching type used are shown in Fig. 6.8 and Fig. 6.9 respectively.



Figure 6.8. Photo of SPD limiting type.



Figure 6.9. Photo of SPD switching type.

Voltages at SPD were measured by a digital oscilloscope Tektronix mod. TDS2002B with maximal samples rate 1 GS/s and bandwidth 60 MHz.

Examples of SPDs voltage  $U_p$  responses for limiting and switching type are shown in Fig. 6.10 and Fig. 6.11. respectively.



Figure 6.10. Oscillogram of voltage on the SPD terminals (limiting type) under stressing overvoltage of 2,5 kV and wave shape 1,2/50 μs.



Figure 6.11. Oscillogram of voltage on the SPD terminals (switching type) under stressing overvoltage of 2,5 kV and wave shape 1,2/50 μs.



### 6.3. Computer simulation of surge protective devices: models development

#### 6.3.1. Introduction

In this paragraph the concept of models development for computer simulation are considered. Typical elements of low-voltage systems are taken into account as well as damage source representation of lightning current.

#### 6.3.2. Lightning source current

The lightning stroke may be simulated as an ideal current generator by means of the following equation accepted by the standards [18] already presented in chapter 2:

$$I = \frac{I_p}{k} \cdot \frac{(t/\tau_1)^{10}}{1 + (t/\tau_1)^{10}} \cdot \exp(-t/\tau_2) \quad (6.1)$$

where:

$k$  – correction factor for the peak current;

$t$  – time;

$I_p$  – peak value of the lightning current;

$\tau_1$  – front time constant;

$\tau_2$  – tail time constant.

Three shapes of lightning current, namely representative of positive stroke (10/350  $\mu$ s), first negative stroke (1/200  $\mu$ s), subsequent negative stroke (0,25/100  $\mu$ s) are considered as well as the normalized shape dedicated for SPD class II test (8/20  $\mu$ s). The relative equation (6.1) parameters to obtain the mentioned wave shapes are reported in Tab. 6.2.

Table 6.2. Equation parameters

Parameters	10/350 $\mu$ s	1/200 $\mu$ s	0,25/100 $\mu$ s	8/20 $\mu$ s
$k$	0,93	0,986	0,993	0,36
$\tau_1$ ( $\mu$ s)	19	1,82	0,454	14,6
$\tau_2$ ( $\mu$ s)	485	285	143	20

A second way to represent the lightning current is reported in [150], where the current front of the first strokes is expressed by the following relation:

$$I = At + Bt^n \quad (6.2)$$

The basic assumption is that the current shape reaches the instant of maximum steepness (90% of amplitude) at a time  $t_n$  dependent on the exponent  $n$ . The two variables are approximated by:

$$n = 1 + 2 \left( s_N - 1 \right) \left( 2 + \frac{1}{s_N} \right) \quad (6.3)$$

$$t_n = 0,6t_f \left( \frac{3s_m^2}{1 + s_m^2} \right) \quad (6.4)$$

$$s_m = s_m \frac{t_f}{I_p} \quad (6.5)$$

where:

$s_m$  – maximum steepness;

$t_f$  – front time.

The constants of equation (6.2) then are given by:

$$A = \frac{1}{n-1} \left( 0,9 \frac{I_p}{t_n} - S_m \right) \quad (6.6)$$

$$B = \frac{1}{t_n^n (n-1)} (S_m t_n - 0,9 I_p) \quad (6.7)$$

For subsequent strokes the current front is given by:

$$I = s_m \cdot t_f \quad (6.8)$$

The current tail equation is:

$$I = I_1 e^{-\frac{(t-t_n)}{t_1}} - I_2 e^{-\frac{(t-t_n)}{t_2}} \quad (6.9)$$

where:

$t_1, t_2$  – time constants;

$I_1, I_2$  – constants;

$t_h$  – time-to-half value.

The constants are found from:

$$t_1 = \frac{(t_h - t_n)}{\ln(2)} \quad (6.10)$$

$$t_2 = 0,1 \frac{I_p}{S_m} \quad (6.11)$$

$$I_1 = \frac{t_1 t_2}{t_1 - t_2} \left( S_m + 0,9 \frac{I_p}{t_2} \right) \quad (6.12)$$

$$I_2 = \frac{t_1 t_2}{t_1 - t_2} \left( S_m + 0,9 \frac{I_p}{t_1} \right) \quad (6.13)$$

A third method for representation of lightning current is introduced in LIOV code [151, 152] for inductive effects on overhead lines. In this case the lightning current is simulated as sum of three lightning current functions already presented in chapter 3.

$$i(0, t) = i_{H1}(0, t) + i_{H2}(0, t) + i_{DE}(0, t) \quad (6.14)$$

where the individual component of lightning current are defined as follows:

$$i_{H1}(0, t) = \frac{I_{01}}{\eta_1} \frac{\left(\frac{t}{\tau_{11}}\right)^{\eta_1}}{1 + \left(\frac{t}{\tau_{11}}\right)^{\eta_1}} e^{-\frac{t}{\tau_{12}}} \quad (6.15)$$

$$i_{H2}(0, t) = \frac{I_{02}}{\eta_2} \frac{\left(\frac{t}{\tau_{21}}\right)^{\eta_2}}{1 + \left(\frac{t}{\tau_{21}}\right)^{\eta_2}} e^{-\frac{t}{\tau_{22}}} \quad (6.16)$$

$$i_{DE}(0, t) = I_D \left( (1 - e^{-\alpha t}) - (1 - e^{-\beta t}) \right) \quad (6.17)$$

$$\eta_1 = e^{-\left(\frac{\tau_{11}}{\tau_{12}}\right) \left(\frac{\tau_{12}}{\tau_{11}}\right)^{\frac{1}{\eta_1}}} \quad (6.18)$$

$$\eta_2 = e^{-\left(\frac{\tau_{21}}{\tau_{22}}\right) \left(\frac{\tau_{22}}{\tau_{21}}\right)^{\frac{1}{\eta_2}}} \quad (6.19)$$

where:

$\alpha$  - front time coefficient;

$\beta$  - tail time coefficient.

The presented methods of lightning current simulation have particular benefits depending on the considered arrangement as well as lightning current effects. In general cases for low-voltage circuits the first representation of lightning current as reported in (6.1) seems to be more proper for all type of damage sources.

### 6.3.3. Low voltage SPD

The typical low-voltage limiting type SPD is simulated in order to match the  $U / I$  characteristic derived by actual voltage-current measurements. Models performance is presented and discussed in chapter 4. An example of characteristic derived by means of model elaborated is shown in Fig. 6.12.

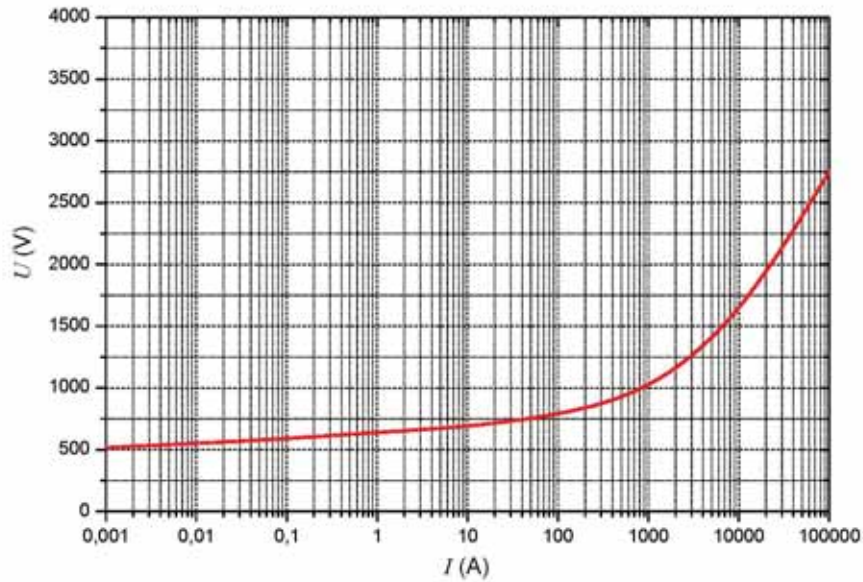


Figure 6.12.  $U/I$  characteristic of SPD limiting type.

It is important to mention that  $U/I$  characteristic is symmetrical and only positive part is reported.

SPD switching type simulation takes into account the volt-time characteristic of the spark gap and the arc resistance. The simulation aspects are reported in chapter 4.

The connection leads of SPD are simulated by means of concentrated inductance.

#### 6.3.4. Supply line

Supply line as well as internal circuit conductors are simulated by means of transmission line model where the parameters typical for the usual LV cable types are inserted. The distributed parameter lined model is shown in Fig. 6.13.

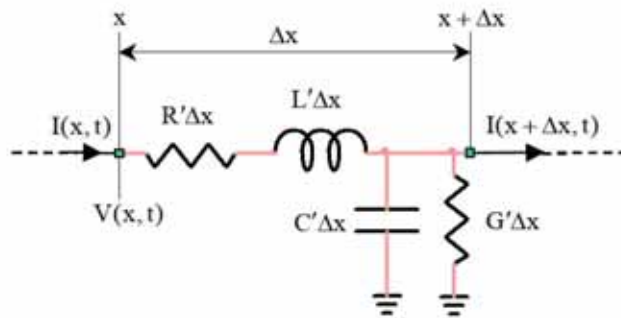


Figure 6.13. Distributed parameter line model.

The basic time domain equations of the single phase distributed parameter line (Fig. 6.12) are [153, 154]:

$$\frac{dV(x,t)}{dx} = -R' I(x,t) - L' \frac{dI(x,t)}{dt} \quad (6.20)$$

$$\frac{dI(x,t)}{dx} = -G'V(x,t) - C' \frac{dV(x,t)}{dt} \quad (6.21)$$

The primed variables are given in per line length. When Laplace transformation is used:

$$\frac{dV(x,s)}{dx} = -Z'I(x,s) \quad (6.22)$$

$$\frac{dI(x,s)}{dx} = -Y'V(x,s) \quad (6.23)$$

where:

$$Z' = R' + sL' \quad (6.24)$$

$$Y' = G' + sC' \quad (6.25)$$

Differentiation of equations (6.22) and (6.23) results into:

$$\frac{d^2V(x,s)}{dx^2} = \gamma^2 V(x,s) \quad (6.26)$$

$$\frac{d^2I(x,s)}{dx^2} = \gamma^2 I(x,s) \quad (6.27)$$

with:

$$\gamma = \sqrt{(R' + sL')(G' + sC')} \quad (6.28)$$

The general solution of equations (6.25) and (6.26) is given by:

$$V(x,s) = V^+ e^{-\gamma x} + V^- e^{\gamma x} \quad (6.29)$$

$$I(x,s) = \frac{1}{Z_c} [V^+ e^{-\gamma x} - V^- e^{\gamma x}] \quad (6.30)$$

with the characteristic impedance:

$$Z_c = \sqrt{\frac{R' + sL'}{G' + sC'}} \quad (6.31)$$

For practical issues the supply line as well as internal circuit conductors can be characterized by propagation velocity given by:

$$v = \frac{1}{\sqrt{LC'}} \quad (6.32)$$

and surge impedance given by:

$$Z = \sqrt{\frac{L}{C}} \quad (6.33)$$

The typical values of these parameters for different type of lines are reported in Tab. 6.3 [154].

Table 6.3. Line parameters.

Parameter	Overhead line	Low-voltage cable	Telecommunication
$v$ (m/s)	$2+3 \cdot 10^8$	$2+3 \cdot 10^8$	$2+3 \cdot 10^8$
$Z$ ( $\Omega$ )	200÷400	40÷60	20÷30

### 6.3.5. Transformer

The MV/LV transformer is simulated in transient conditions by a network representing the winding capacitance  $C$ , inductance  $L$  and resistance  $R$ . The model construction is shown in Fig. 6.14.

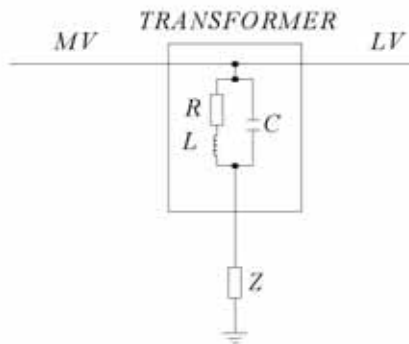


Figure 6.14. Simplified transformer model.

In case of lightning, fast front source, the dominant parameter of this model consist of capacitance [155-157]. The respectively values of this parameter for different types of transformers as suggested by [158] are reported in Tab. 6.4. It is to note that the ranges of capacitance values are different according to the corresponding values of operational voltage.

Table 6.4. Impulse capacitance of power, voltage and current transformer.















Type	10 kV	30 kV	110 kV	220 kV	380 kV
Power transformer	1 – 2,5 nF	1 – 2,8 nF	0,5 – 6 nF	1 – 5 nF	1 – 6 nF
Voltage transformer	0,3 – 0,4 nF	0,3 – 0,4 nF	0,1 – 2 nF	0,1 – 2 nF	0,1 – 2 nF
Current transformer	0,3 – 0,4 nF	0,3 – 0,4 nF	0,1 – 0,7 nF	0,1 – 0,7 nF	0,1 – 0,7 nF

### 6.3.6. Grounding system

Performance of grounding systems under low frequency and slow varying currents is well understood. The methodology of earth resistance calculation according to [159] is reported in Tab. 6.5.



Table 6.5. Formulas for the calculation of ground resistance of different earthing arrangements.

	Hemisphere radius $r$	$R = \frac{\rho}{2\pi r}$
	One ground rod length $L$ , radius $r$	$R = \frac{\rho}{2\pi L} \left( \ln \frac{4L}{r} - 1 \right)$
	Two ground rods $s > L$ ; spacing $s$	$R = \frac{\rho}{4\pi L} \left( \ln \frac{4L}{r} - 1 \right) + \frac{\rho}{4\pi s} \left( 1 - \frac{L^2}{3s^2} + \frac{2L^4}{5s^4} \dots \right)$
	Two ground rods $s < L$ ; spacing $s$	$R = \frac{\rho}{4\pi L} \left( \ln \frac{4L}{r} + \ln \frac{4L}{s} - 2 + \frac{s}{2L} - \frac{s^2}{16L^2} + \frac{s^4}{512L^4} \dots \right)$
	Buried horizontal wire length $2L$ , depth $s/2$	$R = \frac{\rho}{4\pi L} \left( \ln \frac{4L}{r} + \ln \frac{4L}{s} - 2 + \frac{s}{2L} - \frac{s^2}{16L^2} + \frac{s^4}{512L^4} \dots \right)$
	Right-angle turn of wire length of arm $L$ , depth $s/2$	$R = \frac{\rho}{4\pi L} \left( \ln \frac{2L}{r} + \ln \frac{2L}{s} - 0,2373 + 0,2146 \frac{s}{L} + 0,1035 \frac{s^2}{L^2} - 0,0424 \frac{s^4}{L^4} \dots \right)$
	Three-point star length of arm $L$ , depth $s/2$	$R = \frac{\rho}{6\pi L} \left( \ln \frac{2L}{r} + \ln \frac{2L}{s} + 1,071 - 0,209 \frac{s}{L} + 0,238 \frac{s^2}{L^2} - 0,054 \frac{s^4}{L^4} \dots \right)$
	Four point star length of arm $L$ , depth $s/2$	$R = \frac{\rho}{8\pi L} \left( \ln \frac{2L}{r} + \ln \frac{2L}{s} + 2,912 - 1,071 \frac{s}{L} + 0,645 \frac{s^2}{L^2} - 0,145 \frac{s^4}{L^4} \dots \right)$
	Six-point star length of arm $L$ , depth $s/2$	$R = \frac{\rho}{12\pi L} \left( \ln \frac{2L}{r} + \ln \frac{2L}{s} + 6,851 - 3,128 \frac{s}{L} + 1,758 \frac{s^2}{L^2} - 0,490 \frac{s^4}{L^4} \dots \right)$
	Eight-point star length of arm $L$ , depth $s/2$	$R = \frac{\rho}{16\pi L} \left( \ln \frac{2L}{r} + \ln \frac{2L}{s} + 10,98 - 5,51 \frac{s}{L} + 3,26 \frac{s^2}{L^2} - 1,17 \frac{s^4}{L^4} \dots \right)$
	Ring of wire diameter of ring $D$ , diameter of wire $d$ , depth $s/2$	$R = \frac{\rho}{2\pi^2 D} \left( \ln \frac{8D}{d} + \ln \frac{4D}{s} \right)$
	Buried horizontal strip length $2L$ , section $a$ by $b$ , depth $s/2$ , $b <$ $a/8$	$R = \frac{\rho}{4\pi L} \left( \ln \frac{4L}{a} + \frac{a^2 - \pi ab}{2(a+b)^2} + \ln \frac{4L}{s} - 1 + \frac{s}{2L} + \frac{s^2}{16L^2} + \frac{s^4}{512L^4} \dots \right)$
	Buried horizontal round plate radius $a$ , depth $s/2$	$R = \frac{\rho}{8a} + \frac{\rho}{4\pi s} \left( 1 - \frac{7}{12} \frac{a^2}{s^2} + \frac{33}{40} \frac{a^4}{s^4} \dots \right)$
	Buried vertical round plate radius $a$ , depth $s/2$	$R = \frac{\rho}{8a} + \frac{\rho}{4\pi s} \left( 1 + \frac{7}{24} \frac{a^2}{s^2} + \frac{99}{320} \frac{a^4}{s^4} \dots \right)$

In case of lightning, in surge conditions, grounding systems might have different and often complex behavior due to discharge in the soil. Complex processes are characterized by a hysteresis comportment (see Fig. 6.15). Grounding systems behavior in transient conditions of earthed electrodes of various shapes (horizontal conductors, driven-rods, grid systems) from theoretical and experimental points of view is described in [160-165] and [166-170] respectively. Recent models take into account discrete breakdown and filamentary arc paths, but relevant parameters are usually not known for practical cases [171].

The grounding system models can be approached by engineering methods based on circuit concepts or physical methods based on electromagnetic field concepts. In present work the engineering concept is selected. In practical situations often detailed data on the soil properties are unknown.

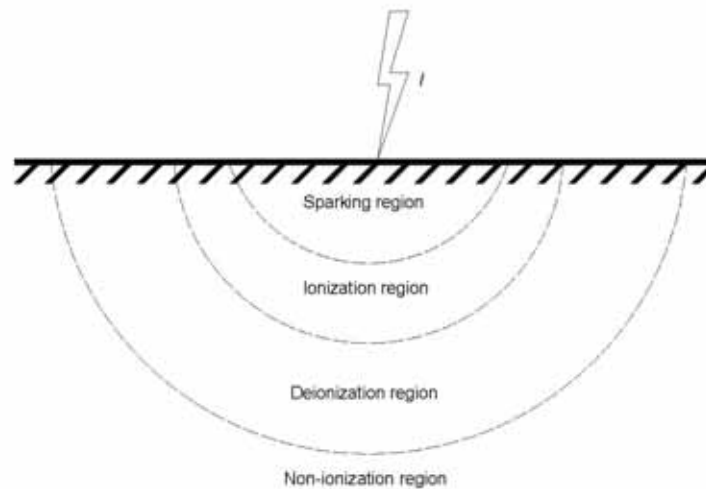


Figure 6.15. Lightning current effects on soil.

Often the soil is formed by different layers. The soil layer division is represented in Fig. 6.16. Usually layered models are applied with apparent resistivity of the layers [172].



Figure 6.16. Soil with two layers.

In practical cases the non-linear behavior of soil due to ionization effects can be ignored which always gives conservative results or can be represented by means of variable resistance [173].

The geometrical features of earthing arrangement have an impact on the electrical characteristics [171]. The Fig. 6.17. shows earthing arrangement behavior for A type rods

defined by [11] for different conductor length value as a function of soil resistivity. It is to note that for the typical situation the earthing arrangement has an inductive behavior. The rate of rise of the front of current impulses is therefore of major importance as it increases the importance of inductive voltage drop in comparison with resistive one [160, 169, 170].

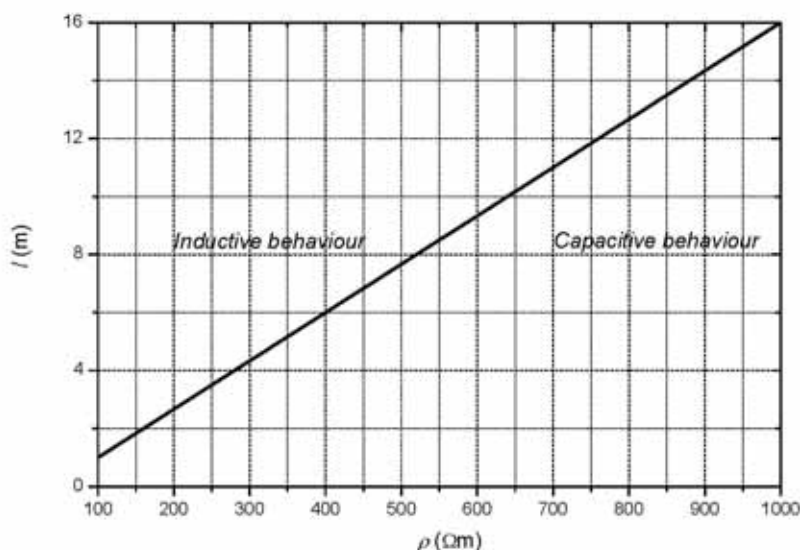


Figure 6.17. Earthing arrangement behaviour for A type rod [11] according to the soil resistivity.

Lightning current, independently from the polarity, propagates into the soil according to the typical laws of conducting means, taking into account the range of frequencies involved in the lightning current (from some hundreds of kHz up to 1 MHz) and for the soil resistivity up to 5000  $\Omega\text{m}$  [164]. It is therefore of basic importance, even for the dimensioning the earth termination system under lightning current, the knowledge of the soil resistivity and attention must be paid to the inhomogeneity of the soil involved in the current discharge. The high values of lightning currents associated with very short front durations can result in high current density in the layers of soil nearest the surface of ground electrodes so that the critical gradients may be exceeded and discharges into the soil can occur [170, 174].

In Fig. 6.18. the influence of conductor length of earthing arrangement on the total value of earth impedance for different value of soil resistivity is shown. This characteristics are obtained with an impulse current wave shape  $7 \mu\text{s} / 17 \mu\text{s}$  and peak value 5 kA. This aspect in details is described in [175].

In order to analyse and to compare the behaviour of different kinds of earth electrodes it is convenient to define some typical involved parameters [164]:

- transient or surge impedance defined as ratio between the instantaneous values of the earth-termination voltage (potential difference between the earth-termination system and the remote earth) and the earth-termination current which, in general, do not occur simultaneously;
- conventional earth impedance, defined as ratio of the peak values of the earth-termination voltage and the earth-termination current. It is used conventionally to indicate the resistance of the earth-termination system when subjected to lightning current;
- the impulse factor, defined as the ratio between the conventional earth impedance and the low frequency resistance of the earth electrode.

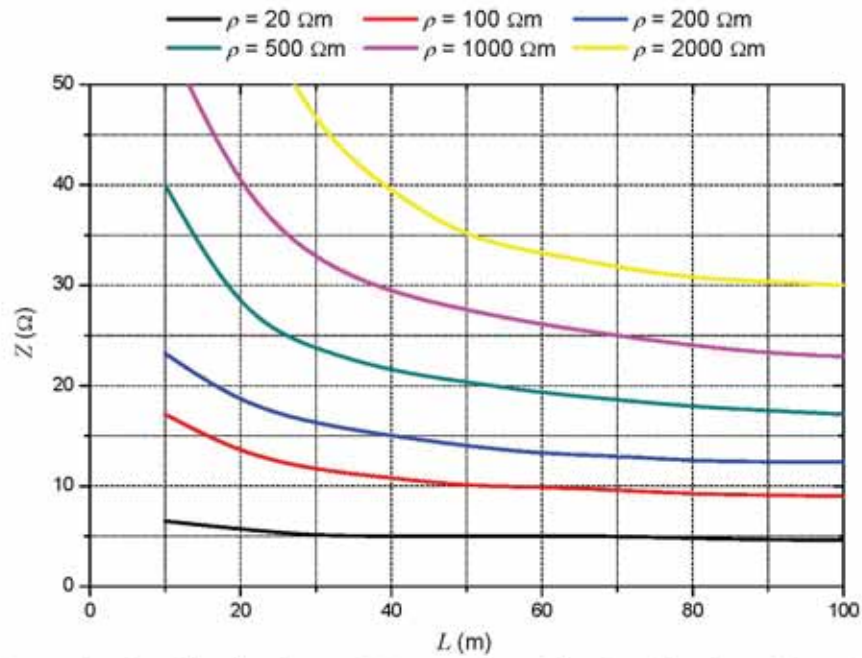


Figure 6.18. Conventional earthing impedance of A type rod as a function of length conductor for six different values of earth resistivity ranging 20 + 2000 Ωm.

The influence of earthing arrangement system dimensions for different configurations on the earthing impedance for different systems and soil resistivity 1500 Ωm is shown in Fig. 6.19 [175].

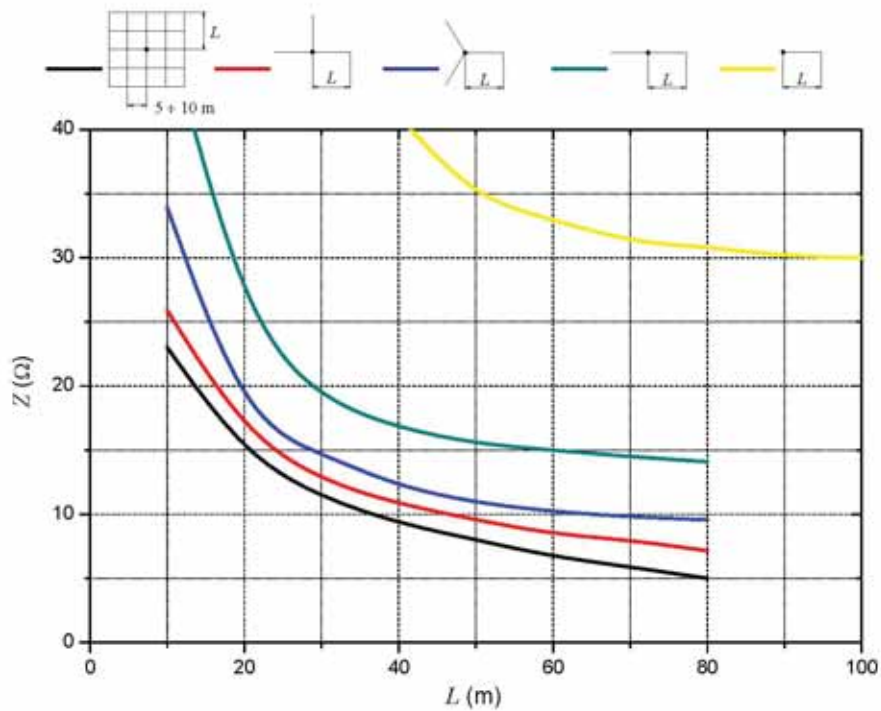


Figure 6.19. Earthing impedance of different earthing systems as a function its dimensions for soil resistivity 1500 Ωm.

The vertical earthing arrangement, namely rod type A according to IEC 62305-3, can be represented by means of  $R, L, C$  elements. The basic configuration is shown in Fig. 6.20.

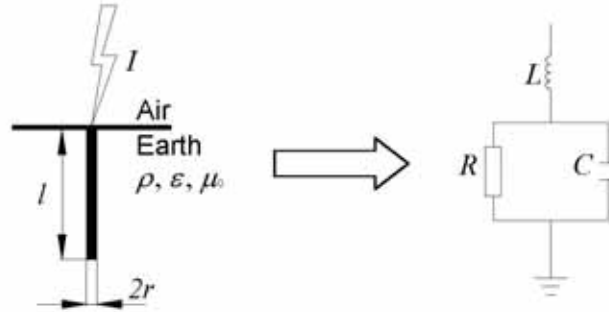


Figure 6.20. Model of vertical rod type A.

The parameters according to the rod features as well as soil parameters can be calculated as follows:

$$R = \frac{\rho}{2\pi l} \ln \frac{2l}{r} \quad (6.34)$$

$$C = 2\pi\epsilon l \ln \frac{2l}{r} \quad (6.35)$$

$$L = \frac{\mu_0 l}{2\pi} \ln \frac{2l}{r} \quad (6.36)$$

where:

$R$  – resistance ( $\Omega$ );

$L$  – inductance (H);

$C$  – capacitance (F);

$\rho$  – resistivity of soil ( $\Omega\text{m}$ );

$\epsilon$  – permittivity of soil (F/m);

$\mu_0$  – permeability (H/m);

$l$  – rod length (m);

$r$  – rod radius (m).

A discrete approximation of the distributed-parameter circuit is often used [176].

More advanced configuration is represented in Fig. 6.21, where the rod is divided into  $N$  fictitious segments and each segment of the rod is represented by a  $R-L-C$  section. Identical parameters are used for each section.

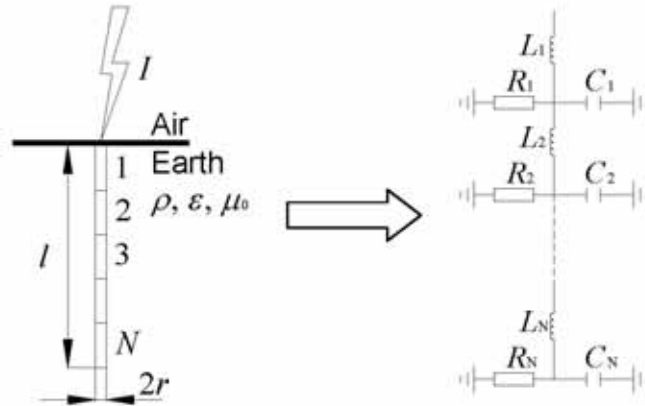


Figure 6.21. Model of vertical rod type A.

The parameters for each section can be calculated as follows:

$$R_n = \frac{1}{G_n} = \frac{\rho N}{2\pi l} \ln \frac{2l}{r} \quad (6.37)$$

$$C = \frac{2\pi\epsilon l}{N} \left[ \ln \frac{2l}{r} \right]^{-1} \quad (6.38)$$

$$L = \frac{\mu_0 l}{2\pi N} \ln \frac{2l}{r} \quad (6.39)$$

The transmission line model can be also adapted in terms of rod type A representation. Per-unit-length parameters can be computed approximately as static parameters since the field structure for the transverse electromagnetic satisfies a static distribution in any transverse plane. Therefore for vertical rod approximate per-unit-length parameters  $G'$ ,  $C'$  and  $L'$  can be simply obtained by dividing  $G$ ,  $C$  and  $L$  with  $l$  [177]. Further simple formulas for  $Z_c$ ,  $\gamma$  and  $Z$  can be applied.

$$R' = \frac{l}{G} = \frac{\rho}{2\pi} \ln \frac{2l}{r} \quad (6.40)$$

$$C' = \frac{C}{l} = 2\pi\epsilon \left[ \ln \frac{2l}{r} \right]^{-1} \quad (6.41)$$

$$L' = \frac{L}{l} = \frac{\mu_0}{2\pi} \ln \frac{2l}{r} \quad (6.42)$$

$$\gamma = \sqrt{j\omega L'(G' + j\omega C')} \quad (6.43)$$

$$Z = Z_c \coth \gamma l \quad (6.44)$$

$$Z_c = \sqrt{Z'/Y'} \quad (6.45)$$





Figure 6.22. Sketch of horizontal rod type A.

Similarly, for a horizontal ground electrode (shown in Fig. 6.22) approximate per-unit-length parameters  $G'$ ,  $C'$  and  $L'$  are [178]:

$$R' = \frac{l}{G} = \frac{\rho}{\pi} \left[ \ln \frac{2l}{\sqrt{2rh}} - 1 \right] \quad (6.46)$$

$$C' = \frac{C}{l} = \pi \epsilon \left[ \ln \frac{2l}{\sqrt{2rh}} - 1 \right]^{-1} \quad (6.47)$$

$$L' = \frac{L}{l} = \frac{\mu_0}{2\pi} \left[ \ln \frac{2l}{\sqrt{2rh}} - 1 \right] \quad (6.48)$$

The transient behaviour of earthing arrangement, namely mesh (type B in standard IEC/EN 62305-3) may be simulated by means of a network of  $\pi$  elements consisting of a capacitance  $C$ , an inductance  $L$  and a conductance  $G$ , what is shown in Fig. 6.23.

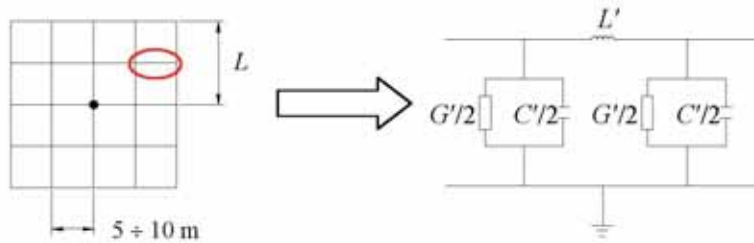


Figure 6.23. Example of mesh model.

The parameters for unit of length can be calculated as follows:

$$G' = \frac{\pi}{\rho} \cdot \left[ \ln \frac{2 \cdot l}{\sqrt{2 \cdot r \cdot d}} - 1 \right]^{-1} \quad (6.49)$$

$$C' = 28 \cdot 10^{-12} (1 + \epsilon_r) \cdot \left[ \ln \frac{2 \cdot l}{\sqrt{2 \cdot r \cdot d}} - 1 \right]^{-1} \quad (6.50)$$

$$L' = 0,2 \cdot 10^{-6} \left( \ln \frac{2l}{r} - 1 \right) \quad (6.51)$$

In case of mesh model, the selection of the parameters values depend on the lightning termination point. Also, it is possible to model complex interactions between the grounding systems and connected complex and distributed electrical systems [179, 180].

#### 6.4. Comparison of numerical and experimental results

In present part of work comparisons of numerical and experimental results are reported; for the discussion the SPD limiting type as protection measure is selected. The first comparison refers to the laboratory results shown in Fig. 6.24. The conditions of test are described in paragraph 6.2.2.



Figure 6.24. Oscillogram of voltage on the SPD terminals (limiting type) under stressing overvoltage of 2,5 kV and wave shape 1,2/50  $\mu$ s.

For the numerical simulation of SPD limiting type the  $U / I$  characteristic obtained during current test of SPD as described in 6.2.1. is used.

The Fig. 6.25. a) and b) represents computed results of SPD response.

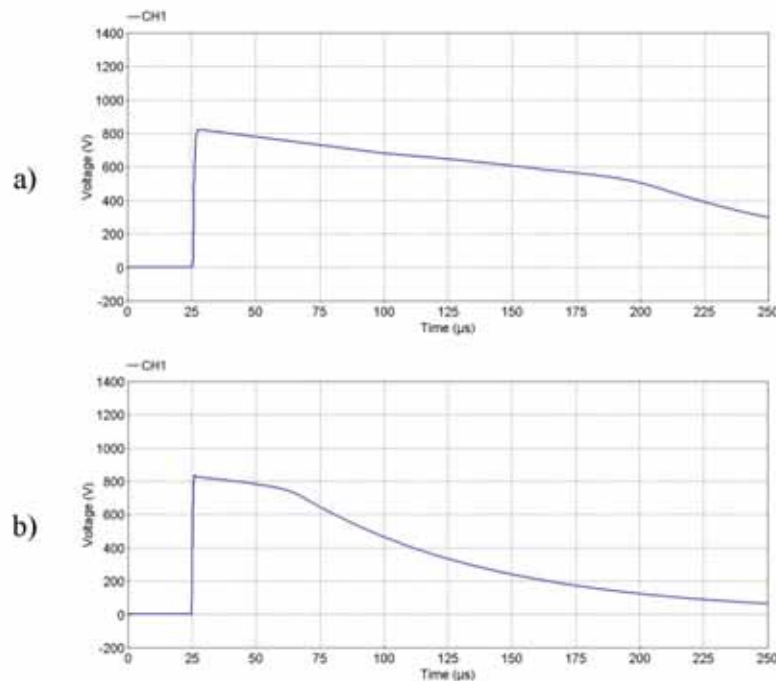


Figure 6.25. Voltage on the SPD terminals: a) in case of use the ideal voltage generator with determinate wave shape 1,2/50  $\mu$ s; b) in case of use the real voltage generator with determinate wave shape 1,2/50  $\mu$ s.

In Fig. 6.25 a) the voltage generator is simulated as an ideal generator, the SPD front time of wave shape ( $T_1$ ) is close to the experimental results, however the time to half value ( $T_2$ ) has different shape. This fact is well spotted after 50  $\mu$ s.

The results of second case (reported in Fig. 6.25 b) when the impulse voltage generator has been reconstructed according to its real features, show a good agreement for the front time ( $T_1$ ) as well for the time to half value ( $T_2$ ). The small difference of voltage values can be tolerated, as shown by comparing Fig. 6.24 and Fig. 6.25 b).

The results shown that the numerical calculation of analytical model are convergence with results from real object in case if the impulse voltage generator is constructed according to the real stressing device and the other physical elements are considered. Moreover present comparison shows that the solution of simulation model for an SPD limiting type is quite proper [107].

A more advanced comparison refers to the arrangement of Fig. 6.26. Such arrangement consists of the impulse voltage generator ( $G$ ) selected to obtain a wave shape 1,2/50  $\mu$ s, the typical low-voltage limiting SPDs, the conductors leading the SPD and the equipment to be protected and some different resistive ( $R$ ), inductive ( $L$ ), and capacitive ( $C$ ) loading elements.

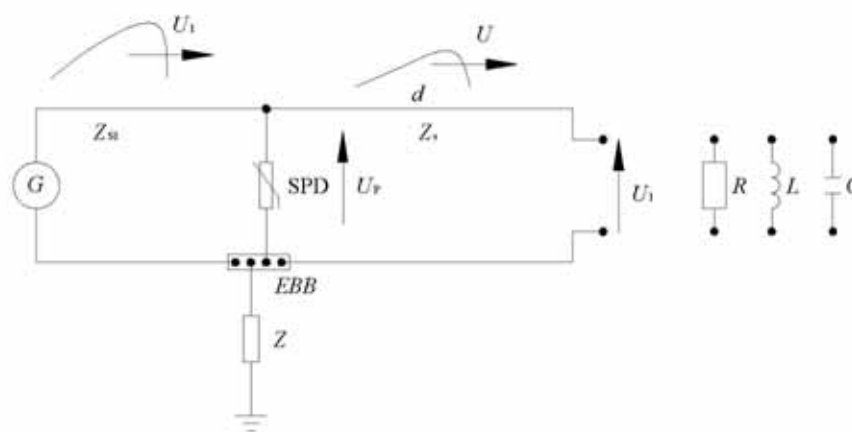


Figure 6.26. Analysed arrangement:  $G$  - impulse voltage generator;  $U_1$  - surge voltage;  $Z_{s1}$  - surge impedance left by the surge;  $EBB$  - equipotential bonding bar;  $Z$  - earth impedance;  $U_p$  - voltage on the SPD terminals;  $d$  - line length;  $Z_s$  - surge impedance right by the line;  $U$  - overvoltage incoming through distant SPD;  $U_1$  - voltage on the terminals of equipment to be protected ( $R, L, C$ ).

The following voltages are measured during the tests and simulations:

- $U_p$  - the voltage on the SPD terminals (CH1);
- $U_1$  - the voltage on the terminal of equipment to be protected (CH2).

Some results obtained by laboratory test and by simulations are reported in Fig. 6.27 a) and b) for  $R$  load, in Fig. 6.28 a) and b) for  $L$  load, in Fig. 6.29 a) and b) for  $C$  load.

In case of resistive load, the  $R = 48 \Omega$  and the line length of 25 m for test and simulation are selected.

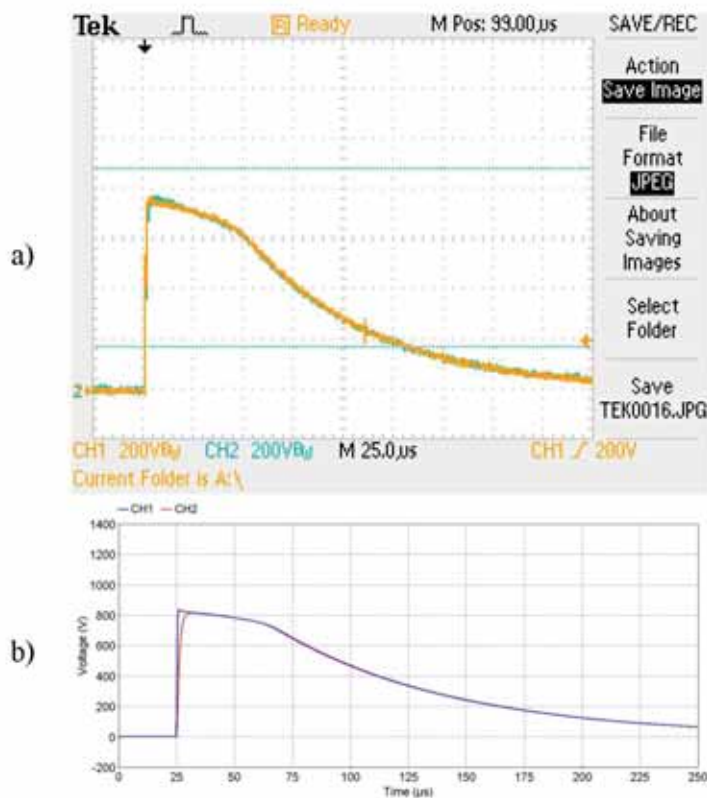
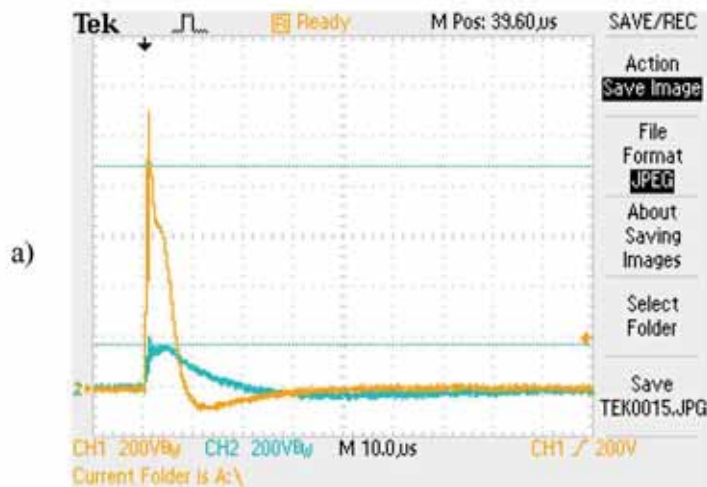


Figure 6.27. Oscillograms of voltage at equipment to be protected for  $R = 48 \Omega$  load condition,  $d = 25\text{m}$ ; CH1 voltage on the SPD terminals; CH2 voltage on the load; a) Experimental results; b) Computed results.

In this case the parameter of resistive load is close to condition of short circuit, so oscillations are not possible. It can be noticed that the value of voltage on the terminal of equipment to be protected (CH2) is similar to the voltage on the SPD terminals (CH1) due to limited length (25 m) of line connecting SPD and load.

In case of inductive load, the  $L = 4,5 \mu\text{H}$  and the line length of 25 m for test and simulation are considered.



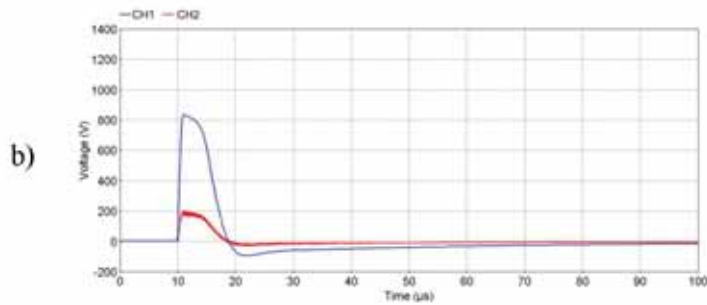


Figure 6.28. Oscillograms of voltage at equipment to be protected for  $L = 4,5 \mu\text{H}$  load condition,  $d = 25 \text{ m}$ ; CH1 voltage on the SPD terminals; CH2 voltage on the load; a) Experimental results; b) Computed results.

It can be noticed that for laboratory test (Fig. 6.28 a) the value of voltage on the terminal of equipment to be protected (CH2) is significant smaller than the voltage on the SPD terminals (CH1). Corresponding simulation (Fig. 6.28 b) exhibits a form similar to the experimental results. In this case the effect of inductive load is visible in the inverse oscillation on the SPD terminals.

In case of capacitive load, the  $C = 0,25 \mu\text{F}$  and the line length of 0,1; 10; 25 m for test and simulation are taken into account.

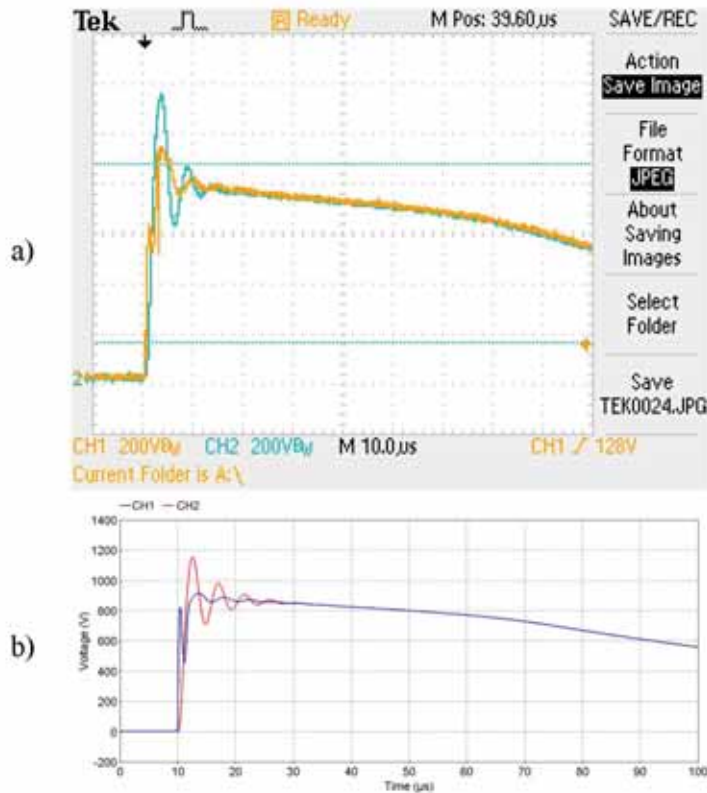


Figure 6.29. Oscillograms of voltage at equipment to be protected for  $C = 0,25 \mu\text{F}$  load condition,  $d = 0,1 \text{ m}$ ; CH1 voltage on the SPD terminals; CH2 voltage on the load; a) Experimental results; b) Computed results.



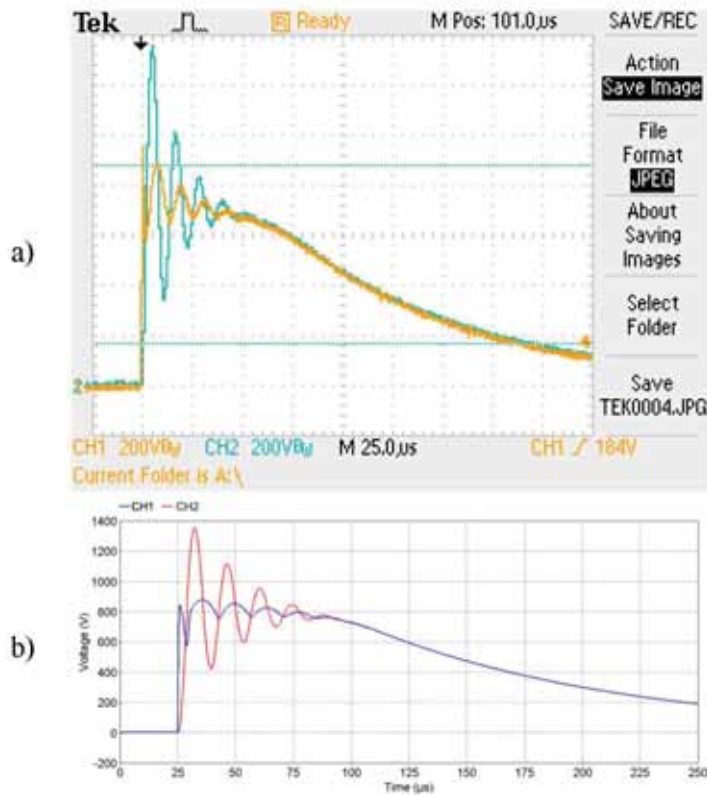


Figure 6.30. Oscillograms of voltage at equipment to be protected for  $C = 0,25 \mu\text{F}$  load condition,  $d = 10 \text{ m}$ ; CH1 voltage on the SPD terminals; CH2 voltage on the load; a) Experimental results; b) Computed results.

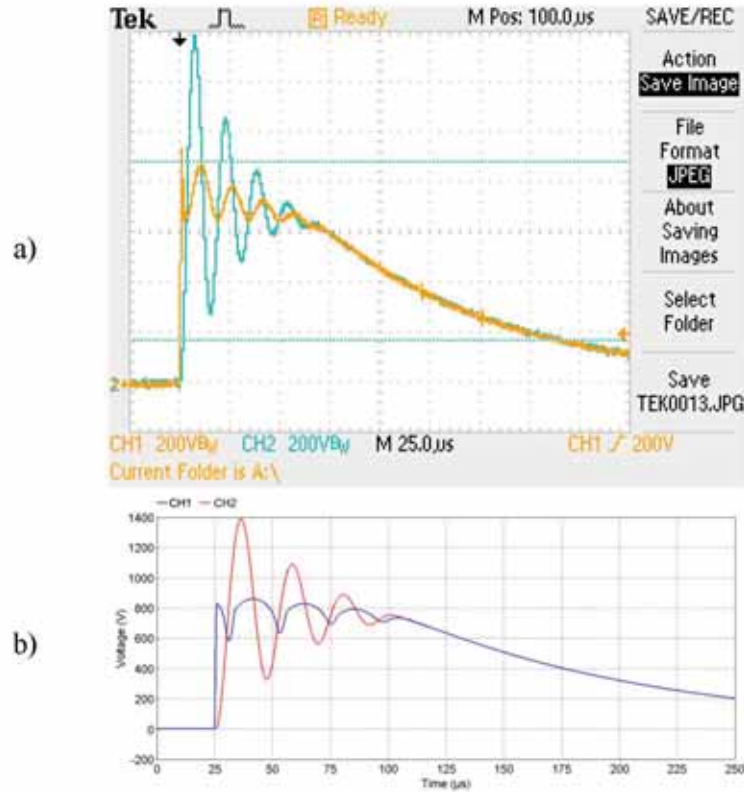


Figure 6.31. Oscillograms of voltage at equipment to be protected for  $C = 0,25 \mu\text{F}$  load condition,  $d = 25 \text{ m}$ ; CH1 voltage on the SPD terminals; CH2 voltage on the load; a) Experimental results; b) Computed results.



It can be noticed that for laboratory tests (Fig. 6.29 a, 6.30 a, 6.31 a) the value of voltage on the terminals of equipment to be protected (CH2) is significant higher than the voltage on the SPD terminals (CH1). This increment ( $\Delta U$ ) depends on the line length. Corresponding simulations (Fig. 6.29 b, 6.30 b, 6.31 b) have the form similar to the experimental results. The results are summarized and reported in Tab. 6.6.

Table 6.6. Measured and simulated values of voltage at apparatus to be protected for  $C = 0,25 \mu\text{F}$  load condition and different line lengths.

Line length (m)	Tests		Simulations	
	$U_1$ (V)	$\Delta U$ (V)	$U_1$ (V)	$\Delta U$ (V)
0,1	1124	324	1162	362
10	1363	563	1381	581
25	1395	595	1398	598

Note:  
 $\Delta U$  – voltage increment respect to the value of voltage on the SPD terminals

On the base of computer simulation model is possible to analyse other electrical circuits, difficult to realize in laboratory. Some results for long leads  $d = 100\text{m}$  and different load conditions are reported in Fig. 6.32 for  $R$  load, in Fig. 6.33 for  $L$  load and in Fig. 6.34 for  $C$  load.

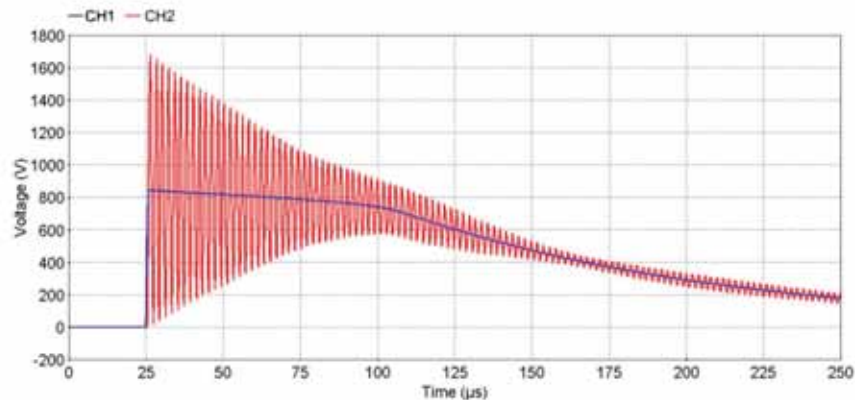


Figure 6.32. Computed oscillograms of voltage at equipment to be protected for  $R = 1 \text{ M}\Omega$  load condition,  $d = 100 \text{ m}$ ; a) voltage on the SPD terminals; b) voltage on the load.

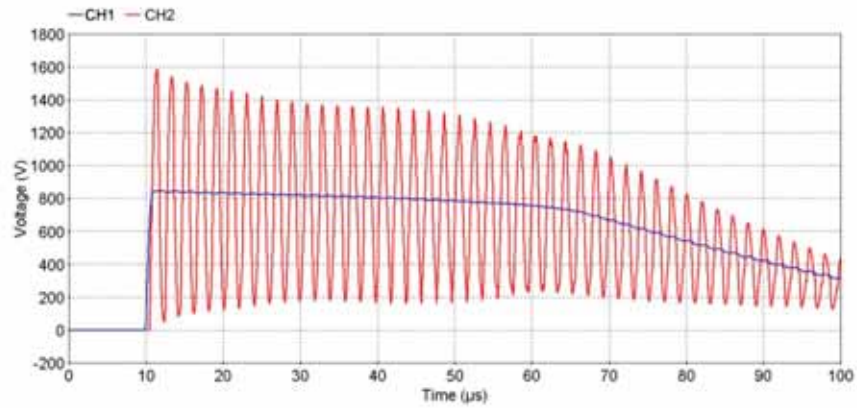


Figure 6.33. Computed oscillograms of voltage at equipment to be protected for  $L = 5$  mH load condition,  $d = 100$  m; a) voltage on the SPD terminals; b) voltage on the load.

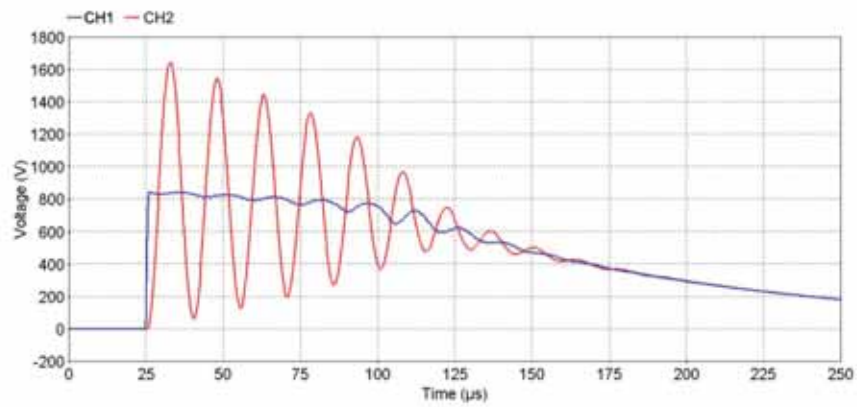


Figure 6.34. Computed oscillograms of voltage at equipment to be protected for  $C = 25$  nF load condition,  $d = 100$  m; a) voltage on the SPD terminals; b) voltage on the load.

From the oscillograms it can be observed that the voltage on the load is doubled, whatever is the load condition due to travelling wave effect on long (100m) line length between SPD and load.

## **6.5. Factors influencing the selection and installation of surge protective devices for low voltage systems: upstream SPD**

### **6.5.1. Introduction**

For a proper selection and installation of SPDs, it is of essential importance to know the stress, which an SPD will experience under surge conditions; such stress, as underlined by the Standard [11, 18], is a function of many complex and interrelated factors. These include: the location of the SPD(s) within the structure; the method of coupling of the lightning strike to the facility (resistive or inductive); the routing of internal circuits and their distance from inducing lightning currents; the sharing of lightning currents within the structure to the earthing system and to the connected services, mainly the current peak value and waveshape, which the SPD will have to conduct under surge conditions. Furthermore the different behaviour of the SPD containing spark gaps (switching type SPD) and SPD containing metal-oxide varistors (limiting type SPD) should be considered.

In the present paragraph only surges due to flashes to the structure (source S1), what consist of worst case, protected by a lightning protection system (LPS), are considered. The influence of the main factors and parameters which affect the selection and installation of an SPD of both types (switching and limiting) installed at entry point of line in the structure are discussed. Investigation relevant to SPD installed downstream are considered in section 6.6. By several computer simulations, simple rules are established for the selection of effective SPD with regard to the discharge current and its protection level.

### **6.5.2. Selection with regard to discharge current**

The selection of the discharge current of an SPD requires the evaluation of the peak value and wave shape of the possible current flowing through the SPD [146, 147, 181-184]. In fact as general rule, SPD shall withstand the energy relevant to the perspective current at the installation point and, at this value, the protection level  $U_p$  shall be lower than the required one. Moreover, the selection of such current has an essential influence on the aging of SPD. In particular, this aspect is more important in an SPD limiting type, such as a varistor, where a degradation is registered due to the effect of single or multiple current pulses that are able to produce microstructural changes in the material.

As shown in the diagram of Fig. 6.35, the lightning current striking the *LPS*, as result of resistive coupling, is shared between the earth arrangement of the structure and the supply line. The current  $I_{SPD}$  flowing through the *SPDI* to the incoming line depends, in amplitude and shape, on the conventional impedance of the earth arrangement ( $Z$ ) and on the impedance of the supply line (mainly on line length) and on the wave shape of the lightning current.

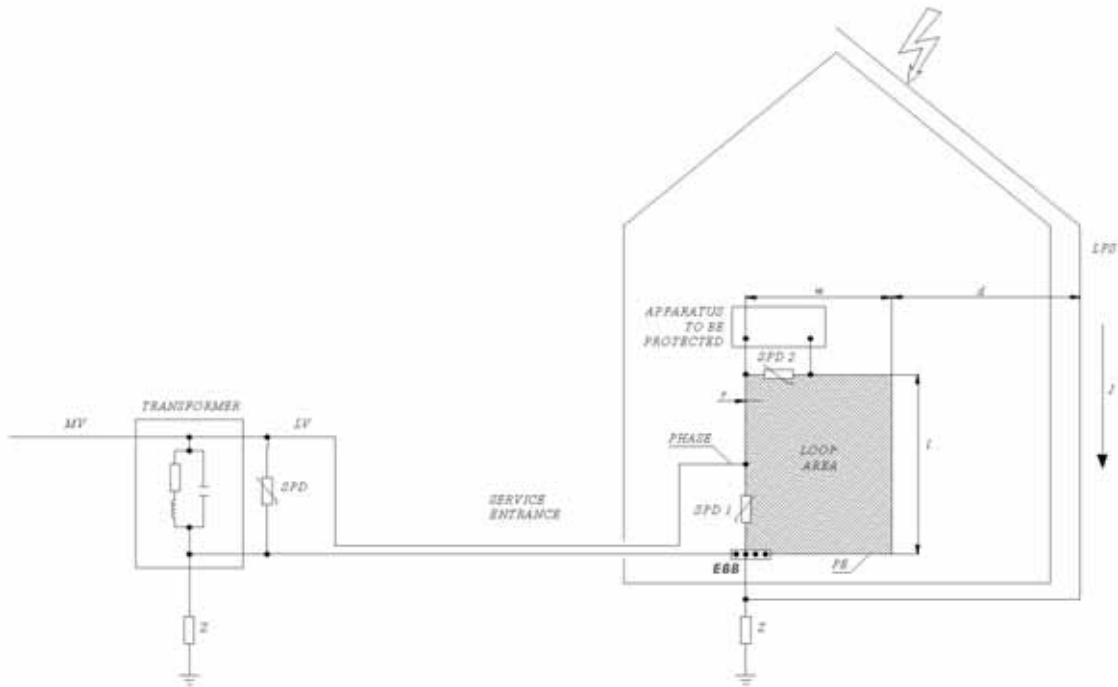


Figure 6.35. Basic diagram of circuit to supply an apparatus and the loop formed by PE, phase conductor and an SPD bonded to a concentrated earth termination arrangement (type A according to IEC/EN 62305-3).

An example of the currents distribution of the considered arrangement is presented in Fig. 6.36 and in Fig. 6.37 for lightning current shape  $10/350 \mu\text{s}$  and  $0,25/100 \mu\text{s}$  respectively.

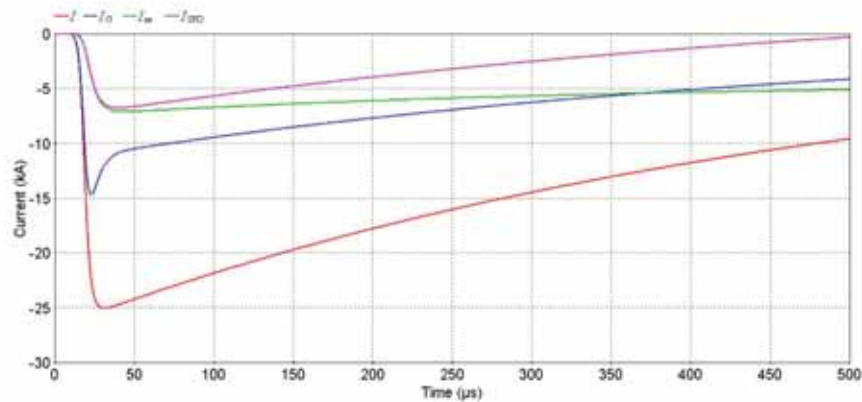


Figure 6.36. Current distribution in the arrangement considered in Fig. 6.35; lightning current wave shape  $10/350 \mu\text{s}$ ; conventional earth impedance  $Z = 10 \Omega$ ; supply line length  $L = 100 \text{ m}$  with two conductors; no external connected services.  $I$  - lightning current;  $I_G$  - current to earth electrode;  $I_N$  - current to the neutral;  $I_{SPD}$  - current to the phase conductor.

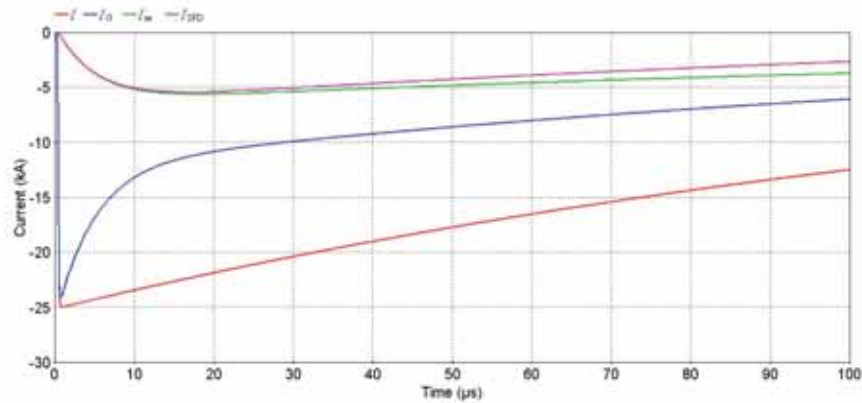


Figure 6.37. Current distribution in the arrangement considered in Fig. 6.35; lightning current wave shape 0,25/100  $\mu\text{s}$ ; earth impedance  $Z = 10 \Omega$ ; supply line length  $L = 100 \text{ m}$  with two conductors; no external connected services.  $I$  - lightning current;  $I_G$  - current to earth electrode;  $I_N$  - current to the neutral;  $I_{SPD}$  - current to the phase conductor.

Indeed shape of lightning current and line length scarcely affect the amplitude of  $I_{SPD}$ , while the rise time  $T_1$  of  $I_{SPD}$  increases with the length of the supply line as reported in Fig. 6.38; this directly affects the voltage drop  $\Delta V$  on the connection conductors of SPD (see 6.5.3).

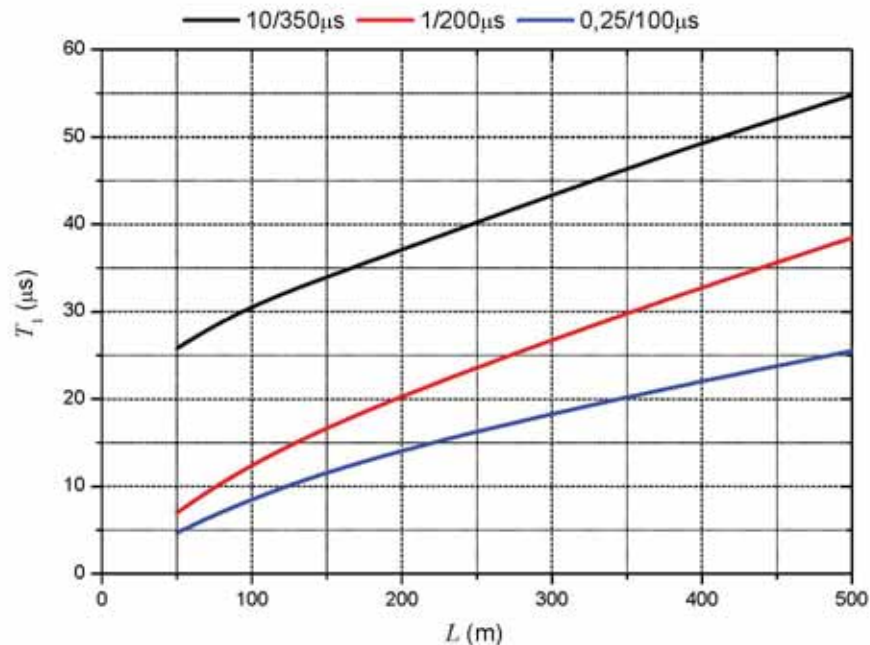


Figure 6.38. Rise time  $T_1$  of the current  $I_{SPD}$  as a function of supply line length  $L$  for three shapes of lightning current.

The highest values of current flowing through the SPD occur where a single line with two conductors is connected to the structure, with no other connected external service and for high values of the conventional impedance of the earth arrangement ( $Z$ ), as shown in Fig. 6.39.



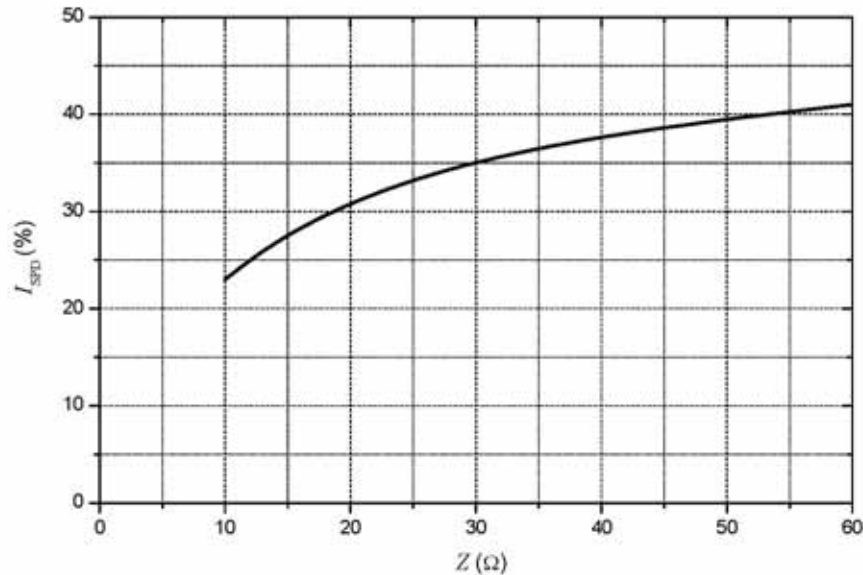


Figure 6.39. Percentage of the current  $I_{SPD}$  as a function of conventional earth impedance for the positive stroke current 10/350  $\mu$ s. Length of supply line  $L = 50$  m; no external connected services.

The  $Z$  value of an earthing arrangement, dimensioned according to IEC/EN 62305-3, increases with the lightning protection level (LPL), i.e.  $Z = 10 \Omega$  for LPL I and  $Z = 15 \Omega$  for LPL II; therefore the current  $I_{SPD}$  is increasing with LPL.

As an example, if  $Z = 10 \Omega$  is assumed and a single supply line with two conductors is connected to the structure, with any other connected external service, the current  $I_{SPD}$  ranges from 27% to 21% for a positive flash (standard shape 10/350  $\mu$ s) and from 23% to 18% for subsequent stroke of negative flash (standard shape 0,25/100  $\mu$ s), as the length of the line  $L$  varies from 50 m to 500 m. These values are in the range of the approximate value (25%) suggested by the IEC/EN 62305-1 independently from the wave shape of lightning current, the length of the line and the protection level LPL.

Furthermore, the results of several simulations show that the current  $I_{SPD}$  is not practically influenced by :

- the type of earthing arrangement, namely rod type (type A according to standard EC/EN 62305-3) or ring or mesh type (type B of standard IEC/EN 62305-3);
- the type of electrical system, TT or TN;
- the type of SPD, switching or limiting .

For a properly designed SPD, the charge for unit of current, associated to the current  $I_{SPD}$ , is increasing with the line length but at least for the line length values  $L < 1000$  m, is always less than 0,5 C/kA, even in the worst case of positive flashes (shape 10/350  $\mu$ s), as shown in Fig. 6.40.

Note that the charge 0,5 C/kA is the value associated to the current with the standard shape 10/350  $\mu$ s, so that indeed such shape appear adequate for SPD class I testing.



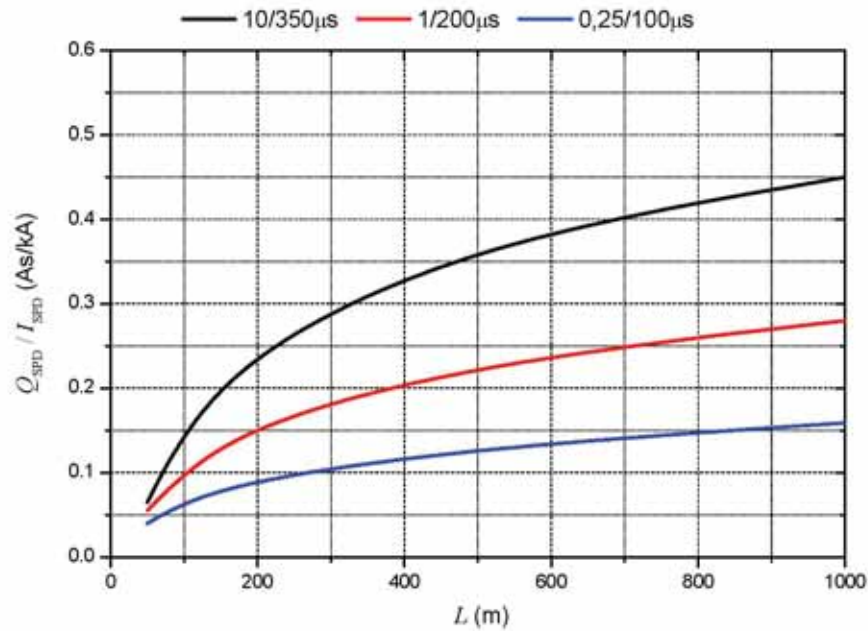


Figure 6.40. Charge per unit of current flowing through SPD as a function of supply line length  $L$  for three shapes of lightning current.

### 6.5.3. SPD selection with regard to protection level

The selection with regard to protection level  $U_p$  of an SPD has a direct influence on the values of the voltage at the terminals of the apparatus to be protected  $U_1$ .

The voltage  $U_1$  depends on:

- the protection level  $U_p$  of SPD;
- the inductive voltage drop  $\Delta V$  of the leads/connections of SPD;
- the effects of surge travelling along the protected circuit;
- the overvoltages  $U_i$  induced by lightning current in the protected circuit.

The inductive voltage drop  $\Delta V$  on the leads/connections of SPD should be combined with the protection level  $U_p$  in order to obtain the so-called “effective protection level”  $U_{p,ef}$  of the SPD [11]. The voltage drop depends on the length of the connecting leads and on the steepness of the current flowing through the SPD, which, depends, as mentioned at the preceding section, on the impedance of the earth arrangement and on the line length.

Moreover, the propagating effect of fast transients along the protected circuit shall be taken into account. Due to oscillation phenomena of fast surges, in the time interval of two times the travel time of surge along the circuit, the voltage  $U_1$  at the apparatus terminals is [146, 147, 185]:

$$U_1 = U_p + k \cdot l \quad \text{if } l < l_2 \quad (6.52)$$

$$U_1 = 2 \cdot U_p \quad \text{if } l \geq l_2 \quad (6.53)$$

where:

$k = \frac{2 \cdot s}{v}$  – increment of the voltage per unit of the circuit length (V/m);

$s$  – front steepness of the voltage at SPD terminals (V/μs);

$v$  – the speed of voltage surge along the circuit (m/ $\mu$ s);  
 $l$  – the distance between SPD and apparatus to be protected,  
 $l_2$  – the distance at which the voltage is doubled on apparatus terminals.

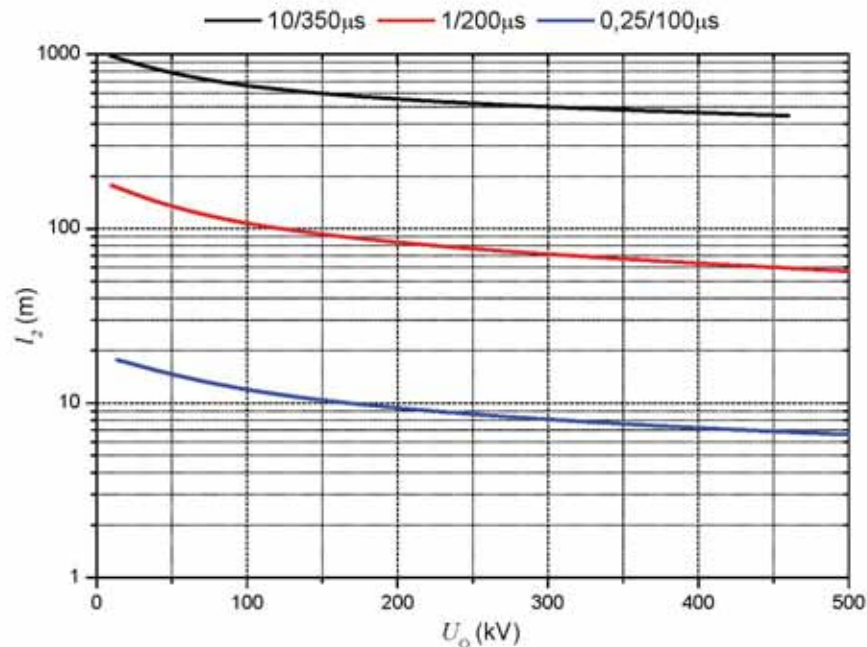


Figure 6.41. Protected circuit length  $l_2$  as function of earth-termination voltage  $U_o$  for three lightning current shapes; protection level of switching type SPD: 1,25 kV.

For the SPD of switching type the voltage  $U_1$  at the SPD terminals may be approximate by a triangular shape reaching the maximum value  $U_p$  at switching time of the SPD.

The distance  $l_2$  at which the voltage is doubled on apparatus terminals decreases with:

- increasing of the front steepness  $s$ ;
- increasing of protection level  $U_p$  of SPD;
- increasing of the amplitude of earth-termination voltage  $U_o = Z I_G$  stressing the SPD, as shown in Fig. 6.41;
- decreasing of the rise time of the stressing overvoltage  $U_o$ .

For the SPD of limiting type the voltage  $U_1$  at the SPD terminals may be approximated by a rectangular shape and the maximum value  $U_p$  is reached in a short time – from 0,1  $\mu$ s for wave shape 0,25/100  $\mu$ s to 3  $\mu$ s for shape 10/350  $\mu$ s of the lightning current; such time is scarcely affected by the line length and by the value of conventional earth impedance  $Z$ .

The distance at which the voltage is doubled on apparatus terminals ( $l_2$ ) increases as the rise time of the lightning current  $I$  is increasing. In Fig. 6.41, 6.42 and 6.43 a summary of the obtained results is reported for negative subsequent strokes current 0,25/100  $\mu$ s, negative first stroke current 1/200  $\mu$ s and positive flash current 10/350  $\mu$ s.

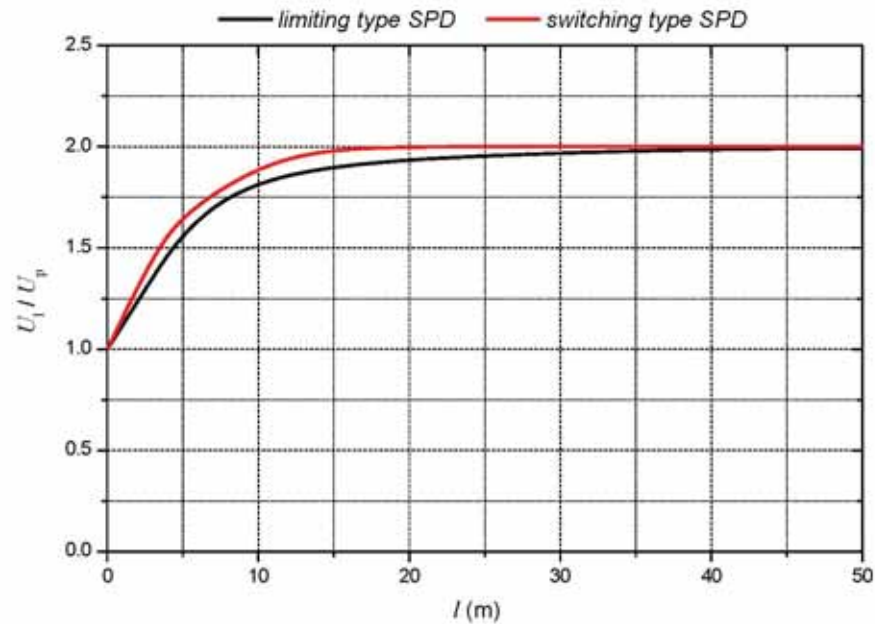


Figure 6.42. Voltage ratio  $U_1 / U_p$  for SPD switching and limiting type as a function of the protected circuit length  $l$ . Protection level of the SPD: 1,25 kV; lightning current 0,25/100  $\mu$ s; earth termination voltage  $U_o = 80$  kV; supply line length  $L = 50 \div 1000$  m.

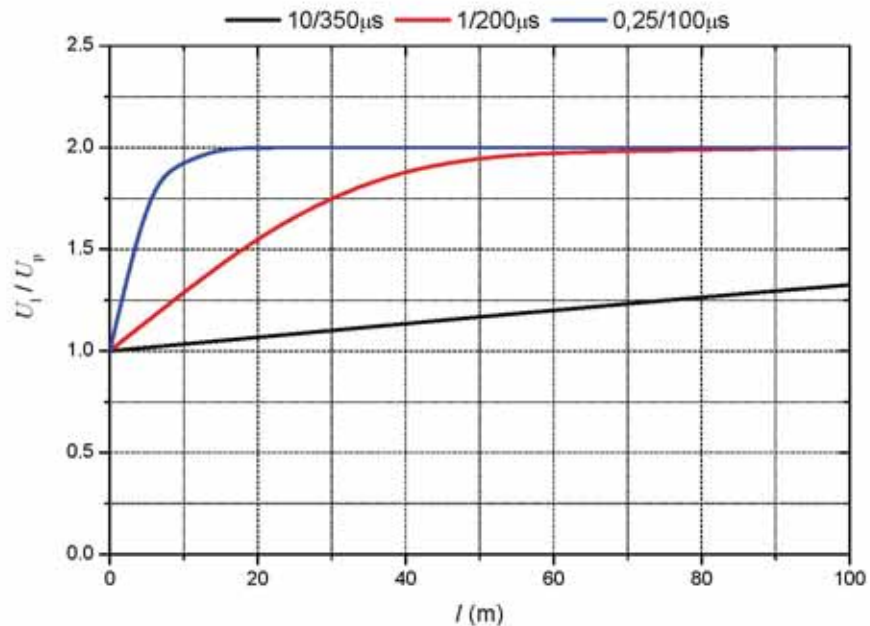


Figure 6.43. Voltage ratio  $U_1 / U_p$  as a function of the protected circuit length  $l$  for three lightning current shapes.

For the fastest lightning current (0,25/100  $\mu$ s), usually the distance  $l_2$  does not overcome a value of 20 m, but at the distance of about 10 m from the SPD the voltage already reaches the value  $U_1 \approx 1,9 U_p$ , as demonstrated in Fig. 6.43. Therefore for practical purposes  $k = 0,1 U_p$  may be assumed. Furthermore, the overvoltage  $U_i$  induced by lightning current in the protected circuit, has to be also considered, and its influence on the protection distance must be taken in account. Simple methods to evaluate the induced voltage  $U_i$  are reported in [11].

Lastly it is noted that the voltage measured at the apparatus terminals may overshoot the SPD nominal protection level [186] even by a factor higher than 2. Such result should be further considered and discussed with particular attention to successive reflections from the LV power line and to the capacitive coupling to earth of the line as well as of the circuit between SPD and apparatus, which cannot be ignored and may influence the voltage at the apparatus terminals.

#### 6.5.4. Inductive voltage drop $\Delta V$ on the connection leads of SPD

The inductive voltage drop  $\Delta V$  on the leads/connections of SPD (Fig. 5.8) depends on the inductance  $L_c$  of such leads and on the steepness of the current  $I_{SPD}$  flowing through the SPD to the incoming lines, and then on its amplitude and rise time.

As discussed in section 6.5.2, amplitude and rise time of the current  $I_{SPD}$  depend on the earthing arrangement and on the line length. Because the amplitude of the current  $I_{SPD}$  is decreasing and the rise time  $T_1$  is increasing with increasing of the supply line length, consequently the voltage drop  $\Delta V$  is decreasing with such length.

The highest value of the voltage drop is due to the flowing of the current of negative subsequent stroke.

For a properly designed SPD, the values of  $\Delta V$  are in most the cases higher than  $\Delta V = 1$  kV/m fixed by the IEC/ EN 62305-4, independently from the length of the connected line, from the sharing of the current among the conductors of the incoming lines and external services as well as from the lightning protection level LPL.

At assumption of  $L_c = 1 \mu\text{H/m}$ , the voltage drop  $\Delta V$  assumes the values reported in Tab. 6.7 according to the protection level LPL and the supply line length.

Table 6.7. Voltage drop  $\Delta V$  in the SPD branch; earth impedance  $Z = 10 \Omega$ ; mono phase supply line length ranging between 50 m and 1000 m.

Source type	LPL I (kV/m)	LPL II (kV/m)	LPL III-IV (kV/m)
First positive stroke (10/350 $\mu\text{s}$ )	6,5 $\div$ 1,5	5 $\div$ 1	3,3 $\div$ 0,7
First negative stroke (1/200 $\mu\text{s}$ )	7 $\div$ 1,6	5,5 $\div$ 1,2	3,5 $\div$ 0,8
Subsequent negative stroke (0,25/100 $\mu\text{s}$ )	8 $\div$ 3,5	6 $\div$ 2,6	4 $\div$ 1,7

From the results summarized in Tab. 6.7 it can be demonstrated that the worst case consist of subsequent negative strokes for LPL I.



### 6.5.5. SPD dimensioning

#### Selection of protection level $U_p$

For the *SPD1* installed at the entry point of the line (main switch board) the selection of protection level  $U_p$  should take into account:

- the inductive voltage drop  $\Delta V$  of the leads/connections of SPD,
- the effects of surge travelling along the protected circuit,
- the voltage  $U_i$  induced by lightning current in the protected circuit formed by the SPD and the apparatus to be protected.

In all the three cases reference should be made to the subsequent strokes of negative flashes, which represent the more severe case, as discussed in 6.5.2.

Following the IEC 62305-4 [11], if an effective protection level  $U_{pf}$  is defined as the voltage at the output of the SPD resulting from its protection level  $U_p$  and the voltage drop  $\Delta V$ , namely:

$$U_{pf} = U_p + \Delta V \quad \text{for limiting type SPD} \quad (6.54)$$

$$U_{pf} = \max(U_p, \Delta V) \quad \text{for switching type SPD} \quad (6.55)$$

the following formulas may help in the selection of  $U_p$  according to the length  $l$  of the protected circuit:

$$U_{pf} \leq U_w \quad \text{for } l = 0 \text{ m} \quad (6.56)$$

$$U_{pf} \leq (U_w - U_i) / (1 + 0,1l) \quad \text{for } 0 < l \leq 10 \text{ m} \quad (6.57)$$

$$U_{pf} \leq (U_w - U_i) / 2 \quad \text{for } l > 10 \text{ m} \quad (6.58)$$

being  $U_w$  the rated impulse withstand voltage of the apparatus to be protected.

It is to note that the value  $U_{pf} \leq 0,8 U_w$  suggested by the IEC/ EN 62305-4 for  $0 < l \leq 10 \text{ m}$  is not on safety side in front of the value given by formula (6.54).

Due to high values of  $\Delta V$ , even if the induced voltage  $U_i = 0$  is assumed, the distance between *SPD1* and apparatus (or the value of  $U_p$ ) should be kept so low that practically in all cases installation of a downstream *SPD2* is required.

Once *SPD2* is provided, the fulfillment of conditions a, b) and c) are no longer required for *SPD1*: only the energy coordination between *SPD1* and *SPD2* should be considered.

#### Selection of SPD discharge current

The impulse current  $I_{imp}$  of a class I test SPD and the nominal current  $I_n$  of a class II test SPD should be selected in such way that :

- the value of  $U_p$  at the current  $I_{SPD}$  expected at the point of SPD installation, does not overcome the rated impulse withstand voltage level  $U_w$  of the equipment to be protected;
- the energy associated to the discharge current does not overcome the value tolerated by the SPD.

If the shape of the  $I_{SPD}$  would be the same of the SPD standard test current (10/350  $\mu$ s for SPD of class I test, 8/20  $\mu$ s for SPD of class II test) both the conditions a) and b) could be verified if:

$$I_{imp} \geq I_{SPD} \quad \text{for SPD of class I test} \quad (6.59)$$

$$I_n \geq I_{SPD} \quad \text{for SPD of class II test} \quad (6.60)$$

Usually the wave shape of expected  $I_{SPD}$  differs from the standardized shape of SPD test current. In this case, condition b) may be considered satisfied as a first approximation if the charge  $Q_{SPD}$  associated to  $I_{SPD}$  does not overcome the tolerable one for the SPD.

If we consider that the charge  $Q_{SPD}$  for unit of current associated to the standard current 10/350  $\mu$ s is  $Q_{imp} = 0,5$  C/kA and to the standard current 8/20  $\mu$ s is  $Q_n = 0,027$  C/kA, the relations to be respected for SPD dimensioning are the following:

for SPD class I test:

$$I_{imp} \geq I_{SPD} \quad (6.61)$$

$$Q_{imp} \geq Q_{SPD} \text{ or numerically } I_{imp} \geq 2 Q_{SPD} \quad (6.62)$$

for SPD class II test:

$$I_n \geq I_{SPD} \quad (6.63)$$

$$Q_n \geq Q_{SPD} \text{ or numerically } I_n \geq 37 Q_{SPD} \quad (6.64)$$

It should be noted (see Fig. 6.40) that an SPD1 class I test is able to withstand the expected charge  $Q_{SPD}$  so that its dimensioning is determined by the current  $I_{SPD}$ .

### 6.5.6. Conclusions relevant to the upstream SPD

From the analysis herewith performed the following conclusions may be drawn:

- The selection of a proper protection level of SPD is affected by the length and the characteristics of the circuit between the SPD and the apparatus and by the shape of lightning current;
- the voltage  $U_i$  at apparatus terminals increases with circuit length and may reach the double of SPD effective protection level  $U_{p/r}$  in ten meters for the negative subsequent stroke (worst case);
- the inductive voltage drop  $\Delta V$  on the leads/connections of SPD may reach several hundred volts even for short connection length (0,1 ÷ 0,2 m);
- due to high values of  $\Delta V$ , even if overvoltage  $U_i$  induced in the circuit is negligible, the distance between SPD1 and apparatus (or the value of  $U_p$ ) should be kept so low that practically in all cases installation of a downstream SPD2 is required;
- the rise time of the current  $I_{SPD}$  flowing through the SPD to the incoming lines is longer than the rise time of the lightning current and is increasing as the length of the line increases, while its amplitude decreases with the line length;
- an SPD1 class I test is able to withstand the expected charge  $Q_{SPD}$  so that its dimensioning is determined by the current  $I_{SPD}$ ;
- the standard lightning current shape 10/350  $\mu$ s appears adequate for SPD testing.



## 6.6. Factors influencing the selection and installation of surge protective devices for low voltage systems: downstream SPD

### 6.6.1. Introduction

The present section intends to give a contribution to the investigation on the expected surge current, peak value and shape, due to lightning electromagnetic impulse (LEMP) by flashes to the structure for the surge protective device (SPD) proper selection in order to assure electronic apparatus operation. The obtained results are discussed with the SPD requirements of international standard [18].

In the previous section (6.5) and in the contributions [107, 143-147, 187, 188] it has been demonstrated that in the case of source of damage S1, an SPD (*SPD1*) installed at the entry point of an incoming line is not able to protect the apparatus internal to the structure (see Fig. 6.35) if the length of the circuit between SPD and apparatus is higher than few meters. In these circuits a second SPD (*SPD2*) is required to be installed close to the apparatus to be protected. *SPD2* should be energy coordinated with *SPD1* taking into account the current and the associated charge values flowing from *SPD1* to the circuit at its operation. The aim of present paragraph is to investigate on the expected surge current, peak value and shape, by flashes to the structure (source of damage S1) for the *SPD2* proper selection in order to assure electronic apparatus operation.

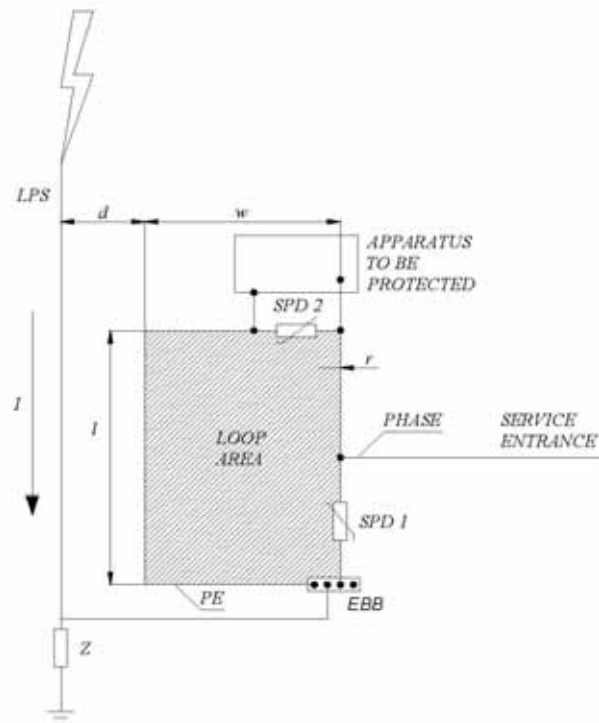


Figure 6.44. Considered basic arrangement: lightning strokes to LPS near an electric circuit.

The analysed arrangement has been already shown in Fig. 6.35 and its simplification is presented in Fig 6.44. Lightning current flowing on LPS down-conductors causes on the loop formed by the circuit between *SPD1* and *SPD2* overvoltages for inductive coupling that overlap the voltage across the *SPD1* increasing the voltage which urges the apparatus.

The discharge current  $I_{SPD2}$  flowing through *SPD2* is the combination of the current  $I_i$  induced in the loop circuit and the current  $I_r$  transmitted (feeding effect) in the circuit from *SPD1* during its operation. The knowledge of the amplitude and waveform of the current  $I_{SPD2}$  is essential for the correct dimensioning of *SPD2*.

Fig. 6.44 represents a simple example of flash to a lightning protection system (LPS) conductor near an electrical circuit loop, where:  $I$  – stroke current;  $d$  – distance between lightning current flowing in the electrical conductor and the induced circuit loop;  $l$  – loop length;  $w$  – loop width;  $r$  – wire radius;  $Z$  – earthing system conventional impedance; *SPD1* – SPD bonding the phase conductor to the equipotential bonding bar (*EBB*); *SPD2* – SPD at the apparatus terminals.

The investigation is focused on the influence of:

- the induced circuit configuration (cross section of the loop wire, width and length of the loop, distance of the loop from the inducing current)
- the installed protection devices, namely switching and limiting *SPD1*,

on the parameters:

- peak value and shape of induced voltages
- peak value and shape of induced currents
- charges associated to induced currents
- peak value and shape of currents fed from *SPD1* to *SPD2*
- charges associated to fed currents
- peak value and shape of currents and values of charge due to combination of inductive and feeding effects.

### 6.6.2. Induced voltage

In case of reported basic circuit the induced voltage  $U_i$  increases with:

- front steepness of the inducing lightning current;
- length of the circuit;
- distance between the circuit and the down-conductor on which the inducing current flows;
- distance between conductors forming the loop (phase and PE conductors);

and decreases with shielding of:

- structure;
- zones of the structure;
- internal circuit.

The standard IEC 62305-4, clause A.4. provides the criteria for the evaluation of the induced voltage  $U_i$ .

The worst case of inductive coupling is where the internal circuit is wiring parallel to the down-conductor, on which the inducing current flows. In such case, as first approximation, it is assumed that the inducing electromagnetic field invests the entire loop practically at the same

instant, and then propagation phenomena of the induced voltage  $U_i$  in the circuit are neglected [11, 68].

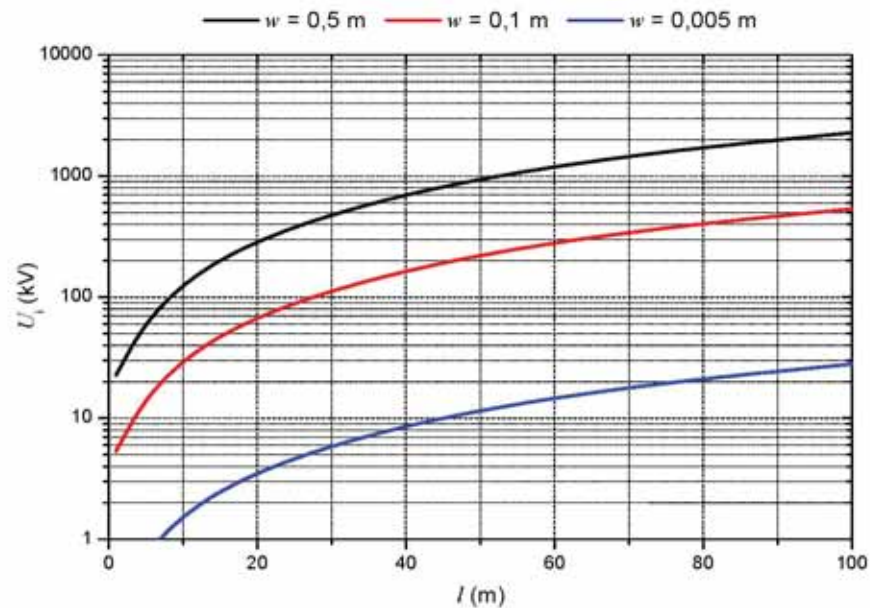


Figure 6.45. Induced voltage  $U_i$  as a function of loop length  $l$  for subsequent stroke;  $w = 0,5$  m;  $w = 0,1$  m;  $w = 0,005$  m.

The high values of the induced voltage  $U_i$  confirm the need to install the second *SPD2* near or at the terminals of the apparatus, as shown in Fig. 6.45.

### 6.6.3. Induced current

The current  $I_i$  induced in the circuit depends, in amplitude and waveform, on the type of installed *SPD1*.

#### In the case of *SPD1* switching type (SG):

- peak value of the induced current does not depend on the waveform of the inducing current;
- waveform of the induced current  $I_i$  is the same of the inducing current  $I$ ;
- under the same conditions (peak value of inducing current, characteristics and location of the loop), the induced charge  $Q_i$  is of one order of magnitude higher than for *SPD1* limiting type.

#### In the case of *SPD1* limiting type (MOV):

- time to peak value  $T_1$  of the induced current  $I_i$  is similar to that of the inducing current  $I$ ;
- time to half value  $T_2$  of the induced current  $I_i$  increases with the dimensions of the loop (length  $l$ , width  $w$ ), as shown in Fig. 6.46, 6.47 and 6.48.

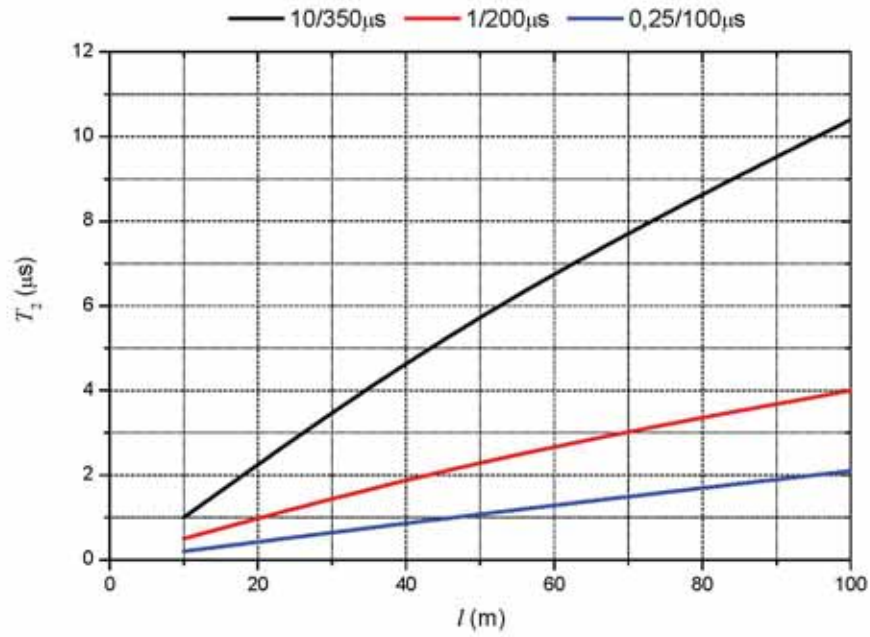


Figure 6.46. Time to half value  $T_2$  of the induced current in a loop with an *SPDI* limiting type as a function of loop length  $l$ , for three current shapes;  $w = 0,005$  m;  $d = 1$  m.

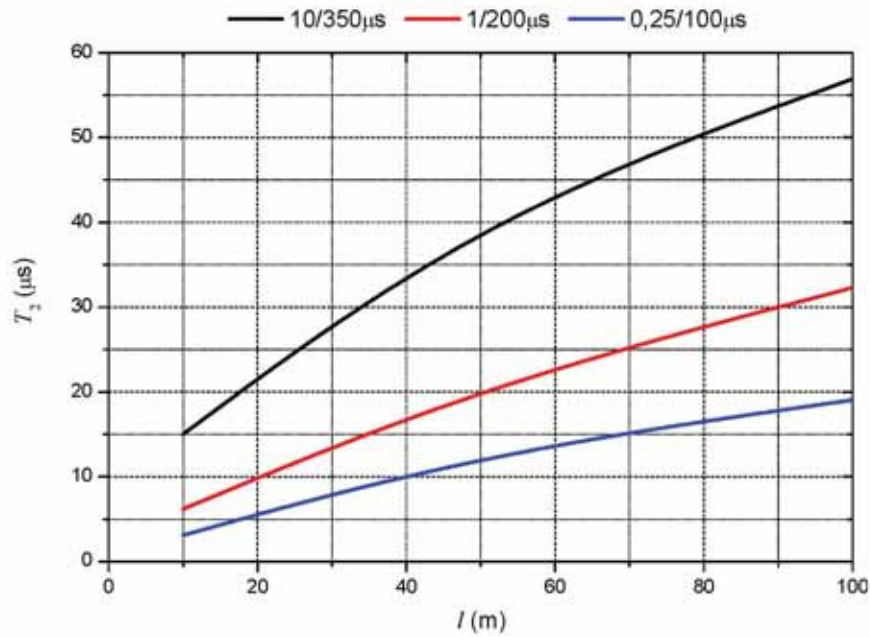


Figure 6.47. Time to half value  $T_2$  of the induced current in a loop with an *SPDI* limiting type as a function of loop length  $l$ , for three current shapes;  $w = 0,1$  m;  $d = 1$  m.

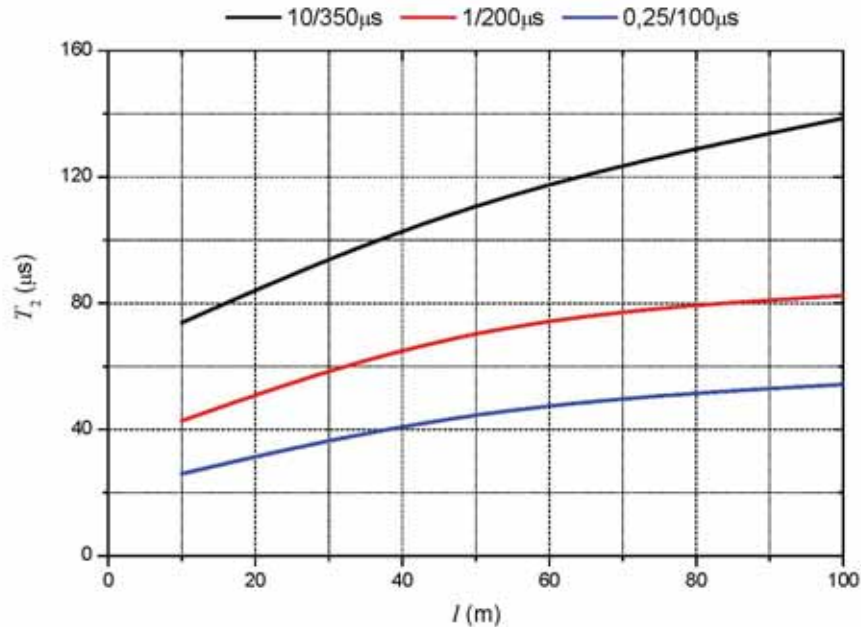


Figure 6.48. Time to half value  $T_2$  of the induced current in a loop with an *SPDI* limiting type as a function of loop length  $l$ , for three current shapes;  $w = 5$  m;  $d = 1$  m.

It is to note that the waveform of the induced current is different (longer) than the standard shape 8/20  $\mu\text{s}$  suggested by standard IEC 62305-1 due to inductive coupling of lightning flashes to the structure (source of damage S1- induced current).

**Regardless of the type of *SPDI* (varistor or spark gap):**

- induced current  $I_i$  slowly increases with increasing of the cross section of loop wire;
- highest values of induced current  $I_i$  are due to the subsequent strokes of negative flashes (0,25/100  $\mu\text{s}$ ), as shown in Fig. 6.49;
- highest values of induced charge  $Q_i$  are due to positive lightning stroke (10/350  $\mu\text{s}$ ), as shown in Fig. 6.50 and Fig. 6.51 obtained for  $w = 0,5$  m and  $w = 0,1$  m respectively;
- charge  $Q_i$  associated to the induced current  $I_i$  increases with the size of the loop (length and width), as shown in Fig. 6.52 For large loops the ratio  $Q_i / I_i$  can be higher than the value 27 mC/kA relevant to the 8/20  $\mu\text{s}$  standard current wave adopted for testing class II SPDs.



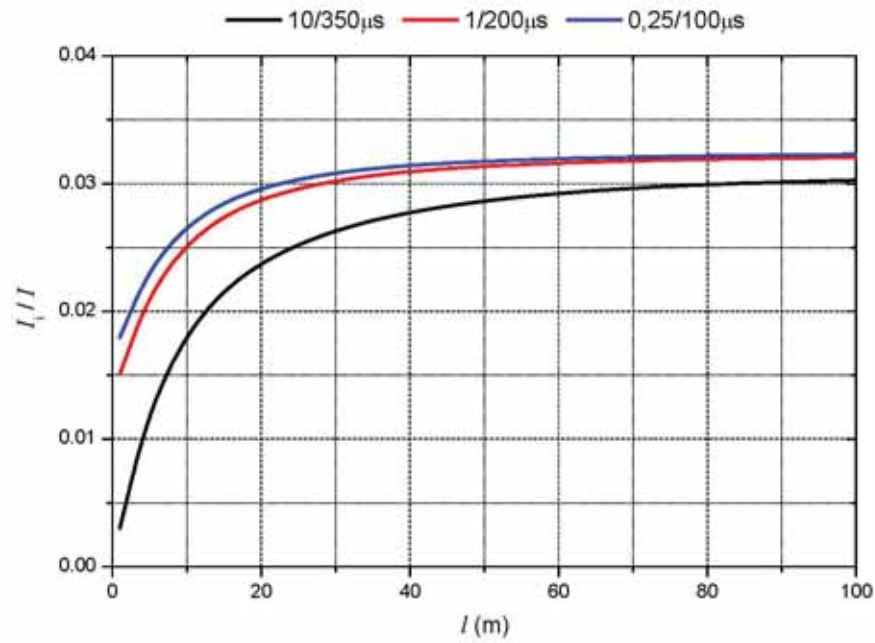


Figure 6.49. Ratio between induced current  $I_i$  and inducing current  $I$  as a function of loop length  $l$  with an *SPDI* limiting type, for three current shapes;  $w = 0,5$  m,  $d = 1$  m.

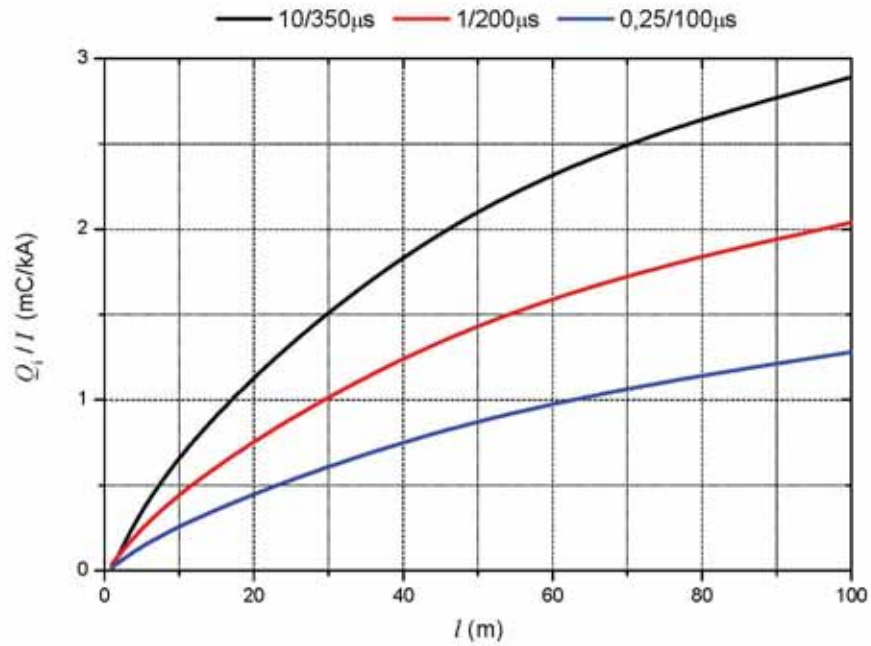


Figure 6.50. Ratio between induced charge  $Q_i$  and inducing current  $I$  in case of loop with an *SPDI* limiting type as a function of loop length  $l$ , for three current shapes;  $w = 0,5$  m,  $d = 1$  m.



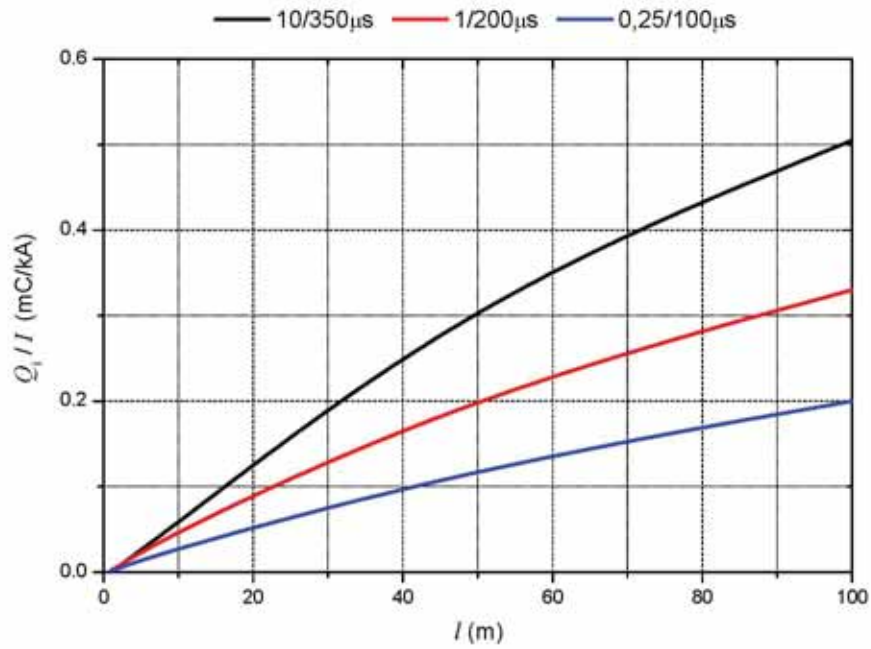


Figure 6.51. Ratio between induced charge  $Q_i$  and inducing current  $I$  in case of loop with an SPD limiting type as a function of loop length  $l$ , for three current shapes;  $w = 0,1$  m,  $d = 1$  m.

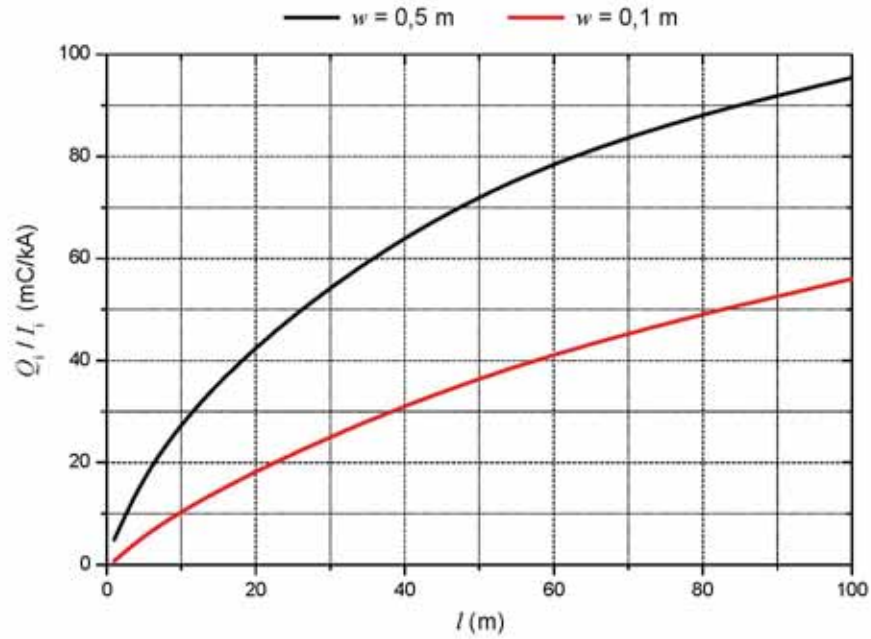


Figure 6.52. Ratio between induced charge  $Q_i$  and induced current  $I$ , in case of loop with an SPD limiting type as a function of loop length  $l$  for positive stroke;  $w = 0,1$  m and  $w = 0,5$  m;  $d = 1$  m.

#### 6.6.4. Voltage drop $\Delta V$ on SPD connecting leads due to induced current

The computed results, summarized in Tab. 6.8 and Tab. 6.9, show that the voltage drop  $\Delta V$  on SPD2 connecting leads:

- increases with the width  $w$  of the loop and weakly with the length  $l$  of the circuit;
- does not depend on the type of SPD1 (SG or MOV);
- is higher for the subsequent strokes of negative lightning flashes (waveform 0,25/100  $\mu$ s).

Table 6.8. Currents on SPD2 and voltage drop  $\Delta V$  on its connection leads for circuit with PE and phase conductors on different routing ( $w = 0,5$  m).

<i>SPDI</i>		SG		MOV	
Effect		Current	Voltage drop	Current	Voltage drop
Induction	$I_1$ (kA)	1,6	--	1,6	--
	$\Delta V$ (kV/m)	--	10,5	--	10,5
	$T_1/T_2$ ( $\mu$ s)	0,5/40	0,35/0,5	0,5/40	0,35/0,5
Lighting current: 50 kA, 0,25/100 $\mu$ s Line length : 1000 m Circuit length : 50 m					

Table 6.9. Currents on SPD2 and voltage drop  $\Delta V$  on its connection leads for circuit with PE and phase conductors on the same cable ( $w = 0,005$  m).

<i>SPDI</i>		SG		MOV	
Effect		Current	Voltage drop	Current	Voltage drop
Induction	$I_1$ (kA)	57	--	52	--
	$\Delta V$ (kV/m)	--	470	--	425
	$T_1/T_2$ ( $\mu$ s)	0,4/2	0,2/0,3	0,35/1	0,2/0,3
Lighting current: 50 kA, 0,25/100 $\mu$ s Line length : 1000 m Circuit length : 50 m					

### 6.6.5. Feeding effect: transmitted current

The current  $I_r$  fed in the circuit depends, in amplitude and waveform, on the type of installed *SPDI*, as shown in Tab. 6.10 and in Tab. 6.11.

Table 6.10. Currents on *SPD2* and voltage drop  $\Delta V$  on its connection leads for circuit with *PE* and phase conductors in different routing ( $w = 0,5$  m).

<i>SPDI</i>		SG		MOV	
Effect		Current	Voltage drop	Current	Voltage drop
Feeding	$I_r$ (kA)	0,12	--	153	--
	$\Delta V$ (kV/m)	--	12	--	4
	$T_1/T_2$ ( $\mu$ s)	0,03/0,05	0,03/0,05	140/400	0,3/70
Lighting current: 50 kA, 0,25/100 $\mu$ s Line length : 1000 m Circuit length : 50 m					

Table 6.11. Currents on *SPD2* and voltage drop  $\Delta V$  on its connection leads for circuit with *PE* and phase conductors in the same cable ( $w = 0,005$  m).

<i>SPDI</i>		SG		MOV	
Effect		Current	Voltage drop	Current	Voltage drop
Feeding	$I_r$ (kA)	0,12	--	153	--
	$\Delta V$ (kV/m)	--	12	--	4
	$T_1/T_2$ ( $\mu$ s)	0,03/0,05	0,03/0,05	140/400	0,3/70
Lighting current: 50 kA, 0,25/100 $\mu$ s Line length : 1000 m Circuit length : 50 m					

**In the case of *SPDI switching type (SG)*** the values of current  $I_r$  and of associated charge  $Q_r$ :

- decrease with increasing of the circuit length  $l$ ;
- practically do not depend on the length  $L$  of the supply line and on the lightning current amplitude  $I$ .

**In the case of *SPDI limiting type (MOV)*** the current  $I_r$  and the charge  $Q_r$ :

- decrease with increasing of the circuit length  $l$ ;
- increase with the length  $L$  of the supply line;
- increase with the lightning current amplitude  $I$ ;

- assume the highest values for positive strokes (10/350  $\mu$ s).

For an *SPDI* properly dimensioned for the current value expected at the point of installation, values of  $Q_r / I_r$  and  $Q_r / I$  are shown in Fig. 6.53 and Fig. 6.54.

For an undersized *SPDI* values of  $Q_r / I_r$  and  $Q_r / I$  are given in Fig. 6.55 and Fig. 6.56.

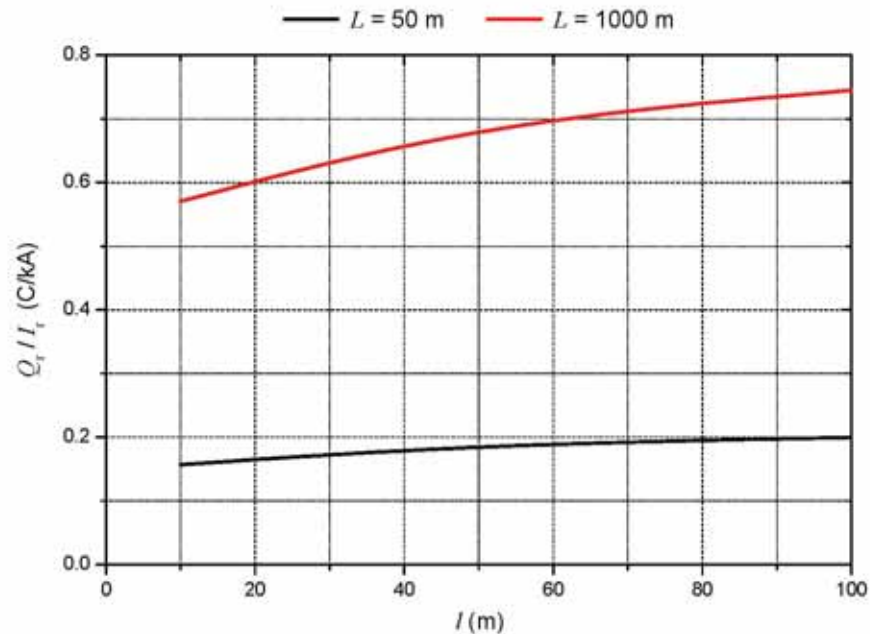


Figure 6.53. Ratio between charge  $Q_r$  and current  $I_r$  for a circuit with an *SPDI* limiting type (properly dimensioned) as a function of its length  $l$  for two values of supply line length  $L$  and positive stroke current.

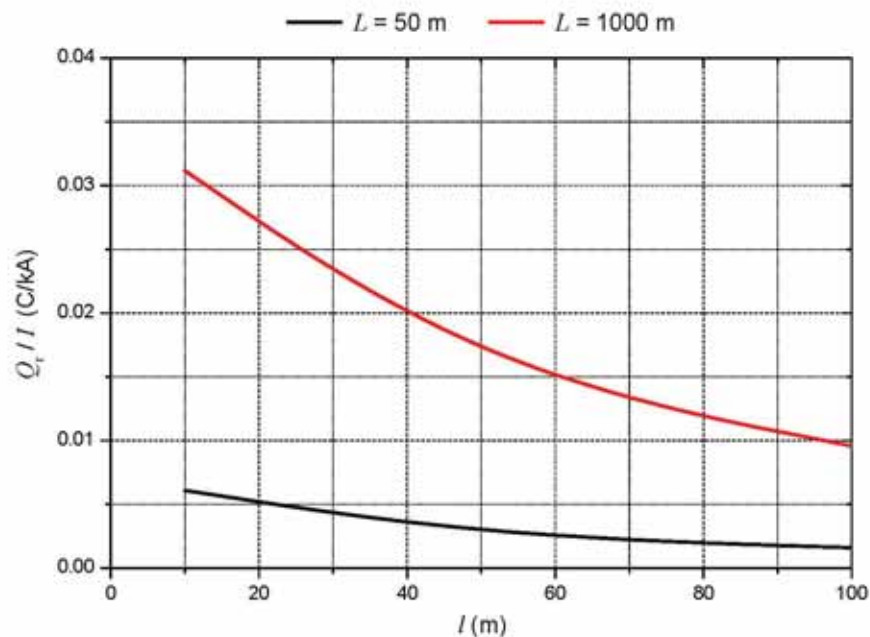


Figure 6.54. Ratio between charge  $Q_r$  and current  $I$  for a circuit with an *SPDI* limiting type (properly dimensioned) as a function of its length  $l$  for two values of supply line length  $L$  and positive stroke current.

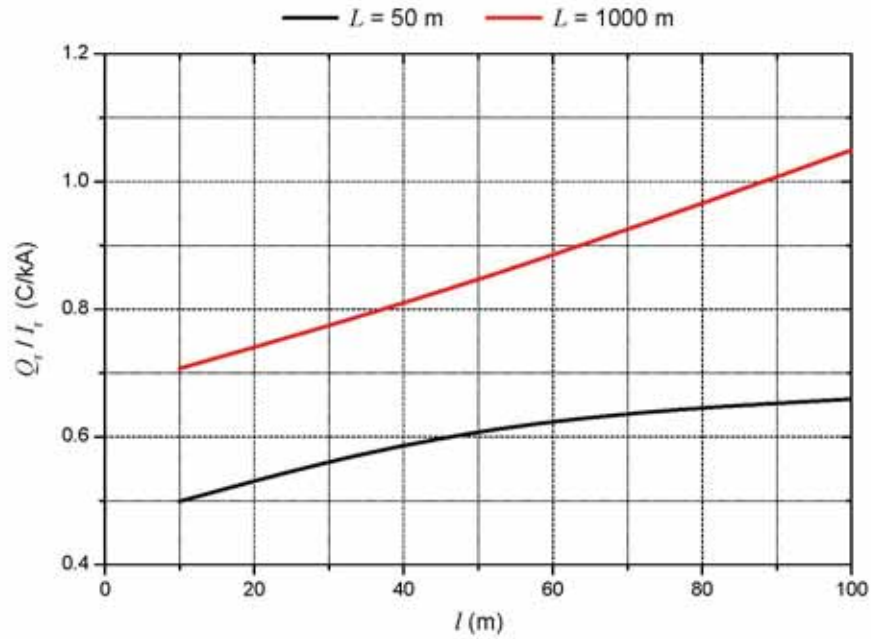


Figure 6.55. Ratio between charge  $Q_t$  and current  $I_t$  for a circuit with an *SPDI* limiting type (undersized) as a function of its length  $l$  for two values of supply line length  $L$  and positive stroke current.

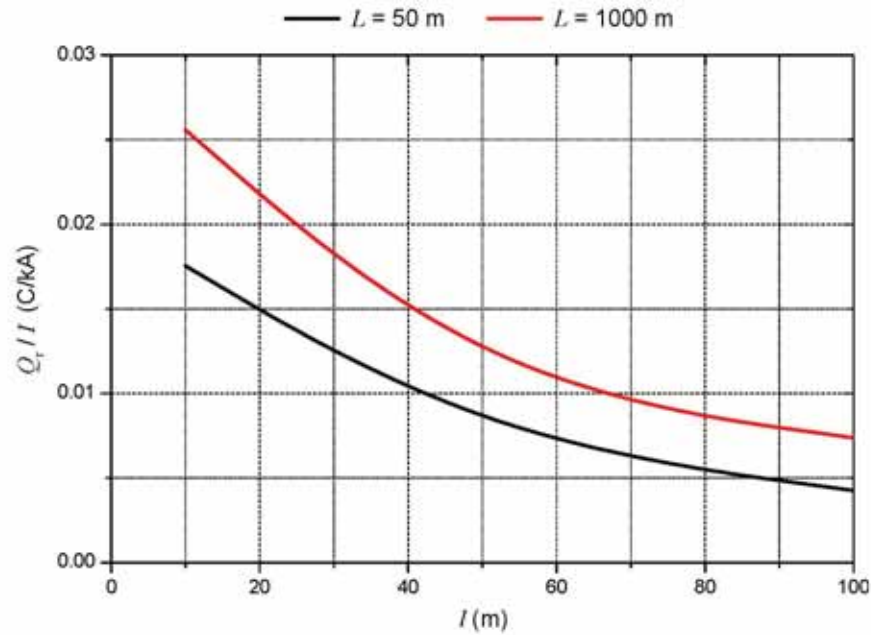


Figure 6.56. Ratio between charge  $Q_t$  and the current  $I$  for a circuit with an *SPDI* limiting type (undersized) as a function of its length  $l$  and for two values of supply line length  $L$  and positive stroke current.

### 6.6.6. Induction and feeding effects composition: current on SPD and voltage drop $\Delta V$ on its connection lead

Values of current flowing through *SPD2* and of voltage drop on its connection leads are reported in Tab. 6.12 and Tab. 6.13, respectively for circuits with PE and phase conductors on different routing and for circuits with PE and phase conductors on the same cable.

Table 6.12. Currents on *SPD2* and voltage drop  $\Delta V$  on its connection leads for circuit with *PE* and phase conductors in different routing ( $w = 0,5$  m).

<i>SPDI</i>		SG		MOV	
Effect		Current	Voltage drop	Current	Voltage drop
Induction	$I_1$ (kA)	1,6	--	1,6	--
	$\Delta V$ (kV/m)	--	10,5	--	10,5
	$T_1/T_2$ ( $\mu$ s)	0,5/40	0,35/0,5	0,5/40	0,35/0,5
Feeding	$I_r$ (kA)	0,12	--	153	--
	$\Delta V$ (kV/m)	--	12	--	4
	$T_1/T_2$ ( $\mu$ s)	0,03/0,05	0,03/0,05	140/400	0,3/70
Lighting current: 50 kA, 0,25/100 $\mu$ s; Line length : 1000 m; Circuit length : 50 m					

Table 6.13. Currents on *SPD2* and voltage drop  $\Delta V$  on its connection leads for circuit with *PE* and phase conductors in the same cable ( $w = 0,005$  m).

<i>SPDI</i>		SG		MOV	
Effect		Current	Voltage drop	Current	Voltage drop
Induction	$I_1$ (kA)	57	--	52	--
	$\Delta V$ (kV/m)	--	470	--	425
	$T_1/T_2$ ( $\mu$ s)	0,4/2	0,2/0,3	0,35/1	0,2/0,3
Feeding	$I_r$ (kA)	0,12	--	153	--
	$\Delta V$ (kV/m)	--	12	--	4
	$T_1/T_2$ ( $\mu$ s)	0,03/0,05	0,03/0,05	140/400	0,3/70
Lighting current: 50 kA, 0,25/100 $\mu$ s; Line length : 1000 m; Circuit length : 50 m					



From the analysis of values summarized in Tab. 6.12 and Tab. 6.13 the following comments arise.

**If an SPD1 switching type is installed:**

- feeding current  $I_r$  is negligible in front of the induced current  $I_i$  in the circuit, even in small loop area (circuit with conductors in the same cable). Therefore the induced current  $I_i$  can be assumed as the  $I_{SPD2}$  flowing through SPD2;
- for voltage drop on connection leads of SPD2, the same conclusion apply as for current flowing through SPD2.

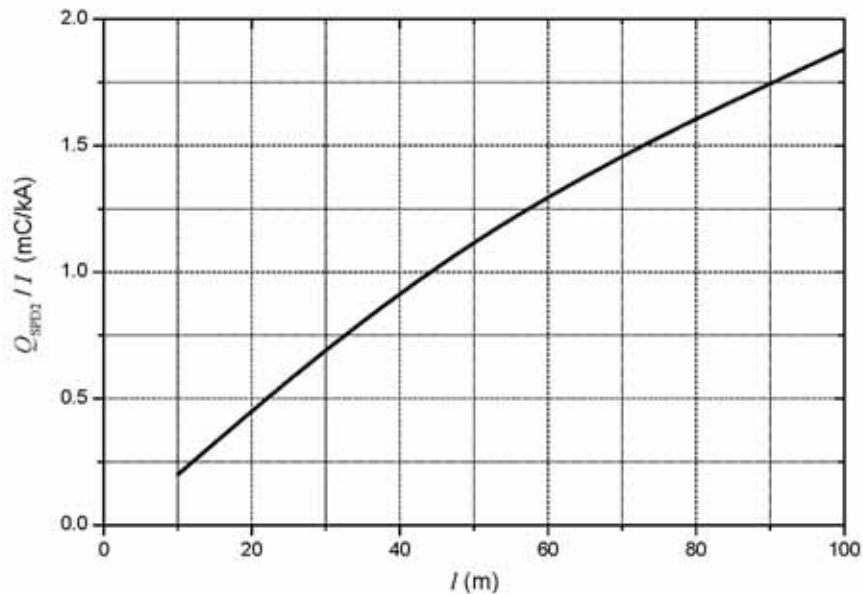


Figure 6.57. Ratio between charge  $Q_{SPD2}$  and the current  $I$  in case of loop with an SPD1 switching type as a function of loop length  $l$  for positive stroke;  $d = 1$  m and  $w = 0,5$  m.

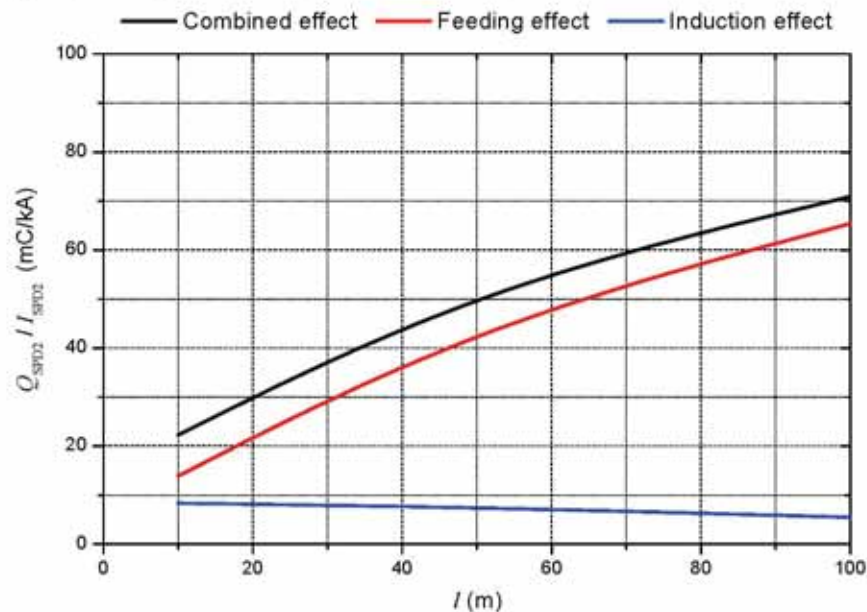


Figure 6.58. Ratio between charge  $Q_{SPD2}$  and current  $I_{SPD2}$  in case of loop with an SPD1 switching type as a function of loop length  $l$  for positive stroke;  $d = 1$  m and  $w = 0,5$  m.

As far as the total charge  $Q_{SPD2}$  associated to the current flowing through  $SPD2$ , such charge is the sum of the  $Q_i$  and  $Q_r$  charges. The worst case is relevant to the first lightning stroke (10/350  $\mu$ s) and to the largest circuit loop, as shown in Fig. 6.57 and Fig. 6.58. Charge due to feeding effect is of minor importance in front of the induced one.

**If an  $SPD1$  limiting type is installed:**

- feeding current  $I_r$  is negligible in front of the induced current  $I_i$  in the circuit, only for large loop area (circuit with PE and phase conductor on different routing) as reported in Tab. 6.12;
- due to shifting in time between the currents due to induction and feeding effects will not build up each other. Therefore the absolute maximum value of the two currents can be assumed as  $I_{SPD2}$  flowing through  $SPD2$ ;
- for voltage drop on connection leads of  $SPD2$ , the highest values are relevant to the induced current even in small loop area (circuit with conductors in the same cable) as shown in Tab. 6.13.

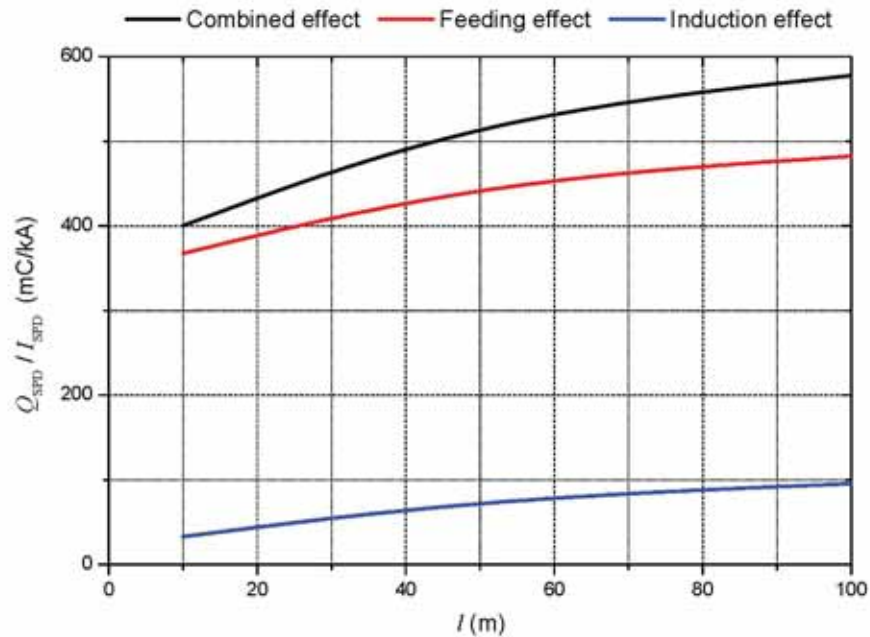


Figure 6.59. Ratio between the charge  $Q_{SPD}$  and inducing current  $I_{SPD}$  in case of loop with an  $SPD1$  limiting type as a function of loop length  $l$  for positive stroke;  $d = 1$  m and  $w = 0,5$  m.

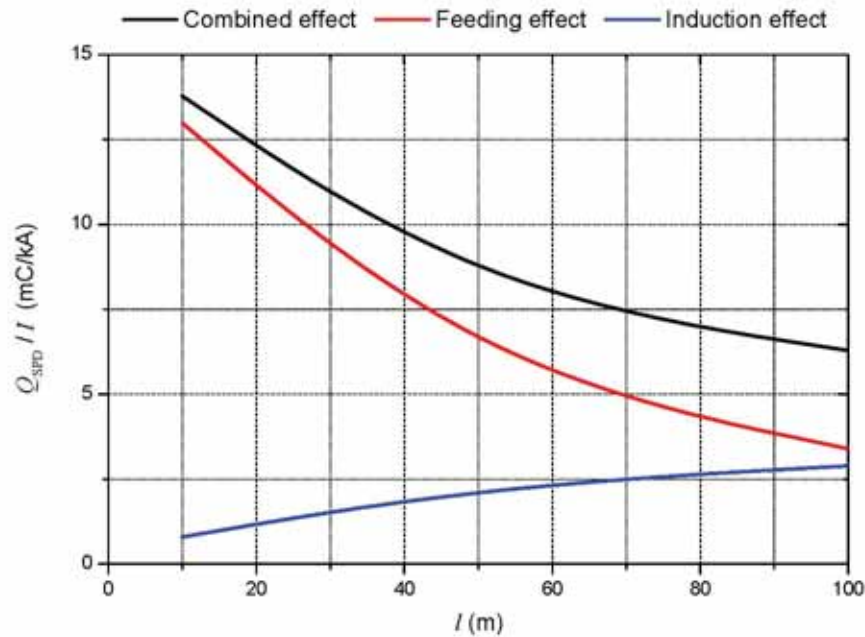


Figure 6.60. Ratio between the charge  $Q_{SPD}$  and current  $I$  in case of loop with an *SPDI* limiting type as a function of loop length  $l$  for positive stroke;  $d = 1$  m and  $w = 0,5$  m.

As far as the total charge  $Q_{SPD2}$  associated to the current flowing through *SPD2*, such charge is the sum of the  $Q_i$  and  $Q_r$  charges. The worst case is relevant to the first lightning stroke (10/350  $\mu$ s) and to the largest circuit loop, as shown in Fig. 6.59 and Fig. 6.60. Charge due to feeding effect is of major importance in front of the charge due to induction effect.

### 6.6.7. SPD dimensioning

#### Selection of protection level $U_{p2}$

For the *SPD2* installed at secondary distribution board, the selection of protection level  $U_{p2}$  should take into account:

- the inductive voltage drop  $\Delta V$  of the leads/connections of *SPD2*,
- the effect of surge travelling along the protected circuit,
- the overvoltages  $U_i$  induced by lightning current in the protected circuit formed by the *SPD2* and the apparatus to be protected.

Reference should be made to the subsequent strokes of negative flashes, which represent the more severe case, as discussed in the preceding paragraphs (6.6.2-6) and in [107].

Following the IEC 62305-4 [11], if an effective protection level  $U_{pf}$  is defined as the voltage at the output of the SPD resulting from its protection level  $U_p$  and the voltage drop  $\Delta V$ , namely:

$$U_{pf} = U_p + \Delta V \quad \text{for limiting type SPD} \quad (6.65)$$

$$U_{pf} = \max(U_p, \Delta V) \quad \text{for switching type SPD} \quad (6.66)$$

the following formulas may help in the selection of  $U_{p2}$  according to the length  $l$  of the protected circuit:

$$U_{p12} \leq U_w \quad \text{for } l = 0 \text{ m} \quad (6.67)$$

$$U_{p12} \leq (U_w - U_i) / (1 + 0,1l) \quad \text{for } 0 < l \leq 10 \text{ m} \quad (6.68)$$

$$U_{p12} \leq (U_w - U_i) / 2 \quad \text{for } l > 10 \text{ m} \quad (6.69)$$

being  $U_w$  the rated impulse withstand voltage of the apparatus to be protected.

It should be noted that it is crucially important to reduce the high values of  $\Delta V$  (see Tab. 6.12 and Tab. 6.13 ) and the induced voltage  $U_i$  caused by inductive coupling in the loop of circuit between *SPD2* and apparatus. Possible suitable installation provisions are:

- reduction of the loop area by using circuit routing with PE and phase conductors in the same cable, better if twisted;
- use of screened circuits or their laying in a closed metallic conduit;
- reduction of the length of *SPD2* leads connection as much as possible.

In the absence of such provisions it is likely that a further SPD (*SPD3*) with  $U_{p13} \leq U_w$  should be installed just at apparatus terminals.

Once *SPD3* is provided, the fulfillment of conditions a), b) and c) is no longer required for *SPD2*: only the energy coordination between *SPD1*, *SPD2* and *SPD3* should be considered.

Selection of discharge current  $I_{SPD2}$

As reported in [107], the impulse current  $I_{imp}$  of a class I test SPD and the nominal current  $I_n$  of a class II test SPD should be selected in such way that both the following conditions are fulfilled:

- a) the value of  $U_{p2}$  at the current  $I_{SPD2}$  expected at the point of *SPD2* installation, does not overcome the rated impulse withstand voltage level  $U_w$  of the apparatus to be protected;
- b) the energy associated to the discharge current does not overcome the value tolerated by the *SPD2*.

Therefore, if we consider that the charge  $Q_{SPD}$  for unit of current associated to the standard current 10/350  $\mu\text{s}$  is  $Q_{imp} = 0,5 \text{ C/kA}$  and to the standard current 8/20  $\mu\text{s}$  is  $Q_n = 0,027 \text{ C/kA}$ , the relations to be respected for *SPD2* dimensioning are the following:

a) for *SPD2* class I test

$$I_{imp} \geq I_{SPD2} \quad (6.70)$$

$$Q_{imp} \geq Q_{SPD2} \text{ or numerically } I_{imp} \geq 2 Q_{SPD2} \quad (6.71)$$

b) for *SPD2* class II test

$$I_n \geq I_{SPD2} \quad (6.72)$$

$$Q_n \geq Q_{SPD2} \text{ or numerically } I_n \geq 37 Q_{SPD2} \quad (6.73)$$

If an *SPD1* switching type is installed, values of  $I_{SPD2}$  and of  $Q_{SPD2}$  are reported respectively in Fig. 6.61 and in Fig. 6.62. In Fig. 6.61 the dominant contribution of inducing effect to the



$I_{SPD2}$  is shown; in Fig. 6.62 the contribution to total charge  $Q_{SPD2}$  of the feeding effect is of minor importance in front of the induced one and may be considered as negligible.

If an *SPD1* limiting type is installed, values of  $I_{SPD2}$  and of  $Q_{SPD2}$  are reported respectively in Fig. 6.63 and in Fig. 6.64. In Fig. 6.63 the dominant contribution of feeding effect to the  $I_{SPD2}$  is evident, while in Fig. 6.64 the total charge  $Q_{SPD2}$  as result of feeding and inducing effect due to positive stroke current is reported.

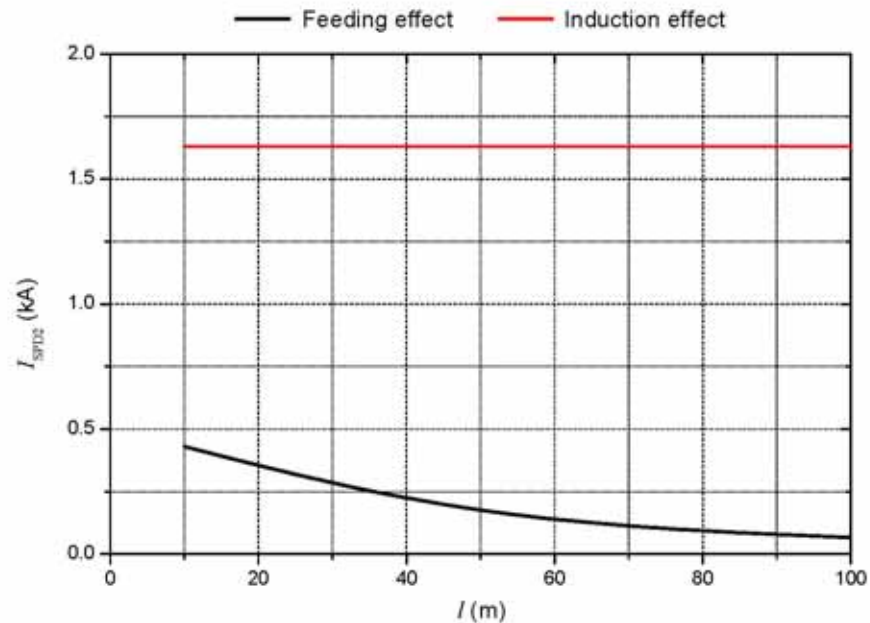


Figure 6.61. Current  $I_{SPD2}$  due to induction and feeding effects in case of loop with an *SPD1* switching type as a function of loop length  $l$  for positive stroke current;  $w = 0,5$  m;  $d = 1$  m.

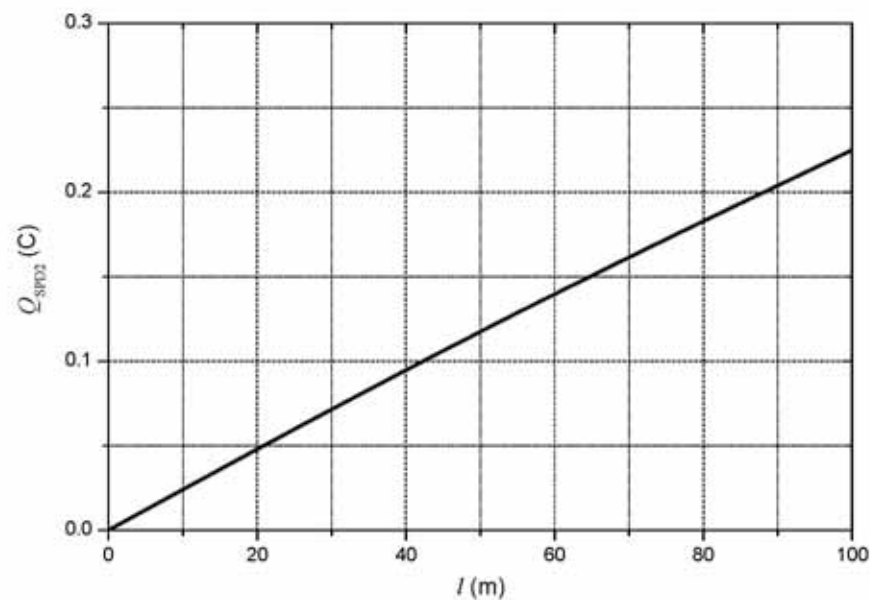


Figure 6.62. Charge  $Q_{SPD2}$  in case of loop with an *SPD1* switching type as a function of loop length  $l$  for positive stroke current;  $w = 0,5$  m;  $d = 1$  m.

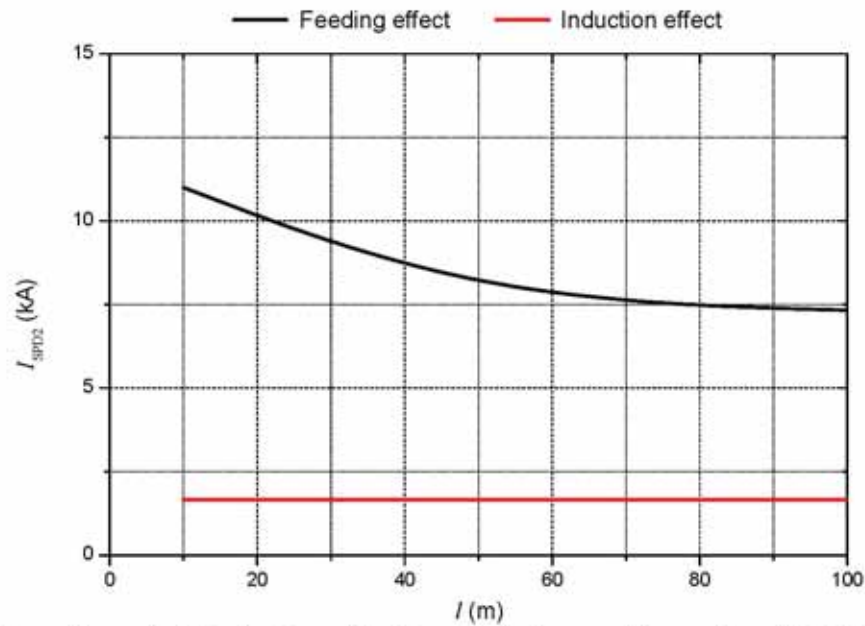


Figure 6.63. Current  $I_{SPD2}$  due to induction and feeding effects in case of loop with an *SPD1* limiting type as a function of loop length  $l$  for positive stroke current;  $w = 0,5$  m;  $d = 1$  m.

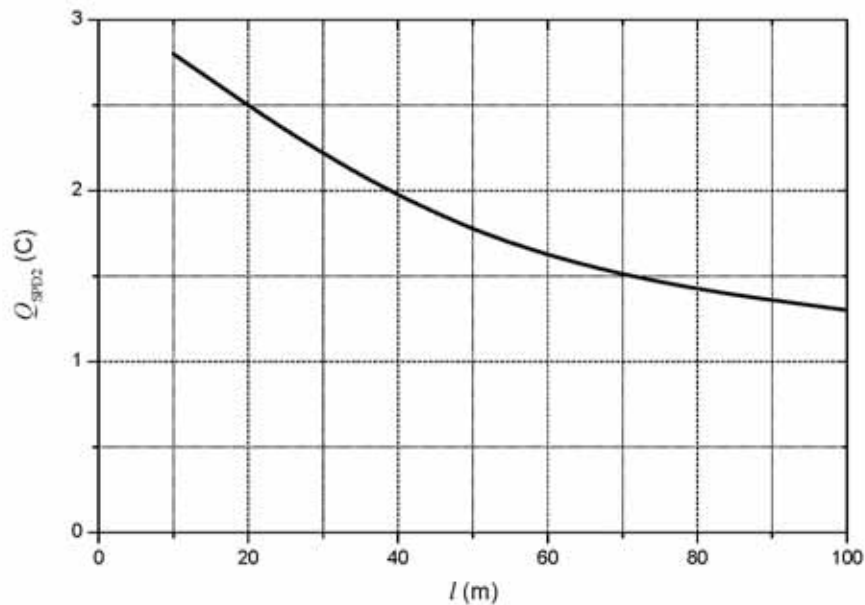


Figure 6.64. Charge  $Q_{SPD2}$  in case of loop with an *SPD1* limiting type as a function of loop length  $l$  for positive stroke current;  $w = 0,5$  m;  $d = 1$  m.

The values of impulse current  $I_{imp}$  of a class I test SPD and of the nominal current  $I_n$  of a class II test SPD to be assigned to *SPD2*, are summarized in Tab. 6.14 where the required values of  $I_{imp}$  are marked in **bold** and the ones of  $I_n$  are marked in *italic*. In the same table the current values suggested by IEC 62305 standard for lightning protection level I (LPL I) are also reported. Note that the values of Tab. 6.14 are obtained in the worst case of induced loop circuit running entirely parallel to the down conductor, as shown in Fig. 6.35.



Table 6.14. Minimum values of discharge current to be assigned to *SPD2* for LPL I according to *SPD1* type range of circuit length 10m ÷ 100m

<i>SPD1</i> type	Calculated values				IEC 62305
	$I_{SPD2}$ (kA)	$Q_{SPD2}$ (C)	$I_{imp} = 2 Q_{SPD2}$ (kA)	$I_n = 37 Q_{SPD2}$ (kA)	$I_n$ (kA)
Switching	1,6	0,02÷0,2	0,04÷0,4	0,8÷8,14	20
Limiting	11	2,8÷1,2	5,6÷2,4	103÷44	20

The results shown in Tab. 6.14, confirm that the values proposed by IEC 62305 for *SPD2* tested with  $I_n$  are on safety side only if an *SPD1* switching type is installed; where *SPD1* is of limiting type an *SPD2* tested with  $I_{imp}$  should be used.

#### 6.6.8. Conclusions relevant to the downstream SPD

From the analysis herewith performed the following conclusions may be drawn:

- induction effect is the decisive factor in determining the current  $I_{SPD2}$  flowing through *SPD2* and the voltage drop  $\Delta V$  on its connection leads:
  - in all cases, if *SPD1* is of switching type;
  - only for large loop area (circuit with PE and phase conductor on different routing), if *SPD1* is of limiting type;
- highest values of total charge  $Q_{SPD2}$  flowing in *SPD2* is due to positive lightning stroke (10/350  $\mu$ s) and to the largest circuit loop;
- total charge  $Q_{SPD2}$  is the sum of the charges due to inducing and feeding effects, but charge  $Q_r$  is of major importance in front of the induced one;
- the high values of the induced voltage  $U_i$  confirm the need to install the downstream *SPD2* near or at the terminals of the apparatus, even for circuits with PE and phase conductors in the same cable;
- because the high values of voltage drop  $\Delta V$  on connection leads of *SPD2* in conjunction with the high values of the induced voltage  $U_i$  on circuit between *SPD2* and apparatus, it is crucially important that suitable installation provisions should be adopted for such circuit, such as:
  - the reduction of the loop area by using circuit routing with PE and phase conductors twisted in the same cable;
  - the use of screened circuits or their laying in a closed metallic conduit;
  - the reduction of the length of *SPD2* connection leads as much as possible;

In the absence of such provisions it is likely that *SPD2* is to be installed at apparatus terminals;
- the values of current proposed by IEC 62305 for *SPD2* class II tested with  $I_n$  are on safety side only if an *SPD1* switching type is installed; where *SPD1* is of limiting type an *SPD2* class I tested with  $I_{imp}$  should be used.

## 6.7. Summary

The present chapter intends to give a criteria for protection measures selection, namely SPD switching and limiting type, against lightning overvoltages.

It is particularly important because nowadays structures are more and more equipped with electrical and electronic apparatus sensitive to lightning surge influences. The operation of these apparatus can be endangered due to flashes to the structure (S1), flashes to ground or to grounded objects near the structure (S2), flashes to the connected lines (S3), flashes nearby the connected lines (S4) [18].

The worst case consists of damage source S1, where failure of apparatus can be caused due to resistive as well as inductive coupling of lightning current flowing to the earthing system. This case is considered in present chapter.

The analyses are developed by several computer simulations adopting suitable computer models validated by experimental tests in HV laboratory of Warsaw University of Technology as well as in the HV laboratory of University of Rome La Sapienza. Examples of experimental results are given.

The analyses are performed by means of commercial transient software EMTP-RV, where models are developed according to the laboratory tests results. The special focus is dedicated for the comparison of the laboratory and computed results to ascertain models correction. The results evaluation seem to be satisfactory and further analyses of apparatus protected by means of SPD are developed.

For the investigation two typical cases, where SPD are installed as protective measures are selected.

The first analysis includes proper selection of SPD installed at the entrance point of structure, namely upstream SPD. The methodology of analyses includes: different behaviour of the SPD containing spark gap (switching type SPD), SPD containing metal oxide varistor (limiting type SPD); location of the SPD within the structure; the shearing of lightning currents within the structure to the earthing system and to the connected services. The results of this part of work demonstrated that the installation of further, downstream SPD is needed.

The second analysis includes the selection of downstream SPD. This SPD has to be coordinated with upstream SPD. The investigation is focused on the influence of the induced circuit configuration, installed protection devices, namely switching and limiting type as the upstream SPD.

Finally, some simple rules for the selection of downstream and upstream SPD are proposed. Comments and comparison with the requirements of the international standard IEC/EN 62305-4 are presented.

# **Chapter 7**

## **7. Criteria for protection measures selection: experimental tests and computer simulations for the isolation transformer**

### **7.1. Introduction**

Operations of electronic and electrical apparatus can be interrupted due to disturbances e.g. coming from connecting lines. These occurrences can be caused due to lightning flashes to the structure (S1), flashes to ground or to grounded objects near the structure (S2), flashes to the lines (S3) and flashes nearby the lines (S4). To reduce apparatus probability failure and assure their continuing service, isolating interfaces as a part of lightning protection system defined by [11, 18, 17, 128] can be applied. The isolation transformer is an effective device, which can also assure additional benefits [118, 189-194]. The present chapter intends to give a contribution to the criteria for protection measures installation as an isolation transformer taking into account lightning threat.

The theoretical background of isolation transformers is already discussed in chapter 4, where general classification as well as construction aspects are presented. Isolating interfaces achieved by means of an isolation transformer upstream of equipment is a powerful protection measure to reduce damages due to overvoltages, but effectiveness of this protection depends on the several factors. These factors include parameters of stressing source, namely overvoltage steepness and peak value, electrical characteristic of apparatus to be protected. Additionally an isolation transformer have to be coordinated with another part of lightning protection system, e.g. SPD. Moreover installation conditions influence on common mode transients. For the proper installation of insolation transformer the particular attention should be paid on its shield grounding conditions.

In following paragraphs the typical installation aspects are presented and discussed. Special focus is dedicated on the overvoltages propagation through an isolation transformer and on the influence of grounding shielding conditions. The attenuation of common mode transient voltage is analysed.

The laboratory test set up and the results obtained on the investigated transformer are presented. The experimental tests are performed in HV Laboratory of University of Rome La Sapienza. For laboratory tests a commercial single-phase low voltage transformer with a floating or grounded screen between the two windings is selected. The computer simulations are performed by means of commercial transient software EMTP-RV. The experimental results are discussed and compared with those obtained from computer simulations.

On the base of performed analysed adequate conclusions useful for a correct installation of an isolation transformer are formulated.

## 7.2. Characteristic of surge transfer by an isolation transformer

From the practical viewpoint when the peak value of transients is higher than the insulation level of the primary winding of the transformer it is necessary to install protective devices as suitable coordinated SPD (see chapter 6.).

Common mode transients from incoming line may occur by resistive coupling. Basic examples of arrangement with an isolation transformer are shown in Fig. 7.1. and Fig. 7.2.

The first case, where protective conductor (*PE*) of the equipment to be protected is not bonded to the same equipotential bonding bar (*EBB*) as SPD is shown in Fig. 7.1.

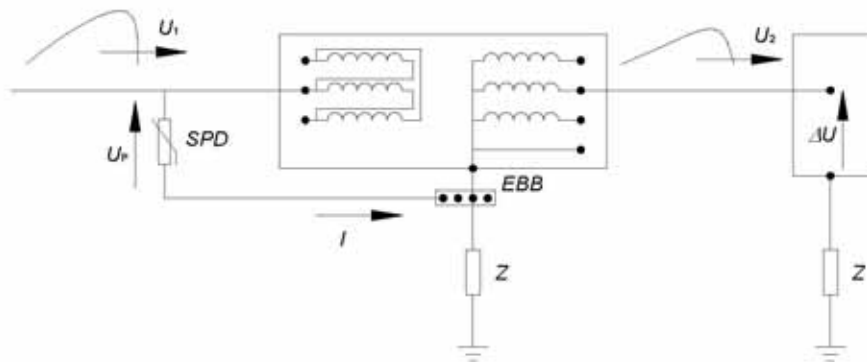


Figure 7.1. Common mode surge transfer by resistive coupling.

In this case (Fig. 7.1) the discharge current  $I$  of the SPD may cause at the secondary winding of transformer a common mode voltage with amplitude  $U_2$  equal to the total voltage across the earth termination as follows:

$$U_2 = Z \cdot I \quad (7.1)$$

where:

$I$  – lightning current;

$Z$  – conventional earth impedance.

The second case, where *PE* of the equipment is bonded to the same *EBB* as the SPD is shown in Fig. 7.2.

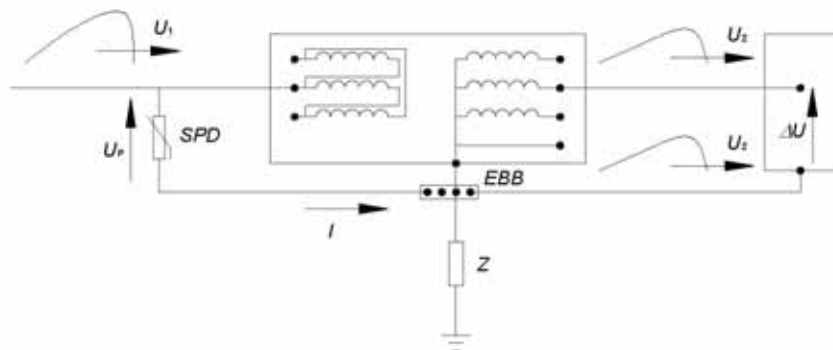


Figure 7.2. Common mode surge transfer by resistive coupling.

In the present situation (Fig 7.2) the voltage  $U_2$  is transferred to both the phase and PE conductors so that common mode transient voltage coming from the connected line may be neglected. However, it is to note that in the first case of Fig. 7.1, if the lightning current reaches the value  $I_f \approx 10$  kA, possible at the strike to the last pole on consumer side of the multiconductor (three phase + neutral) line, and the earthing surge impedance  $Z = 5 \Omega$ , the voltage  $U_2 \approx 50$  kV is transferred to the secondary winding and can cause failure either of the transformer insulation or of the equipment to be protected.

Inductive coupling of source transfer through an isolation transformer mainly affect differential mode transfer and is quite sporadic [1]. In present work this type of source transfer is not considered.

The transfer of common mode transient voltage through a transformer may occur by capacitive coupling due to the primary winding capacitance  $C_1$ , the capacitance  $C_{12}$  between windings, the capacitance  $C_2$  to earth of the secondary winding and of connected circuits, as shown in Fig. 7.3.

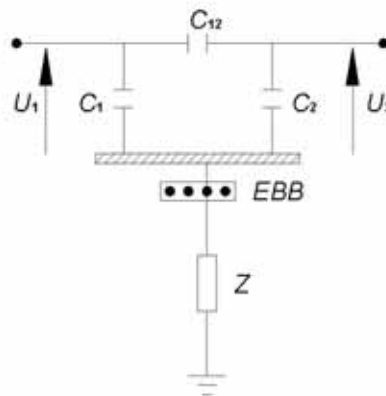


Figure 7.3. Common mode surge transfer by capacitive coupling; where:  $Z$  – conventional earth impedance;  $EBB$  – equipotential bonding bar;  $C_1$  – primary winding capacitance;  $U_1$  – voltage applied at primary winding;  $C_{12}$  – capacitance between windings;  $C_2$  – secondary winding capacitance;  $U_2$  – voltage applied at secondary winding.

The value of overvoltages coming to the apparatus can be calculated by means of following equation:

$$U_2 = \frac{C_{12}}{C_2 + C_{12}} \cdot U_1 \quad (7.2)$$

In the case of transformer with an earthed metal screen between windings (Fig. 7.4) the capacitive coupling between these windings is almost zero so that the transfer of the surge is vanished. The equivalent electric scheme corresponding to the problem is shown in Fig. 7.4.



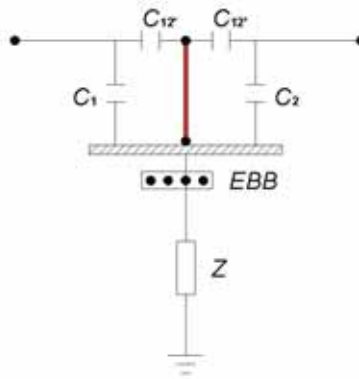


Figure 7.4. Equivalent schemes of transformer with earthed screen between windings.

The simplification of mentioned arrangement is shown in Fig. 7.5.

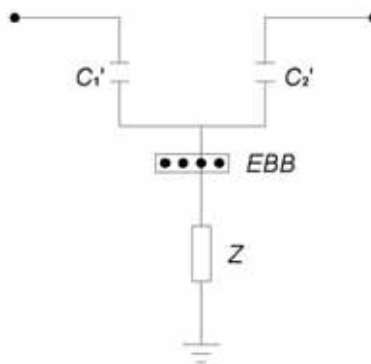


Figure 7.5. Equivalent schemes of transformer with earthed screen between windings: simplified circuit.

$C'_1 = C_1 + C'_{12}$  is the parallel of the ground capacitance  $C_1$  of the primary transformer winding and its capacitance  $C'_{12}$  to the screen.

$C'_2 = C_2 + C'_{12}$  is the parallel of the ground capacitance  $C_2$  of the secondary transformer winding and its capacitance  $C'_{12}$  to the screen.

### 7.3. Laboratory tests of isolation transformers effectiveness

#### 7.3.1. Introduction

The present paragraph intends to demonstrate the practical problems of installation of an isolation transformer. These issues belong mainly to the screen grounding conditions, namely length of connection between an isolation transformer and *EBB*. This connection consist of two series conductor. The internal connection between screen and output transformer always exist, but dominant influence on the protection effectiveness of isolation transformer is due to external connection, which in practice can has a significant length.

The equivalent electrical scheme corresponding to the problem, where the external screen connection is represented by an equivalent self-inductance  $L_{to}$  is shown in Fig 7.6 and in simplification in Fig. 7.7.

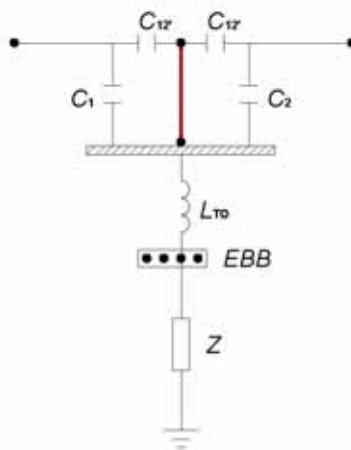


Figure 7.6. Equivalent schemes of transformer with earthed screen between windings.

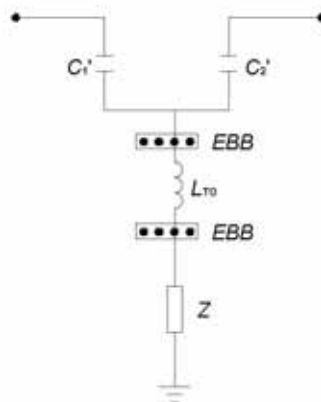


Figure 7.7. Equivalent schemes of transformer with earthed screen between windings: simplified circuit.

In following paragraphs the influence of screen grounding condition is analysed.

### 7.3.2. Determination of tests condition

For laboratory tests a commercial single-phase low voltage transformer with a floating or grounded screen between the two windings is selected. Transformer manufacturing data are following: 230/230 V, 1 kVA and 3% short circuit voltage. The laboratory tests set-up is shown in Fig. 7.8.

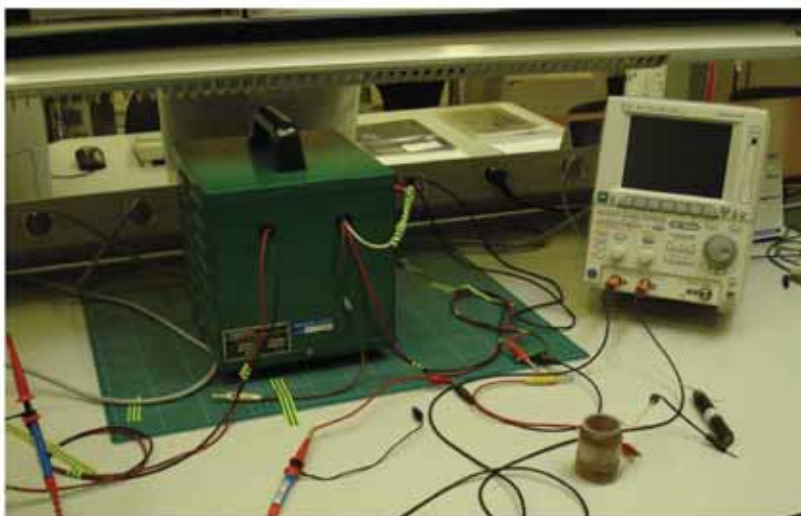


Figure 7.8. Photo of laboratory during tests.

The core is formed with two magnetic circuits tied together up side by side. The core is connected to the tank. The two windings are coiled up around the central column of the core in a concentric construction, in which the primary winding is external in respect to the secondary winding. The second screen also works, if grounded, as a path for the short circuit currents, when a fault occurs between the secondary winding and the core. The screens have two independent sockets in the panel patch board, so they can be kept grounded and ungrounded (floating) individually.

The considered arrangement for the analysis of the transferred transients through the transformer for common mode of propagation is shown in Fig. 7.9. It consists of the impulse voltage generator ( $G$ ) and the isolation transformer. The screen of transformer is connected to the equipotential bonding bar ( $EBB$ ). The primary winding of the transformer is connected to the generator. The second winding of the transformer was connected to the equipment to be protected represented by means of high value of resistance in range of  $M\Omega$ . The arrangement connections are performed by means of a single core wire with  $2.5 \text{ mm}^2$  conductor cross section. Voltages at primary transformer winding (point  $A$ ) and secondary transformer winding (point  $B$ ) are measured by a digital oscilloscope Yokogawa mod. 2022 with maximum samples rate  $2.5 \text{ GS/s}$ , frequency characteristics  $200 \text{ MHz}$  and maximum record length  $62.5 \text{ Mpoints}$ . Two reference points  $T$  at the transformer metallic tank and  $\theta$  at the  $EBB$  are selected. For each measurement point the peak values of phase-to-local earth voltage ( $U_{AT}$  and  $U_{BT}$ ), of phase-to- $EBB$  voltage ( $U_1$  and  $U_2$ ) are taken into account.

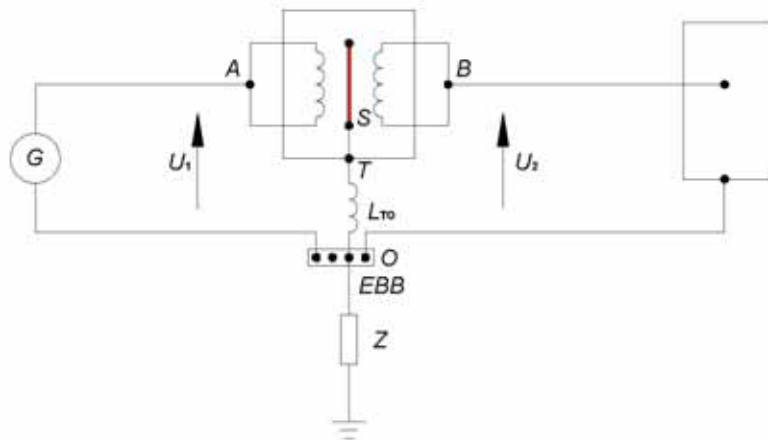


Figure 7.9. Equivalent circuit of considered laboratory set up.

For the generation of the voltage transients a recurrent impulse generator Haefely Type 48, is used. This device has a possibility of generating a different forms of overvoltages. The peak value as well as times  $T_1$  and  $T_2$  generated impulses can be obtained. Equivalent electric circuit of surge generator is shown in Fig. 7.10.

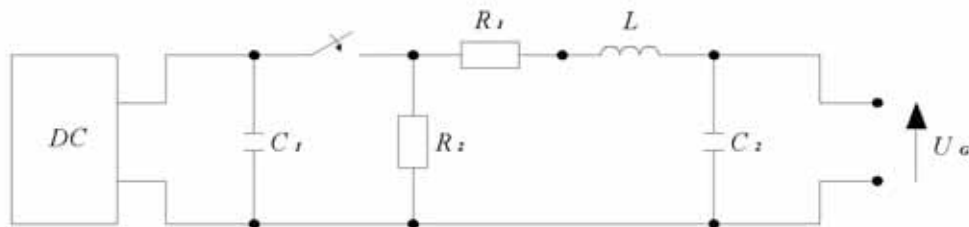


Figure 7.10. Equivalent electric circuit of impulse voltage generator.

The overvoltage shapes selected with corresponding circuit parameters of generator are reported in Tab. 7.1.

Table 7.1. Settings of impulse generator.

Name	Wave shape $T_1/T_2$ ( $\mu\text{s}$ )	$R_1$ ( $\Omega$ )	$R_2$ ( $\Omega$ )	$C_1$ (nF)	$C_2$ (nF)	$L$ ( $\mu\text{H}$ )
WS-1	0,25/50	3,3	68	1000	1	0
WS-2	1,2/50	4,7	68	1000	100	0
WS-3	12/500	47	680	1000	100	0

The wave of type *WS-1* can reproduce a fast front overvoltages on an upstream line [137] and impinging the transformer. The wave shape *WS-2* is the standard lightning shape. The wave of type *WS-3* can represent a long wave shape due to a switching operation although the switching surges in low voltage networks are generally very similar to a fast front wave shape [137].

### 7.3.3. Computer simulation of isolation transformer: models development

The proper representation and simulation transformers in high frequency conditions is an object of many complex studies [124, 195-199]. Generally in transient conditions transformers features are reduced to the filtration behavior. Moreover in case of an isolated transformer the proper representation of shield is needed.

In present analyses the isolation transformer is represented by simplified circuit shown in Fig. 7.11. The circuit model based on the experimental data, where  $R1 = 250 \text{ M}\Omega$ ,  $C1' = 0,5 \text{ nF}$ ,  $C2' = 0,5 \text{ nF}$ ,  $C3 = 0,05 \text{ nF}$ ,  $L_{T0} = \text{variable}$ ,  $R2 = 100 \text{ M}\Omega$ ,  $Z = 10 \text{ }\Omega$  [190]. However it is important to mention that simulation results, mainly voltage at secondary winding  $U_2$ , are strongly influenced by method of impulse voltage representation as well as connection leads. For the analyses the impulse voltage generator is reconstructed according to equivalent scheme shown in Fig. 7.10. The methodology of connection leads representation is already discussed in chapter 6.

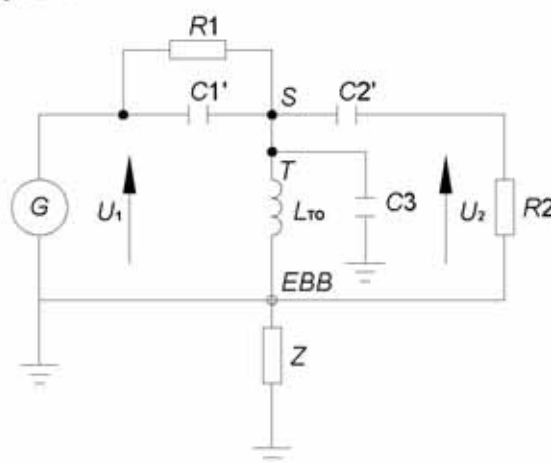


Figure 7.11. Simplified model of isolation transformer.

### 7.3.4. Tests results

For the tests reported in this chapter, the two transformer screens were connected together. The measurements were performed for the screen connected to the transformer tank ( $T$ ) grounded to  $EBB$  by cable of different length. At the same  $EBB$  the  $PE$  conductor of the equipment to be protected is connected. In a real case in which, even if the screen is directly connected to the transformer metallic tank in point  $T$  (Fig. 7.7), this point is then bonded to  $EBB$ , where also the protective conductor ( $PE$ ) of the internal installation is bonded, even with a cable of several metres length. If the value of the self-inductance  $L_{T0}$  is high enough, the effect of the screen in the surge transfer is very limited and may be even vanished. The analyses results are summarised and reported in Tab. 7.2.



Table 7.2. Ratio  $U_2 / U_1$  of voltages obtained in selected points and different conditions.

$U_1$		$U_2$		$ST$	$TO$		$U_2/U_1$
AT	AO	BT	BO		$L_{TO}$ ( $\mu H$ )	$l$ (m)	
<b><i>WS-1</i></b>							
	x		x	x	-	$+\infty$	0,93
	x		x	x	146,3	150	0,82
	x		x	x	5	5	0,27
	x		x	x	2,1	2	0,17
<b><i>WS-2</i></b>							
	x		x	x	-	$+\infty$	0,92
	x		x	-	-	$+\infty$	0,90
x		x		-	-	$+\infty$	0,74
	x		x	x	146,3	150	0,48
	x		x	x	5	5	0,05
	x		x	x	2,1	2	0,03
<b><i>WS-3</i></b>							
	x		x	x	-	$+\infty$	0,91
	x		x	x	146,3	150	0,06
	x		x	x	5	5	0,015
	x		x	x	2,1	2	0,012
Note: $U_1$ – voltage impinging the primary winding $U_2$ – voltage transferred to the secondary winding							

From the results summarized in Tab. 7.2 it can be demonstrated that:

- the strong attenuation of the surge transferred through the transformer, if the screens are grounded to EBB with a very short cable length of 10 cm (equivalent inductance assumed equal to 0,1  $\mu H$ ): such attenuation ranges from 5% for the short front shape type *WS-1* to about 1% for shape type *WS-2* and to 0.5% for the long front shape type *WS-3*;
- the attenuation of transferred surge is clearly reduced, if the length of connecting cable to *EBB* is of the order of some meters: for a cable length of a few meters (between 2 and 5 m) the attenuation is of the order of 15% for the wave type *WS-1*, of 2.5% for the wave type *WS-2* and of 0.5% for the wave type *WS-3*;
- the attenuation of transferred surge is further reduced, if the length of connecting cable to *EBB* is of the order of hundred meters: the attenuation is of the order of 75% for the short front wave type *WS-1*, of 40% for *WS-2* shape and of 5% for the long front voltage shape Type *WS-3*; it means that if the stressing voltage shape exhibits a long front duration, the length of the connecting lead to ground has almost no influence;



- almost 90% of the impinging voltage is transferred to the transformer secondary, and then to the load, if the screens are ungrounded.

In Fig. 7.12 to 7.23 the phase to ground (*EBB* point) voltage wave shapes recorded at primary winding ( $U_1$  – CH1) and secondary winding ( $U_2$  – CH2) are reported. The screens are grounded with different cable length or ungrounded. The shape of stressing voltage is of type *WS-1*, *WS-2* and *WS-3*. The transformer is unloaded at the receiving end.

The results of type *WS-1* stressing voltage are compared with computed oscillograms and reported in Fig 7.12 to 7.15. This group of tests consists of four cases. The first three results are obtained in case where the isolation screen is grounded to earthing arrangement by means of three different cable length  $l$ , namely  $\sim 2$ ,  $\sim 5$  and  $\sim 150$  m. The case with ungrounded screen is also considered.

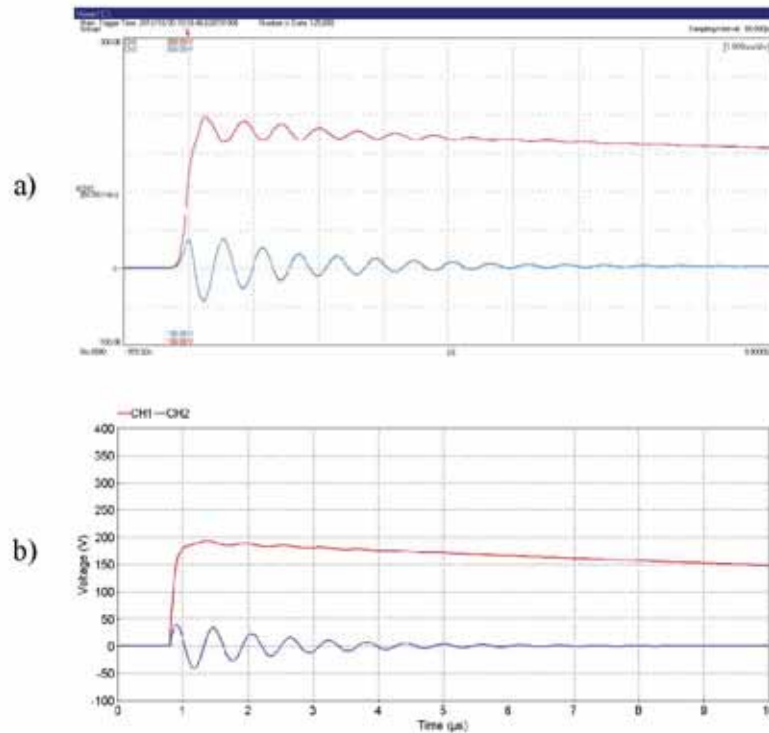


Figure 7.12. Records in the case of screen grounded through inductance  $L_{to} = 2,1 \mu\text{H}$ , at *WS-1* type surge operation; a) experimental result; b) computer simulation.

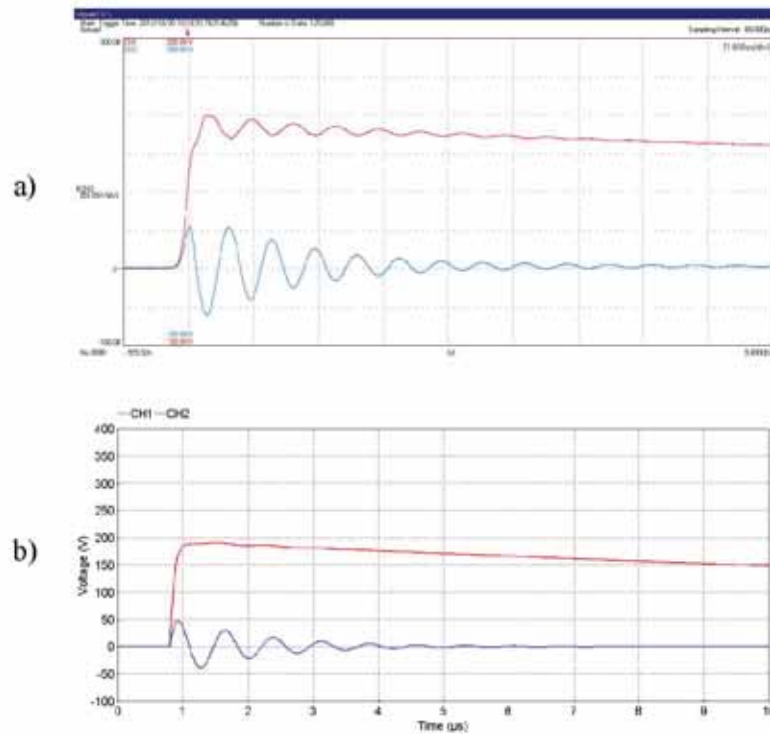


Figure 7.13. Records in the case of screen grounded through inductance  $L_{10} = 5 \mu\text{H}$ , at *WS-I* type surge operation; a) experimental result; b) computer simulation.

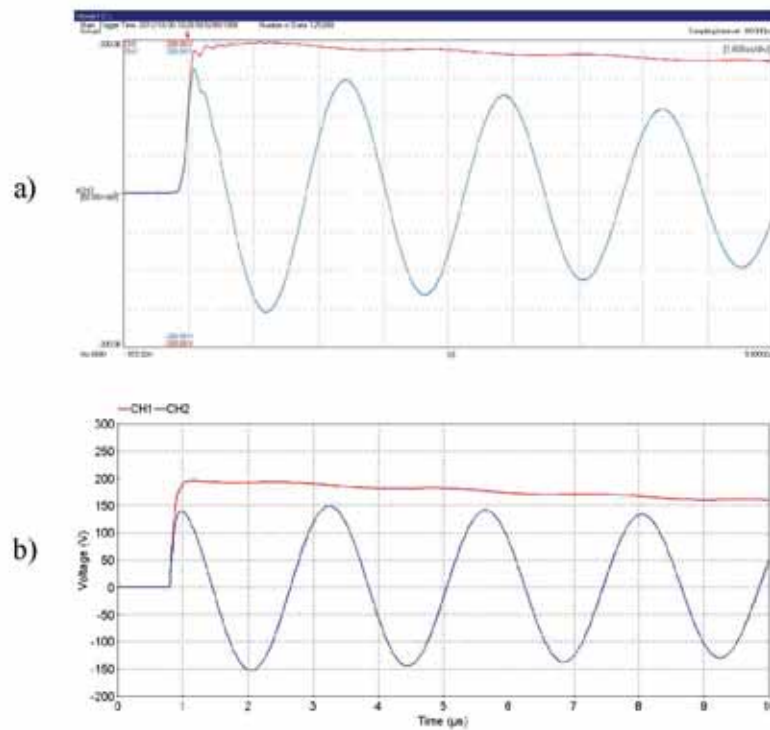


Figure 7.14. Records in the case of screen grounded through inductance  $L_{10} = 146,3 \mu\text{H}$ , at *WS-I* type surge operation; a) experimental result; b) computer simulation.

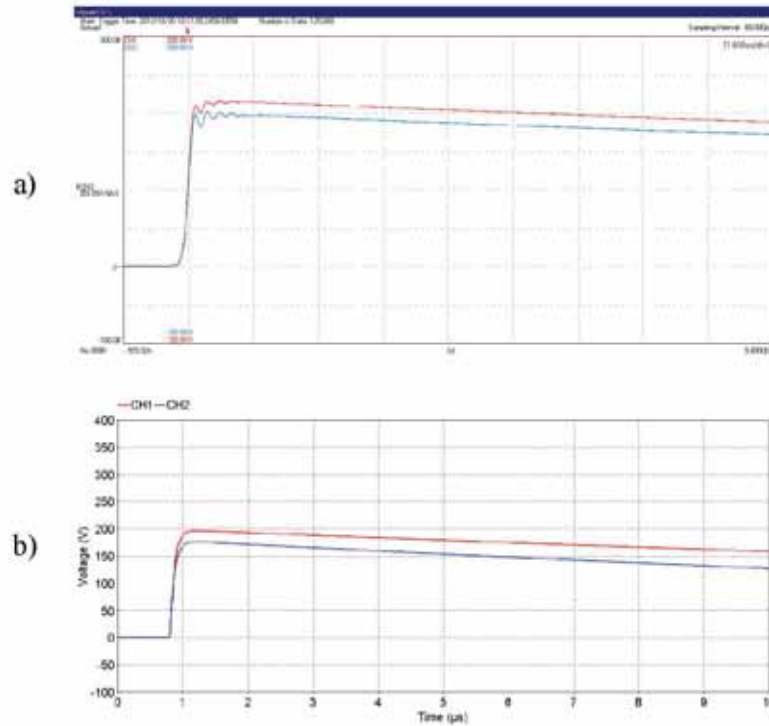


Figure 7.15. Records in the case of ungrounded screen, at *WS-1* type surge operation; a) experimental result; b) computer simulation.

In case of *WS-1* type surge operation and screen grounded through 2 m cable, it is to note that the voltage appears at secondary winding  $U_2$  is less than 50 V and this value is increased with cable length. The registered values  $U_2$  are as follows 50 V, 150 V for 5 m 150 m cable grounding length respectively. The worst case consist of the situation where ungrounded screen is considered. Moreover, the laboratory test and computer simulation results are compared. This comparison shows a good agreement between results, however small tolerable differences of shape and peak value exists.

The results of type *WS-2* stressing voltage are reported only for laboratory tests. In this case similar configurations of grounding screen conditions are considered.

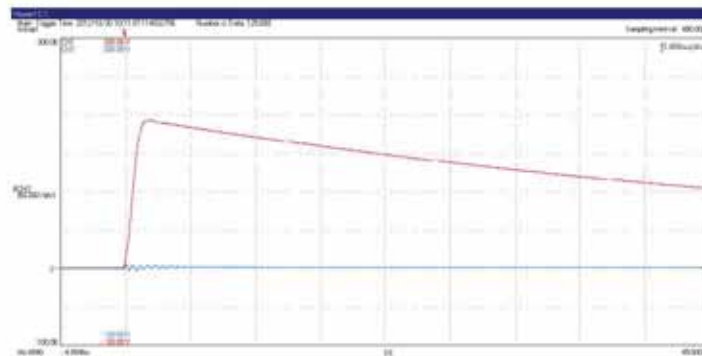


Figure 7.16. Records in the case of screen grounded through inductance  $L_{10} = 2,1 \mu\text{H}$ , at *WS-2* type surge operation; experimental result.

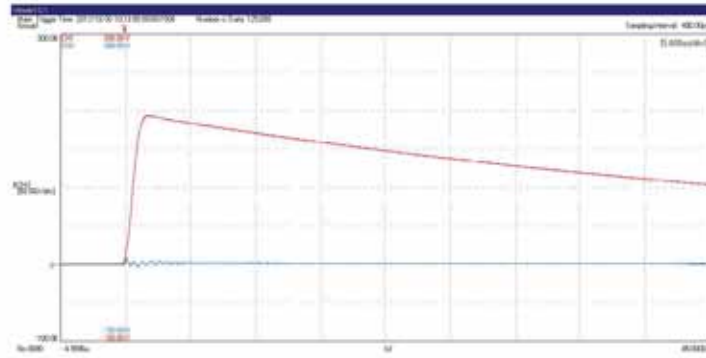


Figure 7.17. Records in the case of screen grounded through inductance  $L_{10} = 5 \mu\text{H}$ , at *WS-2* type surge operation; experimental result.

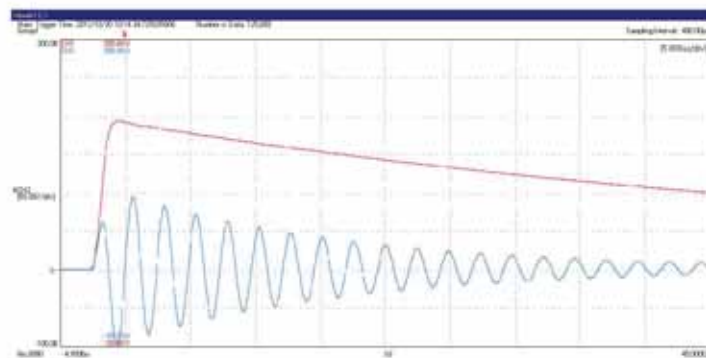


Figure 7.18. Records in the case of screen grounded through inductance  $L_{10} = 146,3 \mu\text{H}$ , at *WS-2* type surge operation; experimental result.

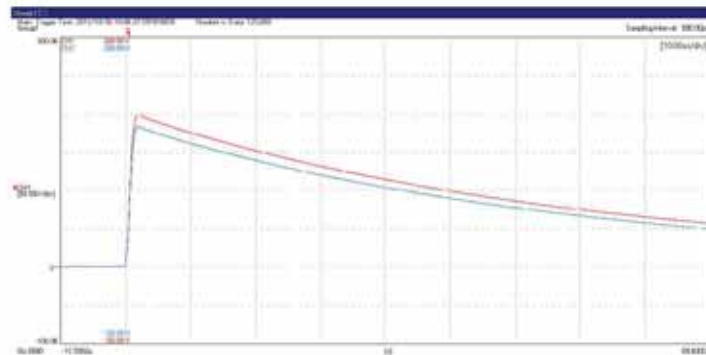


Figure 7.19. Records in the case of ungrounded screen, at *WS-2* type surge operation; experimental result.

The results with *WS-2* type surge, show that reduced efficiency of circuits separation appears when the screen is grounded through extremely long connection or ungrounded due to connection damage. The normal installation conditions seem to be not influenced on the protection effectiveness.

The results of type *WS-3* stressing voltage are reported only for laboratory tests. In this case similar configurations of grounding screen conditions are considered.

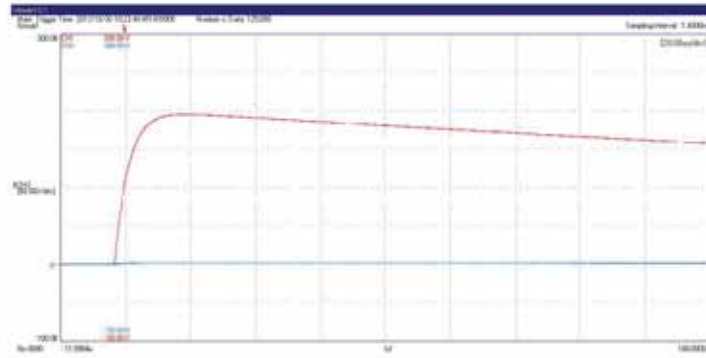


Figure 7.20. Records in the case of screen grounded through inductance  $L_{10} = 2,1 \mu\text{H}$ , at *WS-3* type surge operation; experimental result.

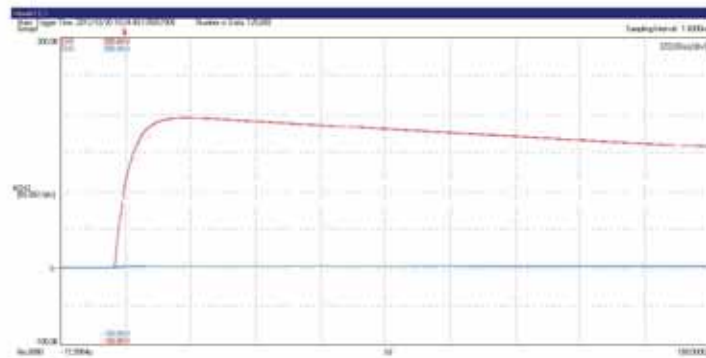


Figure 7.21. Records in the case of screen grounded through inductance  $L_{10} = 5 \mu\text{H}$ , at *WS-3* type surge operation; experimental result.

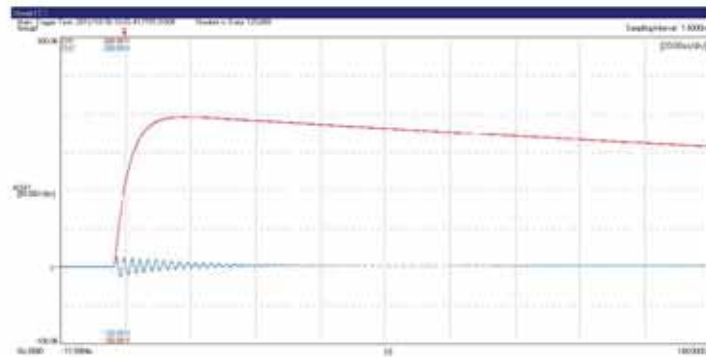


Figure 7.22. Records in the case of screen grounded through inductance  $L_{10} = 146,3 \mu\text{H}$ , at *WS-3* type surge operation; experimental result.



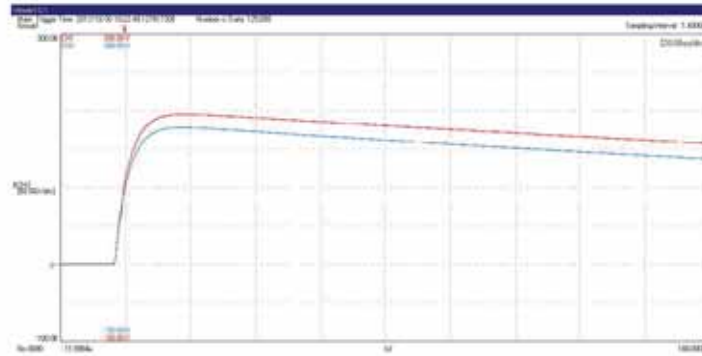


Figure 7.23. Records in the case of ungrounded screen, at *WS-3* type surge operation; experimental result.

The results with *WS-3* type surge, show that reduced efficiency of circuits separation appears where the screen is ungrounded, e.g. due to connection damage.

In Fig. 7.24 the summary of results is reported. The ratio  $U_2 / U_1$  is plotted as the function of length of the connecting cable of the transformer screen to the equipotential bonding bar.

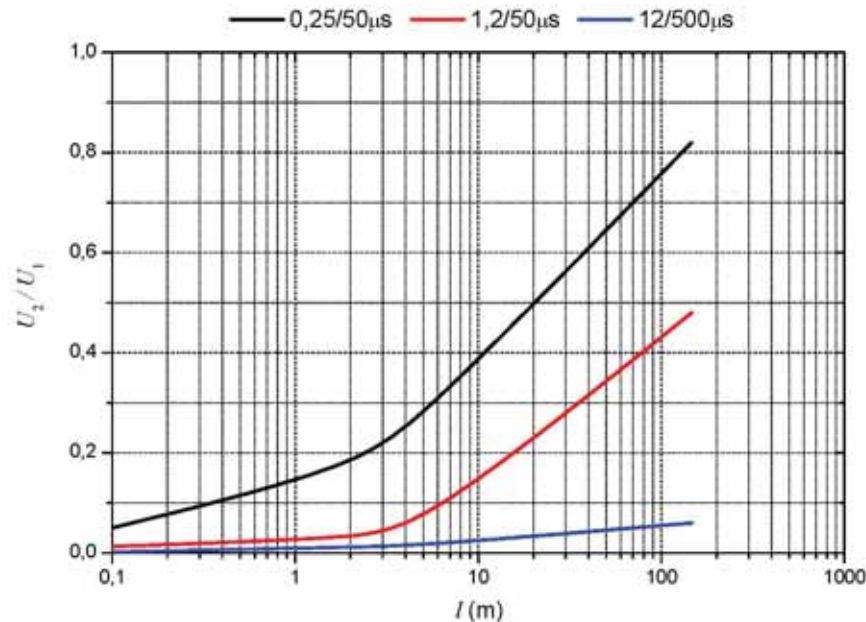


Figure 7.24. Ratio  $U_2 / U_1$  as a function of length of the connecting cable of the transformer screen to the equipotential bonding bar.

The experimental results, confirmed by computer simulations shown that the isolation transformer with screen earthed to the same bonding bar of the apparatus to be protected can be used with aim to attenuate the common mode lightning surges.

The effectiveness of attenuation of the common mode surges by means of an isolation transformer, depends on the characteristic of surge appear as well as on the installation condition. The worst case consist of fast front sources, caused e.g. due to subsequent negative lightning flashes. Moreover, the protective effect may be seriously reduced, if the installation of the transformer is not carefully considered. The effectiveness of protection decreases with the connecting cable of the transformer screen to the bonding bar increase.



#### 7.4. Summary

In the present chapter selected criteria for the electronic and electrical apparatus protection by means of an isolation transformer are presented. For the investigations reported the fast front source are considered. Moreover, special focus is dedicated on the mechanism of common mode surge transfer through an isolation transformer winding.

In case of fast front source e.g. lightning origin, the affecting source of primary winding is mainly transferred on the secondary winding of transformer due to capacitive coupling. This effect can be reduced by means of a screen between windings. In case of isolation transformers their effectiveness, not only depend on the manufacture characteristic, namely screen features, but also on the installation conditions.

The installation conditions include first of all grounding aspects, where the connection between a screen and earthing arrangement has a crucial influence on an isolation transformer effectiveness. In present investigation four length are considered, namely 2 m, 5 m, 150 m and finally damaged connection represented by means of high value of resistance.

The laboratory tests as well as computer simulation confirm that, the grounding condition of screen has an impact on protection effectiveness. This factor is also depends on the steepness of stressing source. The worst cases are for fast front sources with a front time e.g. 0,25  $\mu\text{s}$ . In case of long front sources with a front time e.g. 12  $\mu\text{s}$  the reduced effectiveness of screen appears if the connection between screen and grounding arrangement is damaged.

The laboratory tests and computer simulation results comparison is demonstrated. On the base of comparison performed for *WS-1*, it is to note that a good agreement is obtained, however some small tolerable difference exist.

For practical installation issues of isolation transformers, it is strongly recommended to reduce the length of connection between the screen and earthing arrangement. Moreover, the primary winding of isolation transformer should be protected by means of e.g. SPD.

# Chapter 8

## 8. Case study: selected aspects of lightning protection for photovoltaic power generation systems

### 8.1. Introduction

Photovoltaic power generation systems (PVPGS) can be divided into two categories taking into account maximal output of power generated. The first category consists of domestic photovoltaic arrays, where the power generation range is  $0,5 \div 5$  kW. The second group consists of commercial or industrial photovoltaic power generation systems, where the power generation range is  $10 \div 100$  kW.

The domestic systems are normally single phase connected to the domestic supply at 230V. The photovoltaic arrays are usually fixed over an existing pitched roof or integrated into a new roof, or may be fitted on a suitable wall or free-standing structure. The modules are wired to produce an appropriate voltage and connected to a DC/AC inverter synchronised with the grid.

PVPGS mounted on commercial, industrial or other large buildings will generally be connected to the three phase supply in the building.

Moreover, PVPGS can be further subdivided into two categories, where criterion of division is based on the operational time of power generation. The first group consists of systems called grid connected. A schematic representation of these systems is shown in Fig. 8.1. These configurations in simplification include solar modules, inverter and monitoring system.



Figure 8.1. Schematic representation of grid connected PVPGS.

The second group consists of systems called standalone. A schematic representation is shown in Fig. 8.2. Solar power system consists essentially of four components: photovoltaic modules, solar power controller, inverter, batteries and other accessories. The system uses solar photovoltaic modules during the day transforming solar energy into electrical energy, which through the solar controller, is stored in batteries to provide power.

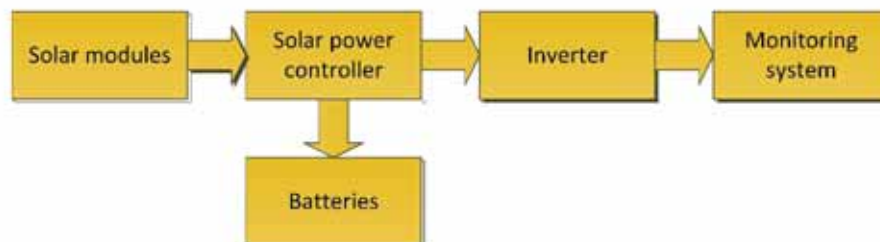


Figure 8.2. Schematic representation of standalone PVPGS.

PVGS, due to their external locations on roofs or facades of buildings and as free-standing installations in open extended areas, are vulnerable to both direct and indirect lightning

flashes. The problem of lightning protection of PVGS is object of many researches [200-207]. For practical issues of lightning protection the IEC 62305 standard [11, 17, 18, 128], can be applied. However to assure PVGS operations and protect against lightning interferences some particularities have to be considered e.g. risk assessment [208].

An example of industrial PVGS is shown in Fig. 8.3. This configuration includes photovoltaic panels installed in open area and the control centre within structure. The PVGS is connected to the local LV network. The operation of this system can be interrupted due to direct flashes to the photovoltaic panels (S1-a), control centre (S1-b) and connected LV lines (S3-a, S3-b). Moreover, indirect influence of lightning current exists, where the system operation can be disturbed due to nearby flashes to the photovoltaic panels (S2-a, S2-b) structure (S2-a, S2-b) and connected LV lines (S4-a, S4-b).

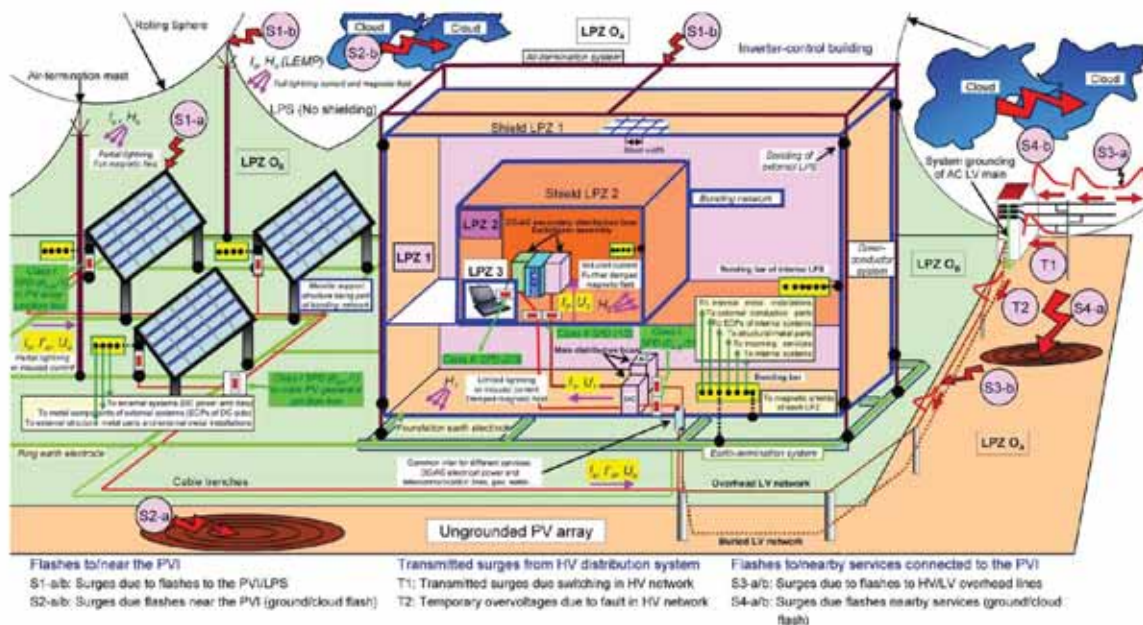


Figure 8.3. Sources of surges and potential LPZs in a large photovoltaic installation [200].

In terms of lightning protection the characteristics of the structure to be protected are crucial. An example of PVGS and its main components is shown in Fig. 8.4.

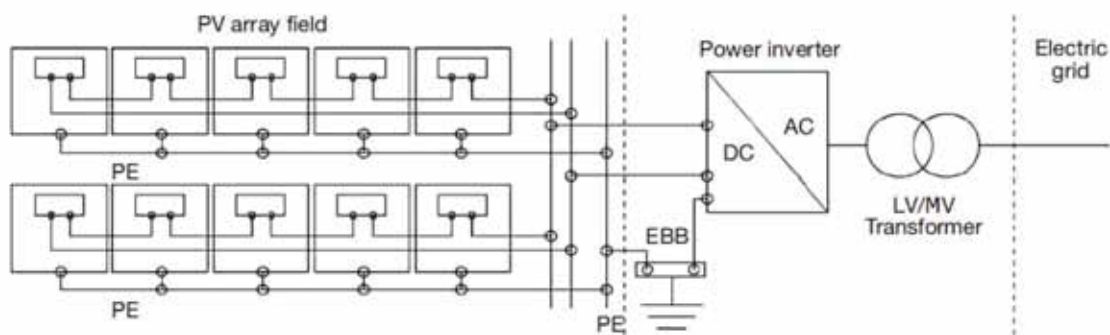


Figure 8.4. Photovoltaic power generating system and its main components [203].

The elements of PVGS can be divided into three group: photovoltaic modules, inverter and general PVGS equipment.

In general, the characteristics of PVGS apparatus, namely the surge withstand capability, are defined in their product specification. If it is necessary, devices should be tested according to their specific standards [209, 210].

Photovoltaic modules safety qualifications are included in [211, 212]. The  $U_w$  of modules according to [202] are reported in Tab. 8.1.

Table 8.1.  $U_w$  of photovoltaic panels under impulsive stress 1,2/50  $\mu$ s.

Nominal voltage (V)	$U_w$ (V)
100	1500
150	2500
300	4000
600	6000
1000	8000

The  $U_w$  of inverters and associated components according to [202] are reported in Tab. 8.2. However the control and measurements apparatus can have different values of this parameter.

Table 8.2.  $U_w$  of inverter and associated components under impulsive stress 1,2/50  $\mu$ s.

Nominal voltage (V)		Category			
		I	II	III	IV
AC	DC	$U_w$ (V)			
50	71	330	500	800	1500
100	141	500	800	1500	2500
150	213	800	1500	2500	4000
300	424	1500	2500	4000	6000
600	849	2500	4000	6000	8000
1000	1414	4000	6000	8000	12000

The schematic representation of possible lightning protection measures for PVGS, in accordance with [11] is shown in Fig. 8.5.



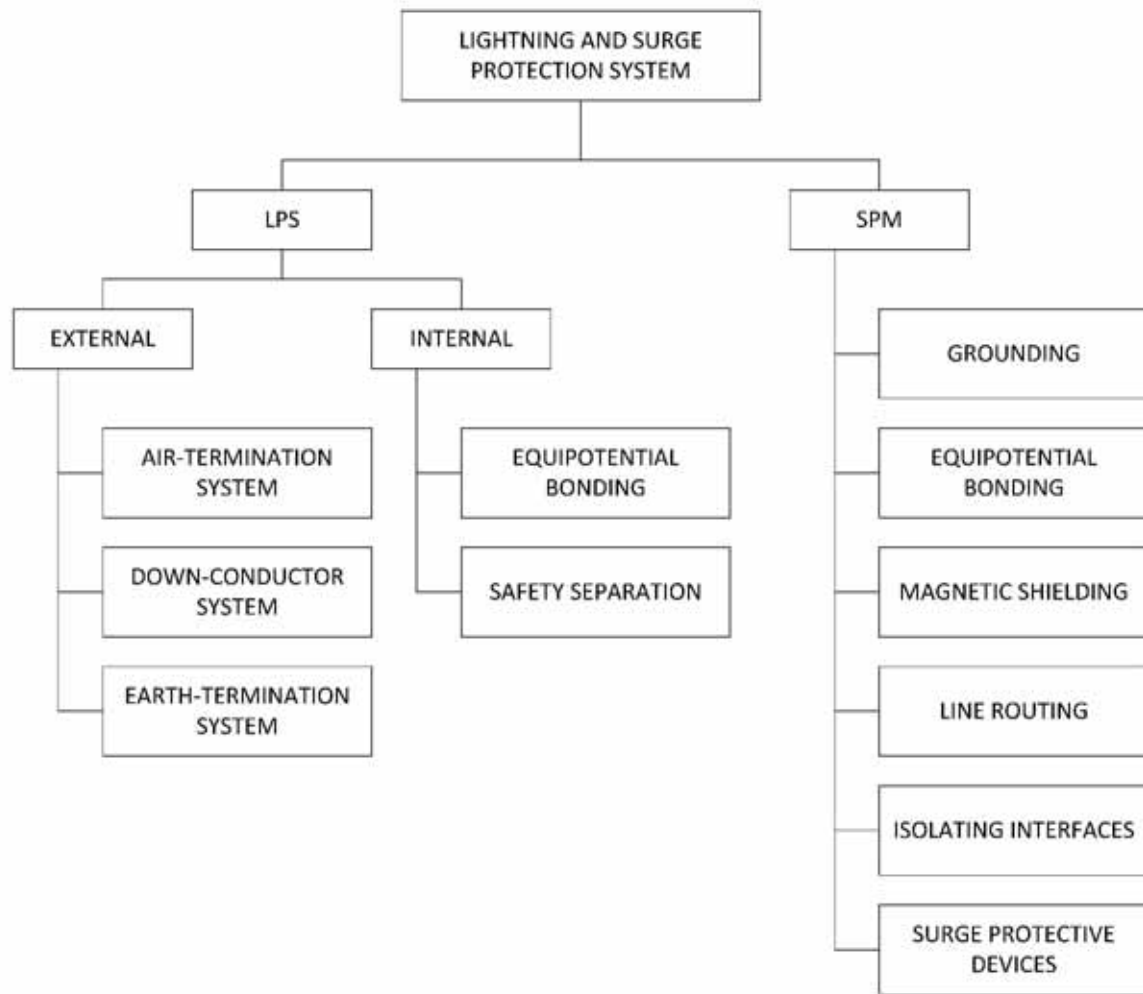


Figure 8.5. Classification of lightning and surge protection measures.



## 8.2. Risk assessment

### 8.2.1. Introduction

For the PVGS to be protected, the lightning protection system can be selected taking into account the lightning risk analysis and its assessment.

The assessment of risk of loss of human life gives values which usually are under the tolerable level  $10^{-5}$  and so the PVPGS did not need any protection measure. On the contrary the values of risk of economic loss are not negligible at all.

The analysis of the risk components of present paragraph outlined that the hazard is due mainly to the effect of nearby flashes and that the risk of failure is greater in the DC side of the system. Taking into consideration the high value (about 20% of the whole installation) of the economic loss expected [208, 213], it is mandatory to adopt some protection measures, otherwise the time of return of the investment increases too much.

In present paragraph, two examples of risk evaluation according to the IEC standard [17] are presented. The first case consists of a roof top PVPGS, with a photovoltaic array field (structure to be protected) which is 45 m wide, 60 m long and 15 m high from ground level (including the metallic frame of the PV modules). The second case consists of a ground based PVPGS, with a photovoltaic array field which is 45m wide, 60m long and 1.5m high.

Each PVPGS considered is about 250 kWp and the distribution system, according to IEC 60364 [214], is IT on the DC side and TN on the AC side.

The structures are assumed as being isolated, as well as having no LPS system and no coordinated SPD set.

For the roof top PV system, the collection area of the structure is equivalent to the collection area of the building that is housing the PV array field.

The DC/AC power inverter and the transformer are located inside the building that is housing the photovoltaic system in case of the roof top mounted system or, in case of the ground mounted system, inside a dedicated technical cabinet (the cabinet is inside the PV array field, so that no contribution to the collection areas is added).

The system is connected to the electric grid with an HV shielded ( $R_s \leq 1 \Omega/\text{km}$ ,  $U_w = 6 \text{ kV}$ ) and buried ( $\rho = 500 \Omega\text{m}$ ) power cable of 1000 m length, in a rural environmental (as defined in the IEC 62305-2 [17]) where there are no adjacent structures.

In Tab. 8.3 and Tab. 8.4 are summarized the data and characteristics of the structures and of their internal systems.

It is assumed that the structures, of an industrial kind, are in a rural place and fenced, so that people stays nearby for a very short time. Nevertheless, in the next paragraph two conservative choices are done about the permanence of people in the zones of interest.

Moreover, the probability of failure of internal systems due to flashes near the incoming line,  $P_{LI}$ , has a different value if compared to that in table B.9 in the IEC 62305-2 [17]. The line location factor is substituted with line installation factor and new parameters ( $C_{LD}$ ,  $C_{LI}$ ) and new probabilities ( $P_{TU}$ ,  $P_{EB}$ ) are introduced [17].

Table 8.3. Characteristics of the structures.

Parameter	Comment	Symbol	Value
PV dimensions (m)	roof top	$L_b \times W_b \times H_b$	60×45×15
PV dimensions (m)	ground based	$L_b \times W_b \times H_b$	60×45×1,5
location factor	isolated	$C_D$	1
shield at external structure boundary	none	$K_{S1}$	1
shield at internal structure boundary	none	$K_{S2}$	1
people in the structure	inside (only for the roof top PVPGS) or outside the structure	$n_i$	n
protection measures	fence	$P_{TA}$	0
	no LPS	$P_B$	1

**Note:** For more information about symbols and values adopted refer to standard IEC 62305-2

Table 8.4. Internal power systems (DC and AC) and relevant incoming power line characteristics.

Parameter	Comment	Symbol	Value
soil resistivity	$\Omega\text{m}$	$\rho$	500
length (m)	m	$L_L$	1000
HV/LV transformer	at building entrance	$C_T$	0,2
line installation factor	isolated	$C_I$	0,5
line environmental factor	rural	$C_E$	1
line shield	shielded power line (bonded to the same bonding bar as the equipment) $R_s \leq 1\Omega / \text{km}$ and $U_w = 6\text{kV}$	$P_{LD}$	0,02
		$P_{LI}$	0,1
		$C_{LD}$	1
		$C_{LI}$	0
internal wiring precaution (DC and AC side of system)	unshielded cable, no routing precaution in order to avoid loops	$K_{S3}$	1
equipment withstand voltage (starting from the DC side to the main circuit of the LV/HV transformer)	$U_w = 1,5\text{ kV}$	$K_{S4}$	0,67
protection against touch voltages	none	$P_{TU}$	1
coordinated SPDs	none	$P_{SPD}$	1
		$P_{EB}$	1

**Note:** For more information about symbols and values adopted refer to standard IEC 62305-2

### 8.2.2. Risk assessment for the roof top PVPG

In Fig. 8.6 a typical domestic photovoltaic power generation system is shown. The photovoltaic panels are imposed on the structure roof. The inverter and possible accompanying apparatus are installed inside the structure.



Figure 8.6. Domestic photovoltaic power generating system [204].

The domestic photovoltaic power generating system in simple case can be represented by electrical circuit given in Fig. 8.7. However, the complexity of the system can be different, according to customers need. In all cases lightning protection issues should be considered taking into account risk components what is discussed in present paragraph.

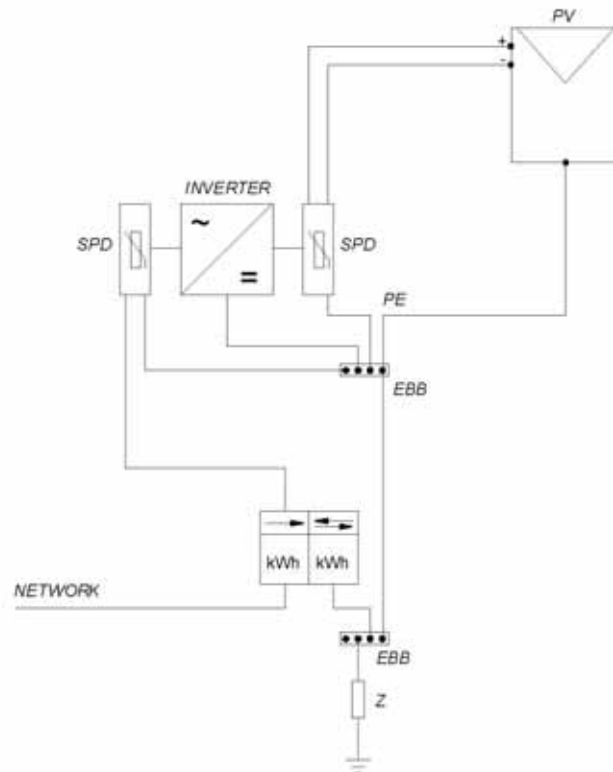


Figure 8.7. Basic circuit of domestic photovoltaic power generating system.

### Risk of loss of human life ( $R_1$ )

According to IEC 62305-2 it is possible to define two zones. In fact the external surface of the building that is housing the PV array field is different from the internal volume. There is a single fire proof compartment and does not exist any spatial shield between the two zones:

$Z_1$  = outside of the building that is housing the PV array field;

$Z_2$  = inside of the building that is housing the PV array field (where the internal systems are located).

Table 8.5.  $Z_1$  zone – roof top mounted PVPG - risk  $R_1$ .

Parameter	Comment	Symbol	Value
Soil surface	Grass around the building; concrete on the roof top	$r_t$	$10^{-2}$
Shock protection	Fence around the building and warning notice for avoiding maintenance on the roof top during thunderstorms	$P_A$	$\approx 0$
Loss	by electric shock	$L_T$	$10^{-2}$

**Note:** For more information about symbols and values adopted refer to standard IEC 62305-2

Table 8.6.  $Z_2$  zone – roof top mounted PVPG - risk  $R_1$ .

Parameter	Comment	Symbol	Value
Floor surface	concrete	$r_t$	$10^{-2}$
Risk of fire	low risk of fire	$r_f$	$10^{-3}$
Hazard	no special hazard	$h_z$	1
Fire protection	one of the following provisions: fire extinguishers; fixed and manually operated extinguishing installations; manual alarm installations; hydrants; fire proof compartments; protected escape routes	$r_p$	0,5
Internal systems	(connected to the main switchboard)		
Loss	by electric shock	$L_T$	$10^{-2}$
Loss	by physical damage	$L_F$	$2 \times 10^{-2}$
Probability of damage, risk component $R_B$	No LPS provided	$P_B$	1
Probability of damage, risk component $R_U$	No SPD set provided, shielded line (bonded to the same bonding bar as the equipment) $R_s \leq 1\Omega / \text{km}; U_w = 6\text{kV}$	$P_U$	0,02
Probability of damage, risk component $R_V$	No SPD set provided, shielded line (bonded to the same bonding bar as the equipment) $R_s \leq 1\Omega / \text{km}; U_w = 6\text{kV}$	$P_V$	0,02

**Note:** For more information about symbols and values adopted refer to standard IEC 62305-2

According to the standard IEC 62305-2 [17] the components of the risk  $R_1$  are expressed by:

$$R_1 = R_A + R_B + R_U + R_V \quad (8.1)$$

where (remember the choices  $n_z/n_1=1$  and  $t_z/8760=1$ ):

$$R_A = N_D \times P_A \times r_t \times L_T \quad (8.2)$$

$$R_B = N_D \times P_B \times r_p \times h_z \times r_f \times L_F \quad (8.3)$$

$$R_U = N_L \times P_U \times r_t \times L_T \quad (8.4)$$

$$R_V = N_L \times P_V \times r_p \times h_z \times r_f \times L_F \quad (8.5)$$

The calculations concerning the risk  $R_1$  have to be repeated for each zone which the structure was divided in. The overall risk is obtained by the sum of the risks of each zone [17].

The probability  $P_A$  is negligible because of the fence and the fact that during thunderstorms on the roof top it is forbidden any maintenance activity. The probability  $P_B$  is equal to 1 since the structure is not protected with a lightning protection system (LPS). The two probabilities  $P_U$  and  $P_V$  are determined by the fact that an SPD set is not installed.

Considering a lightning ground flash density of

$$N_g = 4 \text{ flashes}/(\text{year} \times \text{km}^2) \quad (8.6)$$

which is the maximum value in Italy, it is possible to obtain a number of dangerous events due to flashes to the structure (photovoltaic array field) equal to:

$$N_D = N_g \times C_D \times A_D \times 10^{-6} \quad (8.7)$$

Taking into account the value in Tab. 8.3, formula (8.6) and (8.7) give the following value:

$$N_D = 7,4 \times 10^{-2} \quad (8.8)$$

while  $N_L$ , the number of dangerous events due to flashes to the service (HV power line), is equal to:

$$N_L = N_g \times C_1 \times C_E \times C_T \times A_L \times 10^{-6} \quad (8.9)$$

Taking into account the value in Tab. 8.3, formula (8.6) and (8.9) give the following value:

$$N_L = 1,6 \times 10^{-2} \quad (8.10)$$

Therefore using the values of Tab. 8.3-6 it is possible to obtain the following value for risk  $R_1$  for zone  $Z_2$  (such risk does not includes  $R_A$  that constitutes risk  $R_1$  for zone  $Z_1$ ):

$$R_1 = 7,76 \times 10^{-7} \quad (8.11)$$

Note that risk  $R_1$  for zone  $Z_1$  is negligible, for the fence around the building and the fact that during thunderstorms on the roof top it is forbidden any maintenance activity. Hence, the overall risk  $R_1$  is reduced to the value for the zone  $Z_2$  that is given by (8.11).

By considering a value for the tolerable risk equal to  $R_T = 10^{-5}$ , as suggested by the standard IEC 62305-2 [17], because  $R_1 \leq R_T$ , it follows that it is not necessary any lightning protection system for such risk.

It is important to observe that, taking into account the same conditions, if the building that is housing the plant had an ordinary risk of fire (specific fire load between  $800 \text{ MJ/m}^2$  and  $400 \text{ MJ/m}^2$ ) instead of a low one (specific fire load less than  $400 \text{ MJ/m}^2$ , or structures containing a small amount of combustible materials), then the risk  $R_1$  (equal to  $7,47 \times 10^{-6}$ ) still is not greater than the tolerable value. If the risk of fire is high (specific fire load larger than  $800 \text{ MJ/m}^2$ ), then the risk  $R_1$  (equal to  $7,44 \times 10^{-5}$ ) is greater than the tolerable risk; in such case, the risk  $R_1$  cannot be reduced below the tolerable value only by adopting additional fire protection measures, like fixed automatically operated extinguishing installations (obtaining  $R_1 = 2,98 \times 10^{-5}$ ). Instead, with the procedure described in the 1st edition, even an ordinary risk of fire was enough to have a risk greater than the tolerable value, but in such case the above mentioned additional fire protection measures were enough to re-obtaining tolerable values.

#### Risk of economic loss ( $R_4$ )

To evaluate risk  $R_4$  it is necessary to consider the following risk components:  $R_B$ ,  $R_C$ ,  $R_M$ ,  $R_V$ ,  $R_W$  and  $R_Z$  [17]. In Tab. 8.7 the amount of loss according to Annex C of the standard [17] is given. In Tab. 8.8 the values of the probabilities of damage according to Annex B of the standard [17] are reported.

Table 8.7.  $Z_2$  zone – roof top mounted PVPGS - risk  $R_4$ .

Parameter	Comment	Symbol	Value
Risk of fire	low risk of fire	$r_f$	$10^{-3}$
Special hazard	no special hazard	$h_z$	1
Fire protection	one of the following provisions: fire extinguishers; fixed manually operated extinguishing installations; manual alarm installations; hydrants; fire proof compartments; protected escape routes	$r_p$	0,5
Loss	by overvoltages	$L_O$	0,01
Loss	by physical damage	$L_F$	0,5
<b>Note:</b> For more information about symbols and values adopted refer to standard IEC 62305-2			

It is to note that if a SPD is not provided, the probability reducing failure of internal systems (flashes near a structure) ( $P_{MS}$ ) depends only on shielding, wiring and withstand voltage of equipment and is calculated as the square of the product  $K_{S1} \times K_{S2} \times K_{S3} \times K_{S4}$ . The probabilities  $P_V$  and  $P_W$  and  $P_Z$  are evaluated according to the standard IEC 62305-2, [17].



The risk components for  $R_4$  are expressed by (all relating to the  $Z_2$  zone):

$$R_4 = R_B + R_C + R_M + R_V + R_W + R_Z \quad (8.12)$$

where:

$$R_B = N_D \times P_B \times r_p \times h_z \times r_f \times L_F \quad (8.13)$$

$$R_C = N_D \times P_C \times L_O \times c_s / c_t \quad (8.14)$$

$$R_M = N_M \times P_M \times L_O \times c_s / c_t \quad (8.15)$$

$$R_V = N_I \times P_V \times r_p \times h_z \times r_f \times L_F \quad (8.16)$$

$$R_W = N_I \times P_W \times L_O \times c_s / c_t \quad (8.17)$$

$$R_Z = N_I \times P_Z \times L_O \times c_s / c_t \quad (8.18)$$

Table 8.8.  $Z_2$  zone – roof top mounted PVPGS - risk  $R_4$ .

Parameter	Comment	Symbol	Value
Probability of damage, risk component $R_B$	No LPS	$P_B$	1
Probability of damage, risk component $R_C$	No coordinated SPD set	$P_C$	1
Probability of damage, risk component $R_M$	$K_{S1} \times K_{S2} \times K_{S3} \times K_{S4} = 0,67$	$P_M$	0,44
Probability of damage, risk component $R_V$	shielded line (bonded to the same bonding bar as the equipment) $R_s \leq 1 \Omega/\text{km}; U_w = 6 \text{ kV}$	$P_V$	0,02
Probability of damage, risk component $R_W$	shielded line (bonded to the same bonding bar as the equipment) $R_s \leq 1 \Omega/\text{km}; U_w = 6 \text{ kV}$	$P_W$	0,02
Probability of damage, risk component $R_Z$	shielded line (bonded to the same bonding bar as the equipment) $R_s \leq 1 \Omega/\text{km}; U_w = 6 \text{ kV}$	$P_Z$	0

**Note:** For more information about symbols and values adopted refer to standard IEC 62305-2

The number of events  $N_M$  (8.19) and  $N_I$  (8.20) take into account flashes nearby respectively the structure and the incoming service,

$$N_M = N_g \times A_M \times 10^{-6} \quad (8.19)$$

$$N_I = N_g \times C_1 \times C_E \times C_T \times A_I \times 10^{-6} \quad (8.20)$$

where:

$$A_M = 8,90 \times 10^5 \quad (8.21)$$

and

$$A_1 = 4,00 \times 10^6 \quad (8.22)$$

corresponding to

$$N_M = 3,56 \quad (8.23)$$

and

$$N_1 = 1,60 \quad (8.24)$$

By using the formulas given above, assuming the parameters in Tab. 8.7 and Tab. 8.8 and the values given in (8.8) and (8.10) for the number of dangerous events due to flashes to the structure ( $N_D$ ) and to the service ( $N_L$ ) one has, for the risk components, the values in Tab 8.9.

Table 8.9. Risk component values and their percentages over total economic risk  $R_4$ .

Risk component $R_X$	Value	$(R_X/R_4)\%$
$R_B$	$1,85 \times 10^{-5}$	0,56%
$R_C$	$1,48 \times 10^{-4}$	4,44%
<b><math>R_M</math></b>	<b><math>3,17 \times 10^{-3}</math></b>	<b>94,98%</b>
$R_P$	$8,00 \times 10^{-8}$	0,00%
$R_{IP}$	$6,40 \times 10^{-7}$	0,02%
$R_Z$	0	0%
$R_4$	$3,33 \times 10^{-3}$	100,00%

Considering that risk  $R_4$  is related to the total cost  $c_1$  of the system to be protected through the formula:

$$R_4 = c_1/c_t \quad (8.25)$$

where:

$c_1$  - annual loss, it is possible to see that the loss  $c_1$  for the PVPGS can be obtained as:

$$c_1 = R_4 \times c_t \quad (8.26)$$

Therefore, without protection measures one has an increase of the annual cost of the plant of about 0,3% of the cost of the PVPGS (for large plants this fact can increase consequently the time for the return of the investment).

It is note that if a tolerable risk equal to  $R_T = 1 \times 10^{-3}$  according to the IEC standard 62305-2 [17] is assumed, protection measures are required due to high value of risk component  $R_M$ .

### 8.2.3. Risk assessment for the ground based PVPGS

The industrial or commercial photovoltaic power generation systems generally are installed on the earth through special brackets. An example of considered system is shown in Fig. 8.8.



Figure 8.8. Industrial photovoltaic power generating system [204].

The electrical equivalent circuit in simplification is shown in Fig. 8.9.

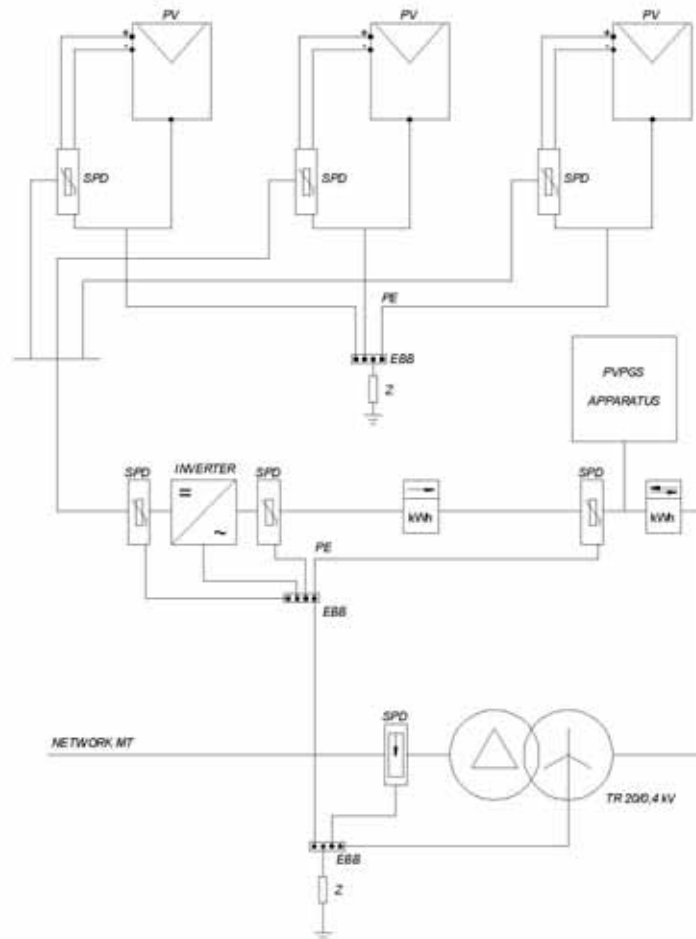


Figure 8.9. Basic circuit of industrial photovoltaic power generating system.

Due to the spatial location of these systems, the selection of adequate protection measures is needed.

### Risk of loss of human life ( $R_1$ )

The same considerations as those already done for the rooftop PVPGS, can be applied to a ground based PVPGS. Indeed, because of the small collection area  $A_D$  ( $3,7 \times 10^3 \text{ m}^2$  instead of  $18,5 \times 10^3 \text{ m}^2$  of the rooftop PVPGS) of a photovoltaic array field with a negligible height (that brings the number of dangerous events to  $N_D=1,5 \times 10^{-2}$  and  $N_L=1,6 \times 10^{-2}$ ) and due to the lack of the fire risk of the building, the value of  $R_1 = 1,84 \times 10^{-7}$  and can be considered as negligible in comparison with  $R_1 = 10^{-5}$ .

### Risk of economic loss ( $R_4$ )

The same considerations as the ones for the rooftop PVPGS also apply here. The values of each risk component are slightly different in comparison with those of Tab. 8.9 and are reported in Tab. 8.10.

Table 8.10. Risk component values and their percentages over total economic risk  $R_4$ .

Risk component $R_X$	Value	$(R_X/R_4)\%$
$R_B$	$3,71 \times 10^{-6}$	0,12%
$R_C$	$2,97 \times 10^{-5}$	0,93%
<b><math>R_M</math></b>	<b><math>3,17 \times 10^{-3}</math></b>	<b>98,93%</b>
$R_V$	$8,00 \times 10^{-8}$	0,00%
$R_W$	$6,40 \times 10^{-7}$	0,02%
$R_Z$	0	0%
$R_4$	$3,20 \times 10^{-3}$	100,00%

**Note:** assuming  $c_s / c_t = 0,2$  in case of damage of systems due to overvoltages and assuming the total loss of the structure and its contents in case of fire

### 8.3. Protection of control and measurement apparatus by means of SPD

#### 8.3.1. Introduction

In Fig. 8.10, an example of domestic photovoltaic power generation system with acquisition and control unit (ACU) is presented. In this situation, during lightning occurrences, the control system can be especially endangered due to peculiar characteristics of signal and data lines for regular operations of the system [144, 145].

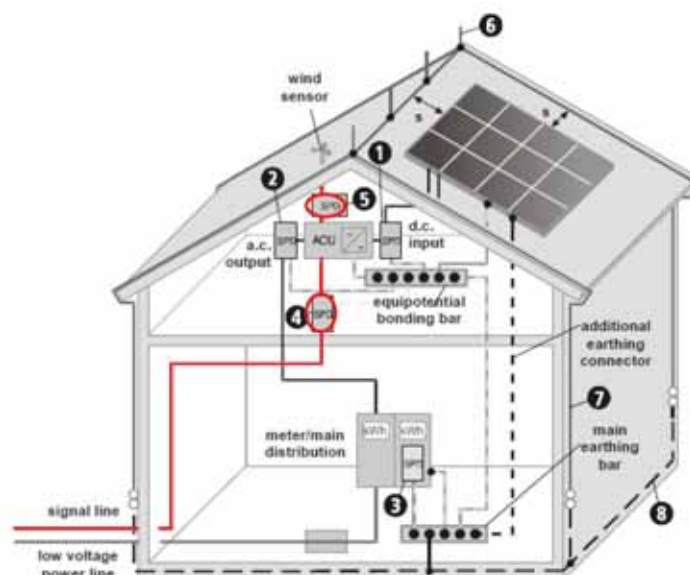


Figure 8.10. Example of PVGS with acquisition and control unit, where: 1 - SPD Type 2 for PV application; 2 - SPD Type 2; SPD Type 1; 4 - combined SPD for low voltage power supply and signal line; 5 - SPD for signal line; 6 - air termination system; 7 - down conductor; 8 - earth termination system [90].

The SPD function in real occurrence results in the initiation of travelling waves caused by lightning current. In analysed example the travelling waves are caused by an impulse voltage generator. However in both cases the wave propagation model is applied. The voltage wave may be reflected and modified along the circuit towards the apparatus [154].

The paragraph deals with influence of lightning overvoltage shape on SPD characteristics for ACU protection. For this aim several laboratory tests are performed in order to ascertain this influence.

The laboratory setup is formed by an impulse voltage generator with peak value of 400 V whose electrical parameters are selected in order to obtain different voltage shapes: 1,2/50  $\mu$ s, 12/50  $\mu$ s, 0,25/50  $\mu$ s, 12/500  $\mu$ s, 8/20  $\mu$ s; typical limiting SPDs which can be applied on data lines, with different protection levels:  $U_p = 40$  V,  $U_p = 80$  V,  $U_p = 100$  V; signalling wires of different length, ranging from 5 to 30 m, connecting SPD to apparatus to be protected, characterized by high value of input resistance.

During investigations the voltages are measured at SPD and apparatus terminals to analyse the influence of front steepness of incoming overvoltage and of connecting leads lengths. The considered basic arrangement is shown in Fig. 8.11.



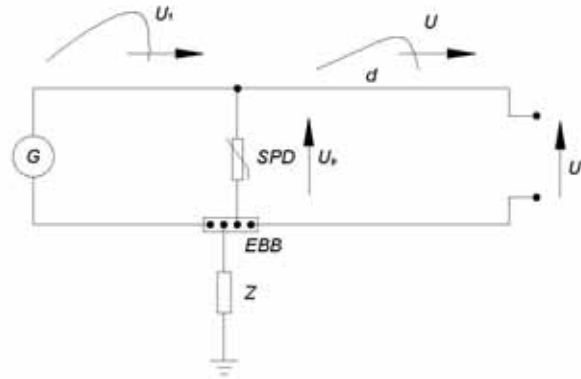


Figure 8.11. Basic arrangement:  $G$  - impulse voltage generator;  $U_1$  - surge voltage;  $EBB$  - equipotential bonding bar;  $Z$  - conventional earthing impedance;  $U_p$  - voltage on the SPD terminals;  $d$  - line length;  $U$  - overvoltage incoming through distant SPD;  $U_1$  - voltage on the terminals of apparatus to be protected.

### 8.3.2. Results of laboratory tests

#### Influence of connecting leads

Voltage surges incoming to the circuits are reduced through the SPD according to its protection level. In real case within a structure the distance between an SPD and apparatus to be protected can have a significant value. In this case, standard impulse wave form 1,2/50  $\mu$ s, resistive load  $R$  (open circuit), SPD with level of protection  $U_p = 40$  V and three line length 5 m, 15 m and 30 m are used.

Some results obtained by laboratory test are reported in Fig. 8.12, 8.13 and 8.14.



Figure 8.12. Oscillograms of voltage at apparatus to be protected: CH1 voltage on the SPD terminals, CH2 voltage on the load; impulse voltage wave shape 1,2/50  $\mu$ s; Resistive load,  $R = 10^6 \Omega$ ; line length  $d = 5$  m.





Figure 8.13. Oscillograms of voltage at apparatus to be protected: CH1 voltage on the SPD terminals, CH2 voltage on the load; impulse voltage wave shape 1,2/50  $\mu$ s; Resistive load,  $R = 10^6 \Omega$ ; line length  $d = 15$  m.



Figure 8.14. Oscillograms of voltage at apparatus to be protected: CH1 voltage on the SPD terminals, CH2 voltage on the load; impulse voltage wave shape 1,2/50  $\mu$ s; Resistive load,  $R = 10^6 \Omega$ ; line length  $d = 30$  m.

It can be noticed that the value of voltage on the terminals of apparatus to be protected (CH2) is higher with respect to the voltage on the SPD terminals (CH1) in each case. However the  $U_p$  doubled is not achieved. Undertaken tests allow to assess the differences between value of voltage on SPD terminals and apparatus to be protected along the considered distance. In Tab. 8.11 is reported, the voltage on the SPD terminals ( $U_p$ ), the voltage on the load ( $U_l$ ), the increasing of the voltage ( $\Delta U$ ) with distance  $d$  and its increment for unit length.

Table 8.11. Measured value of voltages on the SPD terminals and at apparatus to be protected for  $R = 10^6 \Omega$  load condition and different line length  $d$  for stressing wave shape 1,2/50  $\mu\text{s}$ .

$d$ (m)	$U_p$ (V)	$U_1$ (V)	$\Delta U$ (V)	$\Delta U / d$ (V/m)	$\Delta U / U_p$ (%)
5	40,8	55,4	14,6	2,9	36
15	41,4	62,8	21,4	1,4	52
30	39,7	64,7	25	0,8	63

### Influence of cable type

Influence of cable type connecting SPD and load is also investigated and results for different cable velocity values are reported in Tab. 8.12.

Table 8.12. Calculated values of voltage at apparatus to be protected for different cable propagation velocity values,  $R = 10^6 \Omega$  load condition and  $U_p = 40$  V.

$d$ (m)	$v$ (m/ $\mu\text{s}$ )	$U_1$ (V)	$\Delta U$ (V)	$\Delta U / U_p$ (%)
30	180	69,6	29,6	73,9
30	200	66,3	26,3	65,8
30	220	63,6	23,6	59,1
30	240	61,4	21,4	53,4
30	260	59,5	19,5	48,7

The results presented in Tab. 8.12 are obtained at assumptions: the same value of stressing overvoltage steepness; the same distance  $d$ ; the same SPD.

### Influence of lightning overvoltage shape

The voltage on the SPD terminals depends on the current flowing in the branch according to the SPD  $U / I$  characteristics, so that the measured value of  $U_p$  can be less than the nominal values 40V.

In Tab. 8.13 the values of voltage measured on the SPD terminals ( $U_p$ ) and on the load terminals ( $U_1$ ) are reported together with increment of voltage for unit of length of circuit for different stressing wave shapes.

Table 8.13. Measured values of voltage on the SPD and apparatus to be protected terminals for  $U_p = 40$  V,  $R = 10^6 \Omega$  load condition, connecting leads 30 m and different wave forms.

Wave shape $T_1/T_2$ ( $\mu\text{s}$ )	$U_p$ (V)	$U_1$ (V)	$(U_1 - U_p) / d$ (V/m)
0,25/50	39,9	79,5	1,32
1,2/50	39,7	64,7	0,83
8/20	36,5	47,3	0,36
12/50	36,5	46	0,32
12/500	36	45,6	0,32

### Influence of SPD protection level

The present part of work is dedicated to investigate the  $U_p$  influence on the voltage appearing on the apparatus terminals. For this aim, impulse voltage wave form 0,25/50  $\mu$ s, line length  $d = 30$ m, resistive load  $R$  (open circuit), SPDs with different level of protection  $U_p = 40$  V,  $U_p = 80$  V,  $U_p = 100$  V are considered.

From the oscillograms (Fig. 8.15, 8.16 and 8.17) it can be observed that the level of protection  $U_p$  has not a significant influence for the overvoltage shape appearing on the terminals of apparatus.

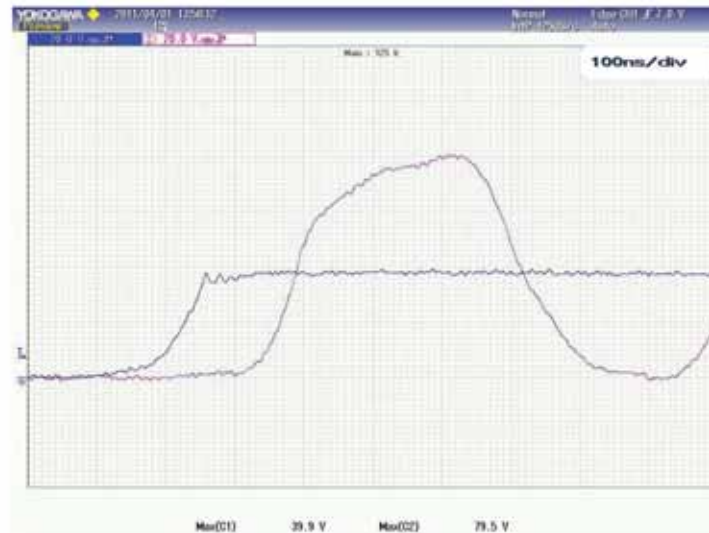


Figure 8.15. Oscillograms of voltage at apparatus to be protected: CH1 voltage on the SPD terminals, CH2 voltage on the load; impulse voltage wave shape 0,25/50  $\mu$ s;  $U_p = 40$  V; resistive load,  $R = 10^6 \Omega$ ; line length  $d = 30$  m.

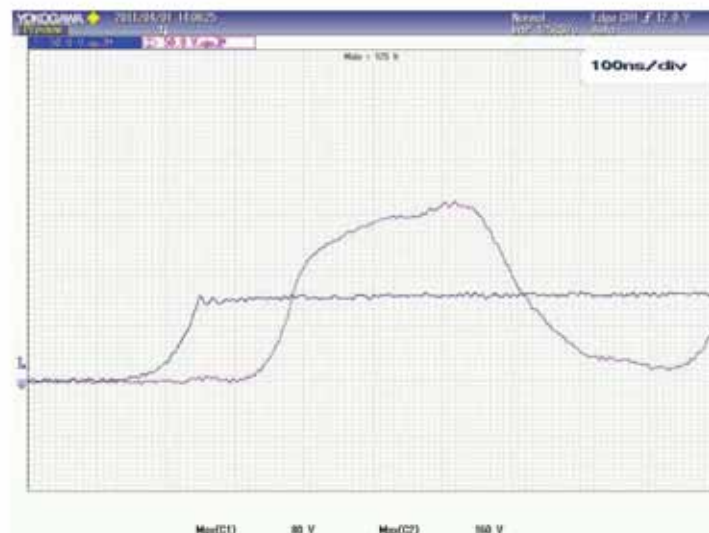


Figure 8.16. Oscillograms of voltage at apparatus to be protected: CH1 voltage on the SPD terminals, CH2 voltage on the load; impulse voltage wave shape 0,25/50  $\mu$ s;  $U_p = 80$  V; resistive load,  $R = 10^6 \Omega$ ; line length  $d = 30$  m.



Figure 8.17. Oscillograms of voltage at apparatus to be protected: CH1 voltage on the SPD terminals, CH2 voltage on the load; impulse voltage wave shape 0,25/50  $\mu$ s;  $U_p = 100$  V; resistive load,  $R = 10^6 \Omega$ ; line length  $d = 30$  m.

The summary of results of voltage peak values are reported in Tab. 8.14.

Table 8.14. Measured values of voltage on the SPD terminals and at apparatus to be protected for  $R = 10^6 \Omega$  load condition, connecting leads  $d = 30$  m and voltage shape 0,25/50  $\mu$ s

$U_p$ (V)	$U_1$ (V)	$\Delta U$ (V)	$\Delta U / U_p$ (%)
40	79,5	39,6	99
80	160	80	100
100	194	94	94

The SPDs used in tests create a new three range of voltage determined by  $U_p$ . However it is possible to notice an effect of SPDs during the front of stressing overvoltage. This situation is caused of the wave shape used in tests where the peak value of voltage is equal 400 V. The results presented in Tab. 8.14 show that the steepness of stressing overvoltage in each case has the same value and allow to obtain a value of voltage equal  $2 U_p$  on the apparatus terminals.

The analyses performed in this paragraph show that the analogies between low-voltage power and signal systems lightning protection exist. Also in the case of signal systems, a proper installation of SPDs has an impact on their effectiveness. The worst case in terms of protection consists of fast front source e.g. due to subsequent negative flashes, where the voltage may be doubled at load terminals in a dozen of meters due to oscillation phenomena. Voltage increment depends on the steepness of stressing overvoltage and on the characteristics of connecting leads.



## 8.4. Influence of load conditions on apparatus protection by means of SPD

### 8.4.1. Introduction

The voltage surges incoming to the structure circuits through the SPD from external lines are reduced but at the end of the circuit they may again significantly increase. The surge increment along the circuit depends on the length of the circuit as shown in previous paragraph and chapter 6, but the influence of the electrical parameters ( $R$ ,  $L$ ,  $C$ ) of the apparatus to be protected is not well recognized [143].

The present paragraph deals with influence of apparatus to be protected on SPD selection. This problem is particular important in case of differential mode of SPD application. In this case the proper selection of protection level of SPD to be applied ( $U_p$ ) depends not only on the parameters of the SPD and phenomena appearing in the circuit between first SPD and the apparatus to be protected (see chapter 6), but also on the transient characteristic of apparatus to be protected. In Fig. 8.18 simple example of industrial photovoltaic power generation system is shown.

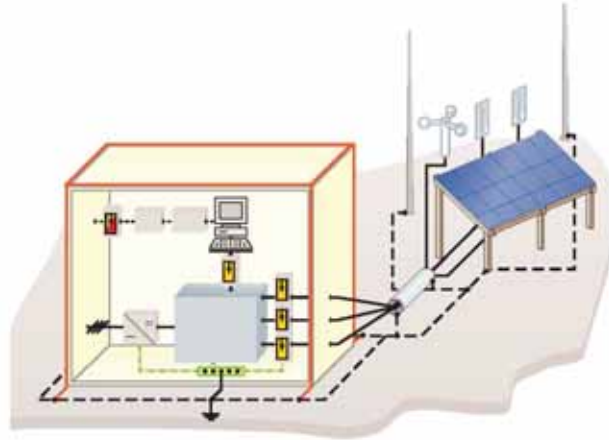


Figure 8.18. Simple example of industrial photovoltaic power generation system and relevant control centre [90].

It is to note that within a control centre structure different apparatus can be placed. This group of apparatus in a basic case consists of inverter and computer. However in real situations, this group of apparatus is much more complex. An example is given in Fig. 8.19.

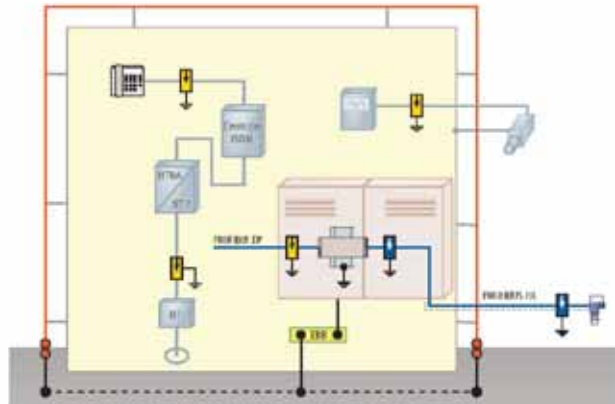


Figure 8.19. Example of apparatus placed within a control centre of industrial photovoltaic power generation system [90].

Each apparatus has different transient characteristics, which can be expressed by concentrated parameters like  $R$ ,  $L$ ,  $C$  or their combination.

The summary of computer simulations results are given in the following paragraph.

#### 8.4.2. Results of computer simulations

The considered basic arrangement is shown in Fig. 8.20 and it is simulated by means of EMTP-RV. For the investigation the impulse current wave shape 0,25/100  $\mu$ s is taken into account. Five types of load are simulated, namely: resistive ( $R$ ), inductive ( $L$ ), capacitive ( $C$ ) and combined ( $RC$ ) and ( $RLC$ ). The distance between SPD and apparatus to be protected is assumed  $d = 10$  m.

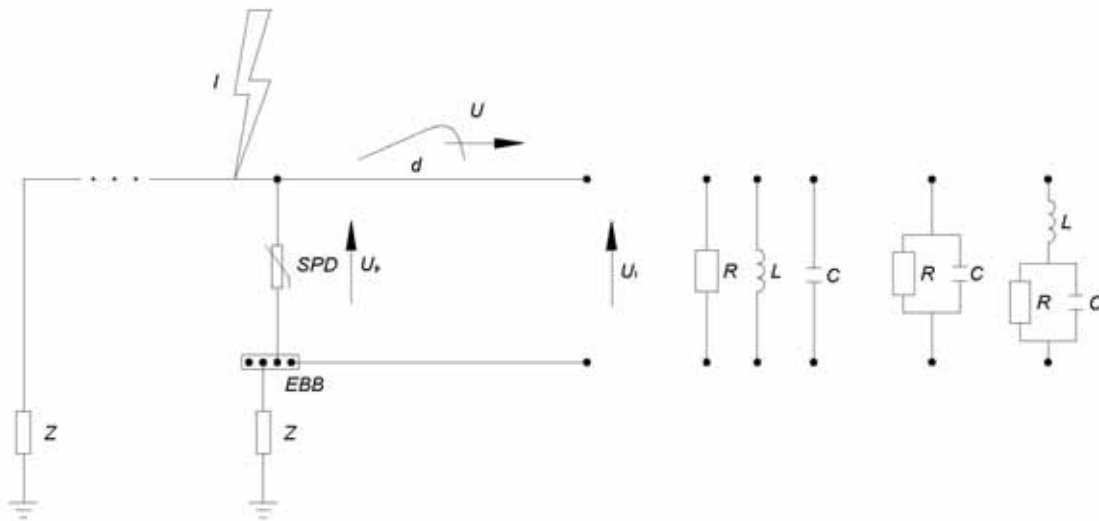


Figure 8.20. Schematic representation of basic analysed arrangement.

On the base of simulations it is stated that in the case of every apparatus there are such circuit parameters (distance  $d$  and  $R$ ,  $L$ ,  $C$  values) at which the stressing voltages may oscillate around the values of SPD residual voltage.

Some results obtained are reported in Fig. 8.21 for  $R$  load, in Fig. 8.22 for  $L$  load, in Fig. 8.23 for  $C$  load, in Fig. 8.24 for  $R$ - $C$  load and in Fig. 8.25 for  $R$ - $L$ - $C$  load.



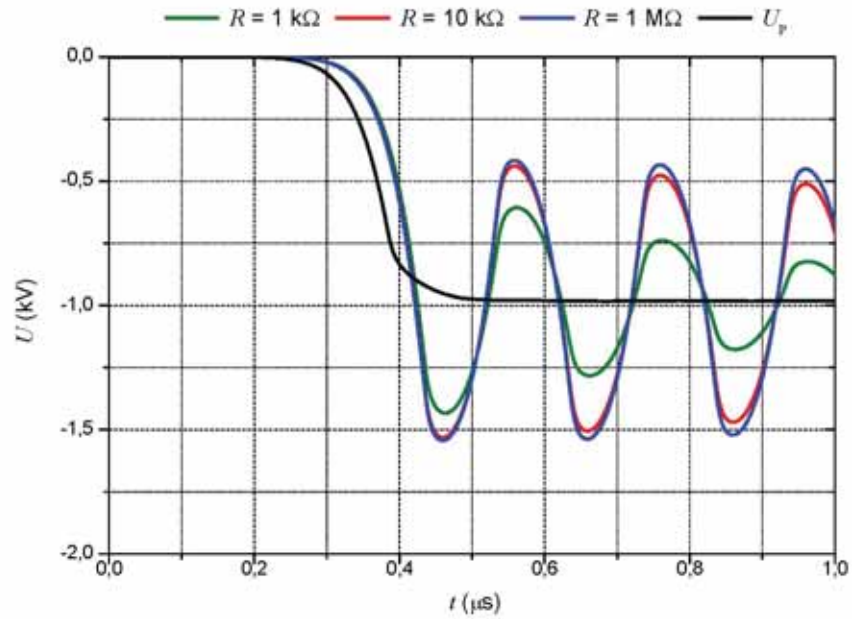


Figure 8.21. Oscillograms of voltage on the SPD terminals and apparatus to be protected for different  $R$  load conditions for impulse current wave shape  $0,25/100 \mu\text{s}$  and  $d = 10 \text{ m}$ .

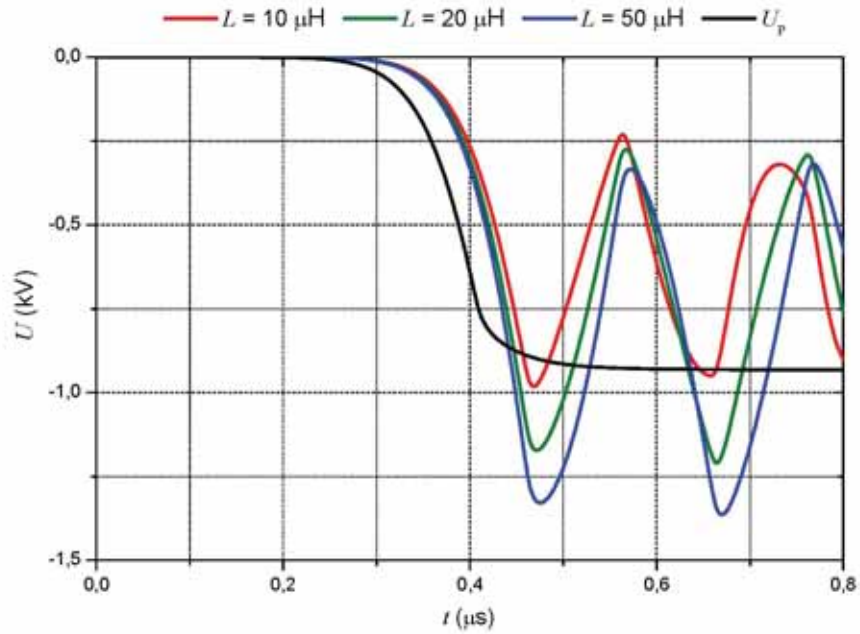


Figure 8.22. Oscillograms of voltage on the SPD terminals and apparatus to be protected for different  $L$  load conditions for impulse current wave shape  $0,25/100 \mu\text{s}$  and  $d = 10 \text{ m}$ .

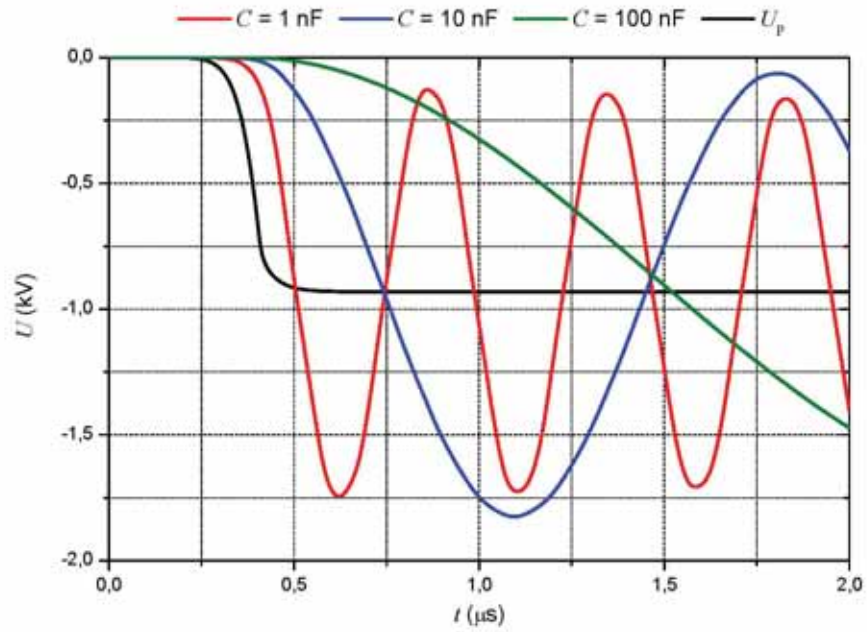


Figure 8.23. Oscillograms of voltage on the SPD terminals and apparatus to be protected for different  $C$  load conditions for impulse current wave shape  $0,25/100 \mu\text{s}$  and  $d = 10 \text{ m}$ .

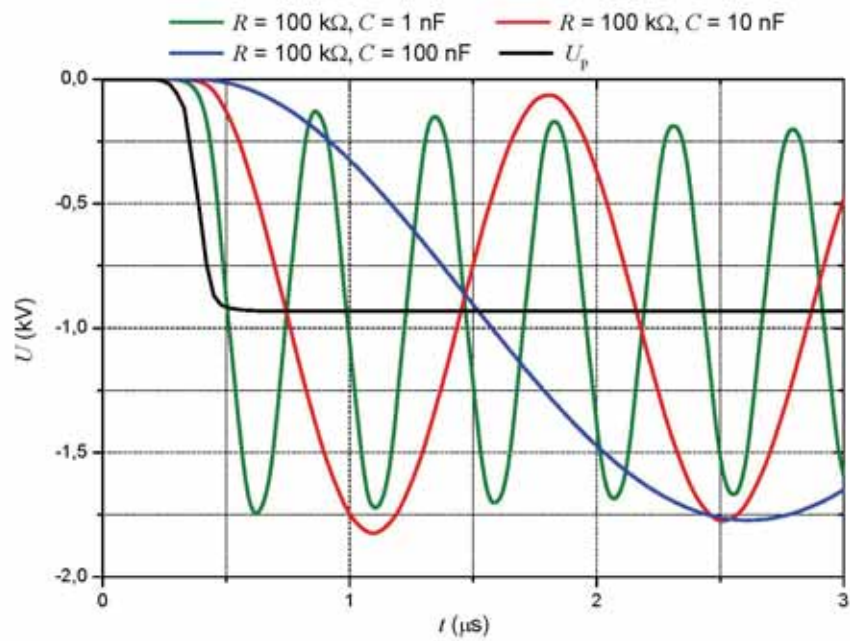


Figure 8.24. Oscillograms of voltage on the SPD terminals and apparatus to be protected for different  $R-C$  load conditions for impulse current wave shape  $0,25/100 \mu\text{s}$  and  $d = 10 \text{ m}$ .

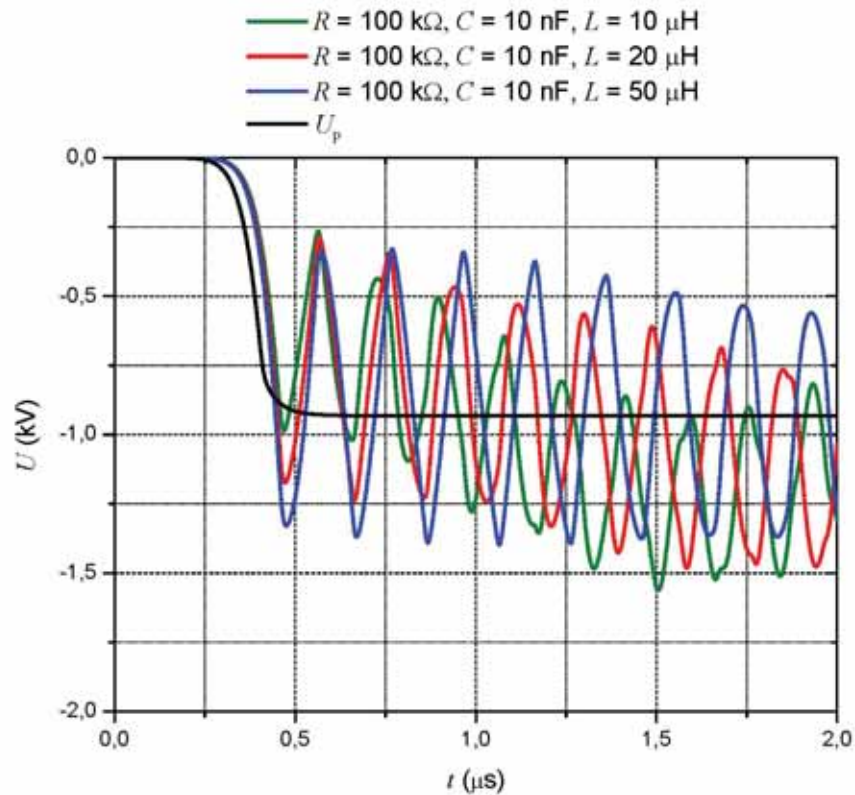


Figure 8.25. Oscillograms of voltage on the SPD terminals and apparatus to be protected for different  $R$ - $L$ - $C$  load conditions for impulse current wave shape  $0,25/100 \text{ }\mu\text{s}$  and  $d = 10 \text{ m}$ .

The results show that in the case of inductive load the surge is immediately doubled and then decreases exponentially to zero. Small parallel resistance may limit the possibility of surge doubling on the inductance. In the case of capacitive load the surge is lowered to zero and then it increases exponentially to doubled value. Small parallel resistance may limit significantly the resulting voltage value. In the case of load combined by series inductance and parallel capacitance the surge on such load is oscillating around the double value and at very high frequency may reach quaternary value. Small parallel resistance may significantly reduce these values.

## 8.5. Influence of parallel consumers on SPD protection features

### 8.5.1. Introduction

In real cases the electrical installation of PVGS can have a complex form. The number of internal circuit as well as external customers can be diversified. An example of PVGS installation is shown in Fig. 8.26.

In present paragraph the influence of parallel consumers on SPD protection features is analysed. For this aim a simple equation (8.27) is used.

$$k = \frac{U_1}{U_{I(N=0)}} \quad (8.27)$$

where:

$k$  – reduction factor;

$U_1$  – voltage on the terminals of apparatus to be protected;

$U_{I(N=0)}$  – voltage on the terminals of apparatus to be protected, without any external circuit.

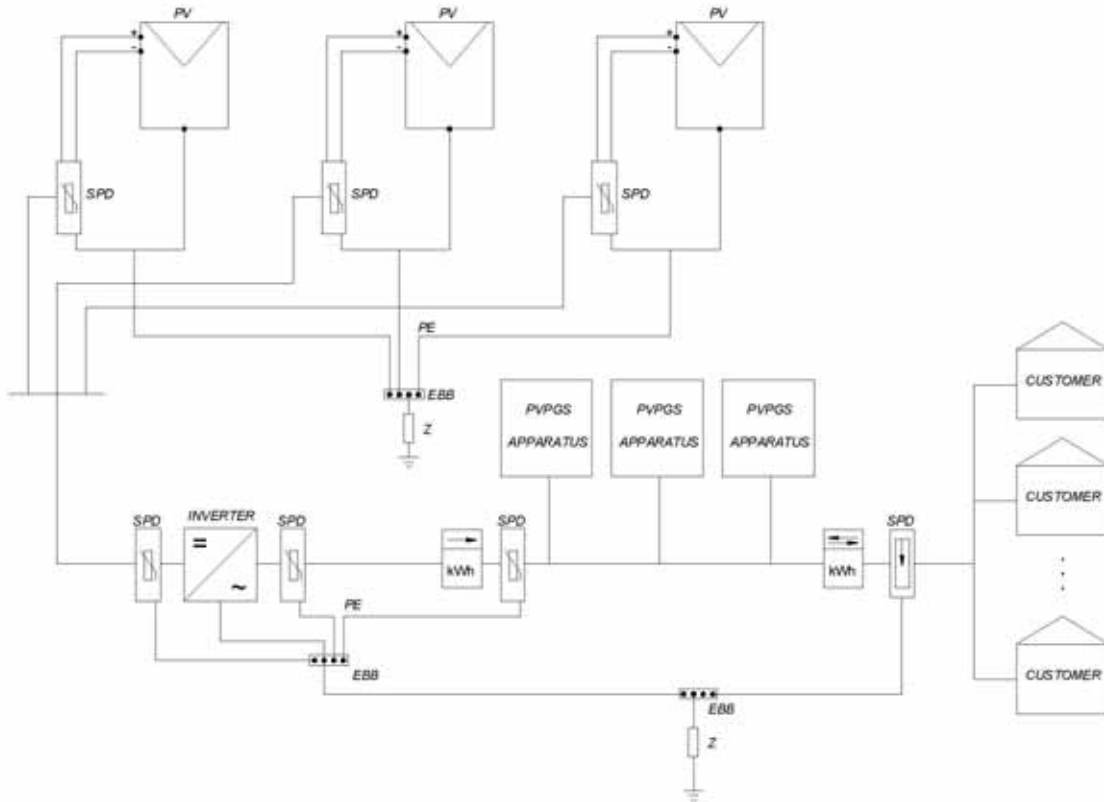


Figure 8.26. Example of PVGS installation.

### 8.5.2. Results of computer simulations

For the investigation two circuit configurations are analysed as shown in Fig. 8.27 and in Fig. 8.30. In both cases the source of damage S3 is taken into account.

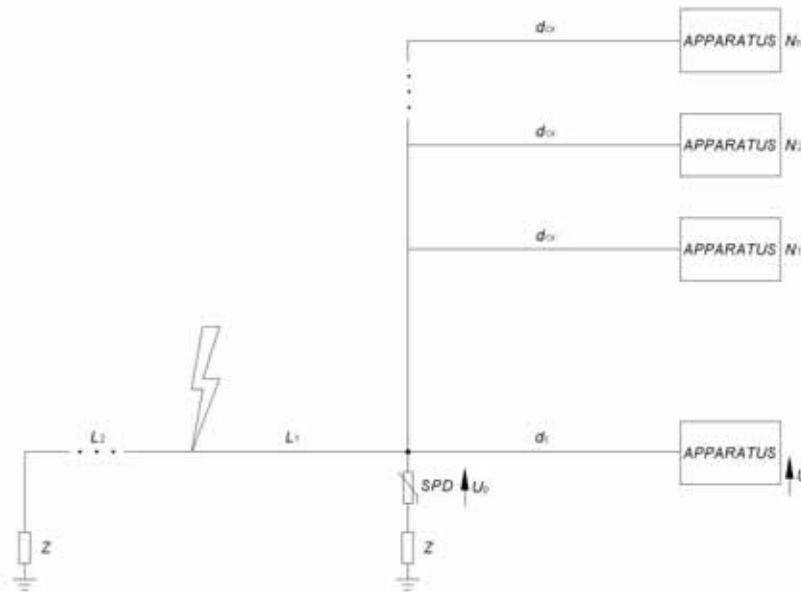


Figure 8.27. Basic configuration of analysed arrangement.

In Fig. 8.28 the summary of analyses for the first case schematic represented in Fig. 8.27, without an SPD installed in a main node is shown. The presented results are obtained for length of external line  $L_2 = \infty$ , striking point distance to the entry point  $L_1 = 50$  m, distance between SPD and apparatus to be protected  $d_c = 50$  m and two lengths of connected external parallel consumers, namely  $d_{ex} = 50$  m and  $d_{ex} = 500$  m.

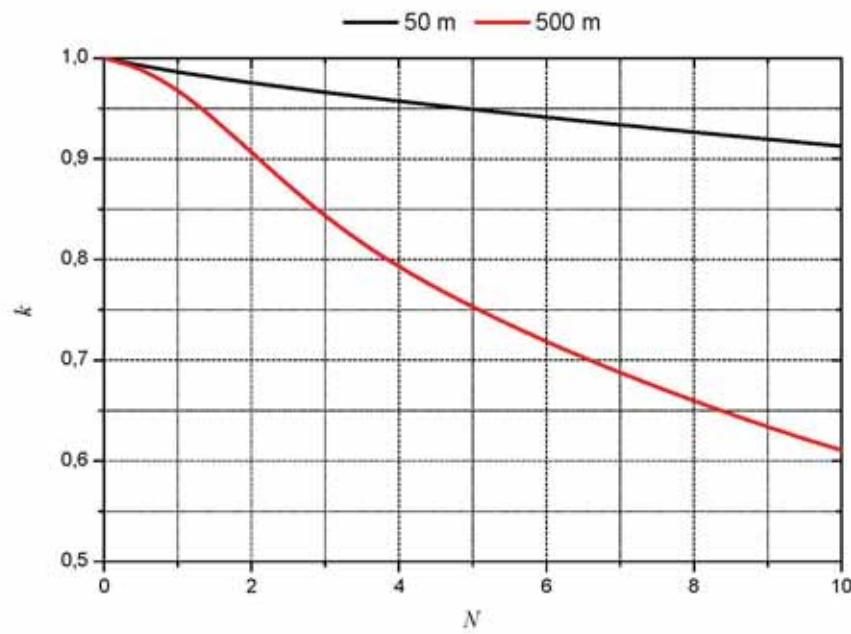


Figure 8.28. Reduction factor  $k$  for a case without SPD in the main node, as a function of number of external connected circuits:  $d_{ex} = 50$  m and  $d_{ex} = 500$  m.

On the base of results presented in Fig. 8.28, it is to observe that in this case without any protection applied in the main point, the number as well as the length of external circuits has an influence on the overvoltage reduction factor.



The results of similar case (Fig. 8.27), but with SPD installed in the main node are presented in Fig. 8.29.

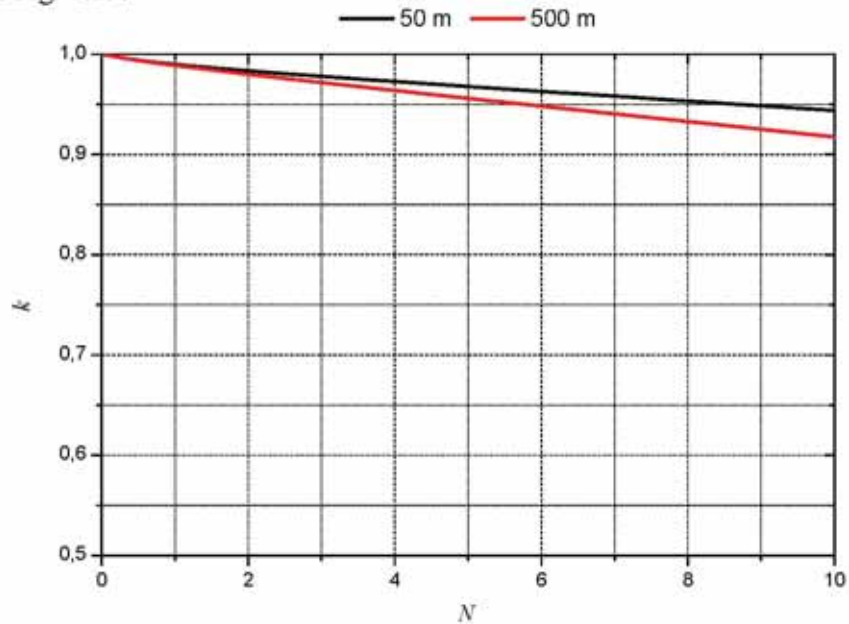


Figure 8.29. Reduction factor  $k$  for a case with SPD installed in the main node, as a function of number of external connected circuits:  $d_{cx} = 50$  m and  $d_{cx} = 500$  m.

The results shown in Fig. 8.514, demonstrated that, the number as well as the length of external connected circuits is no significant influence on reduction factor  $k$ . Moreover further analyses shown that the striking point of lightning flash (e.g.  $L_1 = 1000$  m) is quite no influence on obtained results.

In Fig. 8.30 basic complex configuration of analysed arrangement formed by  $N$  consumers connected in different points is shown. For the investigations and calculations of factor  $k$ , the case without SPD installed in the main node and following parameters are assumed:  $L_4 = \infty$ ,  $L_3 = 50$  m,  $L_2 = 1000$  m,  $L_1 = 1000$  m,  $d_c = 500$  m,  $d_{cx} = 500$  m.

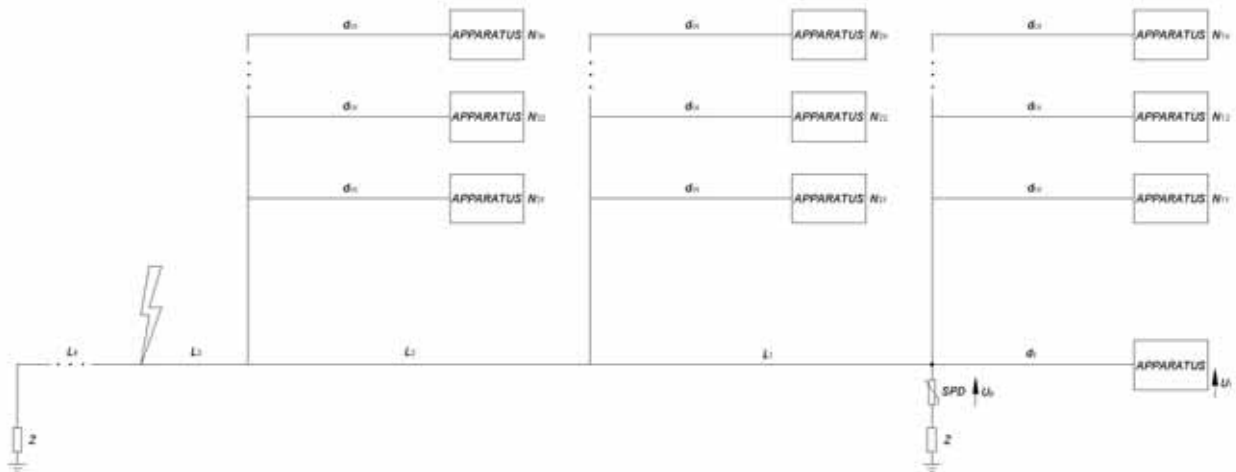


Figure 8.30. Basic complex configuration of analysed arrangement.



Obtained results are summarized in Tab 8.15 and for the basic case are shown in Fig. 8.31.

Table 8.15. Reduction factor  $k$ , in case of  $L_4 = \infty$ ,  $L_3 = 50$  m,  $L_2 = 1000$  m,  $L_1 = 1000$  m,  $d_c = 500$  m,  $d_{ex} = 500$  m for different configuration of connected circuit.

Circuit configuration				$k$
Case	$N_1$	$N_2$	$N_3$	
Basic	0	0	0	1
	10	0	0	0,59
	20	0	0	0,45
	30	0	0	0,36
A	0	10	0	0,67
B	10	10	0	0,49
C	0	0	10	0,72
D	10	0	10	0,54
E	0	10	10	0,51
F	10	10	10	0,47

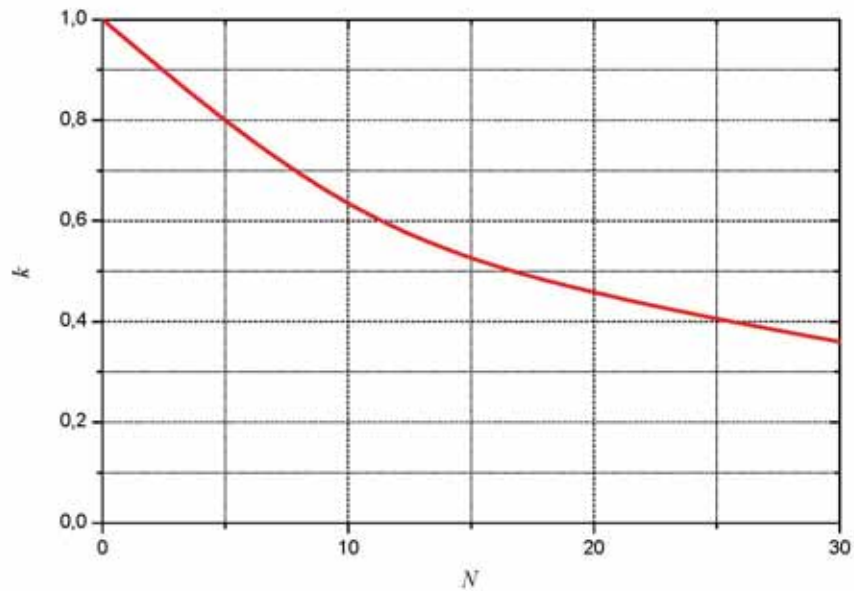


Figure 8.31. Reduction factor  $k$ , in case of  $L_4 = \infty$ ,  $L_3 = 50$  m,  $L_2 = 1000$  m,  $L_1 = 1000$  m,  $d_c = 500$  m,  $d_{ex} = 500$  m as a function of number of external connected circuits for different configuration of connected circuit (basic case of Tab. 8.15).

## 8.6. Grounding conditions influence on apparatus protection by means of SPD

### 8.6.1. Resistive coupling for an extended earth arrangement

In the present paragraph the influence of grounding conditions on apparatus to be protected by means of SPD is recognized.

Fig. 8.32 illustrates the case where the apparatus to be protected is earthed at an EBB different from the main bonding bar at which the SPD1, installed at the line entry point into the structure (main switch board) for the protection of distant apparatus, is connected. In such case if the linear dimensions of the earth arrangement extend more than 10 m (e.g. earthing arrangement of type B according to the IEC/EN standard 62305-3), the equipotentialization of apparatus to be protected (inverter) is not sure.

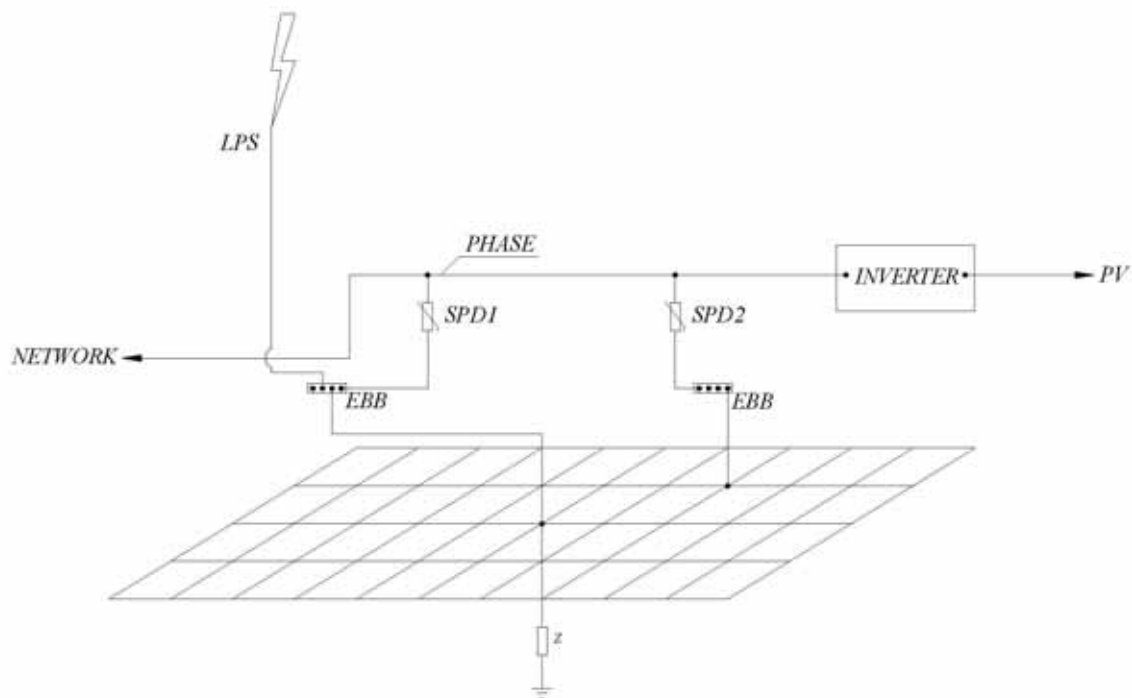


Figure 8.32. Diagram of circuit to supply an apparatus and the loop formed by PE, phase conductors and two SPDs bonded to an extended earth arrangement (type B according to IEC/EN 62305-3).

The flowing of the lightning current to earth gives rise to a common-mode voltage ( $U_0$ ) on the apparatus to be protected ( $U_1$ ); the value of the voltage is such that it is necessary to install an appropriate SPD at the secondary distribution board (SPD2), where the apparatus is connected. The influence of distance ( $L$ ) between point of injection and apparatus to be protected on the ratio  $k = U_1 / U_0$  for different soil resistivity is shown in Fig. 8.33.

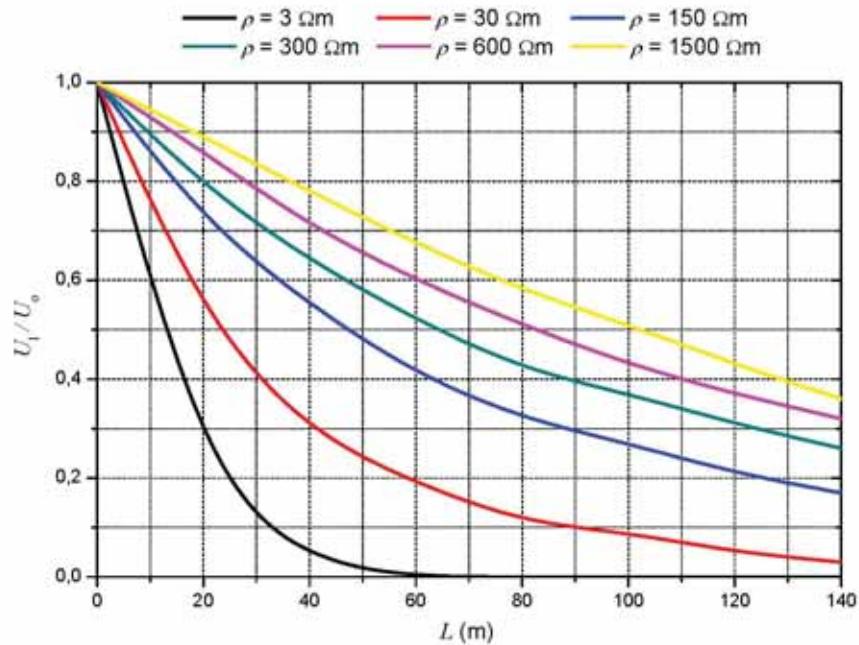


Figure 8.33. Reduction factor ( $k = U_1 / U_0$ ) in a meshed grounding network as a function of the distance  $L$  between the injection point of the lightning current and the point of installation of apparatus to be protected.

In fact the earth-termination voltage  $U_0 = Z I_G$  due to the lightning current  $I_G$  injected into the earthing arrangement of conventional earthing impedance  $Z$  may stress the apparatus in spite of the installed SPD1.

In such condition an SPD2 should be installed at the secondary switch board (or at the apparatus terminals) in order to limit such overvoltage transmitted by resistive coupling. For the correct dimensioning of SPD2 the amplitude and shape of the current  $I_{SPD2}$  flowing through the SPD2 should be known.

The extended earth termination arrangements (e.g. ring electrodes, meshed systems, type B according to the IEC/EN standard 62305-3) are usually dimensioned in order to have a conventional earth impedance of  $Z \sim 10 \Omega$  for lightning current of positive flash 10/350  $\mu\text{s}$  and for the current values associated to LPL I. To obtain such value their radial dimensions increase as the soil resistivity  $\rho$  is increasing (Fig. 8.33). With such dimension the conventional earthing impedance  $Z$  for lightning current of negative subsequent strokes (0,25/100  $\mu\text{s}$ ) associated to LPL I may reach some tents of Ohm.

In all cases, the highest values of  $I_{SPD2}$  and the associated charge  $Q_{SPD2}$  are obtained for the positive flashes as shown in Fig. 8.34.

The charge  $Q_{SPD2}$  for unit of current is increasing with the soil resistivity  $\rho$  but for  $\rho < 2000 \Omega\text{m}$  is always less than the value of 0,5 C/kA associated to the standard current shape 10/350  $\mu\text{s}$  as demonstrated in Fig. 8.35.

As consequence an SPD2 of test class I should be installed, the reference parameter for the selection of their discharge current is the current  $I_{SPD2}$  and not the charge  $Q_{SPD2}$ .

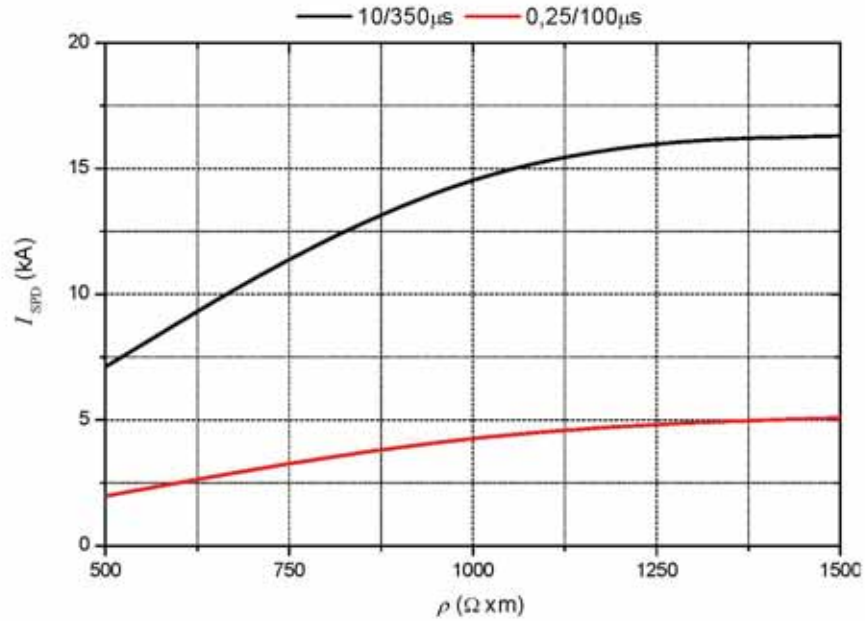


Figure 8.34. Extended earth arrangement - current  $I_{SPD}$  flowing in the circuit with two SPDs due to resistive coupling as the resistivity of soil varies. Assumptions: type B earth arrangement (IEC/EN 62305-3), network configuration 10 x 10 m; lightning current of LPLI injected in the centre of network; apparatus bonded at corner of the network.

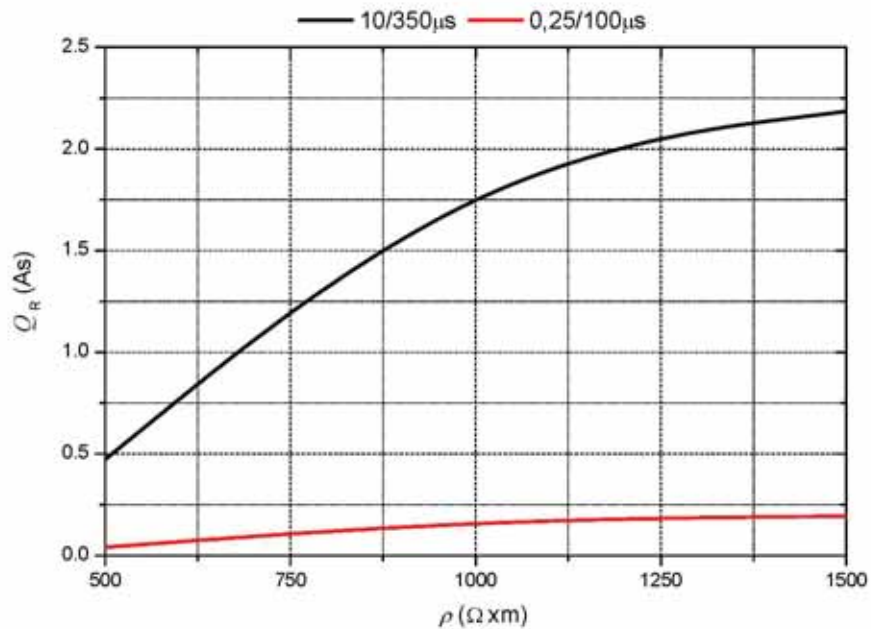


Figure 8.35. Extended earth arrangement - charge  $Q_{SPD}$  associated to the current  $I_{SPD}$  due to resistive coupling as the resistivity of soil varies. Assumptions: type B earth arrangement (IEC/EN 62305-3), network configuration 10 x 10 m; lightning current of LPLI injected in the centre of network; apparatus bonded at corner of the network.



### 8.6.2. Bonding conditions for control and measurement apparatus protection

The aim of paragraph is to investigate the typical problems of selection and installation of an SPD class II test, which can affect its effectiveness. For this investigation a real arrangement of an electric system within a structure is considered (Fig. 8.36) and the schematic electric circuit of such arrangement (Fig. 8.37) is reproduced in laboratory where several tests are performed. Special focus is addressed to ascertain the influence of circuit configuration, especially bonding connection on apparatus to be protected. The influence of different types of apparatus represented by constant parameters ( $R$ ,  $L$ ,  $C$ ) is also investigated.

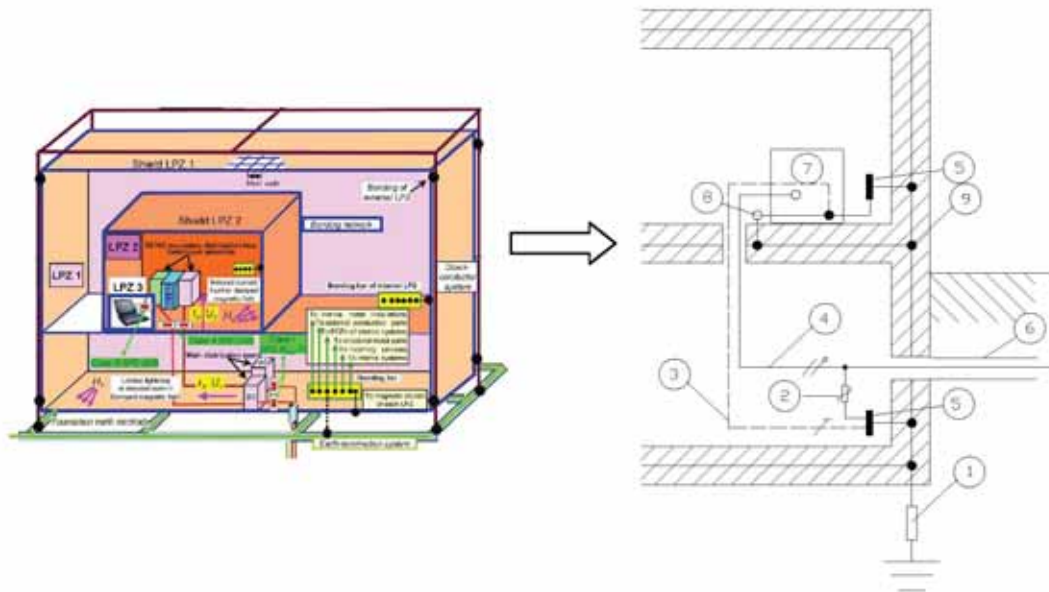


Figure 8.36. Example of electrical system in a structure: 1 – conventional earthing impedance; 2 – surge protective device (SPD); 3 – PE conductor; 4 – power line; 5 – equipotential bonding bar, 6 - common inlet for different services; 7 – apparatus to be protected; 8 - bonding joint; 9 – steel reinforcement in concrete (with superimposed mesh conductors).

A sensitive apparatus (7) is installed in an upper floor within a steel reinforced concrete structure and bonded directly to the steel reinforcement in concrete (9) at the floor level and through the PE conductor (3) at equipotential bonding bar (5) of the switch board. In the same figure is shown also earth impedance (1); surge protective device (2); low voltage feeder (4); common inlet for different services (6) and bonding joint (8).

The schematic circuit in order to reproduce in laboratory the real arrangement is reported in Fig. 8.37, where it is shown the impulse voltage generator ( $G$ ), the typical low-voltage limiting SPD, the conductors of length  $d$  leading the SPD and apparatus to be protected and some different loading elements like resistive ( $R$ ), inductive ( $L$ ) and capacitive ( $C$ ) simulating different input impedance of real apparatus like filters, PC, etc. It is assumed that the resistive part ( $R_c$ ) of the impedance of the considered bonding conductors is prevalent.

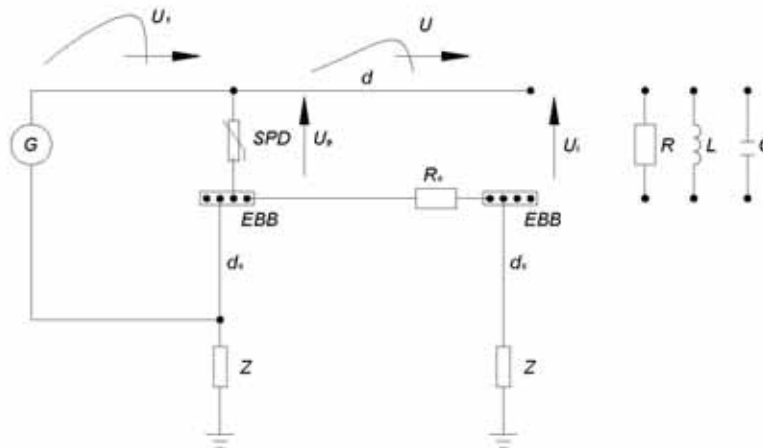


Figure 8.37. Schematic illustration of reproduced arrangement in laboratory:  $G$  - impulse voltage generator;  $U_1$  - surge voltage;  $EBB$  - equipotential bonding bar;  $R_c$  - PE conductor resistance;  $d_c$  - length of conductors connecting EBB and earthing system;  $Z$  - conventional earthing impedance; SPD - surge protective device;  $U_p$  - voltage on the SPD terminals;  $d$  - line length;  $U$  - overvoltage incoming through distant SPD;  $R$  - resistive load;  $L$  - inductive load;  $C$  - capacitive load;  $U_1$  - voltage on the terminals of apparatus to be protected.

### Analyses of bonding condition for resistive load

As suggested in Fig. 8.36 and sketched in Fig. 8.37 the apparatus can be bonded by several points. In the case under consideration the apparatus is connected to the switch board EBB by PE conductor and to the local EBB directly connected to the steel reinforcement of concrete.

The influence of bonding conditions in the case of open end circuit is analysed. Tests are performed with different values of PE conductor equivalent resistance  $R_c = 0 \Omega$ ,  $100 \Omega$  and  $10^6 \Omega$  with a fixed distance  $d = 30\text{m}$  and with two types of stressing overvoltage  $0,25/50 \mu\text{s}$  and  $1,2/50 \mu\text{s}$ .

In Fig. 8.38 and 8.39 the results for  $1,2/50 \mu\text{s}$  stressing wave shape are shown.

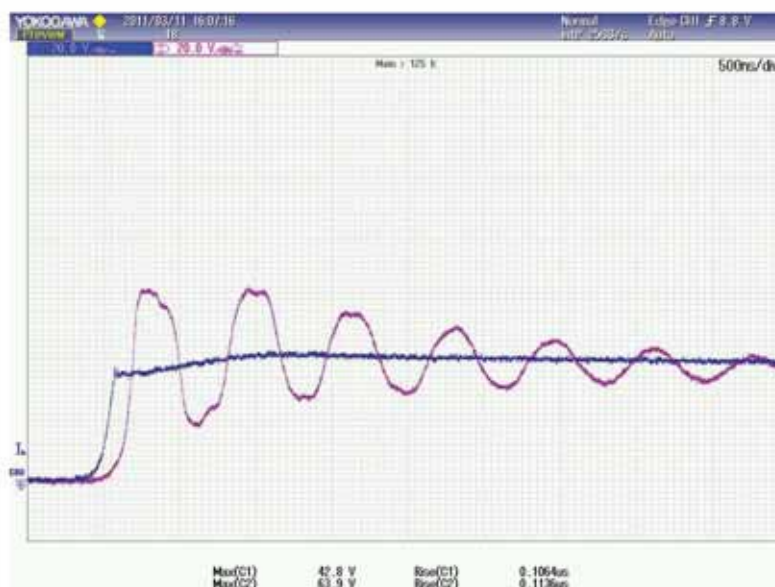


Figure 8.38. Oscillograms of voltage at apparatus to be protected: CH1 voltage on the SPD terminals, CH2 voltage on the load; impulse voltage wave shape  $1,2/50 \mu\text{s}$ ; resistive load  $R = 10^6 \Omega$ ;  $R_c = 0 \Omega$ ; line length  $d = 30\text{m}$ .



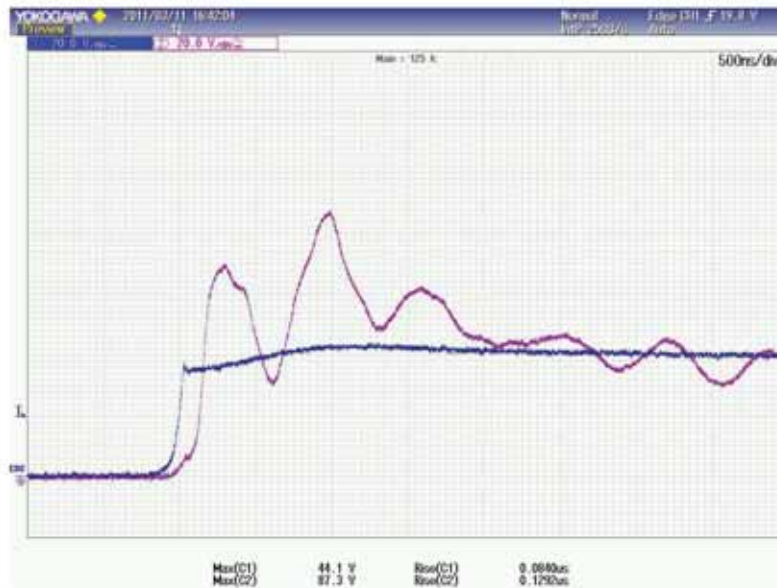


Figure 8.39. Oscillograms of voltage at apparatus to be protected: CH1 voltage on the SPD terminals, CH2 voltage on the load; impulse voltage wave shape  $1,2/50 \mu\text{s}$ ; resistive load  $R = 10^5 \Omega$ ;  $R_c = 10^6 \Omega$ ; line length  $d = 30 \text{ m}$ .

In Fig. 8.40, 8.41 and 8.42 the results for stressing overvoltage  $0,25/50 \mu\text{s}$  are shown.

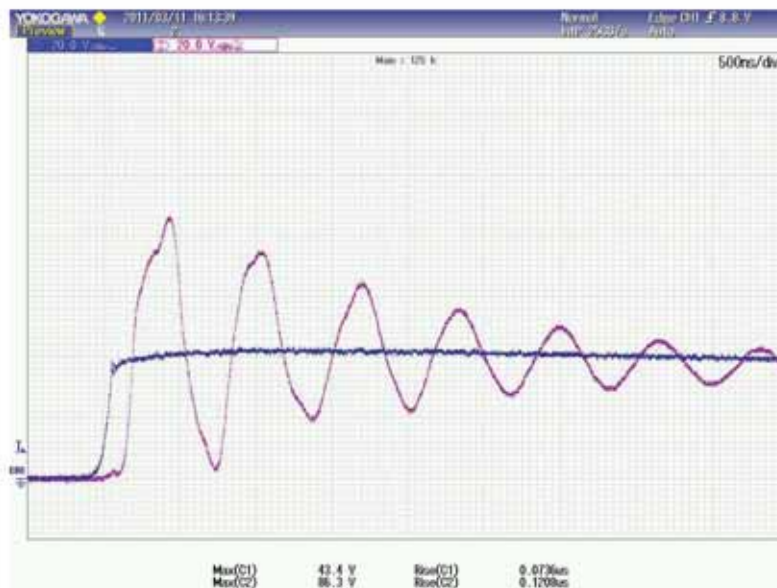


Figure 8.40. Oscillograms of voltage at apparatus to be protected: CH1 voltage on the SPD terminals, CH2 voltage on the load; impulse voltage wave shape  $0,25/50 \mu\text{s}$ ; resistive load  $R = 10^5 \Omega$ ;  $R_c = 0 \Omega$ ; line length  $d = 30 \text{ m}$ .

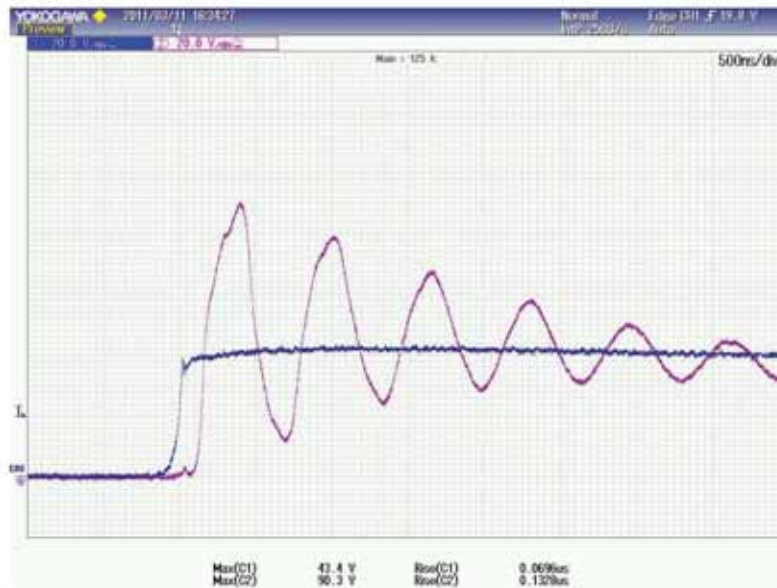


Figure 8.41. Oscillograms of voltage at apparatus to be protected: CH1 voltage on the SPD terminals, CH2 voltage on the load; impulse voltage wave shape  $0,25/50 \mu\text{s}$ ; resistive load  $R = 10^6 \Omega$ ;  $R_c = 100 \Omega$ ; line length  $d = 30 \text{ m}$ .

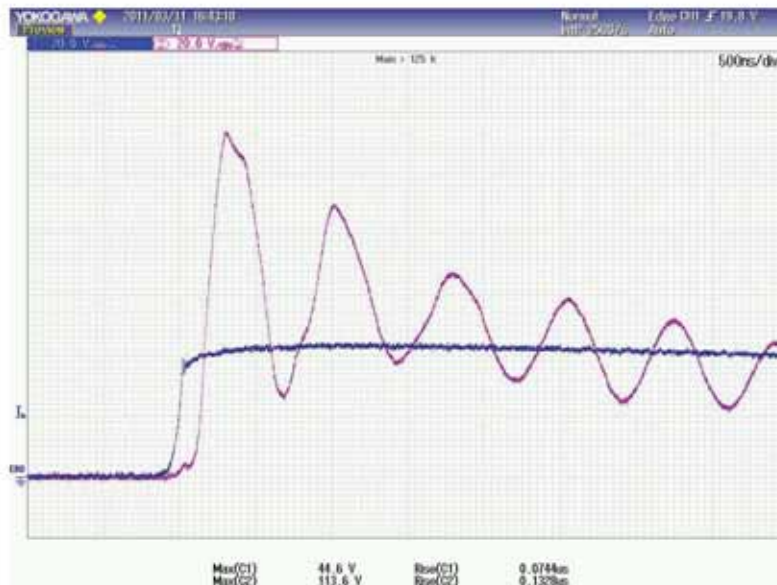


Figure 8.42. Oscillograms of voltage at apparatus to be protected: CH1 voltage on the SPD terminals, CH2 voltage on the load; impulse voltage wave shape  $0,25/50 \mu\text{s}$ ; resistive load  $R = 10^6 \Omega$ ;  $R_c = 10^6 \Omega$ ; line length  $d = 30 \text{ m}$ .

According to the best practice if PE conductor has negligible resistance ( $R_c = 0 \Omega$ ) the expected voltage at the apparatus is less or equal to the double of SPD protection level, according to the rise time of the incoming surge and distance  $d$ .

If the PE conductor is bad connected (simulated by  $R_c = 100 \Omega$ ) or disconnected ( $R_c = 1 \text{ M}\Omega$ ), the voltage at the apparatus terminals may exceed even  $2 U_p$ .

### Analyses of bonding condition for inductive load

In this section results are presented of simulations performed with the same conditions as above for open circuit (resistive load) but connecting the phase conductor and PE to an inductive load of  $L = 5$  mH.

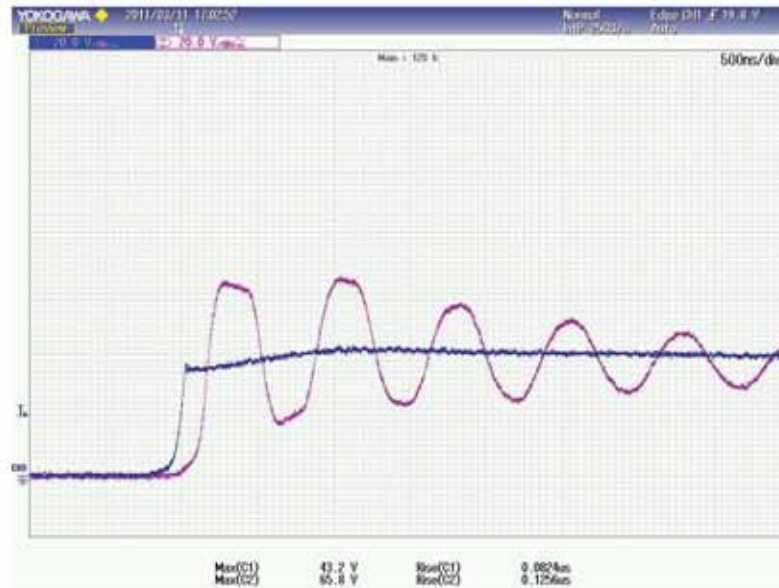


Figure 8.43. Oscillograms of voltage at apparatus to be protected: CH1 voltage on the SPD terminals, CH2 voltage on the load; impulse voltage wave shape 1,2/50  $\mu$ s; inductive load  $L = 5$  mH;  $R_c = 0 \Omega$ ; line length  $d = 30$  m.

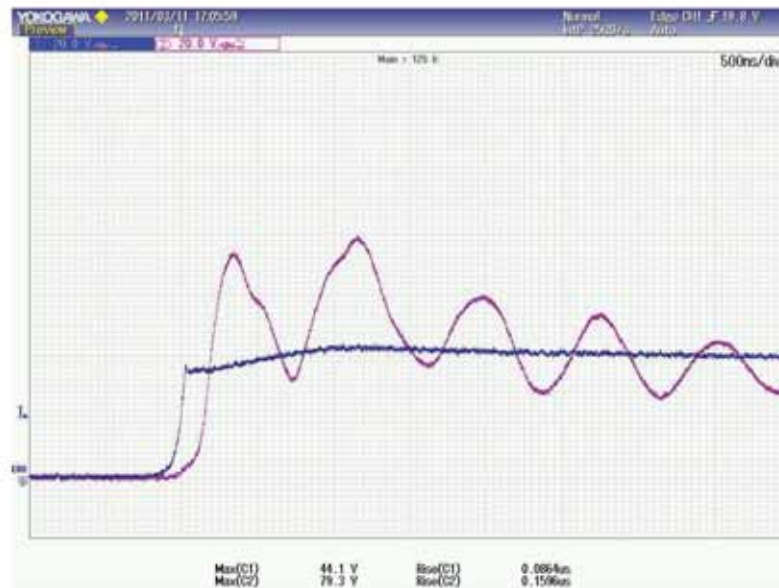


Figure 8.44. Oscillograms of voltage at apparatus to be protected: CH1 voltage on the SPD terminals, CH2 voltage on the load; impulse voltage wave shape 1,2/50  $\mu$ s; inductive load  $L = 5$  mH;  $R_c = 10^6 \Omega$ ; line length  $d = 30$  m.

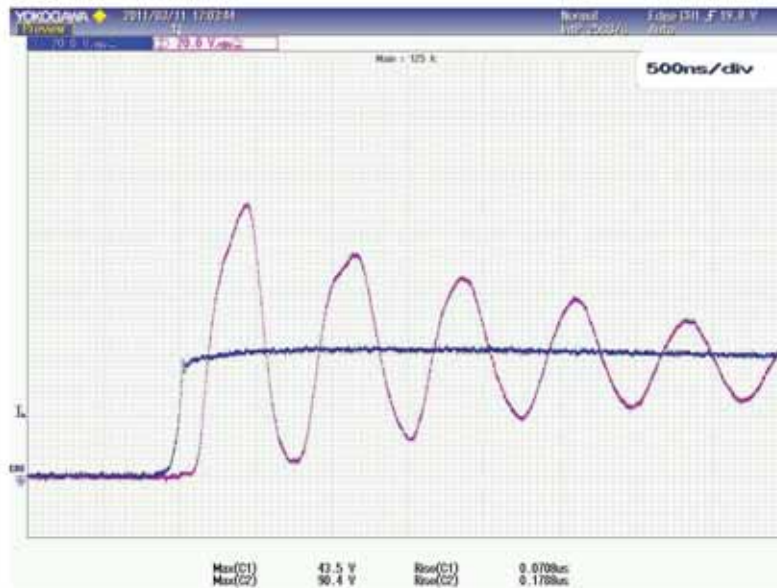


Figure 8.45. Oscillograms of voltage at apparatus to be protected: CH1 voltage on the SPD terminals, CH2 voltage on the load; impulse voltage wave shape  $0,25/50 \mu\text{s}$ ; inductive load  $L = 5 \text{ mH}$ ;  $R_c = 0 \Omega$ ; line length  $d = 30 \text{ m}$ .

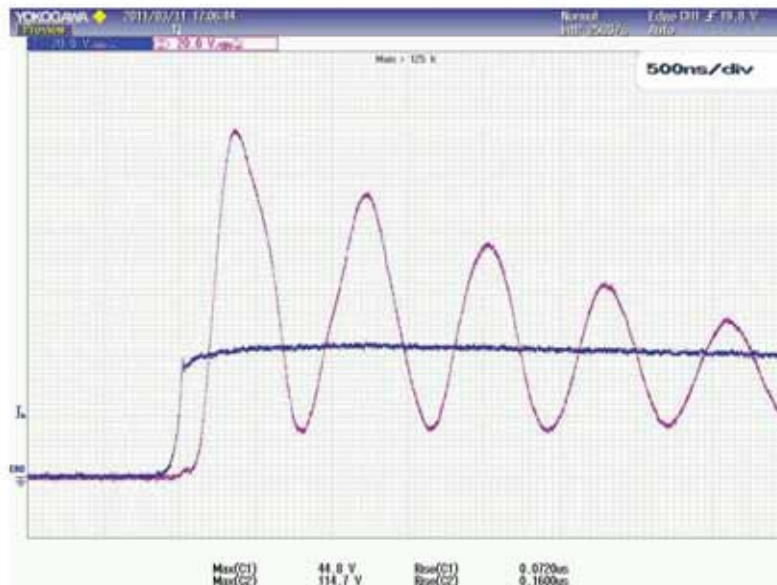


Figure 8.46. Oscillograms of voltage at apparatus to be protected: CH1 voltage on the SPD terminals, CH2 voltage on the load; impulse voltage wave shape  $0,25/50 \mu\text{s}$ ; inductive load  $L = 5 \text{ mH}$ ;  $R_c = 10^6 \Omega$ ; line length  $d = 30 \text{ m}$ .

It is to note that obtained results are in line with open end circuit case as above, at least during the short front time duration of applied surge.



### Analyses of bonding condition for capacitive load

This section is dedicated to the capacitive influence of protected apparatus to the voltage appearing on its terminals, assuming the other conditions equal to the resistance and inductive case. For this aim a capacitive load  $C = 100 \text{ nF}$  is used.

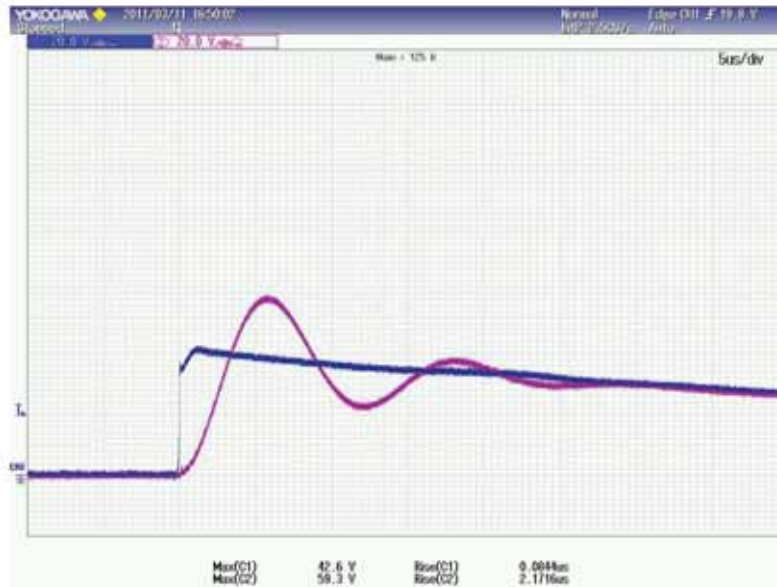


Figure 8.47. Oscillograms of voltage at apparatus to be protected: CH1 voltage on the SPD terminals, CH2 voltage on the load; impulse voltage wave shape 1,2/50  $\mu\text{s}$ ; capacitive load  $C = 100 \text{ nF}$ ;  $R_c = 0 \Omega$ ; line length  $d = 30 \text{ m}$ .

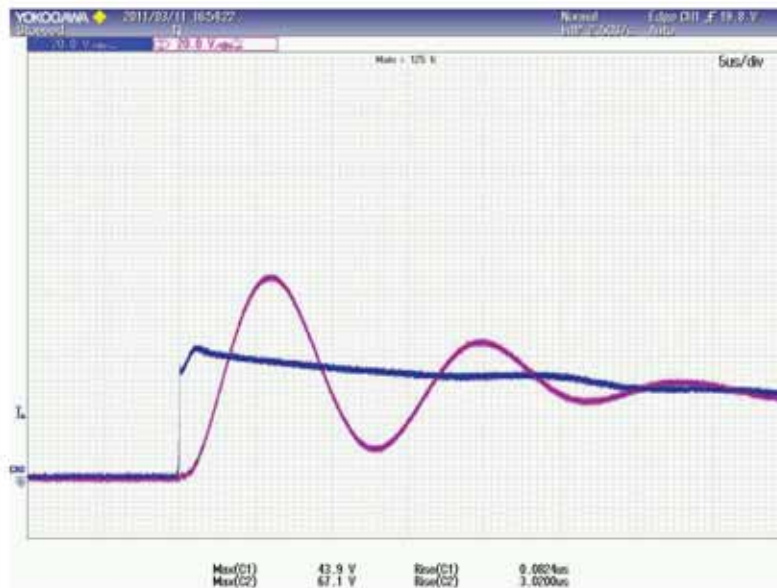


Figure 8.48. Oscillograms of voltage at apparatus to be protected: CH1 voltage on the SPD terminals, CH2 voltage on the load; impulse voltage wave shape 1,2/50  $\mu\text{s}$ , capacitive load  $C = 100 \text{ nF}$ ,  $R_c = 10^6 \Omega$ , line length  $d = 30 \text{ m}$ .



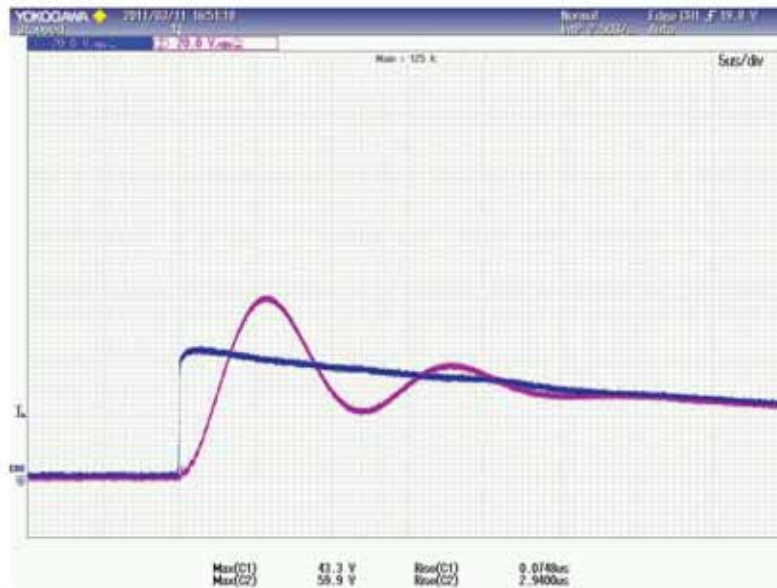


Figure 8.49. Oscillograms of voltage at apparatus to be protected: CH1 voltage on the SPD terminals, CH2 voltage on the load; impulse voltage wave shape 0,25/50  $\mu$ s; capacitive load  $C = 100$  nF;  $R_c = 0 \Omega$ ; line length  $d = 30$  m.

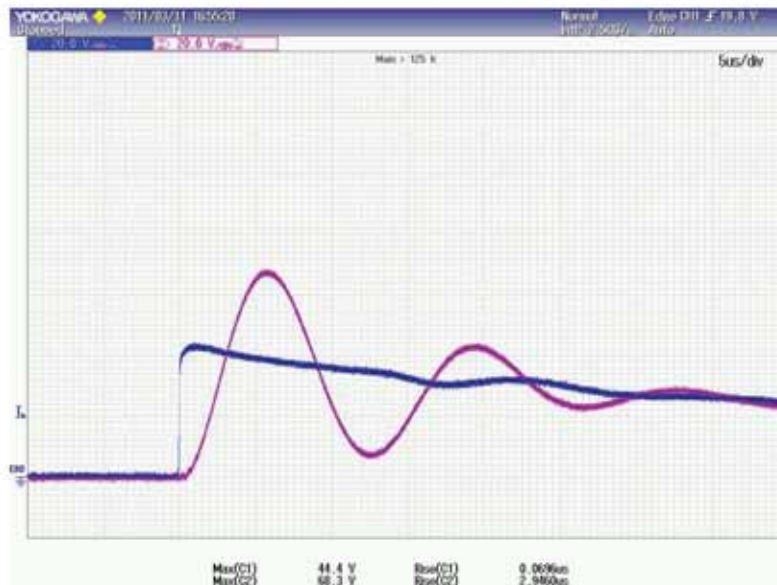


Figure 8.50. Oscillograms of voltage at apparatus to be protected: CH1 voltage on the SPD terminals, CH2 voltage on the load; impulse voltage wave shape 0,25/50  $\mu$ s; capacitive load  $C = 100$  nF;  $R_c = 10^6 \Omega$ ; line length  $d = 30$  m.

The obtained results for capacitive load show that the capacitive character of apparatus has not an influence to exceed the value  $2U_p$ . During the short time of front of surge the capacitance operates a reduction of both the amplitude and steepness of surge. In this case it is seems important to take care about the energetic coordination with the upstream SPD.

The performed tests for  $R$ ,  $L$ ,  $C$  load conditions show that where multi points bonding connection to earth is available for an apparatus within a structure, is important that the PE conductor should have low impedance value in comparison with the other bonding

connections. Unfortunately a not correct designing by under sizing of the PE conductor cross section or a not good routing, may increase the risk of failure of apparatus and the condition suggested by the standard could be not on the safety side. In this case one possibility to reduce the voltage at the apparatus terminals is to adopt a coordinated SPD system where a second SPD should be installed immediately at the apparatus terminals.

### 8.7. Summary

In the present chapter selected aspects of lightning protection for photovoltaic power generation systems are presented.

PVGS from the lightning protection point of view are briefly described. Possible lightning occurrences and fields of disturbance relative to the protected system are shown. Typical components of PVGS are characterized in terms of impulsive withstand voltage ( $U_w$ ). Protection measures recommended by IEC standard and applicable for PVGS are classified and reported.

First investigation intends to present some aspects of risk assessment for PVGS. Two examples of PVGS, namely domestic one and industrial one, with similar characteristic are considered. The performed risk evaluation show that the value of risk of human life is negligible respect to the value of tolerable level suggested by the IEC standard. The selection and installation of protection measures is determined by the risk of economy loss, where  $R_M$  component due to flash near the structure for both cases has dominant value. In this case the lightning risk can be reduced by means of e.g. installation of coordinated SPD system.

Second investigation intends to present some overvoltage protection aspects for acquisition and control unit by means of SPD. The influence of distance between the SPD and apparatus to be protected on protection effectiveness is analysed. The type of connecting leads, SPD protection level as well as stressing overvoltage shape are also considered. The analogies between low-voltage system and signalling systems protection can be concluded.

Third investigation intends to demonstrate load influence on the SPD effectiveness in differential mode of application. The three different type of load, as well as its combination are examined.

Fourth investigation intends to shown the influence of parallel consumer on the SPD selection. The analyses demonstrated that the number and configuration of parallel consumers have no influence on the protection level selection. The number of parallel consumer has an impact on the lightning current division what is examined in chapter 3.

Fifth investigation intends to demonstrate some aspects of grounding system influence on the lightning current transfer due to resistive coupling even if the apparatus to be protected is bonded at the same large grounding network of the LPS.

Sixth investigation intends to show the influence of bonding conditions on control and measurement apparatus protection. The common and differential mode of surge transfer is discussed.

# **Chapter 9**

## 9. Summary and conclusions

In the present thesis selected problems of effective protection for electrical and electronic systems against lightning surges are investigated. Possible surges as sources of damage for sensitive systems are classified and characterized. Natural and random effects of the lightning surges on such systems within a structure are considered.

The worst case consist of damage source S1, it means flashes direct to the structure where failure of apparatus can be caused by resistive as well as inductive coupling of lightning current flowing to the earthing system.

Special focus is dedicated to the reduction of overvoltages in order to limit the probability of damage (and then the risk) to tolerable levels by means of selected protection measures as suggested by IEC standards. The considered protection measures include:

- surge protective device (SPD) – switching type;
- surge protective device (SPD) – limiting type;
- isolation transformer.

The investigation, aimed to the selection, installation and coordination of such protection measures, is mainly performed by means of the commercial transient software EMTP-RV. The simulation models are prepared according to the features of real components of analysed system, namely protection measures (SPDs or isolation transformer), connecting leads, apparatus to be protected, earthing arrangement (A or B type according to the IEC standard), power transformer and for different lightning current values and shapes.

In order to validate models correctness several tests are performed in HV Laboratory of La Sapienza University of Rome and in HV Laboratory of Warsaw University of Technology.

On the base of the computer simulation results new criteria for protection measures selection, installation and coordination are proposed and some general conclusions can be formulated:

- the selection of a proper protection level of an *SPD1*, installed at the entry point of a power line into the structure for reduction of voltages by resistive coupling, is affected by the length and the characteristics of the circuit between the *SPD1* and the apparatus to be protected and by the shape of lightning current;
- the voltage  $U_i$  at apparatus terminals increases with circuit length and may reach the double of *SPD1* effective protection level  $U_{p1}$  in ten meters for the negative subsequent stroke (worst case);
- the inductive voltage drop  $\Delta V$  on the leads/connections of *SPD1* may reach several hundred volts even for short connection length (0,1 ÷ 0,2 m);
- due to high values of  $\Delta V$ , even if overvoltage  $U_i$  induced by lightning current in the circuit between SPD and apparatus is negligible, the value of  $U_p$  should be kept so low that practically in all cases of installation a downstream *SPD2* is required;

- the rise time of the current  $I_{SPD}$  flowing through the *SPD1* to the incoming lines is longer than the rise time of the lightning current and is increasing as the length of the line increases, while its amplitude decreases with the line length;
- an *SPD1* class I test is able to withstand the expected charge  $Q_{SPD}$  so that its dimensioning is determined by the current  $I_{SPD}$ ;
- the standard lightning current shape 10/350  $\mu$ s appears adequate for SPD testing;
- induction effect is the decisive factor in determining the current  $I_{SPD2}$  flowing through a second *SPD2* installed at the apparatus terminals, as well as the voltage drop  $\Delta V$  on its connection leads;
- highest values of total charge  $Q_{SPD2}$  flowing in *SPD2* is due to positive lightning stroke (10/350  $\mu$ s) and to the largest circuit loop;
- total charge  $Q_{SPD2}$  is the sum of the charges due to inducing  $Q_i$  and feeding  $Q_r$  effects, but charge  $Q_r$  is of major importance in front of the induced one;
- the values of current proposed by IEC 62305 for *SPD2* class II tested with  $I_n$  are on safety side only if an *SPD1* switching type is installed.

For the proper installation of isolation transformer the following general conclusions can be formulated:

- common mode lightning surges attenuation achieved by means of an isolation transformer depends on the earthing conditions of the screen;
- the screen of isolation transformer have to be earthed to the same bonding bar of apparatus to be protected;
- the protective effect of isolation transformer can be seriously reduced due to long distance connection of the screen to the equipotential bonding bar.

The results of the investigation obtained for basic LV circuit configurations, are then extended to a case study for lightning protection of photovoltaic power generation systems. Particular attention is paid to:

- the estimation of risk of human life and economical loss due to lightning;
- the protection of control and signaling units;
- the influence of load conditions on apparatus protection by means of SPD;
- the influence of parallel consumer on SPD protection features;
- the grounding and bonding conditions influence on apparatus protection.

The results of present thesis can be helpful in the revision of international standards on lightning protection IEC 62305 series. Moreover some practical aspects can be useful for professional designers and installers of lightning protection systems.



## REFERENCES

- [1] G.B. Lo Piparo, G. Carrescia: *Protezione contro le sovratensioni*, Edizioni TNE, 2008
- [2] P. Hasse: *Protezione da sovratensioni negli impianti a bassa tensione*, Tecniche Nuove Edizioni, 2004
- [3] R. Shariatinasab, B. Vahidi, S.H. Hosseinian: *Statistical evaluation of lightning-related failures for the optimal location of surge arresters on the power networks*, Generation, Transmission & Distribution, IET, vol. 3, no. 2, February 2009
- [4] B.D. Russell, C.L. Benner: *Intelligent Systems for Improved Reliability and Failure Diagnosis in Distribution Systems*, IEEE Transactions on Smart Grid, vol. 1, no. 1, June 2010
- [5] R. Lambert, E. Tarasiewicz, A. Xémard, G. Fleury: *Probabilistic Evaluation of Lightning-Related Failure Rate of Power System Apparatus*, IEEE Transactions on Power Delivery, vol. 18, no. 2, April 2003
- [6] Z. Flisowski, C. Mazzetti, B. D'Elia: *New approach to the assessment of frequency of electronic systems damage due to nearby lightning strokes*, Proceedings of International Symposium on High Voltage Engineering (ISH), London, August 1999
- [7] <http://www.iclp-centre.org>
- [8] [www.iee.usp.br/sipda](http://www.iee.usp.br/sipda)
- [9] <http://www.cigre.org> (CIGRE WG C4)
- [10] IEC 61643-1, *Low-voltage surge protective devices – Part 1: Surge protective devices connected to low-voltage power distribution systems – Requirements and tests*, Ed.2, March 2005
- [11] IEC 62305-4, *Protection against lightning – Part 4: Electrical and electronic systems within the structures*, Ed.2 December 2010
- [12] EPCOS: *SIOV Metal Oxide Varistors*, Application notes, 2011
- [13] R.H. Golde: *Lightning Volume 1 Physics of Lightning*, Academy Press London New York San Francisco, 1977
- [14] V.A. Rakov, M.A. Uman: *Lightning physics and effects*, Cambridge University Press, 2005
- [15] H.J. Christian, R.J. Blakeslee, D.J. Boccippio, W.L. Boeck, D.E. Buechler, K.T. Driscoll, S.J. Goodman, J.M. Hall, W.J. Koshak, D.M. Mach, M.F. Stewart: *Global frequency and distribution of lightning as observed from space by the Optical Transient Detector*, Journal of Geophysical Research, vol. 108, no. D1, 4005, doi:10.1029/2002JD002347, 2003
- [16] S.J. Desch, W.J. Borucki, C.T. Russell, A. Bar-Nun: *Progress in planetary lightning – part of C. Miralles (AeroVironment) and T. Nelson (FMA)*, Institute of Physics Publishing, Reports on Progress in Physics 65, 2002
- [17] IEC 62305-2, *Protection against lightning – Part 2: Risk management*, Ed.2, December 2010
- [18] IEC 62305-1, *Protection against lightning – Part 1: General principles*, Ed.2, December 2010
- [19] F. Heidler, W. Zischank, Z. Flisowski, Ch. Bouquegneau, C. Mazzetti: *Parameters of lightning current given in IEC 62305 - background, experience and outlook*, International Conference on Lightning Protection 2008, Uppsala, Sweden, 23-26 June 2008

- [20] H. Grünwald: *Die Messung von Blitzstromstärken an Blitzableitem und Freileitungsmasten*, Elektrotechnische Zeitschrift, vol. 21, pp 505-509, 1934
- [21] H. Grünwald: *Die Messung von Blitzstromstärken an Blitzableitem und Freileitungsmasten*, Elektrotechnische Zeitschrift, vol. 22, pp 536-539, 1934
- [22] H. Zaduk: *Neuere Ergebnisse der Blitzstromstärkernessungen an Hochspannungsleitungen*, Elektrotechnische Zeitschrift, vol. 17, pp 475-479, 1935
- [23] D. Kulikow: *Blitzströme*, 14<sup>th</sup> International Conference on Lightning Protection, Gdańsk, report R-1.05, 1978
- [24] K. Miladowska: *Vergleichung der Blitzresultate von hohen Schornsteinen und den Zählern*, 14<sup>th</sup> International Conference on Lightning Protection, Gdańsk, report R-1.04, 1978
- [25] F. Popolansky: *Lightning current measurement on high objects in Czechoslovakia*, 20<sup>th</sup> International Conference on Lightning Protection, Interlaken, 1990
- [26] K.B. McEachron: *Lightning to the Empire State Building*, Journal of the Franklin Institute, vol 227, no 2, pp 149 – 217, 1939
- [27] E. Garbagnati, G.B. Lo Piparo: *Lightning Parameters - Results of 10 years investigation in Italy*, International Aerospace Conference on Lightning and Static Electricity ICOLSE, Oxford, Report AI. 1982
- [28] H. Geldenhuys, A. Eriksson, A. Bouon: *Fifteen years' data of lightning current measurement on a 60 m mast*, 19<sup>th</sup> International Conference on Lightning Protection, Graz, report R-1 7, 1988
- [29] W.M. Brechow, W.P. Laronow: *Charakteristiken des Blitzes bei Emschlägen in hohe Objekte*, 16<sup>th</sup> International Conference on Lightning Protection, Budapest, report R-1.08. 1981
- [30] B.N. Gorin, W.I. Lewitow, A.W. Schkiljew: *Einige Ergebnisse der Blitzstationenaufnahmen auf dem Ostankino-Fernsehturm*, 13<sup>th</sup> International Conference on Lightning Protection, Venice, report 1.9, 1976
- [31] B.N. Gorin, W.I. Lewitow, A.W. Schkiljew: *Besonderheiten der Blitzeinschläge in den Ostankino-Fernsehturm*, 13<sup>th</sup> International Conference on Lightning Protection, Venice, report 1.10, 1976
- [32] F. Fuchs, E.U. Landers, R. Schmid, J. Wiesinger: *Lightning current and magnetic field parameters caused by lightning strikes to tall structures relating to interference of electronic systems*, IEEE-Transactions on EMC, vol 40, no 4, pp 444 - 451, November 1998
- [33] G. Diendorfer, M. Mar, W. Schulz, W. Hadrian: *Lightning current measurements in Austria - Experimental setup and first results*, 25<sup>th</sup> International Conference on Lightning Protection, Rhodes, Greece, report 1.14, pp 44 -47, 2000
- [34] W. Janischewskyi, A.M. Hussein, V. Shostak, I. Rusan, J.X. Li, J.S. Chang: *Statistics of lightning strikes to the Toronto Canadian National Tower(1978-1995)*, IEEE-Publication SM 422-6 PWRD, 1996
- [35] E. Montandon, B. Beyerler: *The lightning measuring equipment on the Swiss PTT telecommunication tower at St Chrischona, Switzerland*, 22<sup>nd</sup> International Conference on Lightning Protection, Budapest, Hungary, report R 1 c\_06, 1994
- [36] Y. Goto, K. Nanta, H. Komuro, N. Honma: *Current waveform measurement of winter lightning struck an isolated tower*, 20<sup>th</sup> International Conference on Lightning Protection, Interlaken, report 1.9, 1990
- [37] K. Miyake, T. Suzuki, K. Shmjou: *Characteristics of winter lightning currents on Japan sea coast*, IEEE Transactions on Power Delivery, vol 7, no 3, pp 1450 – 1456, 1992

- [38] F. Heidler, W. Zischank, J. Wiesinger: *Statistics of lightning current parameters and related nearby magnetic fields measured at the Peissenberg tower*, 25<sup>th</sup> International Conference on Lightning Protection, Rhodes, Greece, report 1.19, pp 78 -83, 2000
- [39] M.M. Newman, J.R. Stahmann, J.D. Robb, E.A. Lewis, S.G. Martin, S.V. Zinn: *Triggered lightning channel strokes at very close range*, Journal of Geophysical Research, vol. 72, no 18, pp 4761-4764, 1967
- [40] K. Miyake, K. Horii: *Five years' experiences on artificially triggered lightning in Japan*, Proc of the 7th IEE-Conference "Gas Discharges and their Application, pp. 468-471, 1982
- [41] X. Liu, C. Wang, Y. Zhang, Q. Xiao, D. Wang, Z. Zhou, C. Guo: *Experiment of artificially triggering lightning in China*, Journal of Geophysical Research, vol 99.no D5. pp 10727- 10731, 1994
- [42] P. Depasse: *Statistics on artificially triggered lightning*, Journal of Geophysical Research, vol. 99, no. D9. pp 186515 – 18522, 1994
- [43] M.A. Uman, V. Rakov, K.J. Rambo, T.W. Vaught, M.I. Fernandez, D.J. Codier, R.M. Chandler, R. Bernstein, C. Golden: *Triggered-lightning experiments at Camp Blanding, Florida (1993-1995)*, Transaction on IEE Japan, vol. 117-B, no 4, pp. 446 -452, 1997
- [44] V. Rakov, M.A. Uman, K.J. Rambo: *A review of ten years of triggered-lightning experiments in Camp Blanding, Florida*, Journal of Atmospheric Research, Vol. 76, pp. 503-517, 2005
- [45] E.H. Lay, R.H. Holzworth, C.J. Rodger, J.N. Thomas, O. Pinto Jr., R.L. Dowden: *WWLL global lightning detection system: Regional validation study in Brazil*, Geophysical Research Letters, vol. 31, L03102, doi:10.1029/2003GL018882, 2004
- [46] K. Berger, R.B. Anderson, H. Kröninger: *Parameters of lightning flashes*, CIGRE Electra No 41, p. 23 – 37, 1975
- [47] R.B. Anderson, A.J. Eriksson: *Lightning parameters for engineering application*, CIGRE Electra No 69, p. 65 – 102, 1980
- [48] CIGRÉ WG C4.407: *Lightning parameters for engineering applications*, <http://sc4wg407.ing.unibo.it>, December 2012
- [49] A.J. Eriksson: *Lightning and tall structures*, Transaction SAIEE, p.p. 238–252, August 1978
- [50] C. Romero, M. Paolone, F. Rachidi, M. Rubinstein, A. Rubinstein, G. Diendorfer, W. Schulz, M. Bernardi, C.A. Nucci: *Preliminary Comparison of Data from the Sântis Tower and the EUCLID Lightning Location System*, International Symposium on Lightning Protection (XI SIPDA), Fortaleza, Brazil, 3-7 October 2011
- [51] S.M. Chen, Y. Du, L.M. Fan, H.M. He, D.Z. Zhong: *A Lightning Location System in China: Its Performances and Applications*, IEEE Transactions on Electromagnetic Compatibility, vol. 44, no. 4, November 2002
- [52] F. Suzuki, Y. Onozuka: *Lightning location systems in Japan*, 19th International Lightning Detection Conference 24-25 April, Tucson, Arizona, USA, 2006
- [53] M. Matsui, N. Takano: *Evaluation of Lightning Location Accuracy of JLDN with a Lightning Video Camera System*, 2010 Asia-Pacific International Symposium on Electromagnetic Compatibility, Beijing, China, 12 -16 April 2010
- [54] K.L. Cummins, M.J. Murphy: *An Overview of Lightning Locating Systems: History, Techniques, and Data Uses, With an In-Depth Look at the U.S. NLDN*, IEEE Transactions on Electromagnetic Compatibility, vol. 51, no. 3, August 2009

- [55] G. Diendorfer: *Lightning location systems (LLS)*, IX International Symposium on Lightning Protection, Foz do Iguaçu, Brazil, 26-30 November 2007
- [56] <http://www.euclid.org>, December 2011
- [57] <http://www.vaisala.com>, December 2011
- [58] M. Bernardi, R. Tommasini: *Number of lightning to earth in Italy*, International Conference on Lightning Protection 2012, Vienna, Austria, 2-7 September 2012
- [59] <http://www.fulmini.it>, December 2011
- [60] EN 50536 : Protection against lightning -Thunderstorm Warning Systems, 2011
- [61] Z. Flisowski: *Analiza zagrożenia piorunowego obiektów budowlanych*, Wydawnictwo Politechniki Warszawskiej, Warszawa 1980
- [62] C. Mazzetti, T. Kisielewicz, F. Fiamingo, B. Kuca, Z. Flisowski: *On the lightning hazard and its reduction measures in nuclear plants*, International Conference on Electromagnetic Disturbances 2011, Białystok, Poland, 28-30 September 2011
- [63] Z. Flisowski: *Trendy rozwojowe ochrony odgromowej budowli*, Polska Akademia Nauk Komitet Elektrotechniki, Warszawa 1986
- [64] T. Kisielewicz, C. Mazzetti, Z. Flisowski, B. Kuca, F. Fiamingo: *Natural Danger of Nuclear Power Plants due to Lightning Strokes*, International Nuclear Energy Congress 2012, Warsaw, Poland, 22-24 May 2012
- [65] IEC 71-1: *Insulation co-ordination – Part 1: Definitions, principles and rules*, 1993
- [66] P. Hasse: *Overvoltage protection of low voltage systems*, IET Power and Energy Series 33, 2<sup>nd</sup> Edition, 2000
- [67] P. Hasse, J. Wiesinger: *Manuale per la protezione dalle scariche atmosferiche e la messa a terra*, Tecniche Nuove, 1993
- [68] ITU-T K.67: Series K: *Protection against interference - Expected surges on telecommunications and signalling networks due to lightning*, February 2006
- [69] C. Buccella, S. Cristina, A. Orlandi: *Frequency analysis of the induced effects due to the lightning stroke radiated electromagnetic field*, IEEE Transaction on Electromagnetic Compatibility, vol.34, n° 3, August 1992
- [70] P. Chowduri, E.T.B. Gross: *Voltage surges induced on overhead lines by lightning strokes*, Atti IEE, vol. 114, no 12, pp. 1899-1907, December 1967
- [71] V. Cooray: *Lightning-induced overvoltages in power lines: validity of various approximations made in overvoltage calculations*, 22<sup>nd</sup> International Conference on Lightning Protection, Budapest, September 19-23, 1994
- [72] S. Guerrieri, F. Rachidi, M. Ianoz, P. Zweiaccker, C.A. Nucci: *A time domain approach to evaluate induced voltages on tree-shaped electrical networks by external electromagnetic fields*, International Symposium on Electromagnetic Compatibility, Zurich, March 1995
- [73] F. Heidler: *Analytische Blitzstromfunktion zur LEMP-Berechnung*, 1.9, pagg. 63-66, Monaco, 16-20 September, 1985
- [74] A. Borghetti, S. Guerrieri, M. Ianoz, C. Mazzetti, C.A. Nucci, F. Rachidi: *Sovratensioni indotte da fulminazioni indirette su linee aeree di distribuzione*, Atti della Riunione annuale AEI, pp. 205-217, vol.5, Roma, 24-27 September, 1995
- [75] A. Borghetti, J.A. Gutierrez, C.A. Nucci, M. Paolone, E. Petrache, F. Rachidi: *Lightning-induced voltages on complex distribution systems: models, advanced software tools and experimental validation*, Journal of Electrostatics 60, 2004



- [76] V. Cooray: *The Lightning Flash*, IEE Power Energy Series 34, 2003
- [77] M.J. Master, M.A. Uman: *Lightning Induced Voltages on Power Lines: Theory*, IEEE Transactions on Power Apparatus and Systems. Vol. 103, No.9, pp. 2502-2518, September 1984
- [78] A.J. Eriksson: *The incidence of lightning strikes to power lines*, IEEE Transaction on Power Delivery, Vol. PWRD-2, No.3, July 1987
- [79] S. Rusck: *Induced Lightning Over-Voltages on Power Transmission Lines with Special Reference to Over-Voltage Protection of Low Voltage Network*, Thesis, Royal Institute of Technology, Stockholm, 1957
- [80] C.A. Nucci, V. Bardazzi, R. Brio, A. Mansoldo, A. Porrino: *A code for the calculation of lightning-induced overvoltages and its interface with the ElectroMagnetic Transient Program*, Proceedings of 22nd ICLP, Budapest, 19-23 settembre, 1994
- [81] C.A. Nucci, F. Rachidi, M. Ianoz, C. Mazzetti: *Lightning-induced voltages on overhead lines*, IEEE Trans. on Electromagnetic Compatibility, Vol. 35, No. 1, pp. 75-86, February 1993
- [82] F. Rachidi, C.A. Nucci, M. Ianoz, C. Mazzetti: *Influence of a lossy ground on lightning induced voltages on overhead lines*, IEEE Trans. on EMC, Vol. 38, No. 3, pp. 250-264, August 1996
- [83] M. Paolone, C.A. Nucci, E. Petrache, F. Rachidi: *Mitigation of lightning-induced overvoltages in medium voltage distribution lines by means of periodical grounding of shielding wires and of surge arresters: modeling and experimental validation*, IEEE Trans. Power Delivery 19 (1), 2004
- [84] F. Rachidi, M. Rubinstein, S. Guerrieri, C.A. Nucci: *Voltages induced on overhead lines by dart leaders and subsequent return strokes in natural and rocket-triggered lightning*, IEEE Trans. Electromagnetic Compatibility 39 (2), 1997
- [85] C.A. Nucci, S. Guerrieri, M.T. Correia de Barros, F. Rachidi: *Influence of corona on the voltages induced by nearby lightning on overhead distribution lines*, IEEE Trans. Power Delivery 15 (4), 2000
- [86] F. Rachidi, C.A. Nucci, M. Ianoz, C. Mazzetti: *Response of multiconductor power lines to nearby lightning return stroke electromagnetic fields*, 14<sup>th</sup> IEEE/PES Transmission and Distribution Conference, Los Angeles, also on IEEE Trans. on Power Delivery, Vol. 12, N.3, pp. 1404-1411, July 1997
- [87] F. Rachidi, W. Janischewskyj, A.M. Hussein, C.A. Nucci, S. Guerrieri, J.S. Chang: *Electromagnetic fields radiated by lightning return strokes to high towers*, 24<sup>th</sup> International Conference on Lightning Protection, Birmingham, United Kingdom, pp. 23-28, 1998
- [88] F. Popolansky, F. Prochakzka, M. Schlamp: *Frequency distribution of peak values of lightning overvoltages in a rural low-voltage network*, 21<sup>st</sup> International Conference on Lightning Protection, Berlin 1992
- [89] TR IEC 64/1125/CDV: *Surge overvoltages and surge protection in low-voltage a.c. power systems – General basic information*, June 2002
- [90] Dehn - Blitzplaner: *Manuale per la protezione contro i fulmini*, <http://www.dehn.it/it/service/downloads/bpl.shtml>, 2011
- [91] IEC 61643-1: *Low-voltage surge protective devices – Part 1: Surge protective devices connected to low-voltage power distribution systems – Requirements and tests*, 2005



- [92] S. Ait-Amar, J.B. Ducourneau, G. Serrie, M. Abplanalp: *Arc extinguishing method of SPD type 1*, IEEE Transactions on Dielectrics and Electrical Insulation Vol. 16, No. 3; June 2009
- [93] EPCOS: *SIOV Metal Oxide Varistors*, Data Book, 2008
- [94] EPCOS: *SIOV Metal Oxide Varistors*, General technical information, 2011
- [95] EMTP-RV Model Documentation: *ZnO device*, EMTP - EMTP Works, 2003
- [96] H. Rahaman, B.J. Lee, J. Urban, R. Stark, K. Frank, S.H. Nam: *A spark gap switch with very high repetition rate*, 28th ICPIG, Prague, Czech Republic, July 2007
- [97] IEEE Working Group 3.4.11: *Modeling of metal oxide surge arresters*, IEEE Transaction on Power Delivery, vol. 7, no. 1, pp. 302-309, 1992
- [98] M.J. Kushner, R.D. Milroy, W.D. Kimura: *A laser-triggered spark gap model*, Journal of Applied Physics, Vol.58, Issue: 8, October 1985
- [99] A.J. MacPhee, S.J. Macgregor, S.M. Turnbull: *Electrostatic modelling of a trigatron spark gap*, Pulsed Power Conference, Bristol, UK, July 1995
- [100] A.J. MacPhee, S.J. Macgregor, S.M. Turnbull: *Electromagnetic modelling design considerations for triggered spark gaps*, Pulsed Power Conference, London, UK, March 1997
- [101] A.L. Donaldson, M.O. Hagler, M. Kristiansen, L.L. Hatfield, R.M. Ness: *Modeling of self-breakdown voltage statistics in high-energy spark gaps*, Journal of Applied Physics, Vol.57, Issue: 11, June 1985
- [102] S. Bindu, H.A. Mangalvedekar, S. Umbarkar, A. Sharma, D.P. Chakravarti, P.C. Saroj, K.C. Mittal: *Modelling of a spark gap switch*, Properties and Applications of Dielectric Materials (ICPADM), Bangalore, India, July 2012
- [103] J.G. Zola: *Simple model of metal oxide varistor for Pspice Simulation*, IEEE Transactions on Computer-Aided Design of Integrated Circuits and Systems, vol.23, no.10, pp. 1491- 1494, October 2004
- [104] S.A. Kamali, A. Vahedi, A. Halvai: *Performance analysis of HTS fault current limiter combined with a ZnO varistor*, International Conference on Electrical Machines and Systems, ICEMS 2005, Nanjing, China, September 2005
- [105] H. Jun, W. Long, J. He, J. Liu: *Simulation on surge responses of ZnO varistors by Voronoi network with actual grain boundary model*, Annual Report Conference on Electrical Insulation and Dielectric Phenomena (CEIDP), West Lafayette, USA, October 2010
- [106] S. Dau: *Modelling of metal oxide surge arresters as elements of overvoltage protection systems*, International Conference on Lightning Protection, Vienna, Austria, September 2012
- [107] T. Kisielewicz, F. Fiamingo, C. Mazzetti, D. Krasowski, P. Sul, B. Kuca: *Simulated and tested protection effects on electrical equipment terminals at overvoltages incoming through distant SPD*, International Youth Conference on Energetics 2011 – IEEE Conference, Leiria, Portugal, 7-9 July 2011
- [108] J. Sisira, K. Nihal, S. Alistair, K. Rainer: *Numerical simulation of surge protection circuits and experimental verification using a lightning surge simulator*, IECON 2012, 38<sup>th</sup> Annual Conference on IEEE Industrial Electronics Society, Montreal, Canada, October 2012
- [109] T. Hong, V. Scuka: *Time-domain study of a shielding cable system with a nonlinear load*, IEEE Transactions on Electromagnetic Compatibility, vol.41, no.3, pp.214-220, August 1999
- [110] EMTP-RV Model Documentation: *Flashover switch*, EMTP - EMTP Works, 2003

- [111] EMTP-RV Model Documentation: *Ideal switch*, EMTP - EMTP Works, 2004
- [112] EMTP-RV Model Documentation: *R nonlinear device*, EMTP - EMTP Works, 2003
- [113] P. De Potter: *Application note isolation transformers*, European Copper Institute, Leonardo Energy, September 2011
- [114] M. Izhar, C.M. Hadzer, M. Syafrudin, S. Taib, S. Idns: *Performance for Passive and Active Power Filter in Reducing Harmonics in the Distribution System*, Proceedings of National Power & Energy Conference (PECon), 2004
- [115] T. Chuck: *Power Quality in Medium and Large Commercial Buildings*, Senior PQ Engineer, EPRI, November 2007
- [116] R.D. Henderson, P.J. Rose: *Harmonics: The Effects on Power Quality and Transformers*, IEEE Transaction on Industry Applications, Vol. 30, no. 3, May/June 1994
- [117] IEC 61558-2-4: *Safety of transformers, reactors, power supply units and similar products for supply voltages up to 1 100 V - Part 2-4: Particular requirements and tests for isolating transformers and power supply units incorporating isolating transformers*, March 2009
- [118] M.A. Shafie, H. Singh, M.M.A Rahman: *Harmonic and Neutral to Ground Voltage Reduction Using Isolation Transformer*, 2010 IEEE International Conference on Power and Energy (PECon2010), November/December, 2010, Kuala Lumpur, Malaysia
- [119] IEC 60601-1-2: *Medical electrical equipment: General requirements for basic safety and essential performance – Collateral standard: Electromagnetic compatibility – Requirements and tests*, Ed.3, March 2007
- [120] G.L. Amicucci: *Gestire la sicurezza di impianti e tecnologie biomediche: Proposte per l'innovazione tecnologica in ambito sanitario*, Supplemento di Prevenzione Oggi, no. 1, 2008
- [121] IEC 61558-2-15: *Safety of Power Transformers, Power Supply Units and Similar - Part 2-15: Particular Requirements for Isolating Transformers for the Supply of Medical Locations*, Ed. 2, November 2011
- [122] E.P. Wenaas, R. Wheeler: *EMP isolation transformer*, IEEE Transactions on Nuclear Science, Vol. NS-32, No. 6, December 1985
- [123] CIGRE WG.33.02: *Guidelines for representation of network elements when calculating transients*, October 1991
- [124] A. Piantini, A.G. Kanashiro: *A distribution transformer model for calculating transferred voltages*; International Conference on Lightning Protection 2002, Cracow, Poland, 2002
- [125] R. Bechega, J. De Araujo, A. De Souza, M. Barreira: *Digital models of transformer for application on electromagnetic transient studies*, International Conference on Grounding and Earthing & 3<sup>rd</sup> Brazilian workshop on atmospheric electricity, Rio de Janeiro, Brazil, 2002
- [126] TN CR 0016: *Isolation Transformers and Surge Protection*, www.erico.com, June 2012
- [127] ABB: *Electrical installation handbook: Protection, control and electrical devices*, Technical guide - 6<sup>th</sup> edition, 2010
- [128] IEC 62305-3: *Protection against lightning – Part 3: Physical damage to structures and life hazard*, Ed.2, December 2010
- [129] IEC 60364-5-53: *Electrical installations of buildings – Part 5-53: Selection and erection of electrical equipment – Isolation, switching and control*, 2001

- [130] IEC 61000-4-5: *Electromagnetic compatibility (EMC) – Part 4-5: Testing and measurement techniques – Surge immunity test*, 2005
- [131] IEC 61000-4-9: *Electromagnetic compatibility (EMC) – Part 4-9: Testing and measurement techniques – Pulse magnetic field immunity test – Basic EMC Publication*, 1993
- [132] IEC 61000-4-10: *Electromagnetic compatibility (EMC) – Part 4-10: Testing and measurement techniques – Damped oscillatory magnetic field immunity test – Basic EMC Publication*, 1993
- [133] IEC 61643-12: *Low-voltage surge protective devices – Part 12: Surge protective devices connected to low-voltage power distribution systems – Selection and application principles*, 2008
- [134] IEC 61643-21: *Low voltage surge protective devices – Part 21: Surge protective devices connected to telecommunications and signalling networks – Performance requirements and testing methods*, 2000
- [135] IEC 61643-22: *Low voltage surge protective devices – Part 22: Surge protective devices connected to telecommunications and signalling networks – Selection and application principles*, 2004
- [136] Z. Flisowski: *Technika Wysokich Napięć*, WNT, Warszawa 2005
- [137] R.H. Golde: *Lightning Volume 2 Lightning Protection*, Academy Press London New York San Francisco, 1977
- [138] IEC 60664-1: *Insulation coordination for equipment within low-voltage systems – Part 1: Principles, requirements and tests*, 2007
- [139] ITU-T Recommendation K.20: *Resistibility of telecommunication equipment installed in a telecommunications centre to overvoltages and overcurrents*, 2008
- [140] ITU-T Recommendation K.21: *Resistibility of telecommunication equipment installed in customer premises to overvoltages and overcurrents*, 2003
- [141] ITU-T Recommendation K.45: *Resistibility of telecommunication equipment installed in the access and trunk networks to overvoltages and overcurrents*, 2003
- [142] IEC 62066 TR Ed.1.0: *General basic information regarding surge overvoltages and surge protection in low voltage a.c. power systems*, 2001
- [143] D. Krasowski, T. Kisielewicz, B. Kuca, Z. Flisowski, F. Fiamingo, C. Mazzetti: *On critical distance between an SPD and protected appliance with respect to their voltage coordination*, International Conference on Lightning Protection 2010, Cagliari, Italy, 13-17 September 2010
- [144] T. Kisielewicz, F. Fiamingo, C. Mazzetti, B. Kuca, D. Krasowski: *Influence of lightning overvoltage shape on SPD characteristics for telecommunications and signalling networks*, International Conference on Electromagnetic Disturbances 2011, Bialystok, Poland, 28-30 September 2011
- [145] T. Kisielewicz, F. Fiamingo, C. Mazzetti, B. Kuca, Z. Flisowski: *Selected problems of sensitive apparatus protection against lightning overvoltages by means of SPD*, International Conference on Electromagnetic Disturbances 2011, Bialystok, Poland, 28-30 September 2011
- [146] T. Kisielewicz, F. Fiamingo, Z. Flisowski, B. Kuca, G.B. Lo Piparo, C. Mazzetti: *Factors Influencing the Selection and Installation of Surge Protective Devices for Low Voltage Systems*, International Conference on Lightning Protection 2012, Vienna, Austria, 2-7 September 2012

- [147] T. Kisielewicz, C. Mazzetti, Z. Flisowski, B. Kuca, G.B. Lo Piparo: *Electronic Apparatus Protection Against LEMP: Surge Threat for the SPD Selection*, International Symposium on Electromagnetic Compatibility 2012, Rome, Italy, 17-21 September 2012
- [148] G.L. Amicucci, F. Fiamingo, M. Marzinotto, C. Mazzetti, G. B. Lo Piparo, Z. Flisowski: *Protection against lightning overvoltages of electrical and electronic systems: evaluation of the protection distance of an SPD*, International Conference on Lightning Protection 2004, Avignon, France, September 2004.
- [149] C.F. Barbosa, R. Pomponi, R. Tommasini: *SPD characteristics for equipment protection*, International Conference on Lightning Protection 2010, Cagliari, Italy, 13-17 September 2010
- [150] CIGRE WG 01 of SC 33: *Guide to procedures for estimating the lightning performance of transmission lines*, CIGRÉ, October 1991
- [151] C.A. Nucci: *The Lightning Induced Over-Voltage (LIOV) Code*, IEEE PES Winter Meeting, Singapore, January 2000
- [152] M. Paolone, F. Rachidi, A. Borghetti, C. A. Nucci, M. Rubinstein, V. A. Rakov, M. A. Uman: *Lightning Electromagnetic Field Coupling to Overhead Lines: Theory, Numerical Simulations and Experimental Validation*, IEEE Transactions on Electromagnetic Compatibility, vol. 51, no. 3, August 2009
- [153] EMTP-RV Model Documentation: *Constant Parameter Transmission line*, EMTP - EMTP Works, 2003
- [154] L.V. Bewley: *Traveling Waves on Transmission Systems*, Dover Publications, Inc., New York 1963
- [155] A. Piantini, C.V.S. Malagodi: *Modeling of three-phase distribution transformers for calculating lightning induced voltages transferred to the secondary*, IEEE 5<sup>th</sup> International Symposium on Lightning Protection, Sao Paulo, 1999
- [156] A.G. Kanashiro, A. Piantini, G.F. Burani: *A Methodology for Transformer Modelling Concerning High Frequency Surge*, Proceedings of the VI international Symposium on Lightning Protection (VI SIPDA), pp. 275-280, Sao Paulo, November 2001
- [157] A. Piantini, J.M. Janiszewski, W. Bassi, N.M. Matsuo: *A simple transformer model for analysis of transferred lightning surges from MV to LV lines*, CIRED, International Conference on Electricity Distribution, Nice, 1999
- [158] S. Pack, J. Plesch: *EMTP – RV Course*, Graz, Austria, 18-20 October 2010
- [159] IEEE Std 142™ (green book): *142 IEEE Recommended Practice for Grounding of Industrial and Commercial Power Systems*, 2007
- [160] WG of Italian Electrotechnical Committee (CEI), TC81-Lightning Protection: *Lightning Protection of Structures*, Part IV to Part VI, L'Energia Elettrica, n.11, pp. 447-475, 1985
- [161] A.C. Liew, M. Darveniza: *Dynamic model of impulse characteristics of concentrated earths*, Proc. IEE Vol. 121, n. 2, 1974
- [162] R. Verma, D. Mukhedkar: *Impulse impedance of buried ground wire*, IEEE Trans. on PAS, Vol. PAS-99, n. 5, 1980
- [163] B.R. Gupta, B. Thapar: *Impulse impedance of grounding grids*, IEEE Trans. on PAS, Vol. PAS-99, n. 6, 1980
- [164] C. Mazzetti, G. Veca: *Impulse behavior of ground electrodes*, Paper 83 WM142-7, IEEE PES Winter Meeting, New York, 1983



- [165] A.L. Vainer: *Impulse characteristics of complex earth grids*, Electrical Technology, USSR, Vol. 1, 1966
- [166] R. Kosztaluk, M. Loboda, D. Mukhedkar: *Experimental study of transient ground impedances*, Paper 81 SM 399-5, IEEE PES Summer Meeting, Portland, 1981
- [167] P. Kouteynikonoff: *Reponse impulsionnelle des prises de terre aux courantes de foudre*, CIGRE Symposium 22-81, Stockholm, 1981
- [168] E.E. Oettle: *A new general estimation for predicting the impulse impedance of concentrated earth electrodes*, IEEE Transactions on Power Delivery, vol. 3, n. 4, October 1988
- [169] W.A. Crisholm, W.A. Janischewskyj: *Lightning surge response of ground electrodes*, IEEE Transactions on Power Delivery, vol. 4, n. 2, April 1989
- [170] F. Popolansky: *Impulse characteristics of soil*, 20<sup>th</sup> International Conference on Lightning Protection, Interlaken, September 1990
- [171] L. Grcev: *Grounding Systems for High Frequencies and Transients*, International Symposium on Electromagnetic Compatibility 2012, Rome, Italy, 17-21 September 2012
- [172] V. Arnautovski-Toseva, L. Grcev: *Electromagnetic analysis of horizontal wire in two-layered soil*, Journal of Computational and Applied Mathematics, Vol.168, July 2004
- [173] A.F. Imece, D.W. Durbak, H. Elahi, S. Kolluri, A. Lux, D. Mader, T.E. McDermott, A. Morched, A.M. Mousa, R. Natarajan, L. Rugeles, E. Tarasiewicz: *Modeling guidelines for fast front transients*, IEEE Transactions on Power Delivery, Vol. 11, pp. 493 –506, January 1996
- [174] L. Grcev, M. Heimbach: *Frequency dependent and transient characteristics of substation grounding systems*, IEEE Trans, on Power Delivery, vol.12, n. 1, pp. 172-178, January 1997
- [175] E. Giudice, G.B. Lo Piparo: *Quaderno 3 - I fulmini e le linee elettriche*, Edizione RAI Radiotelevisione Italiana, Torino, 1974
- [176] L. Grcev, M. Popov: *On high-frequency circuit equivalents of a vertical ground rod*, IEEE Transactions on Power Delivery, vol. 20, no. 2, pp. 1598-1603, April 2005
- [177] R. Rudenberg, *Fundamental considerations on ground currents*, Electrical Eng., 64, 1-13, 1945
- [178] E.D. Sunde: *Earth conduction effects in transmission systems*, New York: Dover, 1968
- [179] M. Heimbach, L. Grcev: *Simulation of grounding structures within EMTP*, Proceedings of 10th International Symposium on High Voltage Engineering, Montreal, Canada, August 1997
- [180] F. Menter, L. Grcev: *EMTP-based model for grounding system analysis*, IEEE Transactions on Power Delivery, Vol. 9, pp. 1838-1849, October 1994
- [181] J. Birkl, P. Hasse, P. Zahlmann: *Investigation of the interaction of lightning currents with low-voltage installations and their related lightning threat parameters*, 23<sup>rd</sup> International Conference on Lightning Protection, Florence, Italy, 1996
- [182] J. Birkl, P. Zahlmann: *Lightning currents in low-voltage installations*, 29<sup>th</sup> International Conference on Lightning Protection, Uppsalla, Sweden, 2008
- [183] J. Birkl, C.F. Barbosa: *Modeling the current through the power conductors of an installation struck by lightning*, SIPDA, Fortaleza, Brasil, 2011



- [184] IEEE Std C62.42-2005: *IEEE Guide for the Application of Component Surge-Protective Devices for Use in Low-Voltage [Equal to Or Less Than 1000 V (AC) Or 1200 V (DC)] Circuits*, 2006
- [185] G.L. Amicucci, F. Fiamingo, Z. Flisowski, G.B. Lo Piparo, C. Mazzetti: *Surge protective devices for low voltage systems: practical approach for the protection distance evaluation*, Paper ID 160, IEEE Power Tech Conference, Lausanne, 2005
- [186] I.A. Metwally, F. Heidler: *Enhancement of the SPD Residual Voltage at Apparatus Terminals in Low-Voltage Power Systems*, IEEE Transactions on Power Delivery, Vol. 22, No. 4, October 2007
- [187] T. Kisielewicz, F. Fiamingo, C. Mazzetti, B. Kuca, Z. Flisowski: *A Case Study to Effective Protection of Sensitive Apparatus by Means of Voltage Limiting SPD*, Electrical Review, ISSN 0033-2097, r. 88 no. 8/2012
- [188] T. Kisielewicz, F. Fiamingo, C. Mazzetti, B. Kuca, D. Krasowski: *Impact of Overvoltage Shape Caused by Lightning Stroke on Sensitive Apparatus Protection by Means of SPD*, Electrical Review, ISSN 0033-2097, r. 88 no. 9b/2012
- [189] A. Yagasaki: *Highly Improved Performance of a Noise Isolation Transformer by a Thin-Film Short-Circuit Ring*, IEEE Transactions on Electromagnetic Compatibility, vol. 41, no. 3, August 1999
- [190] G.L. Amicucci, F. Fiamingo, G.B. Lo Piparo, B. Kuca, Z. Flisowski, C. Mazzetti: *Protection of electrical and electronic systems against surges by an isolation transformer*, Electrical Review, ISSN 0033-2097, R.86 NR 3/2010
- [191] R.P. Torrico-Bascopé, D.S. Oliveira, C.G.C. Branco, F.L.M. Antunes: *A UPS With 110-V/220-V Input Voltage and High-Frequency Transformer Isolation*, IEEE Transactions on Industrial Electronics, vol. 55, no. 8, August 2008
- [192] M.M.A. Rahman, A.K.S. Bhat: *A high-frequency transformer isolated single-phase single-stage soft-switched AC-to-DC bridge converter*, Power Electronics Specialists Conference, Vancouver, Canada 2001
- [193] T. Fjield, K. Hynynen: *Method of Reduction of the Number of Driving System Channels for Phased-Array Transducers Using Isolation Transformers*, IEEE Transactions on Biomedical Engineering, vol. 47, no. 1, January 2000
- [194] S.C. Tang, S.Y. Hui, H.S. Chung: *A Low-Profile Low-Power Converter with Coreless PCB Isolation Transformer*, IEEE Transactions on Power Electronics, vol. 16, no. 3, May 2001
- [195] R. Montaña, V. Cooray : *Penetration of lightning induced transient from high voltage to low voltage power system across distribution transformers*; International Conference on Lightning Protection 2004, Avignon, France, 2004
- [196] M. Aguado, B. Hermoso, V. Senosiain, P. Martinez Cid: *A simplified distribution transformer model for calculating transferred surges*; International Conference on Lightning Protection 2002, Cracow, Poland, 2002
- [197] P. M. Pakpahan, H. Svarif: *Study on transient model of transformer for lightning over voltage analyzes*; International Conference on Lightning Protection 2000, Rhodes, Greece, 2000
- [198] A. Borghetti, A. Morched, F. Napolitano, C.A. Nucci, M. Paolone: *Lightning-induced overvoltages transferred through distribution power transformer*; IEEE Transactions on Power Delivery, vol.24, 2009

- [199] M. Fernando, V. Cooray: *Lightning surges at distribution transformer secondary*; 5<sup>th</sup> International Conference Industrial Information System, Mangalore, India, 2010
- [200] J.C. Hernández, P.G. Vidal, F. Jurado: *Lightning and Surge Protection in Photovoltaic Installations*; IEEE Transactions on Power Delivery, Vol. 23, no. 4, October 2008
- [201] J. Birkl, P. Zahlmann, O. Beierl: *Surge protection for PV generators: Requirements, testing procedures and practical applications*, X International Symposium on Lightning Protection, Curitiba, Brazil, 9-13 November 2009
- [202] V. Carrescia: *Le guide blu. N. 15 – Fotovoltaico*, TNE, Torino, 2011
- [203] G.L. Amicucci, F. Fiamingo: *Lightning risk to photovoltaic power generating systems*, Prevention Today Vol. 5, no. 1/2, 2009
- [204] ABB: *ABB solutions for photovoltaics protection and other modular devices*, Germany 2010
- [205] J.C. Hernandez, P.G. Vidal, F. Jurado: *Guidelines to requirements for protection against electric shock in PV generators*, Proc. IEEE Power Eng. Soc. General Meeting, pp. 17–22, June 2005
- [206] M. Drif, P.J. Pérez, J. Aguilera, G. Almonacid, P. Gomez, J. de la Casa, J.D. Aguilar: *Univer project. A grid connected PV system of at jaén university. Overview and performance analysis*, Solar Energy Materials and Solar Cells, vol. 91, pp. 670–683, May 2007
- [207] A. Kern, F. Krichel: *Considerations about the lightning protection system of mains independent renewable energy hybrid-systems. Practical experiences*, J. Electrostatics, vol. 60, pp. 257–263, March 2004
- [208] G.L. Amicucci, F. Fiamingo, T. Kisielewicz: *Risk assessment of photovoltaic installations, due to lightning, according to IEC 62305 – 2<sup>nd</sup> Edition*, International Conference on Lightning Protection 2012, Vienna, Austria, 2-7 September 2012
- [209] Electromagnetic Compatibility—Part 4–5: Testing and Measurement Techniques—Surge Immunity Test, IEC Std. 61000-4-5, 2005
- [210] IEEE Std C62.45: *Recommended Practice on Surge Testing for Equipment Connected to LV (1000 V and less) AC Power Circuits*, 2002
- [211] IEC 61730-2: *PV Module Safety Qualification—Part 2: Requirements for Testing*, 2004
- [212] IEC 61730-1: *PV Module Safety Qualification—Part 1: Requirements for Construction*, 2004
- [213] G.L. Amicucci, F. Fiamingo: *Risk assessment of photovoltaic installations due to lightning*, International Conference on Lightning Protection 2008, Uppsala, Sweden, 23-26 June 2008
- [214] IEC 60364 Ed.5: *Low-voltage electrical installations - Part 1: Fundamental principles, assessment of general characteristics, definitions*, 2005